



This work is protected by copyright and other intellectual property rights and duplication or sale of all or part is not permitted, except that material may be duplicated by you for research, private study, criticism/review or educational purposes. Electronic or print copies are for your own personal, non-commercial use and shall not be passed to any other individual. No quotation may be published without proper acknowledgement. For any other use, or to quote extensively from the work, permission must be obtained from the copyright holder/s.

X-RAY FIBRE DIFFRACTION STUDIES OF THE EFFECT OF  
IONS AND SMALL MOLECULES ON THE STRUCTURE OF NUCLEIC ACIDS

by

NIGEL JOHN RHODES

A thesis submitted for the degree of  
Doctor of Philosophy  
in the  
University of Keele

March 1983

Department of Physics,  
University of Keele,  
Keele,  
Staffordshire.

Abstract

X-ray fibre diffraction techniques have been used to investigate the conformations available to the sodium and lithium salts of poly[d(A-C)], poly[d(G-T)] and the sodium salt of poly[d(A-T)].poly[d(A-T)] as a function of added fibre salt content and relative humidity of the fibre environment.

The A, B and C conformations were obtained for Na poly[d(A-C)].poly[d(G-T)] and the sequence of transitions on increasing relative humidity or fibre salt content was C → A → B.

Semi-crystalline C and B diffraction patterns were obtained from fibres of Li poly[d(A-C)].poly[d(G-T)]. The C conformation appeared stable over a wide range of humidity and added fibre salt content. Particularly well resolved C type diffraction patterns were obtained indicating an unusual  $9_2$  helical symmetry.

In conjunction with Mahendrasingam, 1983, the A, B,  $\alpha$ -B', C and D conformations were obtained for Na poly[d(A-T)].poly[d(A-T)] and a sequence of transitions between these conformations has been proposed. The C conformation has reproducibly been observed for both polynucleotide and random sequence DNA when  $\text{Na}^+$  is the associated cation. Thus the C conformation may be more biologically significant than previously supposed.

A number of techniques were examined to quantitatively determine the amount of salt associated with nucleic acids in solution and in x-ray fibre samples.

The crystallization of steffimycin B in DNA fibres was examined by x-ray fibre diffraction methods and compared with other crystalline and non-crystalline drug/DNA studies. It was concluded that low solubility in aqueous solution and a relatively low binding affinity for DNA are possible indicators that a drug may crystallize in DNA fibres. However, fibre preparation techniques and environmental conditions pertaining at that time probably play an important role in this process.

The interaction between bovine serum albumin and montmorillonite has

(ii)

been undertaken using x-ray diffraction techniques. Results are consistent with adsorption of the protein in the interlamellar regions of the montmorillonite. These results provide a basis for the investigation of surface interactions in more intricate biological systems.

Acknowledgements

I am greatly indebted to Professor W. Fuller for supervising this thesis, for his advice and encouragement and for the provision of excellent research facilities.

I would especially like to thank Dr. W.J. Pigram for his assistance and support throughout the course of this thesis.

I am grateful to Drs. C. Nave, D.C. Goodwin, G. Dougherty and R.J. Greenall and Messrs. A. Mahendrasingam and T. Forsyth who have worked in the Biophysics group and with whom I have had many helpful discussions.

I would like to thank Mr. J. Vergne and Dr. G.J. Brahms for their work in providing purified polynucleotide samples. I wish to express my appreciation of Professor R.A.J. Warren for the generous provision of purified  $\phi$ W-14 DNA samples and for his advice and encouragement in experimenting with this viral DNA. I am grateful to Dr. P.J. Blakeley for the use of his steffimycin B/DNA diffraction patterns and to Mr. F. Bingham who allowed me to use his B.Sc. project results relating to steffimycin B/DNA crystallization. I particularly wish to thank Miss K.M. Mandell and Sir John Randall for the BSA/montmorillonite samples and for much helpful advice and encouragement provided by Sir John Randall with regard to the work on BSA/montmorillonite interactions.

I am grateful to Mr. F. Roweth who in his capacity as laboratory superintendent efficiently dealt with many of the administrative and technical problems encountered during this research. I would like to thank all those at Keele that I have called upon for help from time to time and who have always generously obliged me. In particular I wish to express my appreciation of the work carried out in the maintenance of the x-ray diffraction equipment by Messrs. G. Dudley, T. Greasley, G. Marsh, M. Wallace, P. Clarke and J. Mitchel. I would like to thank Mr. D. Emily of the Department of Geology for his advice and assistance in using the flame emission spectrophotometer and Mr. C. Baker and Miss G.A. Harrod for their

aid in constructing the electrode potentiometer for chloride ion analysis.

I also wish to thank Mr. G. Marsh for his work in the development of the DNA brackets and construction of the DNA models and Mr. T. Greasley for his work on the alignment jig for the Franks cameras. I am indebted to Mr. M. Daniels who did his best to impart to me a small portion of his photographic expertise.

I very much appreciate the efforts of Miss G.A. Harrod who typed this thesis.

I am grateful for the award of a Departmental Studentship throughout the period of my research at Keele.

CONTENTS

	Page
Abstract	(i)
Acknowledgements	(iii)
Contents	(v)
Chapter 1. INTRODUCTION	1
1.1 The occurrence of nucleic acids	1
1.2 The general structure of nucleic acids	1
1.3 The importance of nucleic acids	2
1.4 The terminology of nucleic acid structure	3
1.5 The detailed secondary structure of nucleic acids	5
a) The A conformation	5
b) The B conformation	7
c) The C conformation	8
d) The D conformation	9
e) The E conformation	10
f) The S conformation	10
g) The conformations of ribonucleic acids	10
h) RNA/DNA hybrid structures	11
i) The side-by-side structure	12
j) The Z conformations	13
1.6 The objectives of this research	14
Chapter 2. MATERIALS AND METHODS	
2.1 Materials	17
2.2 Protein extraction from commercial DNA	18
2.3 The determination of DNA concentration in solution	19
2.4 The preparation of fibre samples	20
2.5 The birefringence of x-ray fibre samples	24
2.6 The x-ray diffraction equipment	25

2.7	Measurement of the x-ray diffraction patterns	27
2.8	Interpretation of the x-ray diffraction patterns	27
	a) The program 'Film'	28
	b) The program 'Hex'	28
	c) The program 'Find E'	29
Chapter 3.	AN INVESTIGATION INTO THE CONFORMATIONAL FLEXIBILITY OF THE SODIUM SALT OF POLY[d(A-C)].POLY[d(G-T)]	
3.1	Introduction	30
3.2	Materials and methods	33
3.3	Results	35
3.4	Discussion	46
3.5	An estimation of the error in the determination of the $a\text{Cl}^-/\text{PO}_4^-$ ratio	51
Chapter 4.	AN INVESTIGATION INTO THE CONFORMATIONAL FLEXIBILITY OF THE LITHIUM SALT OF POLY[d(A-C)].POLY[d(G-T)]	
4.1	Introduction	55
4.2	Materials and methods	57
4.3	Results	57
4.4	Discussion	74
Chapter 5.	AN INVESTIGATION INTO THE CONFORMATIONAL FLEXIBILITY OF THE SODIUM SALT OF POLY[d(A-T)].POLY[d(A-T)]	
5.1	Introduction	79
5.2	Materials and methods	85
5.3	Results	86
5.4	Discussion	103
Chapter 6.	EXPERIMENTAL TECHNIQUES TO DETERMINE THE AMOUNT OF SALT RETAINED BY NUCLEIC ACIDS	
6.1	Introduction	112
6.2	The micro-Carius method of chloride analysis	112



6.3	The quantitative increase of sodium chloride concentration in samples for x-ray analysis	113
6.4	The determination of $\text{Na}^+/\text{PO}_4^-$ ratios in DNA solutions using F.E.S.	113
	a) A re-examination of $\text{Na}^+/\text{PO}_4^-$ ratios determined by Blakeley, 1976	113
	b) A modified F.E.S. routine	118
	c) Conclusions	120
6.5	A routine for measuring the ability of $\phi$ W-14 DNA to retain $\text{Na}^+$	122
	a) Introduction: $\phi$ W-14 DNA, a viral DNA	122
	b) $\text{Na}^+/\text{PO}_4^-$ ratios of $\phi$ W-14 DNA gels using F.E.S., Goodwin, 1977	124
	c) An alternative technique for measuring $\text{Na}^+/\text{PO}_4^-$ ratios of $\phi$ W-14 DNA	125
	d) Conclusions	127
6.6	The electrode potential method of chloride analysis	128
6.7	Chloride analysis by amperometric titration	133
6.8	Conclusions	135
Chapter 7.	AN EXAMINATION OF THE FORMATION OF SMALL MOLECULE CRYSTALLITES IN DNA FIBRES	
7.1	Introduction	137
7.2	Previous observations of the crystallization of small molecules in DNA fibres	140
	a) The steffimycins	140
	b) Proflavine	143
	c) Miracil D	145
	d) Toluidine blue	146
7.3	Materials and methods	147
7.4	Results	151
	a) X-ray diffraction patterns of steffimycin B/DNA fibres produced from gels 1 to 6	151

b)	Analysis of the best crystalline steffimycin B/DNA diffraction pattern	153
c)	X-ray diffraction patterns of acridine derivative/DNA fibres	158
7.5	Discussion	161
Chapter 8.	AN X-RAY INVESTIGATION INTO THE COMPLEX FORMED BETWEEN BOVINE SERUM ALBUMIN AND MONTMORILLONITE	
8.1	Introduction	168
8.2	Materials and methods	170
a)	Montmorillonite	170
b)	Bovine serum albumin (BSA)	171
c)	Sample preparation	171
8.3	Results	178
a)	X-ray diffraction patterns of samples A - G recorded at a specimen to film distance, $D \sim 4.7\text{cm}$	178
b)	X-ray diffraction patterns of samples A - F recorded at $D \sim 10.0\text{cm}$	181
c)	X-ray diffraction patterns of samples C, D and F recorded at $D \sim 7.6\text{cm}$	186
d)	X-ray diffraction patterns of samples 1 - 10 recorded at $D \sim 7.0\text{cm}$	189
8.4	Discussion	191
a)	Interpretation of the diffraction patterns of samples A - G	191
b)	Interpretation of the diffraction patterns of samples 1 - 10	195
c)	Future experiments	197
Chapter 9.	CONCLUSIONS	199
Appendix A.	The use of a jig to facilitate the alignment of Franks optics on a Searle camera	207

Appendix B.	A bracket to construct CPK models in the B conformation of DNA	213
References		221

## Chapter 1. INTRODUCTION

### 1.1 The occurrence of nucleic acids

Nucleic acids can be divided into two main classes; deoxyribose nucleic acids (DNA's) and ribonucleic acids (RNA's). In eukaryotic cells DNA is usually found packaged with proteins to form chromatin. This nucleoprotein is the constituent of the chromosomes which are located in the nucleus of eukaryotes. In prokaryotic cells the DNA is virtually free of protein and exists in a less well defined region sometimes termed the nucleoid. DNA is also found in mitochondria, chloroplasts and perhaps other self-replicating organisms.

The ribonucleic acids are distinguished according to their function, thus giving rise to messenger RNA (mRNA), ribosomal RNA (rRNA) and transfer RNA (tRNA). These types of RNA are generally assumed to be functionally localized in the cytoplasm of cells although they are all initially transcribed from the genetic material.

### 1.2 The general structure of nucleic acids

DNA consists of two antiparallel polynucleotide chains wound around each other in the form of a double helix. Each nucleotide consists of a deoxyribose sugar group which has a phosphate group covalently bonded at its C5' position and a nitrogenous base similarly bonded at its C1' site. The base is either purine (generally adenine or guanine) or pyrimidine (usually cytosine or thymine). Nucleotides are covalently bonded to one another by phosphoester linkages at their C3' positions. The bases project into the centre of the helix and hydrogen bonding occurs between each base on one chain and an associated base on the opposite chain. Moreover, adenine always bonds with thymine and guanine with cytosine so that one strand of DNA is always the complement of the other. H-bonding and base pair stacking interactions stabilize the double helical structure of DNA. The first model which described DNA in this manner was proposed by Watson

and Crick, 1953a, and Crick and Watson, 1954.

RNA is usually a single stranded molecule although the chain can fold to enable the formation of double helical structures. The chemical make up of RNA is similar to that of DNA with the principal exception that the deoxyribose sugar residue of DNA is replaced by a ribose sugar in RNA. In addition the pyrimidine base uracil replaces that of thymine.

### 1.3 The importance of nucleic acids

The nucleic acids provide a means of carrying out some of the most essential functions in the cell or cells of a living organism. The linear sequence of bases in DNA acts as a store of inheritable information. The complementary nature of DNA allows it to self-replicate with a high degree of fidelity. This feature was first appreciated by Watson and Crick, 1953a,b. However, DNA retains the ability to mutate to some extent whilst ensuring that successful mutants are reduplicated thereby providing a mechanism for adaptation of the species. In some viruses and bacteriophages DNA is absent and its genetic role is carried out by RNA.

In higher organisms RNA is generally confined to translating the information content of DNA into proteins. In this process mRNA is synthesised on one of the DNA strands where it is endowed with the complementary nucleotide sequence of a portion of that DNA strand. The mRNA migrates to the cytoplasm where it combines with the ribosome and a modified initiation aminoacyl-tRNA molecule. A major constituent of the ribosome is also RNA in the form of rRNA. This complex formation is the initial process in protein synthesis. The initiation tRNA molecule occupies the P binding site of the ribosome leaving the R and A sites vacant. During peptide elongation a specific aminoacyl-tRNA molecule binds to the R site of the ribosome by virtue of a codon-anticodon recognition mechanism. In this process three adjacent nucleotides of mRNA form at least two complementary base pairs with three nucleotides of the anticodon

site on the tRNA molecule. The aminoacyl-tRNA molecule is transferred to the A site of the ribosome where it accepts the amino acid of the initiator tRNA molecule or the nascent peptide chain. The P site tRNA is then released and the A site tRNA takes its place. Elongation of the peptide continues in this manner until a termination sequence on the mRNA ends protein production and releases the protein. Since each of the twenty commonly occurring amino acids only bind to one or more different tRNA molecules, the three nucleotides on the DNA molecule code for a specific amino acid in the protein. In this manner the nucleic acids exert their influence on the chemical, metabolic and morphological activities of the cell which are carried out by the proteins.

#### 1.4 The terminology of nucleic acid structure

Nucleic acid structures can be described in terms of their atomic coordinates. Characteristic features of a given conformation include helix symmetry, pitch, rotation per residue and base pair tilt, twist and displacement with respect to the helix axis. Definitions of these terms as used in this thesis are those according to Arnott and Hukins, 1973. The puckering of the furanose rings are termed endo or exo according to whether a given atom is displaced from the mean plane of the sugar residue to the same side as the C5' atom or to the other side, Sundaralingam and Jensen, 1965. Thus the sugar conformation in A DNA is generally described as C3'-endo while that in B DNA is C2'-endo. Alternatively nucleic acid conformation can be described in terms of its torsion angles. Some of the more popular conventions used for these torsion angles are given in Table 1.1 of Berman, 1982, while Table 1.1 of this work shows the notation of Seeman et al., 1976, for the sugar phosphate backbone and that of Sundaralingam, 1969, applied to the sugar ring. Qualitative terms are used to describe a range of torsion angle. Trans (t) implies a torsion angle of  $180^\circ$ , gauche<sup>+</sup> ( $g^+$ ) an angle of  $+60^\circ$  and gauche<sup>-</sup> ( $g^-$ ) an angle of  $-60^\circ$ . The

Nucleotide Backbone Angles	Symbol	Sugar Conformation Angles	Symbol
C4'-C3'-O3'-P	$\alpha$	C4'-O1'-C1'-C2'	$\tau_0$
C3'-O3'-P-O5'	$\beta$	O1'-C1'-C2'-C3'	$\tau_1$
O3'-P-O5'-C5'	$\gamma$	C1'-C2'-C3'-C4'	$\tau_2$
P-O5'-C5'-C4'	$\delta$	C2'-C3'-C4'-O1'	$\tau_3$
O5'-C5'-C4'-C3'	$\epsilon$	C3'-C4'-O1'-C1'	$\tau_4$
C5'-C4'-C3'-O3'	$\zeta$		
O1'-C1'-N9-C8	$\chi$		

Table 1.1

The conformational nomenclature used to describe the nucleotide backbone according to Seeman et al., 1976, and that used to describe the sugar conformation after Sundarlingam, 1969.

conformation about the glycosyl bond is anti for  $\alpha = 0^\circ - 75^\circ$ , high anti for  $\alpha = 75^\circ - 110^\circ$  and syn for  $\alpha = 180^\circ - 270^\circ$ . Thus the torsion angles of the phosphate backbone can be described in terms of a seven letter conformational code. Arnott, 1982, has divided polynucleotide structures with similar  $\zeta$  values into families, while molecular species having the same code are all classified in the same genera. On this basis there are three families. These are the A family including the A DNA, A, A' and A'' RNA conformations, the B family including the B, B', C, C', C'' and D conformations and the A + B family including the Z and Z' conformations with alternating C3'-endo C2'-endo sugar puckering.

### 1.5 The detailed secondary structure of the nucleic acids

Nucleic acids and their synthetic analogues have been observed in a variety of different conformations. The general features of these conformations have been recorded below and details of the molecular models proposed for these structures can be found in the references given.

#### a) The A conformation

A detailed x-ray fibre diffraction study of DNA in the A conformation was carried out by Fuller et al., 1965. The model was refined by fitting the cylindrically averaged square of its calculated Fourier transform to the cylindrically averaged observed x-ray diffraction data using trial and error methods (TEFT). Their final model was an 11-fold right handed double helix with Watson and Crick base pairing having a pitch of 2.815nm. The base pairs were tilted by  $20^\circ$  to the normal of the helix axis, had a twist of  $-8^\circ$  and a displacement from the helix axis of 0.425nm. Arnott and Wonacott, 1966, developed linked atom least squares (LALS) procedures to minimize the differences between the observed and calculated structure factors of a polynucleotide conformation with constraints appropriate to the observed x-ray data. Using these techniques the A conformation was successively refined by Arnott and Wonacott, 1966, Arnott et al., 1969, and



Arnott and Hukins, 1972. However, the LALS results were essentially similar to those obtained by TEFT methods although the sugar conformation was subsequently defined as being C3'-endo. Indeed the A conformation has been subjected to the least amount of stereochemical change in subsequent refinement procedures.

A single crystal structure analysis of d(iodo-CpCpGpG) by Conner et al., 1982, revealed a fragment of right handed double helical DNA in the A conformation. Two tetramer helices were packed together in the crystal with local helix axes nearly coincident, simulating an eight base pair helix. The x-ray data so far obtained was used to define some parameters of an idealized helix based on this structure and free of distorted lattice interactions due to the presence of iodine atoms. These parameters included 10.7 base pairs in a pitch of 2.461nm. The base pairs were tilted at  $19^\circ$  to the normal of the helix axis and exhibited a propeller twist of  $19^\circ$  while the sugar pucker of the nucleosides was C3'-endo. The sense of the propeller twist in the A conformation of d(iodo-CpCpGpG) was opposite to that obtained from fibre diffraction data, Fuller et al., 1965, Arnott and Hukins, 1972.

A right handed double helical A conformation was also observed in a preliminary investigation of the single crystal structure of d(GpGpTpApTpA~pCpC) and its 5-bromouracil analogue, Shakked et al., 1981. The averaged features of the refined duplex were close to those of classical A DNA. There were 10.9 base pairs in a pitch of 2.94nm with a base pair tilt of  $18^\circ$ . The double helix was bent symmetrically about the internal 2-fold axis of the base sequence by an estimated  $15^\circ$ . This work established the A conformation for an A-T sequence in crystals grown from low salt solution.

Single crystal x-ray analysis of the octamer d(GpGpCpCpGpGpCpC) revealed a modified A conformation, Wang et al., 1982a. In this structure the two base pairs at either end of the sequence were in the A conformation while the four central base pairs were modified such that the conformations of alternate sugar residues were closer to those found in B DNA. The

octamer d(CpCpCpCpGpGpGpG) has given virtually identical diffraction patterns to the d(GpGpCpCpGpGpCpC) octamer and it seems likely that it adopts a similar modified A conformation, Wang et al., 1982a.

b) The B conformation

The B conformation of DNA was first described by the model of Watson and Crick, 1953a, and Crick and Watson, 1954. Their model was based on stereochemical principles and the constraints imposed by the x-ray fibre diffraction studies of Na DNA by Wilkins, Franklin and coworkers. Their model was a 10-fold right handed helix with a pitch of 3.4nm and base pairs arranged in a plane normal to the helix axis. Langridge et al., 1960a,b, gave a detailed analysis of the B conformation of DNA based on x-ray fibre diffraction studies of Li DNA fibres which give more crystalline B diffraction patterns than their sodium counterparts. Using TEFT methods the base pairs were brought nearer to the helix axis than in the model of Crick and Watson and changes were made in the sugar pucker and sugar phosphate chain conformation. Langridge et al.'s B model was a 10-fold helix with a pitch of 3.4nm, a base tilt of  $-2^{\circ}$  and a base twist of  $5^{\circ}$ . The base displacement from the helix axis was  $-0.06\text{nm}$  while the sugar conformation was approximately C2'-endo. This model has also been refined using LALS procedures, Arnott and Wonacott, 1966, Arnott et al., 1969, and Arnott and Hukins, 1972, 1973. In the final B model the pitch was 3.38nm, the base tilt was increased to  $-5.9^{\circ}$  and the base twist decreased to  $-2.1^{\circ}$ . The base displacement was changed to  $-0.014\text{nm}$  while the sugar conformation was altered to C3'-exo to remove undesirable stereochemical features.

Wing et al., 1980, crystallized the dodecamer sequence d(CpGpCpG~pApApTpTpCpGpCpG). This sequence incorporates an EcoRI restriction nuclease site, GAATTC, with ends related to the CGCG structure which is associated with the Z conformation, Drew et al., 1980, Crawford et al., 1980. Despite the CGC end sequences and crystallization under conditions of high salt concentration which favour the Z conformation, this sequence adopted a right

handed B helix. The structure was similar to that obtained from x-ray diffraction analysis of Li DNA with two exceptions. The base pairs were found to have a large propeller twist which increased the overlap between one base and its neighbours up and down the same chain. In addition the overall helix was bent by  $19^{\circ}$  over 11 base pairs, although it was concluded that this feature was the result of packing effects. The structure has been further refined by Drew et al., 1981. These authors describe a helix with an average of 9.8 base pairs per turn in a pitch of 3.25nm. The average propeller twist of the base pairs was  $6.7^{\circ}$  while individual deoxyribose ring conformations exhibited an approximate Gaussian distribution around the C1'-exo conformation with  $\zeta$  average =  $123^{\circ}$  and a range of  $79^{\circ}$  to  $157^{\circ}$ . A detailed examination of the influence of base sequence on this structure has been reported by Dickerson and Drew, 1981, while an investigation into the geometry of hydration for this molecule is given by Drew and Dickerson, 1981a.

The B' conformation is a minor variant of the B conformation. It exists in  $\alpha$  and  $\beta$  crystalline forms which were first observed for the synthetic polynucleotide Na poly(dA).poly(dT), Arnott and Selsing, 1974. The model proposed by these workers for this conformation was a 10-fold helix with a pitch of 3.29nm, a base tilt of  $-7.9^{\circ}$  and a base twist of  $-1.0^{\circ}$ . The sugar conformation was C3'-exo and the detailed geometry was very similar to that of B DNA.

### c) The C conformation

In the presence of the lithium cation DNA has been shown to exist in the C conformation, which is closely related to the B conformation of DNA, Marvin et al., 1961. Li C DNA gives semi-crystalline diffraction patterns with either orthorhombic or hexagonal packing arrangements according to the salt content of the specimens as discussed in chapter 4.1. Marvin et al., 1961, proposed a non-integral helix for C DNA with 8.8 - 9.7 residues in a pitch ranging from 2.92 - 3.22nm. Using TEFT techniques Marvin et al.'s

preferred model had  $28_3$  helical symmetry with a pitch of 3.1nm. The base pairs were tilted at an angle of  $-6^\circ$  to the normal of the helix axis, had a twist of  $5^\circ$  and a displacement of -0.213nm. Arnott and Selsing, 1975, have used LALS procedures to refine the C DNA model of Marvin et al. to a conformation more closely resembling that of B DNA. In particular the conformation angles  $\alpha$ ,  $\beta$  and  $\delta$  were more nearly in agreement with the B and related D structures while the base displacement was reduced to 0.07nm and a C3'-exo sugar conformation was assumed. The tilt was increased to  $-8^\circ$  to remove short contacts and the resultant calculated transform was described as not significantly different from the transform of Marvin et al.'s model. Zimmerman and Pfeiffer, 1980, used x-ray diffraction techniques to examine the DNA conformations of fibres immersed in concentrated salt solutions and organic solvent/water mixtures. They determined a wider range of helical parameters for the C conformation as described in detail in chapter 4.1.

The C' and C'' conformations are two minor variants of the C conformation with  $9_1$  and  $9_2$  helical symmetry respectively, Leslie et al., 1980. They have only been observed for synthetic polynucleotides and may well reflect the increased symmetry of these structures as described in Leslie et al., 1980, and chapter 4.4.

#### d) The D conformation

The D conformation was first observed for Na poly[d(A-T)].poly[d(A-T)] by Davies and Baldwin, 1963, who showed that this conformation exhibited a pitch of 2.45nm and described the general intensity distribution but no further information was available. In a further investigation of the D conformation based on LALS analysis of x-ray diffraction data from Na poly[d(A-T)].poly[d(A-T)], Arnott et al., 1974, proposed an 8-fold right handed double helix with Watson and Crick base pairing. The model had a pitch of 2.424nm while the sugar phosphate conformation angles were similar to those of the B DNA model of Arnott and Hukins, 1973. In particular the

sugar conformation was described as C3'-exo. The base pairs were tilted at an angle of  $-16^{\circ}$  to the normal of the helix axis and had a displacement of  $-0.18\text{nm}$ . This model was also used to explain the data obtained from Na poly[d(I-C)].poly[d(I-C)] fibres by Mitsui et al., 1970, and Na poly[d(G-C)].poly[d(G-C)] fibres by Arnott et al., 1974. More recently left handed models for the D conformation have been proposed by Gupta et al., 1980, and Mahendrasingam, 1983. These are discussed in more detail in chapter 5.

e) The E conformation

Leslie et al., 1980, have described an E conformation for the synthetic polynucleotide Na poly[d(I-I-T)].poly[d(A-C-C)] which gave diffraction patterns indicating  $3_2$  helical symmetry and a pitch of  $4.87\text{nm}$  implying a pentanucleotide asymmetric unit. This structure approximated to a mononucleotide repeating unit with a helical symmetry of  $15_2$ .

f) The S conformation

Arnott et al., 1980, have obtained x-ray diffraction patterns from fibres of Na poly[d(G-C)].poly[d(G-C)] which they interpreted in terms of a left handed double helical S conformation. Models were constructed and refined using LALS procedures assuming that the guanosine and cytidine nucleosides have syn and anti conformations respectively as observed by Wang et al., 1979, for the single crystal structure of d(CpGpCpGpCpG) in the left handed Z conformation. The S conformation has a  $6_5$  helix symmetry with a dinucleotide repeating unit and a pitch of  $4.35\text{nm}$ . The base pairs are tilted  $-5^{\circ}$  to the normal of the helix axis, the angle between the guanine and cytosine of a base pair is  $14^{\circ}$  and the base pair displacement from the helix axis is similar to that found in B DNA. Similar conformations have been observed for Na poly[d(A-C)].poly[d(G-C)] and poly[d(A-s<sup>4</sup>T)].poly[d(A-s<sup>4</sup>T)], Arnott et al., 1980.

g) The conformations of ribonucleic acids

RNA has an A conformation which is very similar to that of A DNA.

This conformation has been shown to exist in two crystalline forms designated  $\alpha$  and  $\beta$  which have similar molecular configurations but different molecular packing, Arnott et al., 1966. Using TEFT methods an A RNA model has been refined by Arnott et al., 1967, giving an 11-fold right handed double helix with a pitch of 3.00nm, a base tilt of  $14^\circ$ , a twist of  $0^\circ$  and a displacement from the helix axis of 0.425nm. Subsequent refinements have been carried out by Arnott et al., 1969, 1973.

For fibres of poly(rI).poly(rC) and poly(rA).poly(rU) containing 20% excess salt a new molecular conformation was found termed A', Arnott et al., 1968. This was a 12-fold helix with a pitch of 3.60nm. TEFT refinement procedures gave a model with a base pair tilt of  $10^\circ$ , a twist of  $-4^\circ$  and a displacement from the helix axis of 0.450nm. This model has again been refined by Arnott et al., 1973. This conformation had previously been observed by Davies, 1960, for poly(rI).poly(rC) but its significance as a conformation for RNA structures was not apparent until the observation of the A  $\rightarrow$  A' transition in synthetic polyribonucleotides by Arnott et al., 1968.

A third type of RNA conformation termed A'' has been characterized for ribosomal fragments of RNA, Fuller et al., 1967. This is a non-integral helix which has also been observed for poly(rG).poly(rC), Arnott et al., 1968, where the number of residues per turn was given as  $11.3 \pm 0.5$ .

In general the A, A' and A'' conformations of native RNA and its synthetic analogues bear a marked similarity to one another and to the A conformation of DNA. The inability of RNA to adopt a B type conformation almost certainly occurs due to the presence of the hydroxyl group on the C2' position of the ribose sugar. This results in a steric hindrance of the ribose sugar adopting a C2'-endo conformation which is believed to be a fundamental feature of the B and related conformations.

#### h) RNA/DNA hybrid structures

Ribo-deoxyribonucleotide hybrid structures tend to adopt RNA type

rather than DNA type conformations, Milman et al., 1967, O'Brien and MacEwan, 1970.

This observation is emphasized by the single crystal study of  $r(\text{GpCpG})\sim d(\text{pTpApTpApCpGpC})$  which has been carried out by Wang et al., 1982b. This molecule forms two DNA/RNA hybrid segments surrounding a central region of double helical DNA. All three parts of the molecule adopt a conformation which is close to that observed for the 11-fold A RNA helix. There were 10.9 residues in a pitch of 2.834nm. The base pair tilt was  $20^\circ$  to the normal of the helix axis. The base pairs had a propeller twist of  $14^\circ$  and the ribose and the deoxyribose sugars were all in the C3'-endo conformation.

A notable exception from A type conformations in hybrid structures was that reported by Zimmerman and Pfeiffer, 1981. Fibres of Na poly(rA). poly(dT) yielded conventional A' RNA like x-ray diffraction patterns at 79% rh while under highly solvated conditions gave patterns with striking similarities to those of B DNA.

#### i) The side-by-side structure

A novel DNA conformation which has been proposed by several workers is that of the side-by-side (SBS) structure. In all these models the two DNA strands are joined by complementary Watson and Crick base pairs and the anti-parallel polynucleotide strands alternate between short segments of right and left handed helix. This is an attractive proposal since it reduces the amount of intertwining of the DNA strands and alleviates the unwinding problem of the strands during DNA replication. The original SBS structure was proposed by Rodley et al., 1976. Of the SBS structures it is the one which most closely resembles that of the B conformation of DNA and is the only one for which detailed coordinates have been published. Rodley et al. claim that their model can account for the B type DNA diffraction patterns. Greenall et al., 1979, have compared the full molecular transform of Rodley et al.'s SBS structure with the observed x-ray data from Li B DNA of Langridge et al., 1960b. They concluded that the agreement between the

observed x-ray data and that calculated for the SBS model was substantially worse than that of the best Watson and Crick type B DNA models proposed by Langridge et al., 1960b, and Arnott and Hukins, 1972. Moreover, while the B→A transition of the Watson and Crick B DNA models is easily explained in terms of a decrease in the rotation per nucleotide, a stereochemically plausible transition of the SBS model to account for the A diffraction pattern has not yet been proposed.

j) The Z conformations

A detailed model of the Z conformation was first proposed by Wang et al., 1979, on the basis of single crystal studies of d(CpGpCpGpCpG). The x-ray data revealed a left handed 12-fold helix with a pitch of 4.458nm. In this structure the cytosines retained their customary anti orientation about the glycosyl bond while the guanines adopted the more unusual syn conformation, thus giving rise to a dinucleotide repeating unit. The sugar pucker was also shown to be of an alternating nature, adopting a C2'-endo conformation in the deoxycytidines like that of B DNA, but a C3'-endo conformation in the deoxyguanosines as found in A DNA. The tilt of the base pairs from the normal to the helix axis was given as 7°.

A conformational change in crystals of d(CpGpCpG) on going from low to high salt was observed by Drew et al., 1978. Crawford et al., 1980, have shown that the low salt conformation in this tetramer is very similar to the Z conformation described by Wang et al., 1979. The high salt conformation has been termed Z' by Drew et al., 1980. They have shown that this is also a 12-fold left handed helix with a pitch of 4.566nm and a similar alternating anti/syn glycosyl conformation. The base pair tilt was increased slightly to 9° compared with Z DNA. However, while the deoxycytidine sugar pucker is C2'-endo that of the deoxyguanosine is C1'-exo rather than C3'-endo as in the Z conformation. The transition from the Z to the Z' conformation occurred on going from intermediate to high salt and arose from the substitution of a bound anion for water at the guanine



amino groups, Drew et al., 1980.

Further studies on the low salt conformation of d(CpGpCpG), Crawford et al., 1980, and other crystals of the hexamer, d(CpGpCpGpCpG), Wang et al., 1981, have revealed an additional conformational feature of Z DNA. Generally the phosphate groups are rotated into the minor groove giving a phosphodiester linkage which is  $g^-t$ . However, at some of the GpC sites in the tetramer and hexamer crystals the phosphate groups are rotated away from the minor groove giving a phosphodiester linkage which is  $g^+t$ . These conformations have been termed  $Z_1$  and  $Z_{11}$  respectively. The  $Z_{11}$  conformation is believed to occur as a result of coordination of the phosphate group to  $Mg^{2+}$  or to water.

In an examination of the conformation and dynamics in the Z conformations Drew and Dickerson, 1981b, suggest that the  $Z_1$ ,  $Z_{11}$  and  $Z'$  conformations do not represent distinct conformations but should be regarded as samplings of the full range of conformations available to the Z helix.

#### 1.6 The objectives of this research

X-ray fibre diffraction analysis of synthetic polynucleotides with simple repeating sequences provides structural information which is not necessarily apparent from naturally occurring random sequence DNA. The ultimate objectives of such an analysis are the prediction of structural features of specific nucleic acid sequences in a range of conditions relating to the in vivo state, an understanding of the relationships between the structures and an appreciation of their biological significance without the need to examine every biologically relevant sequence.

A primary concern of this thesis has been to determine the conformations exhibited by fibres of two synthetic polynucleotides, poly[d(A-C)].poly[d(G-T)] and poly[d(A-T)].poly[d(A-T)]. Also of importance are the conditions which induce transitions between these conformations and the sequence in which these conformational transitions occur.

Synthetic polynucleotides have not normally been available in sufficient quantities to allow the techniques described by Cooper and Hamilton, 1966, for DNA, to be used to systematically investigate the effects of fibre salt content on polynucleotide conformation. To overcome this problem samples were prepared containing as little excess salt as possible and x-ray fibre diffraction techniques were used to determine polynucleotide conformation as a function of added fibre salt content. Investigations of polynucleotide conformation as a function of the type of associated cation and relative humidity of the fibre environment have also been performed.

Poly[d(A-C)].poly[d(G-T)] is of particular interest because it contains equimolar fractions of the four nucleotides commonly found in naturally occurring DNA's and thus its study might be expected to allow effects due to nucleotide sequence to be distinguished from those which occur as the result of nucleotide composition. Poly[d(A-T)].poly[d(A-T)] has a biologically interesting sequence in view of its similarity to that found in satellite DNA of crabs and as a result of its enhanced binding to the lac repressor of *E. coli* compared with random sequence DNA.

An examination of the literature readily demonstrates the critical role of salt in the determination of nucleic acid conformation, Marvin et al., 1961, Cooper and Hamilton, 1966. In view of this fact chapter 6 examines a number of experimental techniques which may quantitatively determine the amount of salt associated with nucleic acids in solution and in x-ray fibre samples. These techniques make use of flame emission and U.V. absorption spectroscopy and electropotential and amperometric titration methods. A routine is also described which measures the ability of different DNA's to retain specific cations in solution. This is a particularly important parameter with respect to modified viral DNA's where such information may be related to their structural variations and biological functions.

In chapter 7 an investigation has been carried out into the formation

of crystallites of small molecules in fibres of DNA. In particular the crystallization of steffimycin B and some acridine derivatives which exhibit potential anticarcinogenic properties have been examined. The crystallization phenomenon is important since it may provide information with regard to DNA structure and the mechanism of interaction of these types of antibiotics with DNA. In addition it may be possible to make use of this crystallization process in drug treatment regimes.

A further type of biological macromolecular interaction has been investigated, again using x-ray diffraction techniques, as described in chapter 8. This is the complex formation between the protein bovine serum albumin (BSA) and the clay montmorillonite. The investigation was carried out at the request of Sir John Randall of the University of Edinburgh in an attempt to determine whether BSA was adsorbed in the interlamellar regions of the montmorillonite and if so what was the orientation of the BSA molecules in the protein/clay complex. In the course of this investigation it was necessary to distinguish between the effects of interlamellar swelling due to water adsorption and the presence of sodium chloride as opposed to that produced by the albumin alone. In this respect certain general parallels are apparent when compared with DNA fibre samples which are also critically affected by water and sodium chloride content. The biological justification for these BSA/montmorillonite experiments lies in the useful resemblance of this system to protein/membrane systems.

## Chapter 2. MATERIALS AND METHODS

### 2.1 Materials

Calf thymus DNA used in this work was obtained from either the Sigma Chemical Company or Miles Research Laboratories. Usually these commercial DNA's were subjected to a phenol purification process to extract protein contaminants as described in section 2.2.

The sodium and lithium salts of poly[d(A-C)].poly[d(G-T)] and the sodium salt of poly[d(A-T)].poly[d(A-T)] were prepared by Mr. J. Vergne and Dr. G.J. Brahms at the Institute of Research in Molecular Biology, University of Paris VII, France. These polynucleotides were enzymatically synthesised using DNA polymerase 1 from either *Escherichia coli* or *Micrococcus luteus*. The polynucleotides were deproteinized by a chloroform isoamyl procedure, dialysed against the appropriate salt and precipitated twice by ethanol from 0.1M salt solution. The purity of the samples was examined by U.V. absorption, high sensitivity differential thermal analysis, laser Raman spectroscopy and circular dichroism.

DNA from the bacteriophage  $\phi$ W-14 was isolated and purified by Professor R.A.J. Warren at the Department of Microbiology, University of British Columbia, Vancouver, Canada. The method is reported in Kropinski, Bose and Warren, 1973.

Steffimycin B was a gift to Dr. W.J. Pigram from Dr. F. Reusser of the Upjohn Company, Kalamazoo, Michigan, U.S.A. The antibiotic had been isolated from *Streptomyces algreteus* and purified as described by Brodasky and Reusser, 1974. The samples supplied were used without further purification.

Albumin/montmorillonite samples were prepared by Miss K.M. Mundell and Professor Sir John Randall of the Department of Zoology, University of Edinburgh, Scotland. The detailed preparation of these samples is given in chapter 8.2.

Analar grade laboratory reagents were in general use throughout the course of this work.

## 2.2 Protein extraction from commercial DNA

The following procedure was carried out in the cold room at 4°C to reduce the possibility of DNA denaturation.

A 30-50mg DNA sample was placed in 3mM sodium chloride solution at a DNA concentration  $\sim 1.0 \text{mg ml}^{-1}$  for a period of 48 hours to dissolve. The resultant solution was centrifuged in conical tubes at 3000rpm for 15 minutes using an MSE bench centrifuge to remove dust particles and other macroscopic contaminants. The solution was then carefully decanted and added to an equal volume of freshly distilled phenol saturated with 0.1M sodium chloride solution. The use of freshly distilled phenol is important since phenol oxidation results in peroxide formation which may cause strand breakage of the DNA. In phenol solutions stored for a relatively long period of time, peroxide formation is apparent from the brown tint of the solution.

The DNA/phenol solutions were gently agitated for  $\sim 20$  minutes and then centrifuged as before. Protein was usually apparent as a white precipitate at the interface of the aqueous and phenolic phases of the solutions. The aqueous phases of the solutions were carefully removed from the centrifuge tubes using hooked Pasteur pipettes and added to an equal volume of propan-2-ol. The DNA immediately precipitated and was wound onto a glass rod. It was then washed in 80% ethanol to remove excess salt, in 95% ethanol to remove water and briefly in acetone to remove ethanol.

The DNA was stored in this form for fibre preparation requiring solid material or immediately dissolved in 3mM sodium chloride solution for fibre preparation from gels obtained by high speed centrifugation.

The pH of the DNA solutions was controlled as desired, by the use of 1-10mM Tris.HCl at pH 7.5 present in all solutions.

### 2.3 The determination of DNA concentration in solution

The optical densities of DNA solutions at 258nm were measured in 1.0cm path length quartz cuvettes using a Cary 118C double beam U.V. visible absorption spectrophotometer. A value of  $6600M^{-1}cm^{-1}$  was used for the extinction coefficient of aqueous DNA solutions at 258nm, as suggested by Blakeley, 1976. DNA concentrations were then calculated according to the Beer-Lambert law as shown in Equation 2.1.

$$O.D._{\lambda_{max}} = E_{\lambda_{max}}cl \quad - \text{Equation 2.1}$$

In this equation O.D. is the optical density of the solution at a specific wavelength,  $E_{\lambda}$  is the extinction coefficient at that wavelength,  $l$  is the optical path length of the solution and  $c$  is the concentration.

The absorption of DNA solutions was plotted on a chart recorder from 290-200nm. This allowed  $E_{\lambda 260}/E_{\lambda 280}$  and  $E_{\lambda 260}/E_{\lambda 230}$  ratios to be conveniently determined. Generally  $E_{\lambda 260}/E_{\lambda 280} \geq 1.9$  and  $E_{\lambda 260}/E_{\lambda 230} \geq 2.0$  imply a reasonable degree of DNA purity relative to protein contamination. All proteins absorb strongly at 230nm while proteins containing a high proportion of aromatic residues also absorb strongly at 280nm.

To obtain U.V. spectra, aliquots of DNA solution were first diluted to 4.0ml with 10mM salt or salt/buffer solution to give a DNA concentration of approximately  $25\mu gml^{-1}$ . An aliquot was placed in one of a matched pair of 1.0cm path length quartz cuvettes while the other cuvette was filled with reference buffer. These two cuvettes were inserted in the spectrophotometer sample holder and a third cuvette containing reference buffer was placed in the reference holder. The two reference buffers were zeroed at 258nm and the background absorption was recorded from 290-200nm. The position of the sample holder was then adjusted to place the cuvette containing DNA solution in the sample beam and the DNA absorption was recorded from 290-200nm above the background absorption. The operation of the spectrophotometer by this method allowed absorption due to DNA alone

to be recorded without switching off the sensitive electronics of the spectrophotometer when the cuvette compartment was opened.

This system was also used to record U.V. and visible spectra of drug and drug/DNA solutions. Further details of these experiments are given in chapter 7.

#### 2.4 The preparation of fibre samples

The fibre samples were produced using fibre stretching cells similar to those described by Fuller et al., 1967. To prepare these cells a glass rod  $\sim 15\text{cm}$  in length and  $\sim 0.4\text{cm}$  diameter was heated in a bunsen flame to red heat, removed from the flame and immediately stretched to a thin rod  $\sim 150\text{cm}$  or more in length. This rod was cut into short sections of about  $5\text{cm}$  in length and  $\sim 50\mu$  diameter which were stored in a petri dish to minimize dust contamination. When required one of these smaller glass rods was cut in half and the ends furthest from the break were inserted into small pieces of plasticine. The protruding ends of the glass rods were rounded in a bunsen flame. The glass rods were made in this manner since it was found easier to round the ends of the rods to a similar shape and size if they were of similar diameter beforehand. This is important since dissimilar rod ends tended to result in tapered or irregularly formed fibres. The diameter of these glass rods is also important and should be similar to that of the intended DNA fibre. If the diameter of the glass rods are too small they do not readily support a gel and are easy to break when mounting in the x-ray cameras. If the rods are too large a significant part of the gel may dry in an unoriented mass around the ends of the rods. After rounding, the rods were carefully aligned on a fibre stretching cell as shown in Plate 2.1.

DNA fibres were prepared directly by the addition of  $\sim 70\text{-}200\mu\text{g}$  of solid DNA to droplets of deionized water  $\sim 10\mu\text{l}$  volume suspended between the slightly separated glass rods of prepared fibre stretching cells.

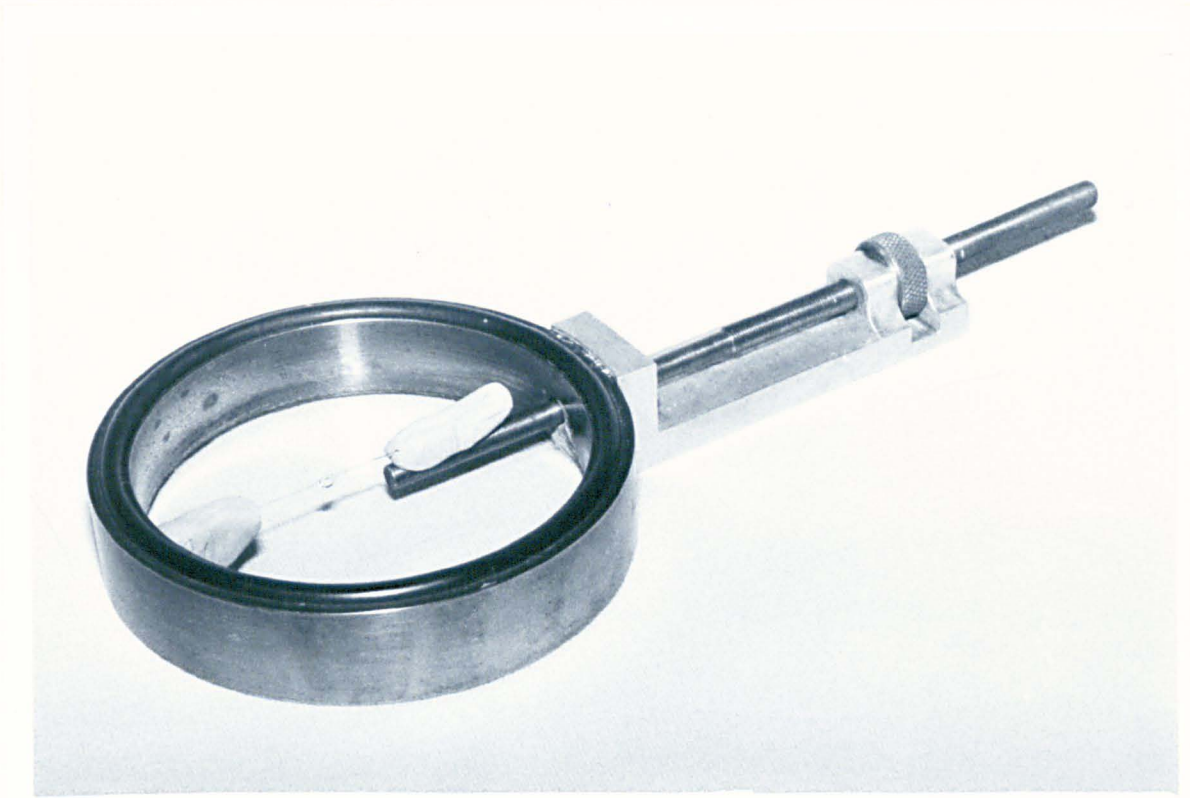


Plate 2.1 A stretching cell for the preparation of DNA fibres after Fuller et al., 1967. A DNA gel is shown supported by glass rods aligned on the cell with the aid of plasticine.

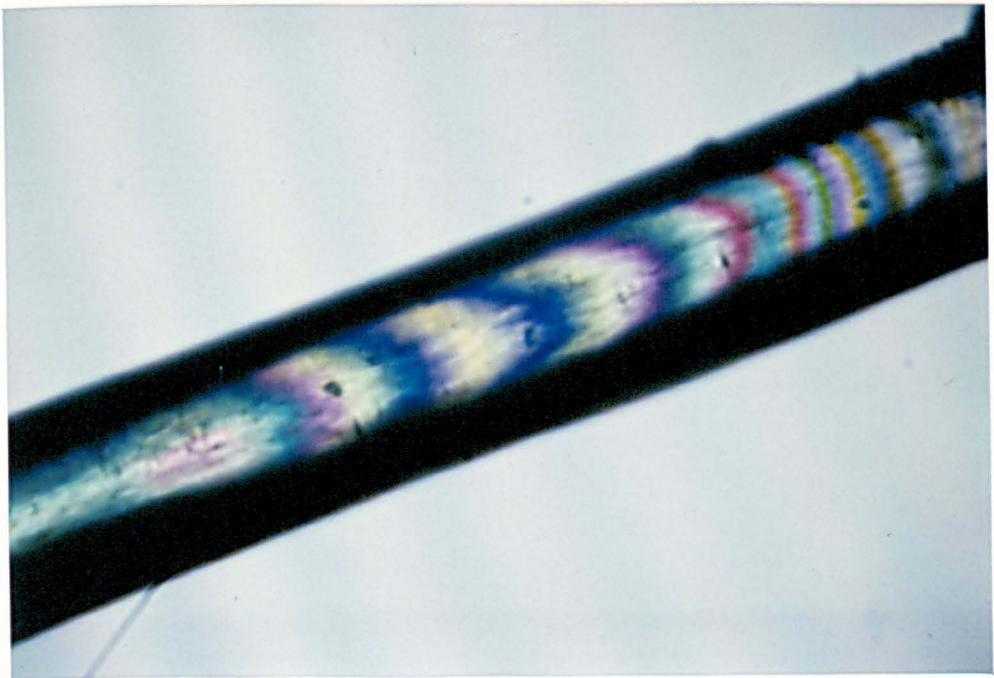


Plate 2.2 A photomicrograph of a Na poly[d(A-T)].poly[d(A-T)] fibre between crossed polaroids with a calcite compensator in the optical pathway.



The droplets were agitated to dissolve the DNA resulting in the formation of gels. Observation of these gels was conveniently achieved with the aid of a  $\times 80$  bifocal dissecting microscope. The fibre cells were manipulated to apply a degree of tension to the gels as they dried. The amount of tension required depended on the concentration and type of DNA or DNA/complex and on the environmental conditions pertaining at the time of fibre formation. Small pots containing saturated potassium chlorate solutions were sealed in the fibre cells of some specimens to produce fibre environments of 98% rh in the belief that slow fibre formation would result in improved crystallinity. Other fibre specimens were allowed to dry in the cold room at  $\sim 4^{\circ}\text{C}$  for a similar reason. However most specimens were prepared under ambient conditions. The amount of salt present in specimens prepared in this manner was dependent on the extent to which the DNA was washed after precipitation.

In some cases it is inconvenient to produce fibres in the manner described above and DNA gels suitable for fibre preparation have been obtained by high speed centrifugation of DNA solutions. This method of preparation has several advantages. In the first instance a gel can be formed from a salt solution of known concentration. This does not imply that the salt concentration in the resultant gel is the same as that of the solution prior to centrifugation since a disproportionate amount of salt may be spun down with the DNA. However, Blakeley, 1976, has shown that if the amount of DNA in the centrifuge tube is kept constant, a variation of salt concentration in the initial solutions results in a similar change in magnitude of the salt content of the resultant gels and hence the fibres. Centrifugation also allows DNA to remain in solution until fibre formation and this is particularly important in the case of  $\phi\text{W-14}$  DNA since once precipitated this viral DNA is extremely difficult to redissolve. Finally centrifugation allows DNA solutions and drug solutions to be mixed in relatively large volumes at easily measured ratios

facilitating the homogeneous distribution of DNA/drug complexes within the fibre samples.

DNA solutions for centrifugation were prepared by the addition of 1.0-2.0ml of 3.0mM DNA, 3.0mM NaCl solutions to appropriate volumes and concentrations of salt and buffer solution to give final volumes of 10.0ml. The final salt concentration of such solutions was generally chosen to be 10.0mM NaCl since Blakeley, 1976, has shown that fibres produced from gels centrifuged from such solutions give A and B diffraction patterns on changing the relative humidity of the fibre environment from 75% to 92%. In preparing DNA/drug solutions for centrifugation, 1.0-2.0ml of 3.0mM DNA, 3.0mM NaCl was diluted to 5.0ml by the addition of the desired salt and buffer solutions while aliquots of drug solutions were made up to similar volumes with the addition of appropriate salt and buffer solutions. The drug solutions were added to the DNA solutions to give solutions of constant DNA content and definitive phosphate to drug, P/D, ratios. Again the final salt content of such solutions was chosen to be 10.0mM NaCl.

The DNA and DNA/drug solutions were transferred to 10.0ml polypropylene centrifuge tubes and spun down at 45,000 r.p.m. for 12 hours at 4°C in an M.S.E. superspeed 50 TC centrifuge with a 10 x 10 ml fixed angle rotor. The top 5.0ml of each supernatant was carefully removed with a Pasteur pipette for subsequent spectroscopic analysis and the remainders of the solutions were decanted. The gel like pellets were sealed in the centrifuge tubes using parafilm and stored at 4°C until required. However it was found better to use the gels as soon as possible since they are quite viscous and even a small amount of drying made the material difficult to handle.

With the aid of an extruded Pasteur pipette drops of a given gel were placed between the rounded ends of glass rods aligned on a fibre stretching cell and fibre samples were then produced as described previously.

The detailed preparation of synthetic polynucleotide fibres of known

added salt concentration is described in chapter 3.2.

## 2.5 The birefringence of x-ray fibre samples

The birefringence of fibre samples was measured before subjecting them to x-ray analysis. A fibre sample was first aligned between the analyser and polarizer of an Olympus BH AP2 polarizing microscope so that the extinction condition was preserved. The specimen table of the microscope was then rotated by  $45^\circ$  and a Carl Zeiss calcite rotary compensator was inserted into the optical path of the microscope between the analyser and the objective. The cross-hairs of the microscope eyepiece were aligned on a point on the fibre corresponding to the black zero zone of the background fringe pattern. The compensator was then rotated until the black zero fringe in the fibre appeared in the cross-hairs of the microscope eyepiece. The vernier of the compensator gave the angle of tilt through which the calcite plate of the compensator had passed and this angle was related to the optical retardation,  $\theta$ , in the fibre sample by tables supplied by the manufacturer. The sample thickness,  $t$ , was conveniently measured using the same microscope in conjunction with a graduated eyepiece and the birefringence of a fibre,  $\Delta n$ , was calculated according to the relationship shown in equation 2.2.

$$\Delta n = \frac{\lambda \theta}{2\pi t} \quad \text{- Equation 2.2}$$

The appearance of interference fringes observed in a fibre sample during birefringence measurements is illustrated in Plate 2.2. The fibre was of Na poly[d(A-T)].poly[d(A-T)] and the fringes are particularly well resolved. Typically the birefringence of DNA or polynucleotide fibres examined in this work was in the range of -0.02 to -0.12. A birefringence of high magnitude tends to indicate a high degree of orientation in fibre samples. However, while fibres producing well resolved diffraction patterns nearly always had a relatively high magnitude of birefringence  $\sim -0.07$  the

converse was not necessarily true since birefringence measurements do not provide information with regard to the crystallinity within the fibre sample.

In practise x-ray diffraction patterns of control DNA fibres were only recorded for those fibres of birefringence  $\geq |-0.06|$ . However, for the synthetic polynucleotide samples, x-ray diffraction patterns were obtained from all samples since the quantity of material available was strictly limited. As a matter of routine birefringence measurements of these samples were recorded beforehand. In the case of DNA/drug samples it was found that the magnitude of the birefringence of these samples was too great to be measured using the system described above.

## 2.6 The x-ray diffraction equipment

Fibres suitable for x-ray analysis were first sprayed with powdered calcium carbonate which produces diffraction rings at known d-spacings on the fibre diffraction patterns. Two forms of calcium carbonate were used. Aragonite gives a principal reflection corresponding to a d-spacing of 0.3396nm while calcite exhibits a principal d-spacing of 0.3035nm. The use of calcite was generally preferred since the aragonite spacing coincides with the 0010 reflection of B DNA.

Nickel filtered  $\text{CuK}\alpha$  x-ray sources were provided by Hilger and Watts microfocuss x-ray generators or a GEC-Elliott GX6 rotating anode x-ray generator. The Hilger and Watts machines were normally operated at 35kV and 2.5mA in conjunction with a 0.1 x 0.1mm spot when viewed at  $\sim 6^\circ$  to the target surface. The GX6 was operated at 35kV and 60mA with a 0.2 x 0.1mm spot size when viewed at  $\sim 6^\circ$  to the target surface.

Pinhole cameras similar to that described by Langridge et al., 1960a, with 100um diameter gold collimators and a maximum specimen to film distance of 3.0cm were used in conjunction with the Hilger and Watts generators. Sample alignment in these cameras was carried out on an optical bench with visible light. Camera alignment was achieved by maximizing the intensity

of the undiffracted beam at the exit of the camera with a mini monitor radiation counter. Searle cameras incorporating toroidal or Franks optics were used on the rotating anode generator. In these cameras alignment was achieved by observing the image of the x-ray beam incident on a thallium activated caesium iodide screen.

X-ray scattering by the sample environment was minimized by continually flushing the cameras with helium gas during x-ray exposure of the samples. Owing to the relatively large volume of the Searle cameras these cameras were flushed with helium for 30 minutes before commencing irradiation of the samples to ensure removal of most of the air. This procedure was not necessary for the pinhole cameras. The relative humidity of the fibre environment was maintained by the helium gas which was bubbled first through a gas bottle containing water to give saturated helium and then through a gas bottle containing an appropriate saturated salt solution. The helium then passed through an empty gas bottle which acted as an excess vapour trap before entering the cameras. All the gas bottles contained sintered glass filters. As a further precaution a pot of the required saturated salt was placed in the cameras before irradiating the samples. The salts used were potassium chlorate, sodium sulphate, sodium tartrate, potassium chloride, sodium chlorate, sodium nitrite, sodium bromide, potassium carbonate and calcium chloride which gave relative humidities of 98%, 95%, 92%, 86%, 75%, 66%, 57%, 44% and 33% respectively according to O'Brien, 1948. To obtain a relative humidity environment ~0% helium gas straight from the cylinder was passed through a bottle containing crystals of silica gel and thence to the camera.

Initially x-ray film used in this work was either Ilford Industrial G or Kodirex. After the withdrawal of these films Kodak No Screen film was used as a replacement. The films were developed and fixed by chemicals supplied by Ilford or Kodak as appropriate.

## 2.7 Measurement of the x-ray diffraction patterns

The positions of reflections on diffraction patterns were measured with a Pye two dimensional travelling microscope which had a sensitivity of  $\pm 0.001\text{mm}$ . An estimate of the accuracy in determining the coordinates of reflections using this device was  $\pm 0.04\text{mm}$ . This corresponds to  $\pm 1/4$  of the width of sharp reflections on well resolved diffraction patterns. The excessive loss of light from the optical system of this microscope rendered it tedious to use and when a Stoe film measuring device became available it was used for less accurate measurements. The sensitivity and probable accuracy of this instrument was  $\pm 0.1\text{mm}$ .

For particular accurate measurements 15" x 12" photographic plates were reproduced from the x-ray negatives and the radii of reflections were determined with a beam compass and steel rule as described in chapter 7.4b.

Measurements of the albumin/montmorillonite and associated diffraction patterns were carried out as described in chapter 8.2.

The intensities of reflections were measured using a Joyce Lobel microdensitometer 3CS. The densitometer was also used to determine the radii of reflections on some occasions.

In cases where relative intensities were estimated by eye a scale of vs, s, m, w and vw was used corresponding to very strong, strong, medium, weak and very weak intensities.

## 2.8 Interpretation of the x-ray diffraction patterns

In determining the type of diffraction patterns obtained during this work and the lattice parameters associated with these patterns, three computer programs have been utilized. These programs were written by Dr. W.J. Pigram in Algol for an Elliott 4130 computer at Keele University and were transcribed by the author to run on the CDC 7600 computer of the Manchester Regional Computer Centre.

a) The program 'Film'

The Film program uses x and y coordinates from points on a calibration ring of known d-spacing to determine the specimen to film distance and the coordinates of the centre of the film. With this data and the x and y coordinates of interesting reflections the corresponding  $\xi$ ,  $\zeta$ ,  $\rho$  and d-spacing of these reflections are calculated. Surprisingly, the analysis of particularly well resolved diffraction patterns gave different coordinates for the centre of the film when determined by a least squares analysis of points on the calibration ring compared with coordinates calculated by averaging the x and y coordinates of appropriate pairs or quartets of sample reflections. This difference was  $\sim 0.2\text{mm}$  and was attributed to the non-homogeneous distribution of calcium carbonate on the fibre samples. When such discrepancies were apparent the specimen to film distance obtained from the calibration ring was used in conjunction with the average value for the coordinates of the film centre to obtain the required data.

b) The program 'Hex'

The Hex program uses  $\rho$ -spacings of given reflections together with their assigned Miller indices to calculate the lattice parameters of an hexagonal unit cell. These parameters are then subjected to a cyclic least squares refinement procedure of  $\sum(\rho_o - \rho_c)^2$  until the difference between  $\rho_o - \rho_c$  in successive cycles is less than a specified value.  $\rho_o$  and  $\rho_c$  are the observed and calculated reciprocal lattice spacings respectively.

For diffraction patterns from which xi-zeta plots had been constructed an estimate of the error in the calculated lattice parameters was obtained from the RMS deviation in  $\rho_o - \rho_c$ . The mean of the unambiguously identified  $\rho_o$  values was calculated and the RMS deviation in  $\rho_o - \rho_c$  was determined as a percentage of this value. This percentage error was applied to the lattice parameters.

c) The program 'Find E'

This program uses the refined lattice parameters to calculate the radii of all possible reflections to a maximum specified value at a specific specimen to film distance.

More specific details of experimental techniques used in this work are given in subsequent chapters.



Chapter 3. AN INVESTIGATION INTO THE CONFORMATIONAL FLEXIBILITY OF THE SODIUM SALT OF POLY[d(A-C)].POLY[d(G-T)]

3.1 Introduction

Poly[d(A-C)].poly[d(G-T)] is one of the two synthetic polynucleotides with a repeating dinucleotide sequence which contains all four of the nucleotides commonly found in naturally occurring DNA's.

In the first report of an x-ray fibre diffraction study of poly[d(A-C)].poly[d(G-T)] by Langridge, 1969, it was stated that good x-ray diffraction patterns were obtained which were identical to those given by native DNA. However, apart from a brief discussion of the intensity of the 11<sup>th</sup> layer line in the A pattern no details were given of the patterns obtained, nor of the conditions required for observing them.

Arnott et al., 1980, reported that Na poly[d(A-C)].poly[d(G-T)] was one of the polynucleotides capable of adopting the S conformation. This conformation was achieved in some fibres after annealing them for prolonged periods. These fibres contained 3-6% retained sodium chloride necessary to reproduce the B conformation in typical DNA specimens.

Leslie et al., 1980, obtained an A pattern from a fibre of Na poly[d(A-C)].poly[d(G-T)] at 66% rh which was indistinguishable from those obtained for other DNA's or polynucleotides. From 66-92% rh they observed a fully crystalline B pattern for the sodium salt of this polynucleotide and point out that this is the first time that a fully crystalline B pattern has been observed for the sodium salt of a DNA or a polynucleotide. These patterns were defined in terms of an orthorhombic lattice with a 10<sub>1</sub> helical symmetry and a pitch of 3.46nm. The patterns suggested a larger unit cell than for the B form of calf thymus DNA.

The experiments carried out during this work on Na poly[d(A-C)].poly[d(G-T)] have established the conditions for the routine observation of the A,B and C conformations in fibres of the sodium salt of this

polynucleotide. While the A and B conformations are readily observed in fibres of naturally occurring Na DNA's, the C conformation is generally associated with Li DNA, Marvin et al., 1961.

Evidence for the C conformation in Na DNA was first apparent when Brahms et al., 1973, interpreted infra-red spectra from Na DNA in terms of a C structure. Bram and Baudy, 1974, found that fibres of the sodium salt of calf thymus DNA dried at 37°C in the relative humidity range of 30-66% on a fixed glass support usually gave C patterns. They reported a layer spacing of 3.1nm. The authors stated that the C conformation was metastable at 66% rh and usually decayed to the A conformation within a day. Furthermore, they found that an immediate transition from the C to the A conformation occurred if the fibre was released from its support at one end.

Arnott and Selsing, 1975, have reported C diffraction patterns from fibres of Na DNA under conditions of low hydration and salt contents intermediate between those appropriate for the A and B conformations of Na DNA.

Zimmerman and Pfeiffer, 1980, have used x-ray diffraction techniques to assay for the C conformation in fibres of Li and Na DNA immersed in various organic solvents and concentrated salt solutions. DNA gels were centrifuged from solutions and used to make fibres as described by Zimmerman and Pfeiffer, 1979. These fibres gave C diffraction patterns at 33% rh, A patterns at 79% rh and B patterns at 98% rh. Of the solutions investigated only t-butanol at 95% or 98% v/v induced the C conformation in Na DNA fibres.

Leslie et al., 1980, have observed the C conformation or the related C' or C'' conformations for a number of synthetic polynucleotides when sodium is the cation. They concluded that the C conformation is stable in a fairly narrow range of fibre salt contents and relative humidities which are both intermediate between those that favour the A and B conformations.

The observation of the C conformation in Na poly[d(A-C)].poly[d(G-T)] fibres initiated a series of experiments carried out by Mahendrasingam, 1983, in order to determine whether the C conformation was apparent in Na DNA fibres under similar environmental conditions. Mahendrasingam examined a wide variety of naturally occurring DNA's including calf thymus, Clostridium perfringens, herring sperm, pollock roe, salmon sperm, Escherichia coli, SP 15, T2 phage, Micrococcus lysodeikticus and  $\phi$ W-14 DNA. The fibres were prepared from gels centrifuged from DNA solutions of 10mM sodium chloride concentration. For fibres containing the lowest amounts of excess salt the C form was observed at relative humidities in the range of 32-75% for all those DNA's. The conformational sequence of transitions for those DNA's was  $C \rightleftharpoons A \rightleftharpoons B$  which was fully reversible, with the exception of fibres of T<sub>2</sub> and SP 15 DNA. Fibres of these DNA's did not exhibit the A conformation, presumably as a result of steric hindrances imposed by the presence of large sugar residues.

These experiments on the sodium salt of poly[d(A-C)].poly[d(G-T)] describe a method for quantitatively varying the amount of added salt in synthetic polynucleotide fibres. The added salt content of such fibres is expressed in terms of the number of added chloride ions per nucleotide phosphate and is denoted by the  $aCl^-/PO_4^-$  ratio. The conditions for routinely observing the A, B and C conformations in fibres of Na poly[d(A-C)].poly[d(G-T)] and the sequence of transitions between these conformations is established. These results are compared with those reported by other workers. Particular attention is drawn to the question of whether the C conformation is intermediate between the A and B conformations as suggested by Arnott and Selsing, 1975, and Leslie et al., 1980, or whether A is the intermediate conformation as reported by Bram and Baudy, 1974, and Zimmerman and Pfeiffer, 1980.

An estimate has been made of the accuracy to which the  $aCl^-/PO_4^-$  ratio

in a fibre can be determined. At the present time there is evidence of a non-homogeneous distribution of salt in fibre samples produced by these methods. An improvement in experimental technique is necessary before the  $a\text{Cl}^-/\text{PO}_4^-$  ratio reflects the  $\text{Cl}^-/\text{PO}_4^-$  ratio in localized regions of the fibre samples.

Attention is drawn to the potential biological significance of the C conformation.

### 3.2 Materials and methods

The sodium salt of the synthetic polynucleotide poly[d(A-C)]. poly[d(G-T)] was prepared at Paris University VII by Dr. G.J. Brahms and Mr. J. Vergne as described in chapter 2.1.

The final precipitation from each batch of synthesized polynucleotide was transferred to a glass microscope slide and allowed to dry under ambient conditions. At this stage the precipitate weighed  $\sim 2.0\text{mg}$ . Small pieces of polynucleotide  $\sim 0.2\text{mg}$  were cut from the original samples and accurately weighed using a Perkin and Elmer electronic microbalance which gave a readout to  $\pm 0.1\mu\text{g}$ .

One of these pieces was allowed to dissolve in 4.0ml of 0.01M sodium chloride solution for a minimum period of 18 hours. The optical density of the solution at  $\lambda_{258\text{nm}}$  was then determined and the polynucleotide concentration of the solution was calculated assuming an extinction coefficient  $E_{\lambda_{258}} = 6600\text{M}^{-1}\text{cm}^{-1}$ , Blakeley, 1976. The expected polynucleotide concentration of the solution was determined from the known mass of the sample using a value of 332.75 for the molecular weight of a Na nucleotide. The percentage difference of the two polynucleotide concentrations was attributed to the presence of water. This value was then used to correct the mass of subsequent pieces of polynucleotide from the same production batch when calculating the  $a\text{Cl}^-/\text{PO}_4^-$  ratio in fibres. Typically the samples were found to contain  $\sim 70\%$  by weight of polynucleotide.

Other pieces of polynucleotide from the same batch were used to make fibres for x-ray analysis. A drop of deionized water was placed on the rounded end of a thin glass rod and then shaken off. Sufficient water remained on the end of the rod so that on touching a piece of weighed polynucleotide with the rod, some of the polynucleotide dissolved and the sample became firmly attached to the rod. Taking care not to dislodge the sample the rod could be aligned on a fibre stretching cell with a second rod of similar size. Further deionized water was added to the sample to produce a gel from which a fibre could be drawn as described in chapter 2.4. A series of gels were formed in this manner and before drawing them out to form fibres, different amounts of standard sodium chloride solutions were added with the aid of a micropipette. It has since been found that Erfurth et al., 1975, used a similar method to prepare DNA fibres for x-ray diffraction and Raman spectroscopy. The concentration and quantity of the sodium chloride solutions were chosen such that the  $a\text{Cl}^-/\text{PO}_4^-$  ratio ranged from 0.0 to approximately 2.0. The error associated with the  $a\text{Cl}^-/\text{PO}_4^-$  ratio is 12 % and an account of this estimation appears in section 3.5.

Since the preparation of  $\text{Na poly}[d(\text{A-C})].\text{poly}[d(\text{G-T})]$  was precipitated from solutions of the same ionic strength and washed in ethanol in the same manner, no significant variation was expected in the ionic content of the samples initially. It should be stressed that the  $\text{Cl}^-/\text{PO}_4^-$  ratio used in this work represents the amount of salt added to a sample and does not take into account salt retained by the polynucleotide material upon precipitation from 0.1M sodium chloride solution. Washing the material in ethanol reduces the excess salt retained by the sample so that the added salt concentration tends to reflect the total salt concentration, but clearly, a method for determining the total ionic content of these samples would be superior.

Cooper and Hamilton, 1966, estimated the total salt content of DNA samples by chloride analysis using a micro-Carius method. However, each assay

required  $\sim 5$ mg of sample and synthetic polynucleotides have not normally been available in sufficient quantities to allow the use of such a technique. Possible procedures for the determination of the total salt content of smaller samples ( $\sim 200$ ug) are discussed in chapter 6.

X-ray diffraction patterns of fibres so prepared were taken using pinhole or Franks optics as described in chapter 2.6.

Some fibres were found to exhibit irreversibility with regard to the variation of their x-ray pattern with the relative humidity of the fibre environment. Hence for each fibre, patterns were first recorded at a low relative humidity of 44% or 57% and then at increasing relative humidities of 66%, 75%, 86% and 92%. If a semi-crystalline B or disordered B diffraction pattern was obtained at 92% rh the relative humidity was not further increased since such a procedure can produce marked changes in the gross features of the fibre, for example, bending or even collapse to an unoriented mass. Typically, only the fibres containing  $a\text{Cl}^-/\text{PO}_4^- \leq 0.3$  were exposed to the higher humidities of 95% and 98%. Diffraction patterns were then taken at decreasing relative humidities of 95%, 92%, 86%, 75%, 66%, 57%, 44%, 32% and 0% followed by a further cycle of humidity changes as appropriate.

### 3.3 Results

Fibres prepared from gels to which no sodium chloride had been added gave diffraction patterns exhibiting two components as the relative humidity was increased from 57% to 92%. The predominant A component did not differ significantly from that observed for the sodium salt of naturally occurring DNA's although it was somewhat ill defined at the lower relative humidities. The prominent features of the minor component in these patterns were the first equatorial reflection and two strong meridional reflections in the region of 0.33nm. These features are identified in Plates 3.1 and 3.2. The variation in the spacing and relative humidity of these reflections as

Plates 3.1 - 3.10 : X-ray diffraction patterns of the sodium salt of  
poly[d(A-C)].poly[d(G-T)] fibres

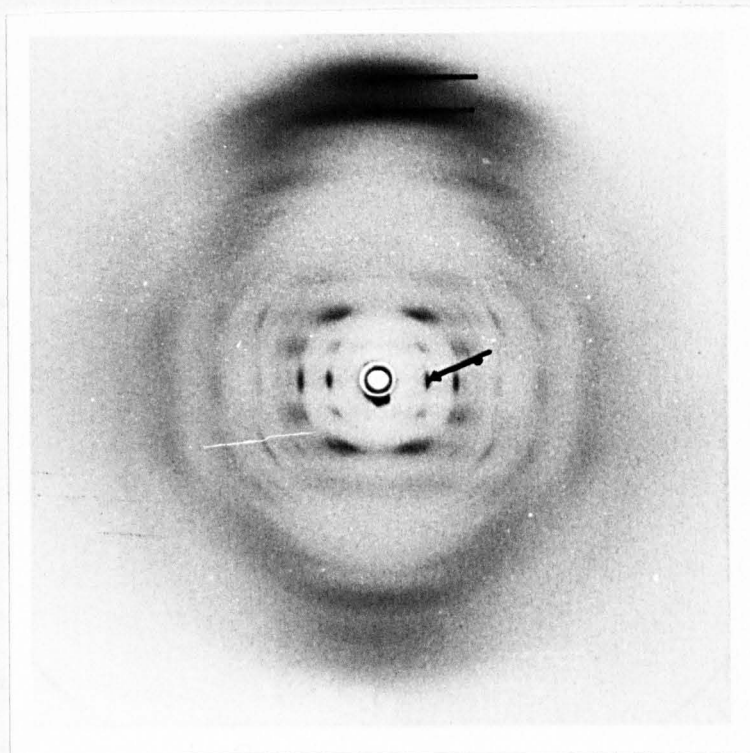


Plate 3.1

Fibre PVII 2,  $aCl^-/PO_4^- = 0.0$ ,  $rh = 66\%$ . This is predominantly an A type diffraction pattern, but there is a minor component characterized by three reflections which are indicated by the arrows.

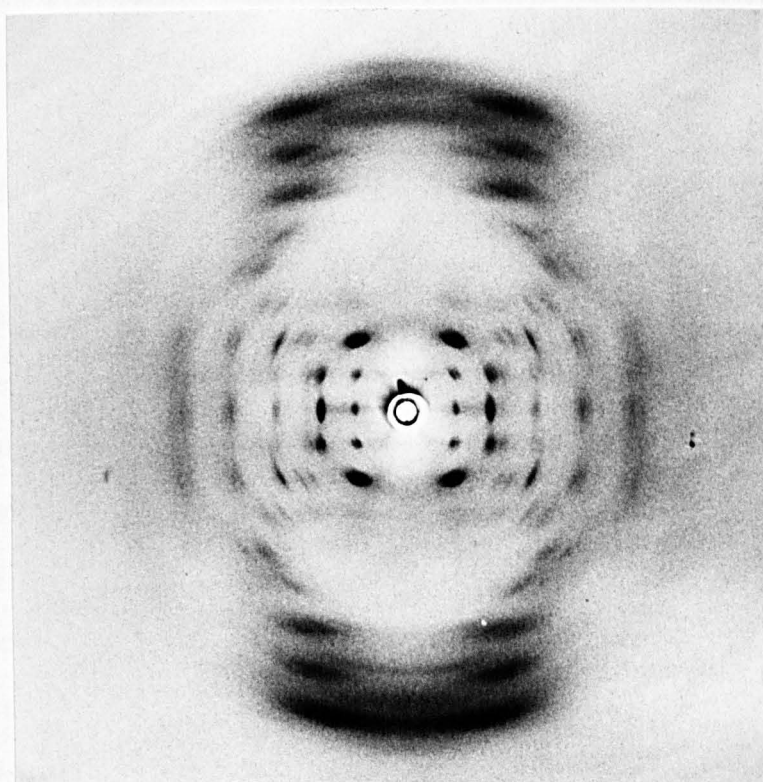


Plate 3.2

Fibre PVII 1/R,  $aCl^-/PO_4^- = 0.0$ ,  $rh = 75\%$ . After passing through a relative humidity cycle the fibre was reformed to retrieve the minor component. This pattern is similar to that of Plate 3.1, but the A component is more crystalline while the minor component is less intense.

a function of relative humidity is summarized in Table 3.1. It was not possible to identify with any certainty the family of conformations which were exhibited by the minor component as the relative humidity was increased. However, a comparison of the data in Table 3.1 with that of the known DNA and polynucleotide structures given in Table 3.2 suggested that the minor component was related to a highly wound C conformation at low relative humidities  $\sim 44\%$ . At 92% rh the minor component of these diffraction patterns was reminiscent of a semi-crystalline B structure as shown in Plate 3.3.

When the relative humidity was raised to 98% only semi-crystalline hexagonal B diffraction patterns were observed which were particularly well defined as shown in Plate 3.4.

Decreasing the relative humidity resulted in the reappearance of the A conformation at 92% rh, but on further decreasing the relative humidity there was no evidence of the two meridional reflections or the equatorial reflection which previously characterized the minor component. Furthermore, the minor component was not observed in fibres whose relative humidity had been decreased prior to reaching 98%, before the occurrence of the  $A \rightleftharpoons B$  transition. This irreversibility is illustrated by a comparison of Plate 3.1 with Plate 3.5. Both diffraction patterns were obtained from the same fibre at the same relative humidity of 66% but in the case of Plate 3.5 the fibre had previously been exposed to a maximum relative humidity of 92%. The complete absence of any equatorial reflection before the 130 reflection of the A conformation in Plate 3.5 is of interest since it is unusual to see an A pattern completely free of intensity contributions from the semi-crystalline B form in this region.

As the relative humidity was further decreased from 33% to 0% the A pattern became much less well defined as shown in Plate 3.6 indicating a progressive collapse of the structure. On increasing the relative humidity from 0% to 66% the A structure was reformed and a further increase in



Relative Humidity	Spacing of Reflection 1/nm	Spacing of Reflection 2/nm	Spacing of Reflection 3/nm	Comparison of the Intensities of Reflections 2 and 3
44%	1.69	0.348	Absent	Reflection 3 absent
57%	1.78	0.351	0.316	Reflection 2 stronger
66%	1.79	0.355	0.319	Reflection 2 stronger
75%	1.86	0.352	0.320	Reflection 3 stronger
86%	1.93	0.358	0.321	Reflection 3 much stronger
92%	2.01	Absent	0.328	Reflection 2 absent

Table 3.1 The effects of relative humidity on the spacings and relative intensities of the reflections which characterize the minor component of Na poly[d(A-C)].poly[d(G-T)] patterns at  $aCl^-/PO_4^- = 0.0$ . The error associated with these spacings is  $\sim \pm 0.06nm$ .

Conformational Type	Cation	Rh%	Helix Symmetry	Unit Cell Dimensions/nm			Crystal System	Axial Rise/Residue nm	First Equatorial Reflection/nm	hkl of First Equatorial Reflection
				a	b	c				
A	Na	66-98	11 <sub>1</sub>	2.22	4.06	2.82-2.87	M	0.256-0.261	1.16	130
B	Li,Na	43-98	10 <sub>1</sub>	3.08-3.61	2.24-3.79	3.34-3.46	O	0.334-0.346	1.81-2.61	110
B*	Na	98	9.95 <sub>1</sub>	-	-	3.31	H	0.331	2.26	110
α-B'	Na	66-92	10 <sub>1</sub>	2.28-2.33	2.28-2.33	3.21-3.29	H	0.324-0.329	2.28-2.33	100
β-B'	Na	31-70	10 <sub>1</sub>	1.77-1.78	1.99-2.00	3.20-3.24	O	0.320-0.324	1.77-1.78	100
C	Li	57-66	28 <sub>3</sub>	3.50	3.50	3.08	H	0.330	2.02	110
C	Li	44	28 <sub>3</sub>	3.22	2.02	3.11	O	0.333	1.71	110
C	Li	66	9 <sub>1</sub>	-	-	-	-	-	-	-
C	Na	81-92	28 <sub>3</sub>	-	-	-	-	-	-	-
C*	Na	33	8 <sub>1</sub>	-	-	2.60	-	0.336(0.325)	1.67	110
C'	Na	74-84	9 <sub>1</sub>	3.32	3.32	2.95	H	0.328	2.32	110
C''	Na	66	9 <sub>2</sub>	2.21	2.21	5.82	H	0.323	2.21	100
D	Na	75	8 <sub>1</sub>	1.70-1.75	1.70-1.75	2.43-2.50	T	0.304-0.313	1.70-1.75	100
D	Na	66	8 <sub>1</sub>	1.98-2.04	1.98-2.04	2.11-2.51	H	0.301-0.314	1.98-2.04	100
D	Na	66	8 <sub>3</sub>	2.04	2.04	7.38	H	0.308	2.04	100
E	Na	66	3 <sub>2</sub>	3.63	2.10	4.87	O	0.325	1.82	110
S	Na	43-66	6 <sub>5</sub>	1.91	1.91	4.35	H	0.363	1.91	100

**Table 3.2** This table shows the conditions of relative humidity and cation type found for the known DNA and polynucleotide conformations. Data is abstracted from Table 7 of Leslie et al., 1980, and is presented irrespective of DNA source or polynucleotide sequence. From the information given the helical pitch and first equatorial spacing have been calculated. Additional data for the C and the semi-crystalline B conformations of Na DNA has been taken from Zimmerman and Pfeiffer, 1980, and is denoted by an asterisk. In these cases the observed values of pitch and first equatorial spacing are given. There seems to be a contradiction in this data for the C conformation and the supposed value for the axial rise per residue is given in brackets.

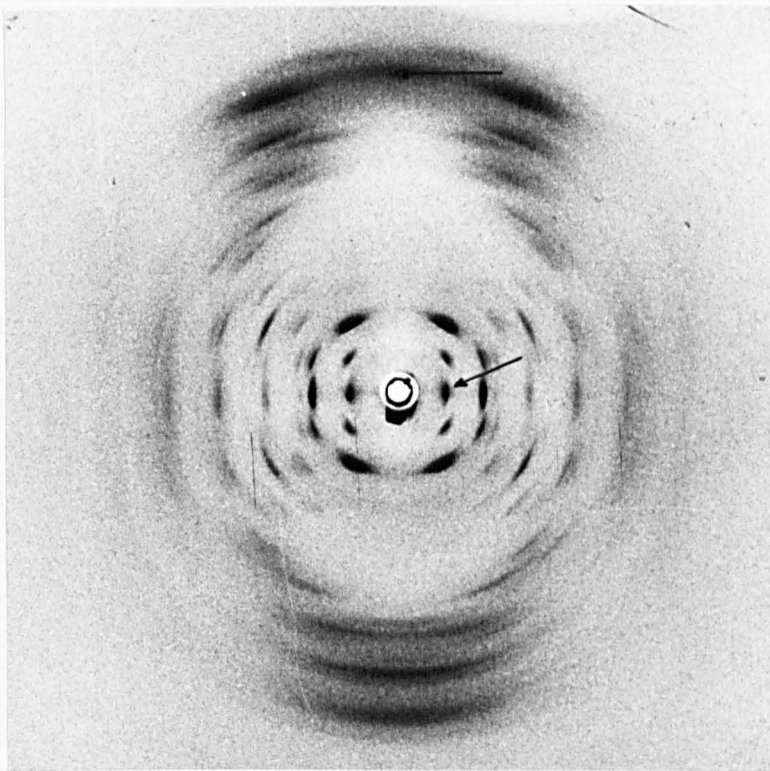


Plate 3.3

Fibre PVII 2,  $a\text{Cl}^-/\text{PO}_4^- = 0.0$ ,  $rh = 92\%$ . Again this is an A type diffraction pattern, but the minor component is now characterized by two reflections which are indicated by the arrows and imply a B conformation.

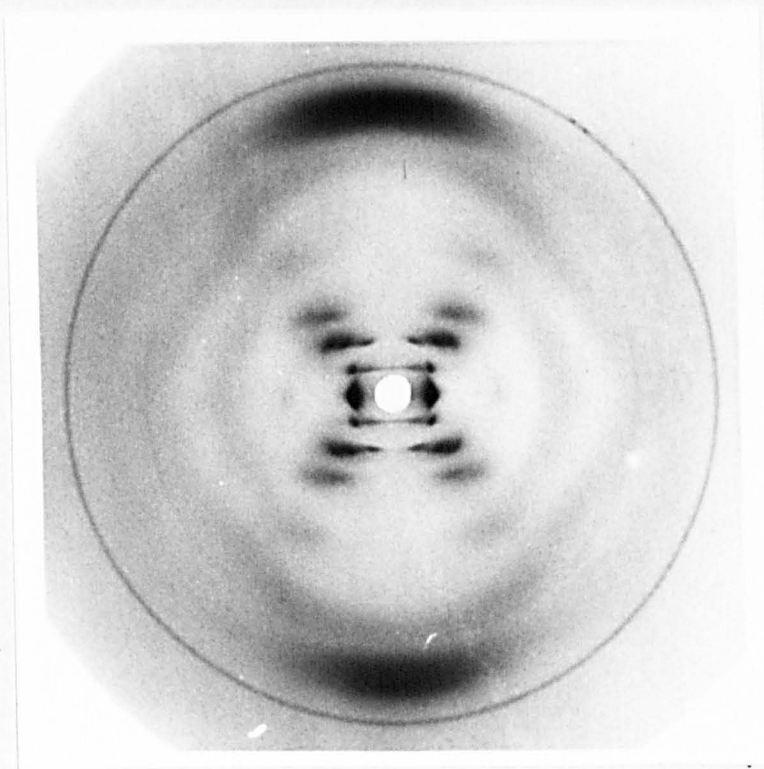


Plate 3.4

Fibre PVII 1/R,  $a\text{Cl}^-/\text{PO}_4^- = 0.0$ ,  $rh = 98\%$ . A well defined hexagonal semi-crystalline B diffraction pattern.

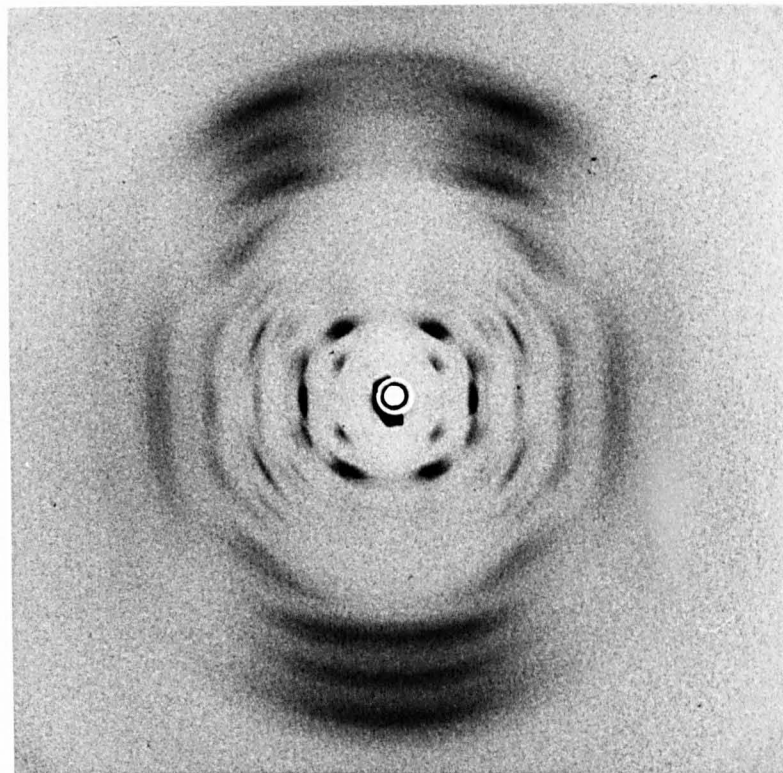


Plate 3.5

Fibre PVII 2,  $a\text{Cl}^-/\text{PO}_4^- = 0.0$ ,  $\text{rh} = 66\%$  after being exposed to a maximum relative humidity of  $92\%$ . The reflections which previously characterized the minor component of this pattern as seen in Plate 3.1 are absent.

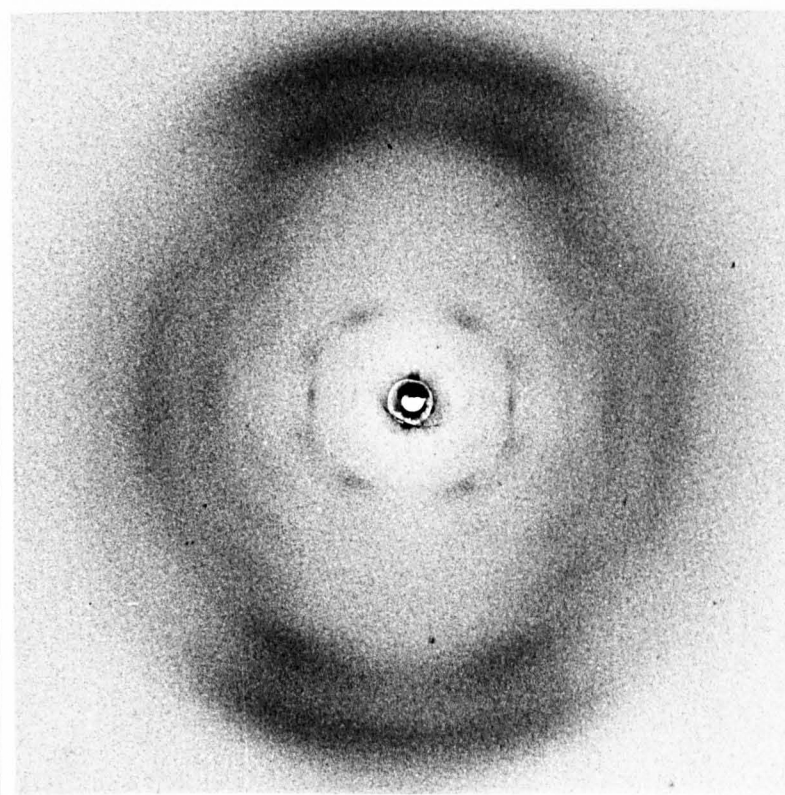


Plate 3.6

Fibre PVII 1,  $a\text{Cl}^-/\text{PO}_4^- = 0.0$ ,  $\text{rh} = 33\%$ . The A structure is beginning to collapse at low relative humidity.

humidity gave rise to the A→B transition at 98% as expected, but again there was no evidence of an intensity distribution characteristic of the minor component.

Despite the apparent irreversibility of the minor component it was reobtained if a fibre which had previously been subjected to a humidity cycle like that described above was rewetted to form a gel and drawn into a new fibre. This new fibre was found to exhibit exactly the same sequence of diffraction patterns as the original fibre beginning with the two component pattern at low relative humidity as seen in Plate 3.2.

Fibres prepared from gels to which sufficient sodium chloride had been added to give  $a\text{Cl}^-/\text{PO}_4^- \leq 0.3$  gave poorly defined diffraction patterns with some similarity to the C type intensity distribution at relative humidities from 44% to 57%. At higher humidities up to and including 92% rh these fibres gave A type patterns. A transition to the B structure occurred when the relative humidity was raised to 98% and on lowering the humidity this transition was found to be reversible.

Fibres prepared from gels which contained 0.4-0.8  $a\text{Cl}^-/\text{PO}_4^-$  gave semi-crystalline patterns at relative humidities from 44% to 57% or 66% as shown in Plate 3.7. These patterns were very similar to that of the hexagonal semi-crystalline C form of the lithium salt of naturally occurring DNA's described by Marvin et al., 1961. The relatively large layer line spacing compared with that of B DNA, the strong intensity of the layer line immediately below the meridional reflection and the presence of diffracted intensity at  $\xi = 1.0\text{nm}^{-1}$  on the first layer line are all features indicative of the C conformation as observed by Marvin et al., 1961. Analysis of the best of these patterns (Plate 3.7) gave a layer line spacing of  $2.81 \pm 0.04\text{nm}$ , an axial repeat of  $0.340 \pm 0.008\text{nm}$  and hence  $8.3 \pm 0.3$  residues per turn. While the number of residues per turn

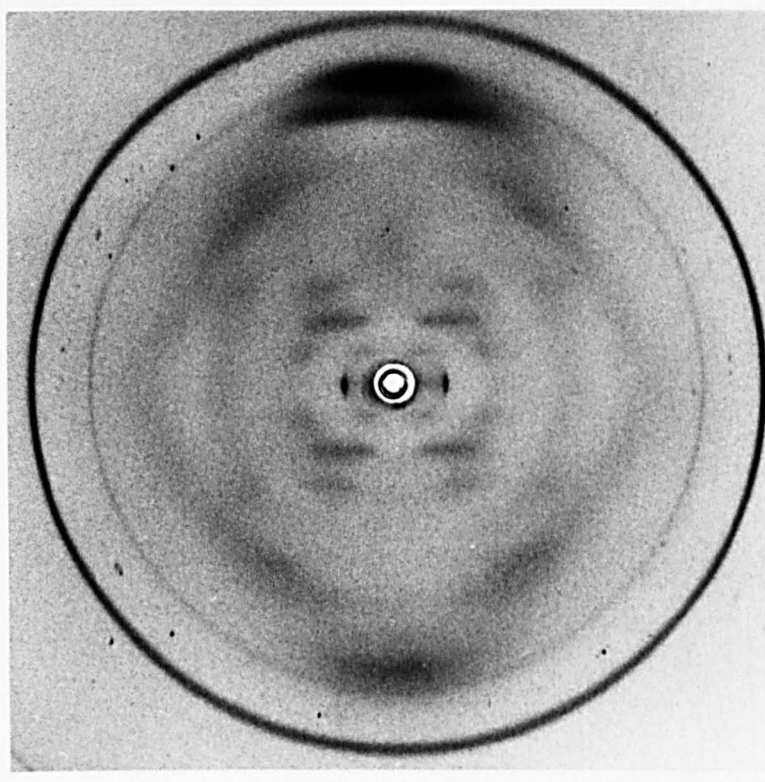


Plate 3.7

Fibre KE 29/R,  $a\text{Cl}^-/\text{PO}_4^- = 0.54$ ,  $\text{rh} = 57\%$ . A semi-crystalline C diffraction pattern with a layer line spacing of 2.81nm and an axial rise per residue of 0.340nm. The diffraction rings at 0.282 and 0.324nm are due to sodium chloride.

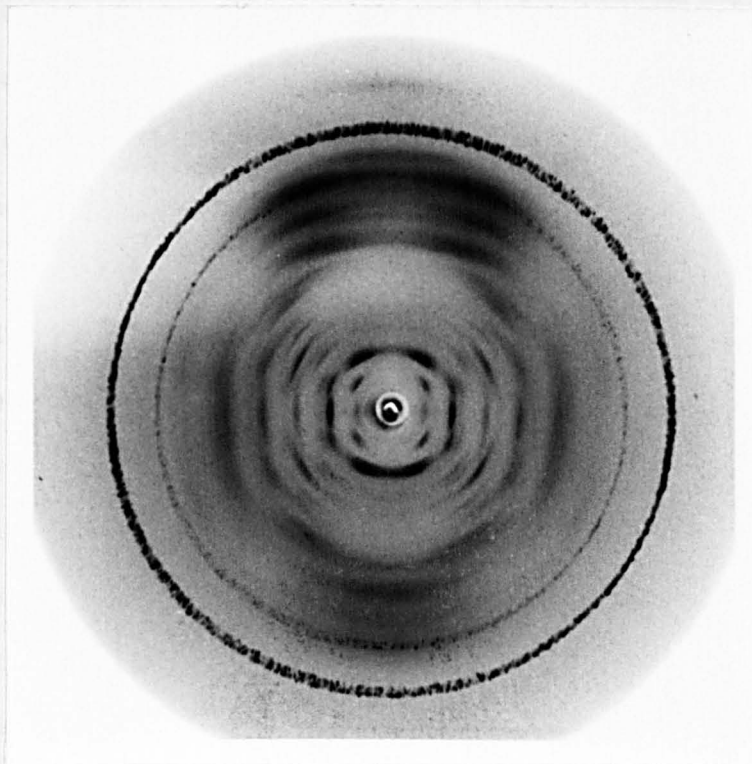


Plate 3.8

Fibre PVII 6,  $a\text{Cl}^-/\text{PO}_4^- = 0.6$ ,  $\text{rh} = 66\%$ . An A type diffraction pattern replaces the lower humidity C pattern. Again the diffraction rings are due to sodium chloride.

found for this pattern lies outside the value of 8.8-9.7 residues per turn of the C conformations of Marvin et al., 1961, it lies within the extended range of 8.0-9.7 residues per turn found by Zimmerman and Pfeiffer, 1980.

Such fibres gave crystalline A patterns at 66% or 75% rh as shown in Plate 3.8 and semi-crystalline hexagonal B patterns at 92% rh as in Plate 3.9. These A and B diffraction patterns were generally indistinguishable from those observed for the naturally occurring DNA's, although the crystallinity exhibited by these patterns was not as good as that of similar patterns of Na poly[d(A-C)].poly[d(G-T)] fibres to which no excess sodium chloride had been added.

Upon reduction of the relative humidity of the fibre environment to 75% the B→A transition was apparent, but A patterns persisted even when the relative humidity had been reduced to 44%. Further reduction of the relative humidity to 0% again resulted in the formation of a disordered structure. As the relative humidity was increased the A structure reformed at about 66% rh but further cycling of the relative humidity failed to induce the fibres to revert to a C conformation. This irreversibility of the C structure exactly paralleled that of the structure represented by the minor component in fibres containing no added sodium chloride.

The C conformation was reobtained if a fibre which had gone through a relative humidity cycle like that described above was rewetted and drawn into a new fibre. As in the case of fibres where the  $a\text{Cl}^-/\text{PO}_4^- = 0.0$ , such new fibres behaved in exactly the same manner as the original fibres.

For one fibre of  $a\text{Cl}^-/\text{PO}_4^- = 0.6$  a further distinct type of diffraction pattern was occasionally obtained as shown in Plate 3.10. Such patterns were obtained at relative humidities associated with the transition between the A and B structures at ~75% rh. The arms of the distinctive cross of intensity distribution are steeper in Plate 3.10 compared with Plate 3.9. This indicates a reduction in pitch compared with the 3.40nm pitch associated with the B conformation and it is therefore tempting to identify

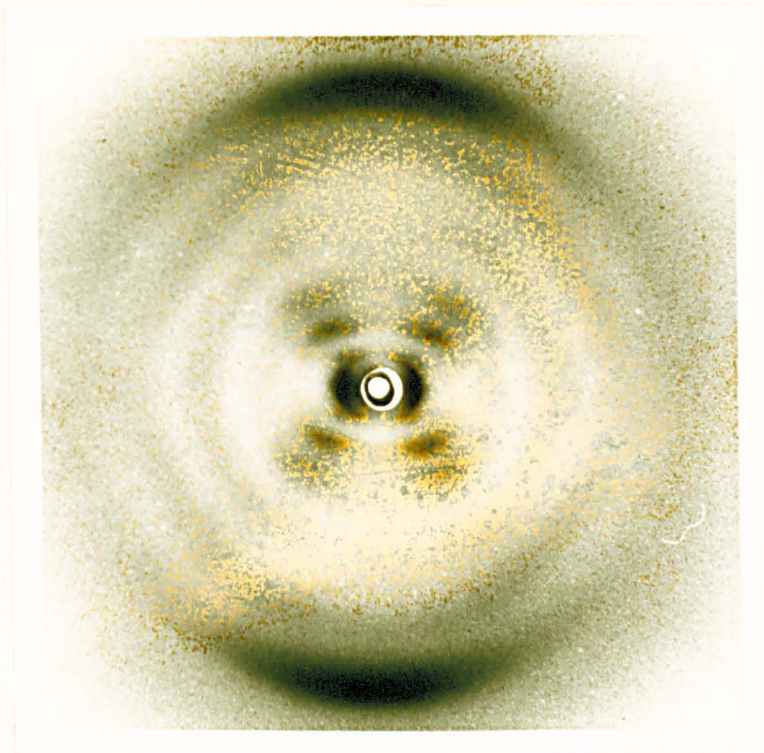


Plate 3.9

Fibre PVII 6,  $a\text{Cl}^-/\text{PO}_4^- = 0.6$ ,  $\text{rh} = 92\%$ . A semi-crystalline B diffraction pattern. The sodium chloride diffraction rings associated with patterns of this fibre at lower rh's are no longer present.

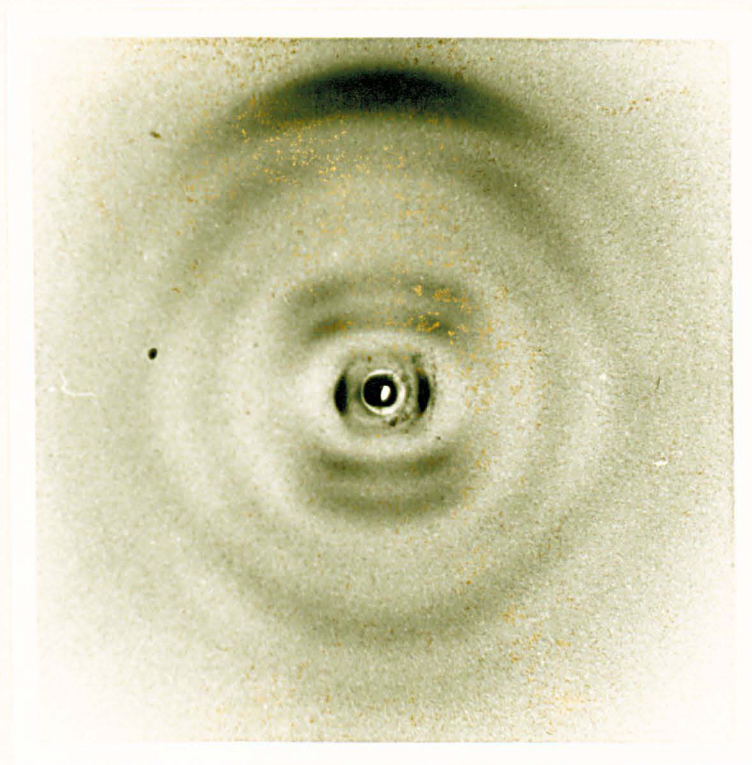


Plate 3.10

Fibre PVII 6,  $a\text{Cl}^-/\text{PO}_4^- = 0.6$ ,  $\text{rh} = 75\%$ . A peculiar semi-crystalline diffraction pattern with a reduced pitch compared with that of the B conformation.



this structure as an intermediate in the  $A \rightleftharpoons B$  transition.

An obvious feature of the C type patterns as in Plate 3.7 was the presence of diffraction rings at 0.282nm and 0.324nm which are characteristic of crystalline sodium chloride. The intensity of these rings was found to decrease with increasing relative humidity of the fibre environment. At 92% rh these rings were completely absent as shown in Plate 3.9. These observations can be attributed to the presence of sodium chloride in these fibres in the form of small crystallites at low relative humidities, but which gradually dissolve as the humidity is increased. A decrease in relative humidity resulted in the reappearance of the sodium chloride diffraction rings which was consistent with this explanation.

Fibres prepared from gels containing 0.9-2.0  $aCl^-/PO_4^-$  tended to show surface irregularities which became more marked with increasing salt content. This effect was attributed to the presence of large crystals of sodium chloride on or near the surface of the fibres. Essentially such fibres showed no crystallinity in the packing of the polynucleotide molecules although there was some orientation in those fibres at the lower end of this range of  $aCl^-/PO_4^-$  ratio. At low relative humidities the patterns of all these fibres were dominated by diffraction from sodium chloride crystals. As the relative humidity was increased the sodium chloride diffraction became weaker and eventually disappeared  $\sim 92\%$  rh giving non oriented poorly crystalline patterns with an intensity distribution similar to that of B DNA. Diffraction patterns were also recorded for these fibres as a function of decreasing relative humidity from 92% to 0%. The sodium chloride diffraction began to return  $\sim 75\%$  rh and at 57% rh the process was complete.

### 3.4 Discussion

These results show that the A, B and C conformations found for the naturally occurring DNA's are all available to the sodium salt of

poly[d(A-C)].poly[d(G-T)]. The conditions of relative humidity and salt content for observing the A and B conformations of this Na polynucleotide are similar to those for naturally occurring Na DNA's as reported by Cooper and Hamilton, 1966. Similar conditions for the observation of the C conformation of Na DNA have not been published previous to Mahendrasingam, 1983, and Rhodes et al., 1982.

Early studies of the C conformation of Na DNA by Bram and Baudy, 1974, and Arnott and Selsing, 1975, have suggested that it is at best a poorly favoured conformation. However, these results show that the C conformation is reproducibly observed under specific conditions. Even so, the degree of crystallinity apparent from Na poly[d(A-C)].poly[d(G-T)] patterns (for example Plate 3.7) and from Na DNA patterns published to date (Bram and Baudy, 1974, Arnott and Selsing, 1975, Zimmerman and Pfeiffer, 1980, Leslie et al., 1980, Mahendrasingam, 1983, and Rhodes et al., 1982) is much poorer than that observed for C patterns from Li DNA (Marvin et al., 1961) and Li poly[d(A-C)].poly[d(G-T)] (chapter 4). No satisfactory explanation has so far been reported of the marked differences in the effect of the lithium and sodium ions on the conformation of DNA and its synthetic analogues.

It was not found necessary to keep fibres under tension as suggested by Bram and Baudy, 1974, in order to observe the C conformation and the effect of tension on fibres of Na poly[d(A-C)].poly[d(G-T)] was not examined.

This work emphasizes that low relative humidity, typically ~44-66%, is a necessary criterion for the observation of the C conformation of Na poly[d(A-C)].poly[d(G-T)]. This is in agreement with studies on the sodium salt of native DNA's by Bram and Baudy, 1974, Arnott and Selsing, 1975, Zimmerman and Pfeiffer, 1980, Mahendrasingam, 1983, and Rhodes et al., 1982. In addition, the C conformation of Na DNA has also been found for fibres immersed in high concentrations of t-butanol ~95% or 98% v/v which also indicates that the C conformation is associated with low hydration,

Zimmerman and Pfeiffer, 1980. These results are in contrast with the study on the polymorphism of a number of polynucleotides by Leslie et al., 1980. They concluded that generally for polynucleotides containing guanine the C form in fibres is stable in a fairly narrow range of fibre salt contents and relative humidities intermediate between the A and B forms. This is rather a surprising conclusion since of the nineteen Na polynucleotides studied only poly[d(A-G-C)].poly[d(G-C-T)] was observed in all three conformations. The humidities recorded for the C, A and B conformations were 74-84%, 92% and 95% respectively. This is in accordance with the work reported here for Na poly[d(A-C)].poly[d(G-T)].

A sodium chloride concentration of between 0.4 and 0.8  $\text{aCl}^-/\text{PO}_4^-$  was found necessary in order to obtain well defined C type patterns of poly[d(A-C)].poly[d(G-T)]. This is in agreement with the rather qualitative observations of Arnott and Selsing, 1975, for Na DNA and Leslie et al., 1980, for various polynucleotides, that the C conformation is stable at salt concentrations intermediate between those of A and B. However, in the former case there was no indication as to how this conclusion was arrived at, while in the latter case the samples were obtained by precipitation and quantitative information on the amount of salt in the fibres is obscure. Bram and Baudy, 1974, and Zimmerman and Pfeiffer, 1980, did not examine the effects of salt concentrations on their samples. In the analysis by Mahendrasingam, 1983, on naturally occurring DNA's the C conformation emerged as characteristic of fibres containing a minimum amount of retained salt.

These results demonstrate that the sequence of conformational transitions for Na poly[d(A-C)].poly[d(G-T)] is  $C \rightarrow A \rightleftharpoons B$ . Although this may have been inferred from the results of Bram and Baudy, 1974, and Zimmerman and Pfeiffer, 1980, the C conformation is more closely related to the B than to the A conformation, Marvin et al., 1961, Arnott and Selsing, 1975. Thus the sequence transition  $A \rightleftharpoons C \rightleftharpoons B$  for Na DNA suggested by Leslie et al.,

1980, seemed more likely. This is clearly not the case for Na poly[d(A-C)], poly[d(G-T)] and this result is supported by the work of Mahendrasingam, 1983, and Rhodes et al., 1982, on Na DNA's.

As well as the relative humidity of the fibre environment and the  $a\text{Cl}^-/\text{PO}_4^-$  ratios, the conformation of Na poly[d(A-C)].poly[d(G-T)] has also been shown to depend on the range of relative humidity to which a fibre has previously been exposed. Thus neither the C conformation from fibres containing 0.4-0.8  $a\text{Cl}^-/\text{PO}_4^-$ , nor the structure characterised by the minor component from fibres containing no added salt, could be retrieved by changes in the relative humidity once the relative humidity had been raised above a critical limit. A possible explanation for this irreversibility for the C conformation and the structure represented by the minor component is the crystallisation of excess salt in a separate phase as gels dry during fibre preparation. This would leave the salt content in the polynucleotide phase low enough to favour the low salt conformation at low relative humidity. As the relative humidity is gradually increased the salt crystals in the fibres dissolve leading to a more uniform salt distribution. Subsequent reduction in the relative humidity may not result in the crystallisation of the salt as a separate phase because the sodium chloride ions aggregate less readily in the wet fibre than in the gel. Consequently the concentration of excess salt in the vicinity of the polynucleotide may be above the level at which the low salt conformation is favoured.

This effect of irreversibility does not seem to be related to peculiar conditions pertaining at the time of fibre preparation since the C conformation and that characterised by the minor component were recoverable upon the production of new fibres from the originals.

In contrast to this irreversible C→A transition for fibres of Na poly[d(A-C)].poly[d(G-T)], only reversible C⇌A transitions have been observed for Na DNA's by Mahendrasingam, 1983, Rhodes et al., 1982. A similar discrepancy has emerged between C→A transitions in Na poly[d(A-T)].

poly[d(A-T)] fibres prepared by the author compared with those prepared by Mahendrasingam, 1983, and this has been attributed to different methods of sample preparation as described in chapter 5.4. In view of these results it is likely that the difference between C - A transitions in Na poly[d(A-C)].poly[d(G-T)] fibres and Na DNA fibres occurs as a result of differences in sample preparation rather than any manifestation of the structural differences between Na poly[d(A-C)].poly[d(G-T)] and Na DNA. In view of this suggestion the  $aCl^-/PO_4^-$  ratio required to stabilize the C conformation of Na poly[d(A-C)].poly[d(G-T)] may be much lower than the value of 0.4-0.8  $aCl^-/PO_4^-$  initially suggested by these results. Thus it maybe less than that required to stabilize the A conformation and compatible with the results for the C conformations of Na DNA's.

A comparison of the C patterns obtained for Na poly[d(A-C)].poly[d(G-T)], Plate 3.7, with those so far obtained for natural Na DNA's shows much better definition in the higher layer lines near the meridian. This may be due to a more regular conformation for the synthetic polynucleotide than is possible for native DNA.

Although in this study the conditions of relative humidity and salt content of fibres has been systematically varied in order to obtain the types of conformations available to the sodium salt of poly[d(A-C)].poly[d(G-T)], not all the conformations reported by other workers have been found here. In the case of the S conformation of poly[d(A-C)].poly[d(G-T)], Arnott et al., 1980, Leslie et al., 1980, this is not surprising since although fibres were prepared with 3-6% retained salt necessary to reproduce the B conformation in typical DNA specimens, the S conformation was only observed after prolonged annealing of some of these fibres. However, the inability to obtain a fully crystalline B pattern for Na poly[d(A-C)].poly[d(G-T)] as reported by Leslie et al., 1980, is rather more difficult to explain.

This work has attempted to express some of the conditions pertaining

to polynucleotide conformation in a quantitative manner. However, just as Cooper and Hamilton, 1966, concluded that there were factors other than relative humidity and salt content which affected the  $A \rightleftharpoons B$  transition and which they were unable to identify, these results also indicate that there are significant factors which generally influence DNA and polynucleotide conformation in fibres other than the traditional parameters of retained salt and relative humidity. Particular regard for factors influencing salt crystallization in terms of crystal growth and nucleation rate may prove to be worth investigation in the future.

In particular these results suggest that the C conformation is routinely observed when sodium is the associated cation in poly[d(A-C)].poly[d(G-T)] fibres. This work is supported by the observation of the C conformation for the Na salts of a wide variety of naturally occurring DNA's by Mahendrasingam, 1983, Rhodes et al., 1982. Under physiological conditions DNA is most likely to be associated with the sodium cation. The routine observation of the C conformation in Na DNA's suggests that this conformation may be of greater biological significance than has so far been assumed.

### 3.5 An estimation of the error in the determination of the $aCl^-/PO_4^-$ ratio

There are three errors which are thought to significantly contribute to the  $aCl^-/PO_4^-$  ratio error. These are the error in calculating the content of the polynucleotide samples, the weighing error and the error associated with pipetting aliquots of standard sodium chloride solutions.

The error in calculating the water content of the polynucleotide samples was determined experimentally using Sigma calf thymus Na DNA, since poly[d(A-C)].poly[d(G-T)] was too precious to use for analysis in this fashion. The water content of twelve Na DNA samples was estimated in the same manner as the Na poly[d(A-C)].poly[d(G-T)] samples and the results are recorded in Table 3.3. For a given DNA sample this table shows the mass of the sample, the expected concentration of the sample in 4.0ml of 0.01M

Sample Number	Weight ug	Expected Concentration $\times 10^{-5}M$	Measured Concentration $\times 10^{-5}M$	Percentage Ratio
1	113.5	8.53	6.14	71.98
2	48.9	3.67	2.61	71.12
3	172.9	12.99	9.54	73.44
4	118.8	8.93	6.36	71.22
5	138.5	10.41	7.65	73.49
6	146.2	10.98	8.03	73.13
7	148.2	11.13	8.33	74.84
8	136.4	8.20*	5.74	70.00
9	122.4	7.36*	5.36	72.83
10	97.7	7.34	5.39	73.43
11	119.5	7.18*	5.46	76.04
12	124.0	9.32	6.99	75.00

**Table 3.3** Data relating to the determination of the water content and associated error in weighed Na DNA samples. Samples dissolved in 5.0ml of 0.01M NaCl solution are denoted by \*. The mean value of the expected/measured percentage ratio is  $73.04 \pm 3.04$  or  $\pm 4.16\%$ .

Tare Weight/mg	1.0	2.0	3.0	5.0	10.0
Measured Value/mg	0.98	1.93	3.07	4.94	10.05
Percentage Difference	-2.0	-3.5	+2.3	-1.2	+0.5

**Table 3.4** Data relating the measured masses of the tare weights to their stipulated values. The average percentage difference between the stipulated and measured weights is  $-0.8\%$ .

sodium chloride solution, the concentration of the dissolved sample determined from the optical density of the solution and the ratio of these two concentrations. From these results the Na DNA samples were shown to have a percentage DNA content of  $73.0 \pm 3.0$ . This gave a percentage error of  $\pm 4.2\%$  in the determination of DNA content. This analysis does not take into account any systematic errors associated with weighing the sample, determining the absorbance of the dissolved samples or in assuming a value of  $6600\text{M}^{-1}\text{cm}^{-1}$  for the extinction coefficient of DNA at  $\lambda_{258\text{nm}}$ . In the latter case an indication of this error may be obtained from reference to the various published values. Thus Peacocke and Walker, 1962, give an average value of  $E_{\lambda_{258}} = 6640\text{M}^{-1}\text{cm}^{-1}$ , while Rusconi, 1966, give  $E_{\lambda_{258}} = 6530\text{M}^{-1}\text{cm}^{-1}$ . Hence the value  $E_{\lambda_{258}} = 6600\text{M}^{-1}\text{cm}^{-1}$  used in these results may represent an error of  $\pm 1.1\%$ . For simplicity these errors have been added to produce an overall error in the water content of  $\pm 5.3\%$ . It is thought that other systematic errors in the water content are negligible compared with the above value.

In considering the error in determining the mass of the polynucleotide samples the recommended procedure for using the microbalance was to calibrate it with the aid of a 150mg class M standard weight. According to the operating manual the design of the balance is such as to give an accuracy of  $\pm 0.1\%$  on all scale ranges after such calibration. It was not possible to confirm this statement since no other standard weights were available at the time. The smallest tare weights were weighed on the balance and the results are recorded in Table 3.4. The difference of the measured masses of the individual weights compared with the stipulated values is larger than the average difference of  $-0.8\%$ . Thus, the discrepancy between the stipulated and measured masses is thought to more nearly reflect variations in the masses of the tare weights rather than any systematic weighing error incurred as a result of incorrect calibration of the microbalance. This suggests that on the 0-10mg scale the balance is accurate



to at least  $\pm 0.8\%$ .

In considering the pipetting errors, the volume of standard sodium chloride solutions added to gels to obtain specific  $\text{aCl}^-/\text{PO}_4^-$  ratios varied from 1.0-10.0ul. The 10.0ul Oxford pipette was used to transfer 5.0ul aliquots of water to the pan of the electronic microbalance in order to determine the reproducibility of the delivery of the pipette. An analysis of twenty-four deliveries gave an average weight of  $4.71 \pm 0.08\text{mg}$  or  $\pm 1.70\%$  per 5.0ul aliquot. Taking into account the density of water at ambient temperature, 5.0ul of water should weigh 4.990mg. The 5.6% discrepancy in the measured and calculated masses of the aliquots is significantly greater than the 1.70% reproducibility of the pipette and is attributed to spluttering and capillary action. Both of these effects cause a small part of the delivery to be retained within the pipette tip. The average time taken to weigh an aliquot was  $20 \pm 2\text{s}$  and the rate of evaporation was  $2.25\text{ugs}^{-1}$ . Thus the determination of the mass of an aliquot was not significantly affected by the rate of evaporation of water. A reduction in the pipetting error may be obtained by using a micropipette of constant bore. Although this type of pipette is less convenient to use than the auto pipette, capillary and spluttering effects might be expected to be less. Alternatively, the  $\text{aCl}^-/\text{PO}_4^-$  ratios could be decreased by  $\sim 6\%$  to account for the low delivery of the auto pipette. However, in this work no such corrections were made and the pipetting error is taken as  $\pm 5.6\%$ .

The addition of these errors results in an overall estimation of the error in the  $\text{aCl}^-/\text{PO}_4^-$  ratio of  $\pm 12\%$ .

This error does not take into account any inhomogeneity in the distribution of the added salt within the fibre samples. Such effects may well give higher or lower  $\text{Cl}^-/\text{PO}_4^-$  ratios in localized regions of the fibres in excess of the estimated error value. It is necessary to improve methods of fibre preparation in order to minimize these effects.

Chapter 4. AN INVESTIGATION INTO THE CONFORMATIONAL FLEXIBILITY OF THE LITHIUM SALT OF POLY[d(A-C)].POLY[d(G-T)]

4.1 Introduction

A variety of diffraction patterns have been obtained from the lithium salt of calf thymus DNA. Langridge et al., 1960a, gave details of fully crystalline orthorhombic B patterns, semi-crystalline orthorhombic and hexagonal B patterns and semi-crystalline orthorhombic and hexagonal C patterns. Marvin et al., 1961, have analysed the type of diffraction pattern obtained from lithium calf thymus DNA as a function of relative humidity and salt concentration in the specimen. They obtained B diffraction patterns when 1 - 6% by weight of lithium chloride was precipitated with the DNA during preparation, but found that the optimum value of lithium chloride was between 2.5% and 4%, while the optimum humidity was 66%. Specimens containing less than 1% lithium chloride gave only C or semi-crystalline B patterns while specimens containing much more than 6% lithium chloride either gave high humidity B patterns or were too deliquescent to use. Generally fibres which gave crystalline B patterns at 66% rh gave orthorhombic C patterns at low relative humidity while fibres of low chloride content gave hexagonal C patterns at 66% or lower relative humidity. All fibres gave semi-crystalline B patterns at 92% rh. However, the relative humidity with which one type of pattern changed to another usually varied with the fibre. Hysteresis effects influenced the type of patterns obtained and these effects were not removed by equilibrating the specimens at constant relative humidity for several days. The lithium chloride concentrations in the DNA samples used in fibre preparation were determined using a micro-Carius method which is briefly described in chapter 6.2.

Davies and Baldwin, 1963, have shown that Li salts of poly[d(A-T)].poly[d(A-T)] and the chemically modified poly[d(A-brU)].poly[d(A-brU)] can

exist in the semi-crystalline B form.

Zimmerman and Pfeiffer, 1980, have observed B and C conformations in fibres of lithium salmon sperm DNA. For fibres prepared from pellets centrifuged from 1mM lithium chloride solutions a C→B transition occurred between 79% and 98% rh. B and C conformations were also apparent for Li DNA fibres immersed in aqueous methanol, aqueous ethanol and high concentration lithium chloride solutions while only the B conformation was observed for Li DNA fibres immersed in ethylene glycol. In all cases the C conformation was adopted in more dehydrating media than the B conformation. The range of helical parameters attributed to the C conformation has been further extended by the results of Zimmerman and Pfeiffer. In particular, the range of residues per turn has increased from 8.8 - 9.7 to 7.9 - 9.6 while the range of pitch values has increased from 2.92 - 3.22 to 2.68 - 3.18 compared with the data of Marvin et al., 1961. Zimmerman and Pfeiffer suggest that a continuous smooth transition can occur between members of the C family. They point out that the number of residues per turn for the C family range from almost that of the B form to that of the D form, Davies and Baldwin, 1963, Arnott et al., 1974, or the T form, Mokul'skii et al., 1972, Mokul'skaya et al., 1975.

Leslie et al., 1980, have obtained diffraction patterns from fibres of the lithium salt of various synthetic polynucleotides. As in the case of native DNA's only the B and C conformations were observed in the presence of the lithium cation. Thus Li poly[d(G-C)].poly[d(G-C)], Li poly[d(I-I-T)].poly[d(A-C-C)], Li poly[d(A-G-T)].poly[d(A-C-T)] and Li poly[d(G-G-T)].poly[d(A-C-C)] all exhibited the B conformation, while the latter two polynucleotides also gave the C conformation at lower relative humidities.

In this work an investigation of the lithium salt of poly[d(A-C)].poly[d(G-T)] has been carried out in a similar manner to that of the sodium salt of this polynucleotide reported in chapter 3. Conditions for the

observation of C and semi-crystalline B diffraction patterns in terms of relative humidity of the fibre environment and added fibre salt content are described. The results are compared with those obtained for other lithium polynucleotides and lithium native DNA's reported by other workers. Particularly well resolved C diffraction patterns have been obtained for Li poly[d(A-C)].poly[d(G-T)] which displays an unusual helical symmetry. Further analysis of these patterns may yield a more accurate model of the C conformation.

#### 4.2 Materials and methods

The lithium salt of the synthetic polynucleotide poly[d(A-C)].poly[d(G-T)] was prepared at Paris University VII by Dr. G.J. Brahms and Mr. J. Vergne as described in chapter 2.1. From this material a series of fibres was prepared containing 0.0, 0.24, 0.55, 0.82, 1.4 and 1.6  $\text{aCl}^-/\text{PO}_4^-$ , in the same manner as described in chapter 3.2 for the sodium salt of this polynucleotide. The sample of  $\text{aCl}^-/\text{PO}_4^-$  ratio = 1.6 was found too deliquescent to be used, having quickly absorbed water from the atmosphere with a resultant loss of shape. However, x-ray diffraction patterns were obtained for all the other samples at a series of ascending and descending relative humidities using pinhole and Franks optics.

#### 4.3 Results

The fibre containing no added LiCl gave a C type diffraction pattern at 44% rh as shown in Plate 4.1. This pattern was characterized by strong intensity on the first layer line in the region of  $\xi = 1.0\text{nm}^{-1}$  and on the  $1\text{m}^{-1}$  layer line, immediately below the meridional reflection as described by Marvin et al., 1961, for C patterns of Li DNA. In addition a pitch of  $2.77 \pm 0.04\text{nm}$  was apparent which is lower than the value obtained by Marvin et al., 1961, but well within the extended range of 2.68 - 3.18nm for Li C DNA reported by Zimmerman and Pfeiffer, 1980. This pattern was more crystalline than previously reported and in particular the intensity

Plates 4.1 - 4.7 : X-ray diffraction patterns of the lithium salt of  
poly[d(A-C)].poly[d(G-T)] fibres

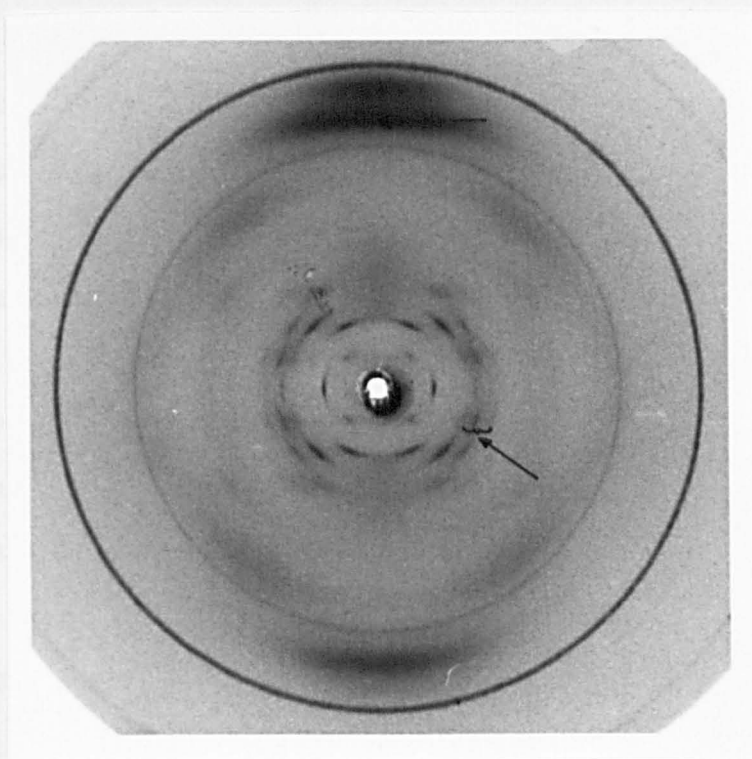


Plate 4.1

Fibre KE 14,  $aCl^-/PO_4^- = 0.0$ ,  $rh = 44\%$ . A C type diffraction pattern as characterized by the strong intensity in the regions indicated by the arrows and a pitch of  $2.77 \pm 0.04nm$ .

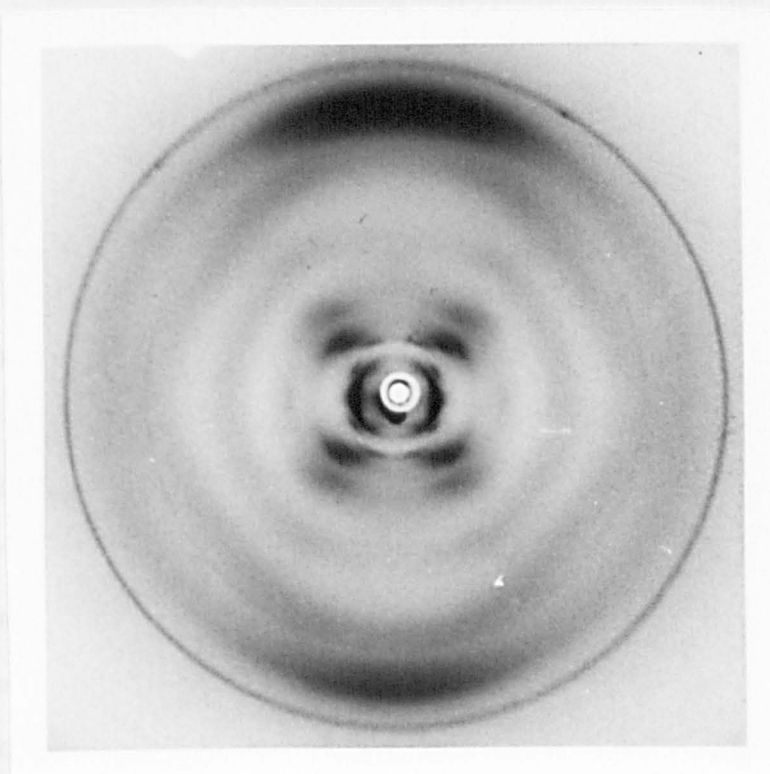


Plate 4.2

Fibre KE 14,  $aCl^-/PO_4^- = 0.0$ ,  $rh = 98\%$ . A semi-crystalline B diffraction pattern with a pitch of  $3.27 \pm 0.09nm$ . Note the absence of strong intensity compared with the arrowed regions in Plate 4.1.

on the first layer line in the region of  $\xi = 1.0\text{nm}^{-1}$  could be resolved into three separate reflections.

Diffraction patterns recorded for this fibre at increasing relative humidities of 57%, 66%, 75%, 86% and 92% showed no distinct conformational changes. At 98% rh a semi-crystalline B diffraction pattern was obtained as shown in Plate 4.2. The pitch obtained from this pattern had increased to  $3.27 \pm 0.09\text{nm}$  and the strong intensity on the first layer line and on the  $1m-1$  layer line which characterized the previous C patterns is no longer apparent. On reducing the relative humidity to 92% a C pattern was once more obtained and this conformation remained stable as the relative humidity was further reduced to 86% and 75%.

Similar series of diffraction patterns were obtained for the fibres of  $a\text{Cl}^-/\text{PO}_4^- = 0.24, 0.55$  and  $0.82$ . The most crystalline and well oriented diffraction patterns were obtained from the fibre having an  $a\text{Cl}^-/\text{PO}_4^-$  ratio  $\approx 0.55$ . Measurements of the set of diffraction patterns obtained from this fibre showed an increase in the d-spacing of the 110 reflection with increasing relative humidity. The reflections are described in terms of an hexagonal lattice as was later shown to be the case for the diffraction patterns which were subjected to a more detailed analysis. This increase is quite marked and corresponds to an increase in intermolecular spacing of 8.6% at 86% rh when the fibre is still clearly in the C conformation, as shown in Plate 4.3. The spacing of the 110 reflection, the corresponding intermolecular spacing and the percentage increase in the spacing as a function of relative humidity are recorded in Table 4.1. d-spacings of the intense 102, 202 and 212 reflections have also been measured and tended to increase with increasing rh. However, the ratios between the  $\xi$ -values of these spacings as a function of relative humidity did not generally differ by more than  $\pm 2\%$  which was the accuracy of the measurements. This suggests that the changes observed in the d-spacings are not an indication of the change in molecular packing, but that an overall expansion

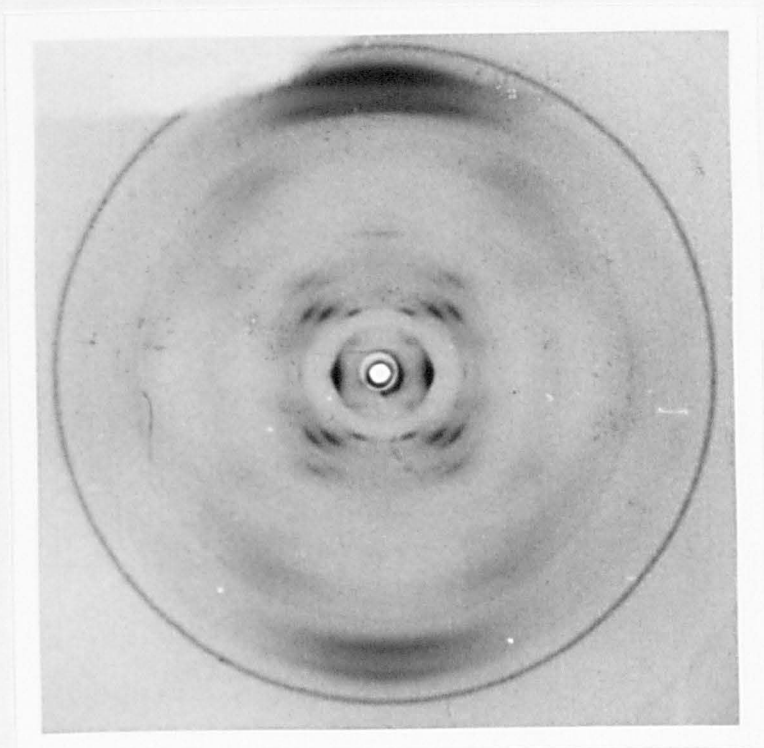


Plate 4.3

Fibre KE 19,  $a\text{Cl}^-/\text{PO}_4^- = 0.55$ ,  $\text{rh} = 86\%$ . A C type diffraction pattern with an increased IMS of  $8.6\%$  and increased 102, 202 and 212  $\xi$ -spacings by an average value of  $-8.4\%$  compared with the same fibre recorded at 57% rh.

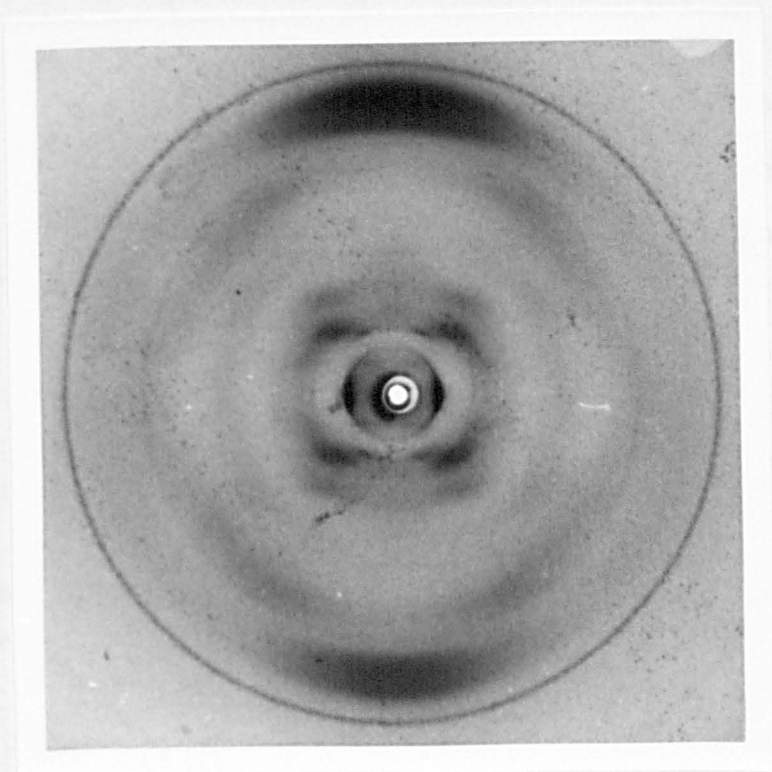


Plate 4.4

Fibre KE 19,  $a\text{Cl}^-/\text{PO}_4^- = 0.55$ ,  $\text{rh} = 86\%$  after passing through a humidity cycle which reached a maximum of 98%. A C type diffraction pattern as characterized by the intensity on the 1m-1 layer line. However, the central reflections are much more diffuse compared with previous C patterns.

%Rh	$d_{110}$ Spacing/nm	IMS/nm	% Increase in IMS	Average % Increase in $\xi$ values of the 102, 202 and 212 Reflections /nm <sup>-1</sup>	Pitch /nm	% Increase in Pitch
57	1.75	2.02	0.05	0.0	2.92	0.0
66	1.73	2.00	-1.4	-2.4	2.86	-2.1
75	1.80	2.08	2.8	-3.6	2.91	-0.3
86	1.90	2.20	8.6	-8.4	2.92	0.0
92	2.01	2.32	14.7	-11.1	3.02	3.4
98	2.20	2.54	25.4	-	3.06	4.8
92	2.11	2.43	20.3	-	3.02	3.4
86	1.99	2.30	13.7	-21.3	2.89	-1.0
75	1.71	1.98	-2.2	-0.3	2.86	-2.1
66	1.70	1.96	-3.0	2.7	2.85	-2.4
57	1.67	1.93	-4.8	3.3	2.88	-1.4
44	1.66	1.91	-5.5	4.7	2.89	-1.0

Table 4.1

Data from the diffraction patterns of the Li poly[d(A-C)].poly[d(G-T)] fibre of  $aCl^-/PO_4^- = 0.55$  showing changes of specific parameters as a function of relative humidity. The average percentage increase in the  $\xi$  values of the 102, 202 and 212 reflections were not obtained at 98% and 92% rh. Under these conditions the fibre gave semi-crystalline B diffraction patterns where the second layer line appeared as a continuous streak of intensity.



of the lattice is occurring. This effect is almost certainly due to the uptake of water molecules and was found to be reversible as the relative humidity was decreased. An average percentage increase in the  $\xi$ -values of the 102, 202 and 212 reflections is recorded in Table 4.1. Measurements from the first, second and third layer line spacings of these patterns were used to calculate the helical pitch as a function of relative humidity. No significant change in this value was observed up to 86% rh. At 92% rh a large change in pitch occurred and at 98% rh a semi-crystalline B diffraction pattern was apparent as evidenced by the decrease in intensity of the  $lm-1$  layer line. As the relative humidity was decreased to 92% the diffraction pattern obtained still retained the overall appearance of a semi-crystalline B pattern. At 86% rh the pitch decreased considerably but the reflections on this pattern, although indicative of the C conformation, were rather diffuse as shown in Plate 4.4. At relative humidities of 75% and lower the C patterns were once more obtained with very sharp central reflections. Pitch values and the percentage increase in these values are also recorded in Table 4.1. Upon reducing the relative humidity the pitch, percentage increase in  $\xi$  and the intermolecular spacing values obtained from the diffraction patterns of this fibre all indicate a contraction of the lattice to a point beyond that obtained for patterns recorded at ascending relative humidities.

One effect of increasing the  $aCl^-/PO_4^-$  ratio in these fibres was an initial improvement in the crystallinity apparent from the diffraction patterns. Beyond an  $aCl^-/PO_4^- = 0.55$  the fibre crystallinity was still good, but the orientation of the molecules within the fibre deteriorated. The diffraction spots on patterns from the fibre of  $aCl^-/PO_4^- = 0.82$  appeared as long drawn out arcs and this effect was even more marked for the fibre of  $aCl^-/PO_4^- = 1.4$  as shown in Plate 4.5.

The transition from C patterns to semi-crystalline B patterns occurred at lower relative humidities as the  $aCl^-/PO_4^-$  ratio increased. For the

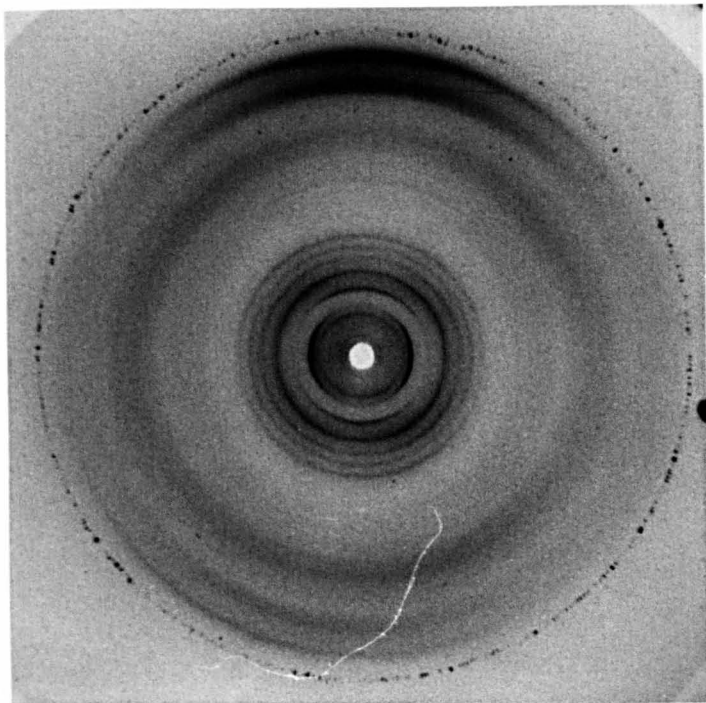


Plate 4.5

Fibre KE 18,  $\overline{aCl}/\overline{PO}_4 = 1.4$ ,  $rh = 44\%$  after passing through a humidity cycle which reached 86%. This is probably a C type diffraction pattern as suggested by the strong intensity on the  $lm-1$  layer line. This pattern demonstrates good crystallinity, but poor molecular orientation observed in fibres of high  $\overline{aCl}/\overline{PO}_4$  ratio.

fibres of  $a\text{Cl}^-/\text{PO}_4^-$  ratios of 0.82 and 1.4 this transition occurred at 92% and 86% rh respectively. In some cases the C  $\rightarrow$  B transition occurred at higher relative humidities than the corresponding B  $\rightarrow$  C transition for a specific fibre. This effect was more pronounced in fibres of higher  $a\text{Cl}^-/\text{PO}_4^-$  ratio and probably reflects the deliquescent nature of lithium chloride. The conformations exhibited by these fibres as a function of relative humidity and  $a\text{Cl}^-/\text{PO}_4^-$  ratio is given in Table 4.2. The symbol C<sup>+</sup> in this table is used to denote diffraction patterns which were still characteristic of the C conformation as defined by Marvin et al., 1961, but which exhibited an increase in the 102, 202 and 212 d-spacings of more than 3% compared with the initial patterns of a given fibre. The symbol m in this table has been used to describe patterns which show strong intensity on the  $lm-1$  layer line, but give rather diffuse central reflections as in Plate 4.4 compared with the sharp central reflections of the low humidity C patterns.

For the fibre of  $a\text{Cl}^-/\text{PO}_4^- = 1.4$ , only the patterns obtained at low relative humidities of 44% and 57% showed sharp central reflections. At higher relative humidities these patterns exhibited very diffuse intensity distributions and little information was obtained. However, these patterns were never dominated by diffraction from salt crystallites as were the Na poly[d(A-C)].poly[d(G-T)] patterns. Before this feature became apparent Li poly[d(A-C)].poly[d(G-T)] fibres were found too deliquescent to be used. C or semi-crystalline B patterns for this fibre were assigned according to the presence or absence of strong intensity on the  $lm-1$  layer line. No attempt has been made to determine any degree of lattice expansion or contraction as a function of relative humidity for this fibre.

Two of the best resolved C diffraction patterns obtained to date for Li poly[d(A-C)].poly[d(G-T)] are shown in Plates 4.6 and 4.7. These were both obtained from the fibre of  $a\text{Cl}^-/\text{PO}_4^- = 0.55$ . Plate 4.6 was recorded at 57% ascending relative humidity and Plate 4.7 at 44% descending relative humidity. An obvious difference between the two diffraction patterns is

%Rh	$a\text{Cl}^-/\text{PO}_4^-$				
	0.00	0.24	0.55	0.82	1.40
44	C	C	Cnm	C	Cnm
57	C	C	C	C+	-
66	C+	C	C	C+	Cnm
75	C+	C	C	C+	Cnm
86	C+	-	C+	m	semi-B
92	C+	C+	C+	semi-B	-
98	semi-B	semi-B	semi-B	-	-
92	C+	m	semi-B	-	-
86	C+	-	m	semi-B	-
75	C+	C+	C	m	Cnm
66	-	-	C	C+	Cnm
57	-	-	C	C+	Cnm
44	-	-	C	Cnm	Cnm

Table 4.2

The occurrence of the C and semi-crystalline B conformations in Li poly[d(A-C)].poly[d(G-T)] fibres as a function of relative humidity and fibre salt content. The symbols m and + are described in the text. No attempt has been made to classify the C conformations of the fibres of  $a\text{Cl}^-/\text{PO}_4^- = 1.4$  in this manner. nm indicates that the pattern was not measured.

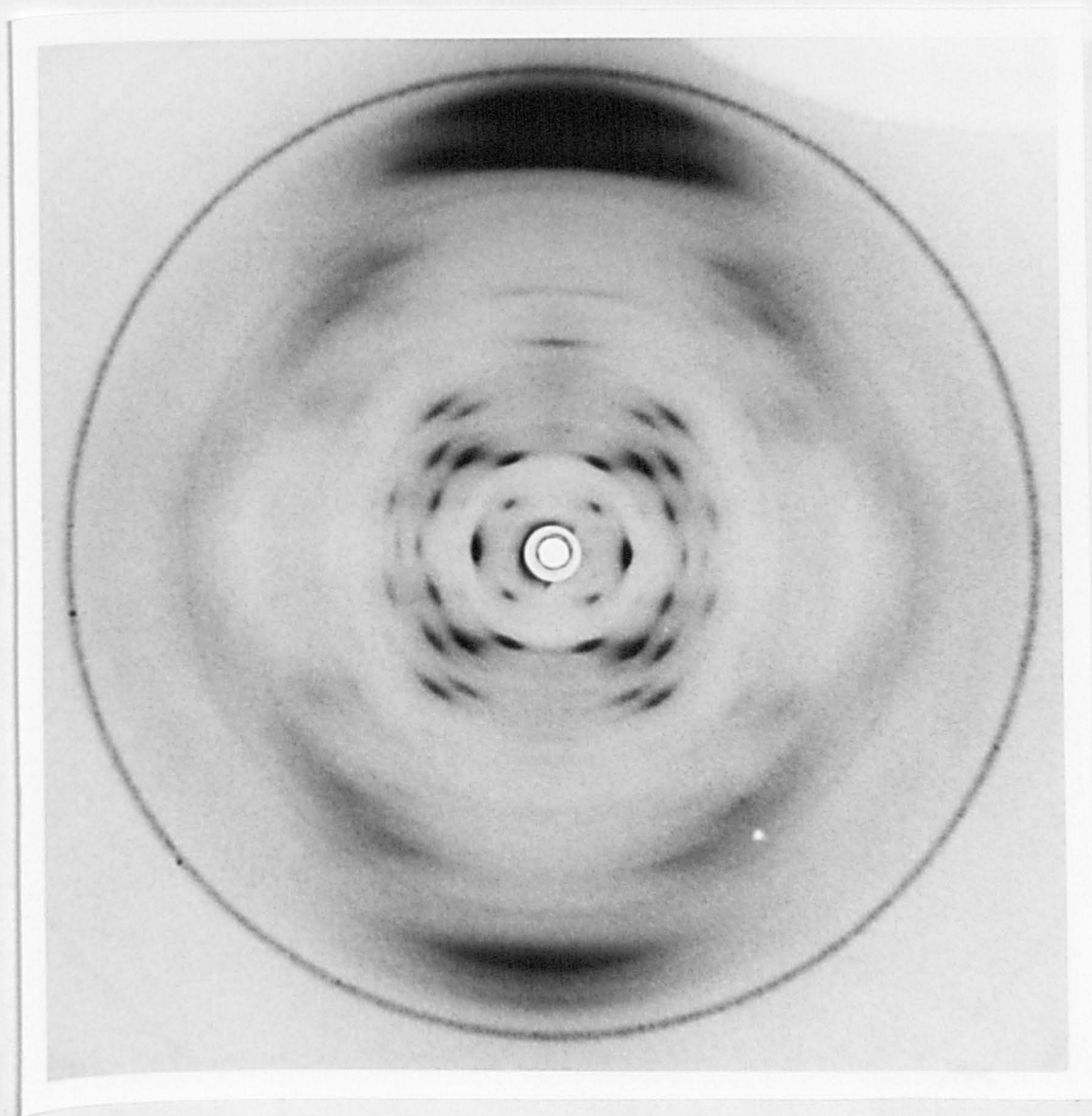


Plate 4.6

Fibre KE 19,  $aCl^-/PO_4^- = 0.55$ ,  $rh = 57\%$ . The fibre is in the C conformation and the molecular packing is hexagonal. Only Bragg reflections are apparent in the central regions of the first and third layer lines.

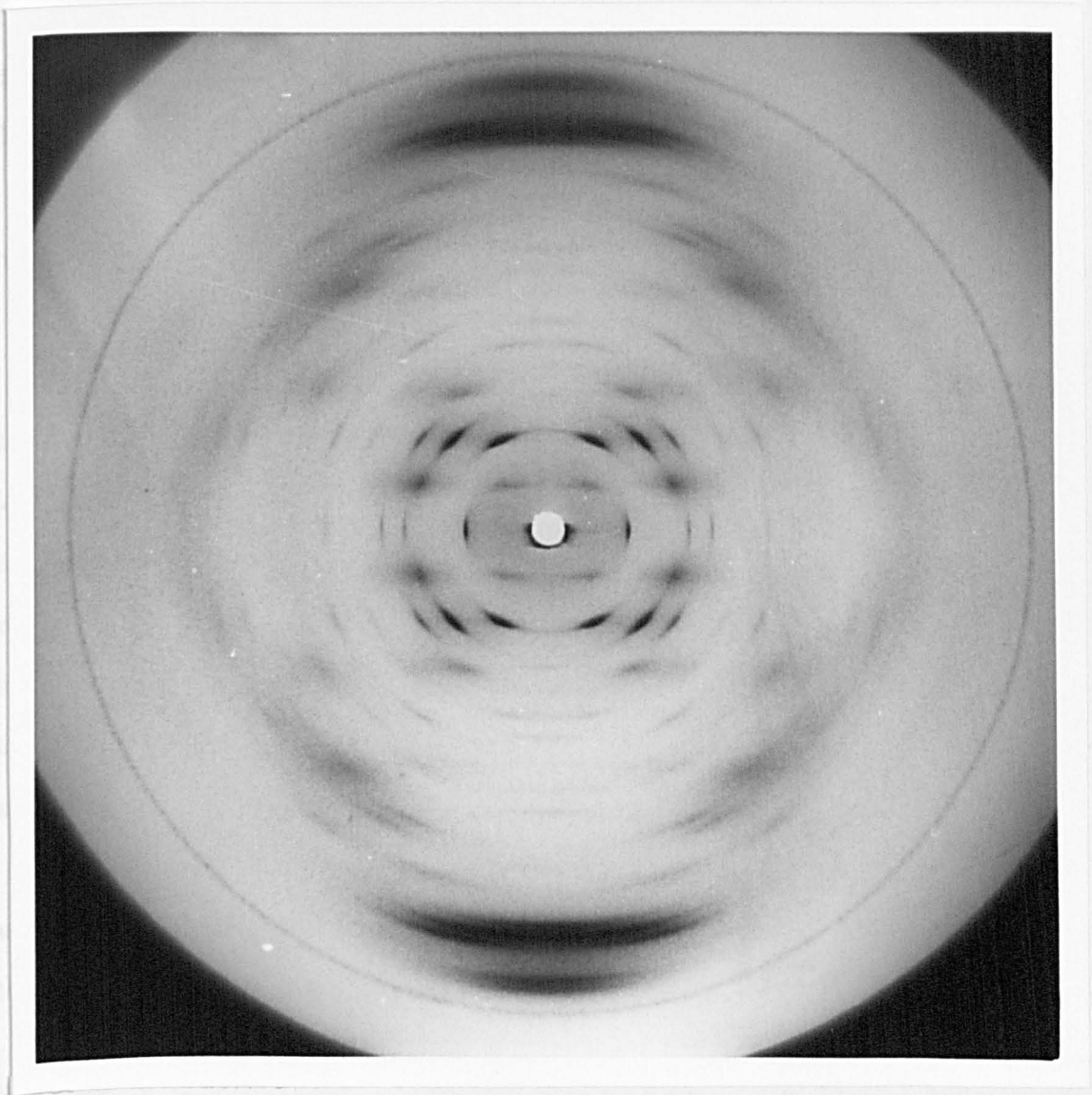


Plate 4.7

Fibre KE 19,  $aCl^-/PO_4^- = 0.55$ , rh = 44% after passing through a relative humidity cycle which reached a maximum of 98%. The fibre is in the C conformation and the molecular packing is hexagonal. Intensity streaks are visible on first, third and fifth layer lines.

the presence of intensity streaks on low numbered odd layer lines as seen in Plate 4.7 where only Bragg reflections are apparent in Plate 4.6. An examination of other diffraction patterns from this fibre showed that intensity streaks first appeared at 86% ascending relative humidity as shown in Plate 4.3 and were present on patterns obtained at 75%, 66%, 57% and 44% descending relative humidity. The intermediate patterns at 92%, 98%, 92% and 86% rh were either semi-crystalline B patterns or closely related to them. Intensity streaks similar to that observed in Plate 4.7 were not apparent in any of the C patterns from fibres of  $aCl^-/PO_4^-$  ratio of 0.0 and 0.82. For the fibres of  $aCl^-/PO_4^- = 0.24$ , some evidence of intensity streaks on the first and third layer lines was observed at 57% and 66% rh. However, the remaining C patterns in this series and those from the fibre of  $aCl^-/PO_4^- = 1.4$  were too diffuse or too weakly exposed to provide information on this phenomenon. Thus only in the patterns from the fibre of  $aCl^-/PO_4^- = 0.55$  were such intensity streaks distinctive and there seems little correlation between the presence of these streaks and relative humidity or fibre salt content. The streaking indicates a tendency for the molecules to be randomly translated by  $\pm 1/2 z$  in the  $z$  direction of the unit cell, Marvin et al., 1961. The presence of faint Bragg reflections superimposed on these streaks in some cases indicates that this random  $z$  translation is not uniform throughout the fibre and that some regions have retained a higher crystalline order.

The patterns shown in Plates 4.6 and 4.7 have been subjected to a more detailed examination.  $x$  and  $y$  coordinates from the diffraction spots of these patterns were measured with the aid of a two dimensional travelling microscope.  $\xi$ ,  $\zeta$ ,  $\rho$ , and  $d$  values were calculated using the computer program 'Film' and  $\xi$ - $\zeta$  plots were constructed for each pattern. Assuming a helical symmetry of  $9_1$ , some reflections were found to occur exactly half way between layer lines and the helical symmetry is thus described as  $9_2$ . In the text, reflections which have so far been referred to by Miller

indices based on a  $9_1$  helical symmetry are henceforth described according to a  $9_2$  helical symmetry. xi-zeta plots for the patterns shown in Plates 4.6 and 4.7, based on a  $9_2$  helical symmetry are given in Figures 4.1 and 4.2 respectively. Both patterns were found to index on an hexagonal system although the higher layer lines of the pattern at 57% rh were not well resolved and could not be indexed unambiguously.  $q$ -spacings of unambiguously identified spots were used in conjunction with their assigned indices to calculate lattice parameters. These were subjected to a cyclic least squares refinement procedure using the computer program 'Hex'. The observed and calculated  $q$ -spacings, together with their assigned Miller indices are given in Tables 4.3 and 4.4. The refined lattice parameters were  $a = 3.480 \pm 0.017\text{nm}$  and  $c = 5.840 \pm 0.028\text{nm}$  for the pattern at 57% rh and  $a = 3.216 \pm 0.004\text{nm}$  and  $c = 5.807 \pm 0.007\text{nm}$  for the pattern at 44% rh. Approximate intensities of the observed reflections have been assigned by eye. These assignments have been included in Figures 4.1 and 4.2 and Tables 4.3 and 4.4.

Apart from the superior crystallinity of the pattern in Plate 4.7 and the presence of intensity streaks on what are now termed the second, sixth and tenth layer lines there is essentially little difference between it and the pattern in Plate 4.6. The xi-zeta plots in Figures 4.1 and 4.2 show good agreement on the zero and fourth layer lines. The difference in the refined lattice parameters is probably due to the difference in relative humidity at which the patterns were recorded. However, it may also occur partly as the result of the random molecular translation by  $\pm 1/2 z$  which allows a smaller  $a$  lattice dimension to be assumed. A comparison of Plates 4.3, 4.4 and 4.6 with 4.1 shows an additional reflection on the second layer line of the latter pattern at  $\xi = 1.09\text{nm}^{-1}$ . This reflection was apparent on patterns of the fibre of  $\text{aCl}^-/\text{PO}_4^- = 0.0$  from 44% to 75% ascending relative humidity and has not been observed on any of the patterns from the other fibres. Measurements suggest that the additional reflection is the 302 reflection, while the two adjacent reflections index as the 202



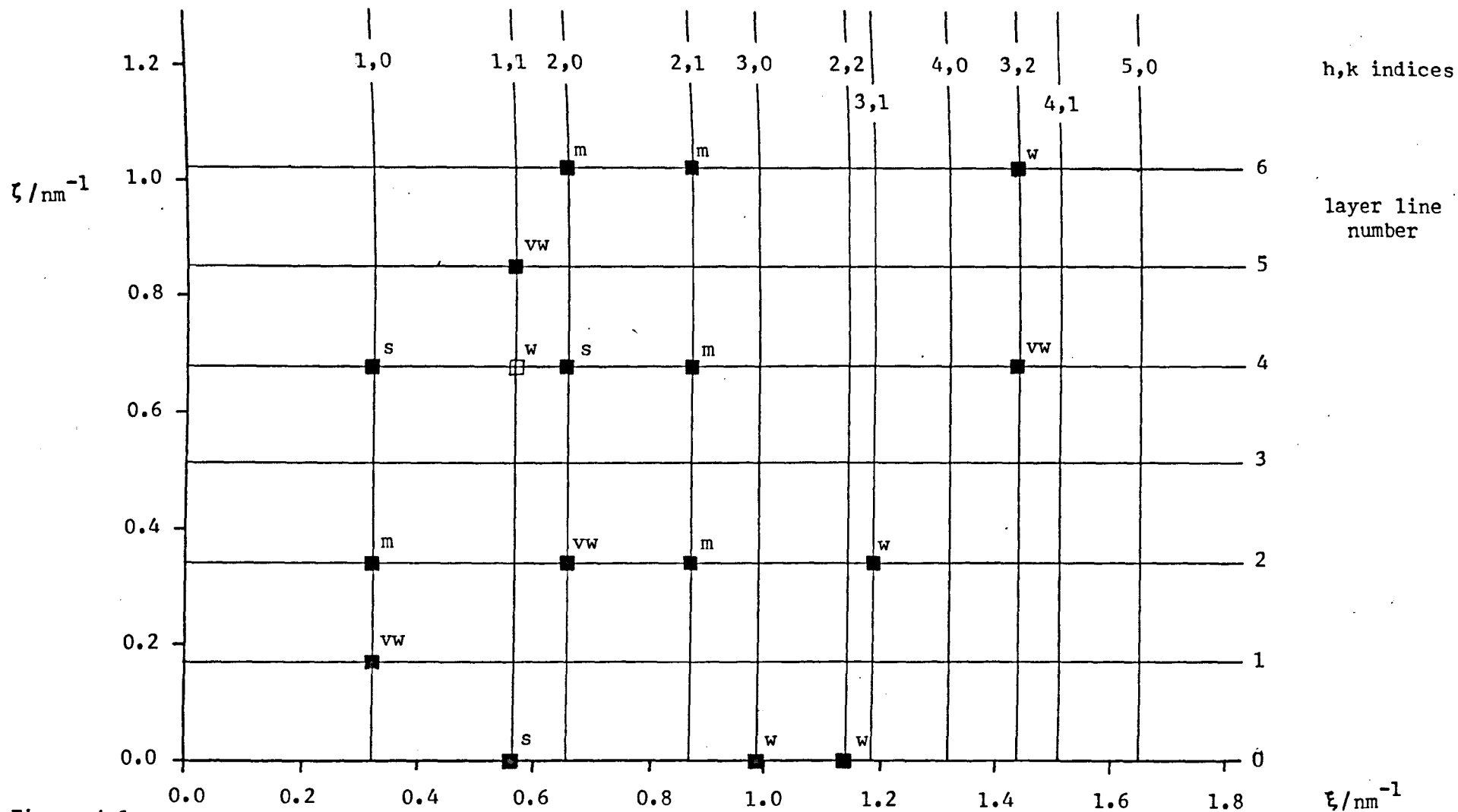


Figure 4.1

A xi-zeta plot of the first six layer lines of the diffraction pattern shown in Plate 4.6. ■, □ indicates the observation of Bragg reflections, while shading indicates the use of the  $q$ -spacing of that reflection in the lattice refinement program. The letters s, m, w or vw indicate the apparent relative intensity of the reflections. The plot corresponds to a hexagonal lattice with  $a = 3.48\text{nm}$  and  $c = 58.4\text{nm}$ .

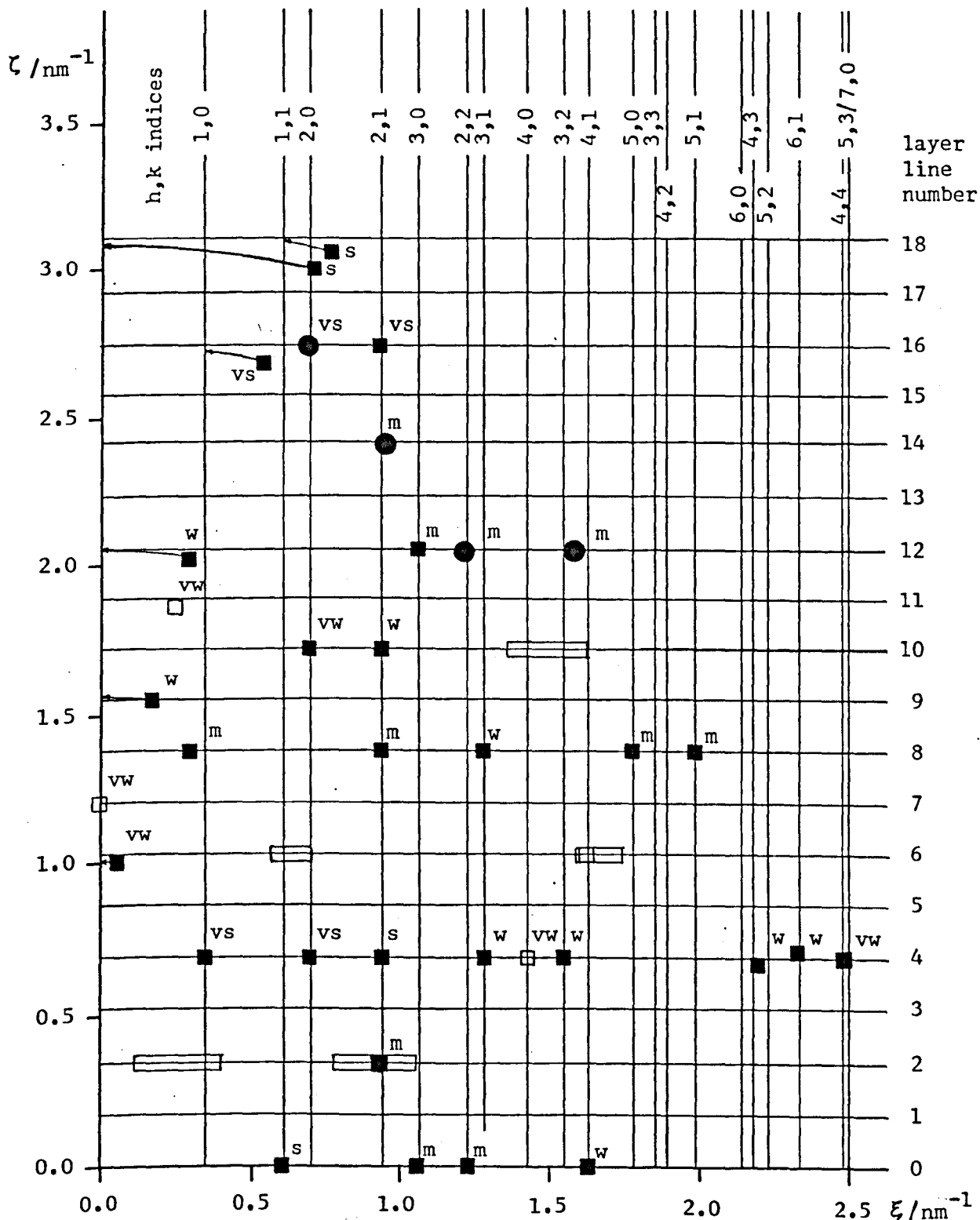


Figure 4.2

A xi-zeta plot of the diffraction pattern shown in Plate 4.7. ■, □ indicates the observation of a Bragg reflection, ●, indicates a broad reflection, ◻, indicates streaked intensity, shading indicates the use of the  $\rho$ -spacing of probable position of a higher layer line reflection. The letters vs, s, m, w and vw refer to the apparent relative intensity of the reflections. The plot corresponds to a hexagonal lattice with  $a = 3.216\text{nm}$  and  $c = 5.807\text{nm}$ .

Assigned h,k,l Value	$\rho$ Observed /nm <sup>-1</sup>	$\rho$ Calculated /nm <sup>-1</sup>	Apparent Relative Intensity
110	0.569	0.575	s
300	0.998	0.995	w
220	1.152	1.149	w
101	0.368	0.373	vw
102	0.474	0.477	m
202	0.751	0.747	vw
212	0.943	0.942	m
312	1.242	1.244	w
104	0.760	0.761	s
114	0.883	-	s
204	0.952	0.954	s
214	1.109	1.113	vw
324	1.598	1.600	vw
115	1.028	1.031	vw
206	1.224	1.223	m
216	1.350	1.351	m
326	1.781	1.774	w
009 or 109	1.550	-	m
1011	1.914	1.912	w
1016 or 1116	2.776	-	s
-	2.863	-	s
-	2.881	-	s
1018 or 1118	3.117	-	s

Table 4.3

Observed and calculated  $\rho$ -spacings together with their assigned Miller indices for the C pattern of Plate 4.6. Also indicated are the corresponding relative intensities.

Assigned h,k,l Value	$\rho$ Observed /nm <sup>-1</sup>	$\rho$ Calculated /nm <sup>-1</sup>	Apparent Relative Intensity
110	0.619	0.622	s
300	1.075	1.077	m
220	1.241	1.244	m
410	1.647	1.645	w
212	1.006	1.010	m
104	0.776	0.777	vs
204	0.994	0.995	vs
214	1.171	1.173	s
314	1.465	1.466	w
404	1.581	-	vw
324	1.708	1.710	w
434	2.296	2.290	w
614	2.461	2.453	w
534 / 704	2.596	2.606	vw
006	1.027	1.033	vw
007	*	-	vw
108	1.422	1.424	m
218	1.672	1.673	m
318	1.888	1.890	w
508	2.269	2.263	m
518	2.430	2.428	m
009	1.556	1.549	w
2010	1.865	1.866	vw
2110	1.970	1.967	w
0011 or 1011	1.909	-	vw
0012	2.067	2.067	w
3012	2.329	2.330	m
2212	2.412	2.412	m
4112	2.636	2.641	m
2114	2.596	2.591	m
1016	2.774	2.779	vs
2016	2.849	2.847	vs
2116	2.918	2.914	vs
0018	3.098	3.100	s
1118	3.161	3.162	s

Table 4.4

Observed and calculated  $\rho$ -spacings together with their assigned Miller indices for the C pattern of Plate 4.7. Also indicated are the corresponding relative intensities. The '\*' denotes that the  $\rho$ -spacing of this reflection was not measured.

and 2 2 2 reflections. At 92% ascending relative humidity and 92%, 86% and 75% descending relative humidities only two of the three reflections were observed. Strong reflections on the equator and fourth layer lines of these patterns indexed according to the xi-zeta plots in Figures 4.1 and 4.2. Why such changes should occur in some patterns of this fibre and not others, or why these changes were not apparent on patterns of other fibres remains unclear.

The analysis of these diffraction patterns is being continued by Mr. T. Forsyth. It will be interesting to further examine the effects of chloride content and relative humidity on the lattice parameters of the C conformation. Mr. Forsyth is involved in intensity measurements of these patterns in order to provide more extensive experimental data for use in model building studies of the C conformation than is currently available.

#### 4.4 Discussion

C and semi-crystalline B diffraction patterns have been obtained from fibres of Li poly[d(A-C)].poly[d(G-T)]. The observation of just these two conformations when Li is the associated cation is in keeping with results from native DNA's, Marvin et al., 1961, Zimmerman and Pfeiffer, 1980, and synthetic polynucleotides, Davies and Baldwin, 1963, Leslie et al., 1980. The A conformation has never been observed for Li DNA's or Li polynucleotides and despite investigation into this apparent anomaly no satisfactory explanation has yet been reported. The A, B and C conformations have been observed for both native Na DNA's and synthetic Na polynucleotides. Additional conformations such as the D and S forms which have been exhibited by Na synthetic polynucleotides have not been observed for their Li counterparts.

The relative humidity and  $a\text{Cl}^-/\text{PO}_4^-$  ratio with which the C and B conformations were observed in fibres of Li poly[d(A-C)].poly[d(G-T)] were similar to that found in fibres of Li calf thymus DNA by Marvin et al., 1961. There was a tendency for semi-crystalline B patterns of Li

poly[d(A-C)].poly[d(G-T)] fibres to be observed at lower relative humidity as the  $aCl^-/PO_4^-$  ratio increased. However, C patterns were obtained from fibres of Li poly[d(A-C)].poly[d(G-T)] at  $aCl^-/PO_4^-$  ratios in excess of those reported by Marvin et al., 1961, for Li DNA. The most crystalline patterns were obtained from fibres of both Li DNA, Marvin et al., 1961 and Li poly[d(A-C)].poly[d(G-T)] at the same  $aCl^-/PO_4^-$  ratio = 0.5.

Fully crystalline B diffraction patterns obtained from Li DNA fibres, by Langridge et al., 1960a, were not apparent for the fibres of Li poly[d(A-C)].poly[d(G-T)] examined in this work. Marvin et al., 1961, has pointed out that while it is possible to obtain crystalline Li DNA patterns from fibres prepared by the addition of lithium chloride solutions to small quantities of chloride free DNA, better patterns were obtained from specimens in which lithium chloride was precipitated with the DNA during preparation. The first of these methods was adopted in the preparation of the Li poly[d(A-C)].poly[d(G-T)] fibres owing to the small quantity of this synthetic polynucleotide available. This method may have resulted in the failure to detect the fully crystalline B patterns for Li poly[d(A-C)].poly[d(G-T)], but in view of the highly crystalline C patterns obtained from fibres of this polynucleotide as seen in Plate 4.6 and 4.7 this supposition seems unlikely. Therefore perhaps the absence of fully crystalline B patterns is related to the more regular structure of the synthetic polynucleotide which has a preferred helical symmetry compared with Li DNA. It is notable that for the five Li synthetic polynucleotides examined by Leslie et al., 1980, no fully crystalline B pattern has been reported.

The size of the unit cell of Li poly[d(A-C)].poly[d(G-T)] in the C conformation changes with relative humidity, but no change was observed in the packing of the molecules which remained hexagonal. In contrast Li C DNA exhibits both hexagonal and orthorhombic packing.

Little variation in pitch was observed in fibres of Li poly[d(A-C)].poly[d(G-T)] in the C conformation as a function of relative humidity

and fibre salt content. The values obtained lie well within the range reported for the C conformation of Li DNA by Marvin et al., 1961, and Zimmerman and Pfeiffer, 1980. The a lattice parameters obtained from the 110 reflections of Li poly[d(A-C)].poly[d(G-T)] C patterns at low relative humidity are similar to those reported by Marvin et al., 1961, and Zimmerman and Pfeiffer, 1980. The a parameters increase with increasing relative humidity to a value of 4.06nm which is well beyond the values obtained for Li C DNA. It is reminiscent of the a value of 4.60nm obtained for hexagonal semi-crystalline B DNA by Langridge et al., 1960a, while the a value obtained for Li poly[d(A-C)].poly[d(G-T)] of 4.32nm which is also supposedly hexagonal semi-crystalline B is more similar. Perhaps this observation lends some weight to the suggestion of Zimmerman and Pfeiffer, 1980, that smooth transitions can occur not only between members of the C family, but also between members of the B and C families.

Hysteresis effects in terms of the type of diffraction pattern obtained as a function of relative humidity have been described by Marvin et al., 1961. In this work there was a distinct tendency for semi-crystalline B diffraction patterns to be observed at lower descending than ascending relative humidities. Despite Marvin et al.'s stipulation that such effects were not removed by equilibrating at constant relative humidity for several days it still seems that the most likely explanation for such effects is the retention of water by the fibres after being subjected to a high humidity environment. Water retention is probably enhanced by the presence of high concentrations of lithium chloride. Irreversible transitions like those found for fibres of Na poly[d(A-C)].poly[d(G-T)] and Na poly[d(A-T)].poly[d(A-T)] described in chapters 3 and 5 respectively have not been observed for fibres of Li poly[d(A-C)].poly[d(G-T)]. These effects have been attributed to inhomogeneous salt distributions within the fibre samples. While such effects have not been apparent in Li poly[d(A-C)].poly[d(G-T)] samples it would be interesting to prepare some Li poly[d(A-C)].poly[d(G-T)]

samples according to the method of Mahendrasingam, 1983, which is described in chapter 5.2. However, it may be that owing to the greater solubility of lithium chloride as opposed to sodium chloride in aqueous solution it is easier to obtain homogeneous salt solutions in lithium chloride fibre samples.

Hexagonal patterns of Li C DNA showed streaks on the first and third layer lines indicating a tendency for the molecules to be translated by  $\pm 0.5$  in the z direction, Marvin et al., 1961. While similar C patterns have been obtained for Li poly[d(A-C)].poly[d(G-T)] fibres not all the C patterns showed this type of disorder. No correlation of this phenomenon with the type of packing, relative humidity or chloride content was apparent.

Minor variations in the C conformation have been denoted by C' or C'' by Leslie et al., 1980. C' has been assigned to C conformations of the synthetic polynucleotides of Li poly[d(A-G-T)].poly[d(A-C-T)] and Li poly[d(G-G-T)].poly[d(A-C-C)] where the helical symmetry is  $9_1$  and probably reflects the trinucleotide repeating base sequence of these structures. C'' has been assigned to the C conformation of Na poly[d(A-G)].poly[d(C-T)] which has a  $9_2$  helical symmetry. This is in contrast to the helical symmetry of  $28_3$  favoured by Marvin et al., 1961, and Arnott and Selsing, 1975, to describe the C conformation of native Li DNA. In this work at least some C patterns of Li poly[d(A-C)].poly[d(G-T)] show  $9_2$  helical symmetry which reflects the dinucleotide repeating base sequence of this structure. However, whether this helical symmetry arises as a result of the difference in electron density of the purine and pyrimidine bases, or whether there is a difference in the sugar phosphate backbone conformation of neighbouring nucleotides, as proposed by Klug et al., 1979, for poly[d(A-T)].poly[d(A-T)], has yet to be determined. In support of the latter suggestion, Leslie et al., 1980, state that the intensities of the additional layer lines on their C'' pattern of Na poly[d(A-G)].poly[d(C-T)] is greater than can be accounted for simply by the chemical nature of the dinucleotide repeat. Intensity



measurements from the Li poly[d(A-C)].poly[d(G-T)] patterns should help to resolve this question.

Plates 4.6 and 4.7 probably represent the most well resolved C patterns yet obtained from natural DNA's or synthetic polynucleotides. The analysis of the intensity distributions of these patterns should help to provide a more accurate model of the C conformation than is currently available. Perhaps a greater understanding of the flexibility of this conformation as a function of relative humidity and  $\text{Cl}^-/\text{PO}_4^-$  ratios may be forthcoming. Further knowledge of the C conformation may be important in view of the potential biological significance of this conformation as implied by the results of chapter 3, Mahendrasingam, 1983, and Rhodes et al., 1982.

Chapter 5. AN INVESTIGATION INTO THE CONFORMATIONAL FLEXIBILITY OF THE SODIUM SALT OF POLY[d(A-T)].POLY[d(A-T)]

5.1 Introduction

The synthetic polynucleotide poly[d(A-T)].poly[d(A-T)] provides a useful comparison with natural DNA's of high adenine and thymine content. Such polynucleotides have the advantage of sequence homogeneity and may provide structural information which is not readily available from the analysis of native random sequence DNA. The structure of poly[d(A-T)].poly[d(A-T)] is of particular biological interest in that it closely approximates to a known satellite DNA found in the crabs of the genus *Cancer*, Sueoka and Cheng, 1962a,b. Another feature of poly[d(A-T)].poly[d(A-T)] is that it binds to the lac repressor of *E.coli* about 100 to 1000 times more strongly than calf thymus DNA, Riggs et al., 1972.

In an x-ray fibre diffraction study Davies and Baldwin, 1963, found that fibres of the sodium salt of poly[d(A-T)].poly[d(A-T)] gave diffraction patterns like those of the A form patterns of Na DNA. This conformation remained stable even at 98% rh, although they concluded that this behaviour was due to fibres of low salt content. One of their preparations of Na poly[d(A-T)].poly[d(A-T)] which gave A form fibres was later found to yield fibres in a new conformation which they designated the D form. Fibres exhibiting the D form were found to do so over a large range in relative humidity of 42%, 66% and 92%. Some fibres of Na poly[d(A-T)].poly[d(A-T)] gave A/D mixtures which after a time generally changed to the D form. The D form was also apparent in ammonium poly[d(A-T)].poly[d(A-T)] fibres although fibres of the sodium salt proved to be more crystalline. That poly[d(A-T)].poly[d(A-T)] could exist in other conformations was demonstrated by the ammonium salt of this polynucleotide which exhibited a C form with the same screw disorder as that of C DNA but with a different lattice arrangement. This material could also be induced into the B form of semi-crystalline Na

DNA by dissolving in a 5% glycerol solution. The lithium salt of this polynucleotide and of a chemically substituted analogue poly[d(A-brU)].poly[d(A-brU)] were shown to exist in a crystalline B conformation with dimensions identical to those of Li DNA. Thus, although the conformational diversity of poly[d(A-T)].poly[d(A-T)] had been established, Davies and Baldwin, 1963, obtained only the A and D conformations for the sodium salt of this synthetic polynucleotide.

In structural studies of alternating purine and pyrimidine sequences Arnott et al., 1974, obtained fibres of Na poly[d(A-T)].poly[d(A-T)] in the D conformation under conditions of minimum retained salt which they stated would normally have yielded the A conformation in DNA fibres. The specimens were more crystalline than those of Davies and Baldwin, 1963, and it was shown that the molecules pack in a tetragonal lattice with unit cell dimensions  $a = 1.70 \pm 0.01 \text{ nm}$  and  $c = 2.43 \pm 0.01 \text{ nm}$  standard deviation. Similar patterns were obtained for poly[d(G-C)].poly[d(G-C)] fibres and Arnott et al., 1974, suggested that the D conformation was not specific to a particular purine-pyrimidine sequence. These authors also stated that the addition of sodium chloride to a fibre in the D conformation induced a change to the B conformation.

Leslie et al., 1980, obtained one fibre of Na poly[d(A-T)].poly[d(A-T)] which gave an A DNA diffraction pattern over a period of six months even at 95% rh. Thus they suggested that there were conditions under which the A conformation of Na poly[d(A-T)].poly[d(A-T)] was stable although they were unable to determine precisely what these conditions were. They also reported D  $\rightarrow$  A  $\rightarrow$  B transitions in one fibre of impure Na poly[d(A-T)].poly[d(A-T)] as the relative humidity of the fibre environment was increased. However, no indication was given of the nature of the impurities in this fibre nor of the quality of the patterns which were obtained. Leslie et al., 1980, concluded that poly[d(A-T)].poly[d(A-T)] normally displayed the B or D conformations in fibres and that the A conformation of this synthetic

polynucleotide was a metastable state which usually changed to the D form after a few days.

With regard to the molecular structure of the D conformation, Arnott et al., 1974, have used their diffraction data in conjunction with linked atom least square refinement methods to propose a right-handed eight fold double helical model with an axial rise per residue of 0.303nm. Sugar pucker and conformational angles were reminiscent of the B conformation of DNA. Arnott et al., 1974, also interpreted data on Na poly[d(I-C)]. poly[d(I-C)] from Mitsui et al., 1970, in terms of a D conformation very similar to that of Na poly[d(A-T)].poly[d(A-T)]. They dismissed the left handed double helical model with unusual furanose ring shapes proposed by Mitsui et al., 1970, as bizarre.

In a survey of duplexes, Gupta et al., 1980, proposed left handed and right handed structures for the A, B and D conformations which were stereochemically satisfactory and in agreement with the observed x-ray intensity data.

Mahendrasingam, 1983, has criticized these models and proposed a new left handed model for the D conformation. The calculated intensity data from this model is in better agreement with the experimental data of Arnott et al., 1974, than that calculated for the previous D models.

An important aspect of nucleic acid conformation is to what extent base sequence and base composition may affect nucleic acid secondary structure. Bram, 1971, Bram and Tougard, 1972 and Bram, 1973, suggested that the detailed secondary structure of DNA in the B conformation is dependent on base sequence and composition. Their conclusion was based on the results of x-ray solution scattering and x-ray fibre diffraction experiments on a wide variety of DNA's of increasing A,T content. Their B type diffraction patterns from oriented DNA's displayed a progressive decrease in intensity of the second layer line with respect to the first and third layer lines as the percentage of A,T increased.

Pilet and Brahms, 1973, investigated the infra red spectra of oriented DNA films of various A,T content containing 3-4% sodium chloride as a function of relative humidity. Normally, these spectra indicated B  $\rightarrow$  A  $\rightarrow$  disordered form transitions as the relative humidity was reduced. However, they found that it was much more difficult to obtain the A conformation in DNA samples of high A,T content. For crab satellite DNA which contains more than 95% A,T they observed only the B  $\rightarrow$  disordered form transition. They concluded that base composition was probably an important factor in the B  $\rightarrow$  A transition.

In an x-ray diffraction investigation of *C. perfringens* DNA (A,T = 68%) and *C. johnsonii* DNA (A,T = 65%) Selsing and Arnott, 1976, observed only the 'orthodox' A and B conformations for these DNA's. However, fibres of *C. perfringens* DNA which had not been purified were found to give patterns resembling semi-crystalline B DNA but with a low pitch of 0.329nm. They suggested that such patterns may be due to the presence of teichoic acid contaminant. They concluded that the conformations adopted by these DNA's were not significantly affected by their high A,T content. Their results showed that DNA's of high A,T content could adopt the A conformation but they did not exclude the possibility of base composition affecting the ease with which the A  $\rightleftharpoons$  B transition occurs as suggested by Brahms et al., 1973.

In an x-ray fibre diffraction study of satellite DNA's from *G. lateralis*, *D. virilis* and *M. musculus*, Selsing et al., 1976, observed only the classical DNA duplex structures. In particular crab satellite DNA was found to exhibit a stable A conformation under appropriate conditions. Selsing and Arnott, 1976, stated that so far only poly(dA).poly(dT), poly[d(A-T)].poly[d(A-T)], which they suggest is metastable in the A conformation and changes to the D form in time, poly[d(G-C)].poly[d(G-C)] and poly[d(A-T-T)].poly[d(A-A-T)] have not been found in the A conformation.

Goodwin, 1977, examined x-ray diffraction patterns from fibres of *M. lysodeikticus* (A,T = 28%), calf thymus (A,T = 60%) and *C. perfringens*.

(A,T = 69%) DNA's and poly[d(A-T)].poly[d(A-T)]. The fibres were prepared from gels centrifuged from solutions of 2mM Tris.HCl pH 7.6 and 5mM, 10mM, 20mM or 50mM NaCl. Goodwin did not find any distinct new conformations of DNA. The A  $\rightleftharpoons$  B transition was observed in all fibres except those of *C. perfringens* at the highest concentration of retained salt. Generally the A conformation persisted at higher relative humidities for fibres of low retained salt as expected from the results of Cooper and Hamilton, 1966. For some fibres of calf thymus and *C. perfringens* DNA Goodwin obtained B patterns of low pitch and intermolecular spacing. In some of these cases the second layer line intensity was enhanced with respect to those of the first and third layer lines when compared with classical semi-crystalline B patterns. For the natural DNA's Goodwin did not observe any enhancement in intensity of the first and third layer lines of his B patterns as reported by Bram and Tougard, 1972, and Bram, 1973. He pointed out that such changes had only been observed in poorly oriented fibres. He suggested that such changes may be caused by (dA)<sub>n</sub>.(dT)<sub>n</sub> regions in the fibres assuming a B' conformation, Arnott and Selsing, 1974, but that such an effect was unlikely to be apparent in patterns of well oriented fibres. Goodwin only prepared fibres of Na poly[d(A-T)].poly[d(A-T)] from a gel centrifuged from solutions containing 2mM sodium chloride. One such fibre at 44% rh was found to give a semi-crystalline B like diffraction pattern with a low pitch of 3.1nm. At 75% rh this fibre exhibited an A diffraction pattern which remained stable as the relative humidity was returned to 44%. As the relative humidity was again increased the A conformation persisted up to 92% rh and at 98% rh a semi-crystalline B conformation was observed. Goodwin reported that this latter pattern did show some increase in intensity of the first and third layer lines with respect to the second compared with the intensity distribution normally observed. No specific suggestions were put forward to explain this result.

Leslie et al., 1980, found that B diffraction patterns from oriented

polycrystalline specimens of poly[d(I-I-T)].poly[d(A-C-C)], poly[d(A-C)].poly[d(G-T)] and poly[d(G-C)].poly[d(G-C)] gave identical distributions of intensity over successive layer lines to that observed from fibres of calf thymus DNA, in spite of the wide variation in base composition. They found this was true even for the polynucleotide complexes poly[d(G-C)].poly[d(G-C)] and poly[d(A-C)].poly[d(G-T)] which crystallise in much larger unit cells. However, they did observe intensity variations analogous to those of Bram and Tougard, 1972, in B patterns which were oriented but not polycrystalline. Leslie et al., 1980, pointed out that although such less well ordered systems may have sequence or composition variants of the B conformation, it is also true that different semi-crystalline packing arrangements of isomorphous molecules would produce the observed modulations of intensity.

An investigation has been initiated into the conformational flexibility of the sodium salt of the synthetic polynucleotide poly[d(A-T)].poly[d(A-T)] in a similar manner to that carried out for the sodium and lithium salts of poly[d(A-C)].poly[d(G-T)]. Only a single fibre has been examined in these experiments, but the x-ray diffraction patterns were particularly well defined and a number of interesting features have emerged. Investigations of Na poly[d(A-T)].poly[d(A-T)] structure have been further extended by Mahendrasingam, 1983, in terms of nucleic acid conformation as a function of excess fibre salt content and his results are summarised. The initial data collected from the single x-ray fibre sample was shown to be representative of Mahendrasingam's results. Conditions for the observation of the C, A,  $\alpha$ -B', semi-crystalline B and D conformations are described and an equation is proposed to relate the transitions between these conformations.

The biological significance of the Na poly[d(A-T)].poly[d(A-T)] conformations are considered with regard to satellite DNA and in the enhanced binding of the lac repressor of E. coli. The difficulties of determining the effects of base sequence and base composition on nucleic acid

conformation in relation to Na poly[d(A-T)].poly[d(A-T)] are also discussed.

## 5.2 Materials and methods

The sodium salt of poly[d(A-T)].poly[d(A-T)] was prepared at Paris University VII by Dr. G.J. Brahms and Mr. J. Vergne as described in chapter 2.1. A small portion of the final poly[d(A-T)].poly[d(A-T)] precipitate was dissolved in distilled water to form a gel as described in chapter 2.4. No sodium chloride solutions were added to the gel as it dried. The resultant fibre was particularly transparent, had a thickness of 145 $\mu$ m and a birefringence of -0.056. The clarity of the interference fringes of this fibre during birefringence measurements is shown in the photomicrograph reproduced in Plate 2.2. From this one fibre a number of x-ray diffraction patterns have been recorded at various relative humidities using Franks optics.

In continuing this work Mahendrasingam, 1983, used a different method of fibre preparation. Na poly[d(A-T)].poly[d(A-T)] prepared by Dr. G.J. Brahms and Mr. J. Vergne or purchased from Boehringer was dissolved at a polynucleotide concentration  $\sim 1.0 \text{ mg ml}^{-1}$  in deionized water or saline solutions ranging from 1mM to 50mM NaCl. These solutions were centrifuged at 50,000 rpm for 12 hours in a 3 x 3 ml swinging bucket rotor using a superspeed 50 TC MSE centrifuge. An estimate of the excess sodium chloride per phosphate in the resultant gels was obtained from the polynucleotide concentration in the solutions prior to centrifugation and the polynucleotide concentration,  $\text{Na}^+$  concentration and volume of the supernatants. The polynucleotide concentration was measured by U.V. absorption spectroscopy and  $\text{Na}^+$  concentration was measured by flame emission spectroscopy.

Owing to the small quantities of Na poly[d(A-T)].poly[d(A-T)] available,  $\text{Na}^+$  concentrations were determined from F.E.S. measurements on the supernatants of the polynucleotide solutions after centrifugation. Since poly[d(A-T)].poly[d(A-T)] may retain a higher salt concentration in



the sedimented gel than is present in the supernatant after centrifugation, this  $\text{Cl}^-/\text{PO}_4^-$  ratio is not necessarily the total  $\text{Cl}^-/\text{PO}_4^-$  in the polynucleotide gel or resultant fibres. It is thus given the suffix c to distinguish it from the a $\text{Cl}^-/\text{PO}_4^-$  ratios described in chapters 3 and 4 and the total  $\text{Cl}^-/\text{PO}_4^-$  ratios described in chapter 6. Fibres were made from these gels as described in chapter 2.4 and x-ray diffraction patterns were recorded using pinhole and toroidal optics.

Once sufficient fibres had been made from a given gel its c $\text{Cl}^-/\text{PO}_4^-$  ratio could be reduced by redissolving it in distilled water and recentrifuging. Mahendrasingam has not yet estimated the error in determining c $\text{Cl}^-/\text{PO}_4^-$  ratios using this method. He suggests that such errors arise largely from the inhomogeneous distribution of excess sodium chloride in the centrifuged gels. Nevertheless his work represents a more extensive analysis of the effects of sodium chloride on Na poly[d(A-T)].poly[d(A-T)] conformation than has so far been reported.

### 5.3 Results

Two component diffraction patterns were obtained from the Na poly[d(A-T)].poly[d(A-T)] fibre at 57%, 66% and 75% rh and an example is shown in Plate 5.1. These patterns were very similar to those obtained from fibres of Na poly[d(A-C)].poly[d(G-T)] to which no salt had been added. The predominant component in these patterns is characteristic of the A conformation of DNA. The quality of these types of patterns is rather poor, but the positions of six spots were measured from the pattern shown in Plate 5.1 using a Stoe film measuring device. Within the limits of experimental error the positions of these spots were found to agree with  $\rho$ -spacings obtained from the A conformation of calf thymus DNA, Fuller, 1961. The minor component of these patterns is represented by the first equatorial reflection at  $1.775 \pm 0.01\text{nm}$  and an intense meridional reflection at  $0.335 \pm 0.01\text{nm}$ . Comparing these types of patterns with those obtained

Plates 5.1 - 5.9 : X-ray diffraction patterns of the sodium salt of poly[d(A-T)].poly[d(A-T)] fibres.

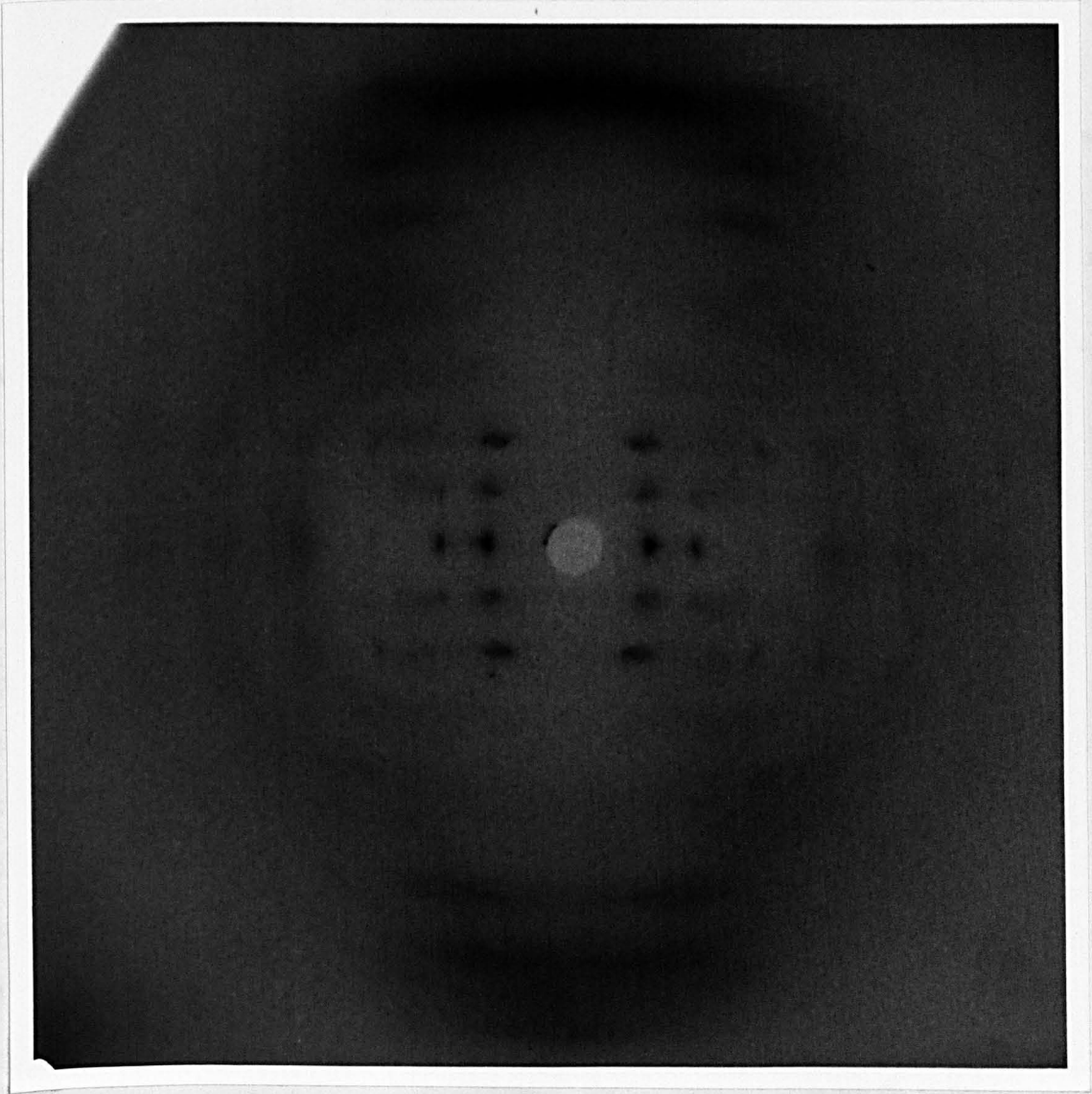


Plate 5.1

Fibre SP 16 at 66% rh. A two component diffraction pattern which is predominantly in the A conformation but has in addition an equatorial reflection at 1.78nm and an intense meridional reflection at 0.335nm.

from Na poly[d(A-C)].poly[d(G-T)] and with later patterns of Na poly[d(A-T)]. poly[d(A-T)] by Mahendrasingam, 1983, it appears likely that this minor component is representative of the C conformation of Na poly[d(A-T)]. poly[d(A-T)].

At 92% rh the minor component of the previous diffraction patterns disappeared and a remarkably well characterised A pattern was obtained similar to that shown in Plate 5.2. As the relative humidity was decreased patterns were recorded at 75%, 66% and 57% rh. They showed an improvement in the molecular orientation within the fibre as evidenced by a decrease in the length of arc of individual diffraction spots, but the A conformation remained stable. Thus the A/C  $\rightarrow$  A transition in this Na poly[d(A-T)]. poly[d(A-T)] fibre was irreversible with respect to relative humidity as was the case for fibres of Na poly[d(A-C)].poly[d(G-T)].

At 44% rh the diffraction pattern indicated a collapse of the A structure as shown in Plate 5.3. Similar patterns have been observed for fibres of Na DNA, Mahendrasingam, 1983, and Na poly[d(A-C)].poly[d(G-T)], Plate 3.6, under conditions of low relative humidity and salt content. In particular Plate 5.3 shows diffraction spots only in the centre of the pattern while reflections at high  $\rho$ -spacings are much less well resolved compared with the patterns at higher relative humidities. There is also an apparent reduction in the intensity of the seventh layer line of Plate 5.3. The first equatorial reflection of the higher humidity A patterns is hardly visible and is not due to diffraction from the A lattice, but may arise from a small fraction of the material being in the B or C conformations. In Plate 5.3 the intensity of this reflection is greatly enhanced. This effect may be due in part to more parasitic scatter in the centre of Plate 5.3, but the apparent increase in intensity of this reflection seems to be more than can be accounted for by this explanation. The d-spacing corresponding to this reflection was  $1.98 \pm 0.05$ nm and did not change as the relative humidity of the fibre environment was reduced from 92% to 44%.

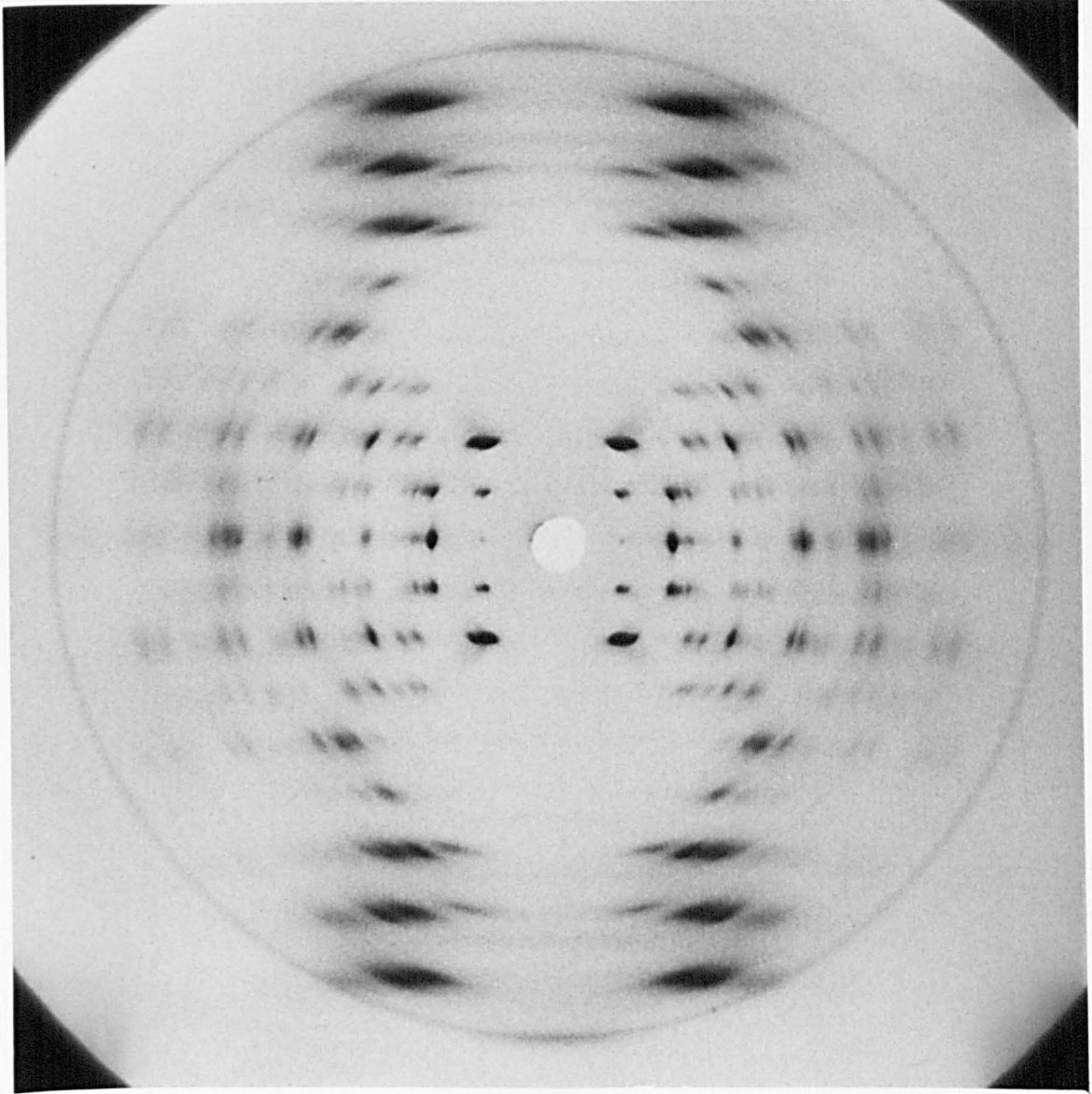


Plate 5.2

Fibre SP16 at 75% rh. The fibre is in the A conformation with good orientation and crystallinity. The concentric ring at 0.3035nm on this and subsequent patterns is due to calcite.

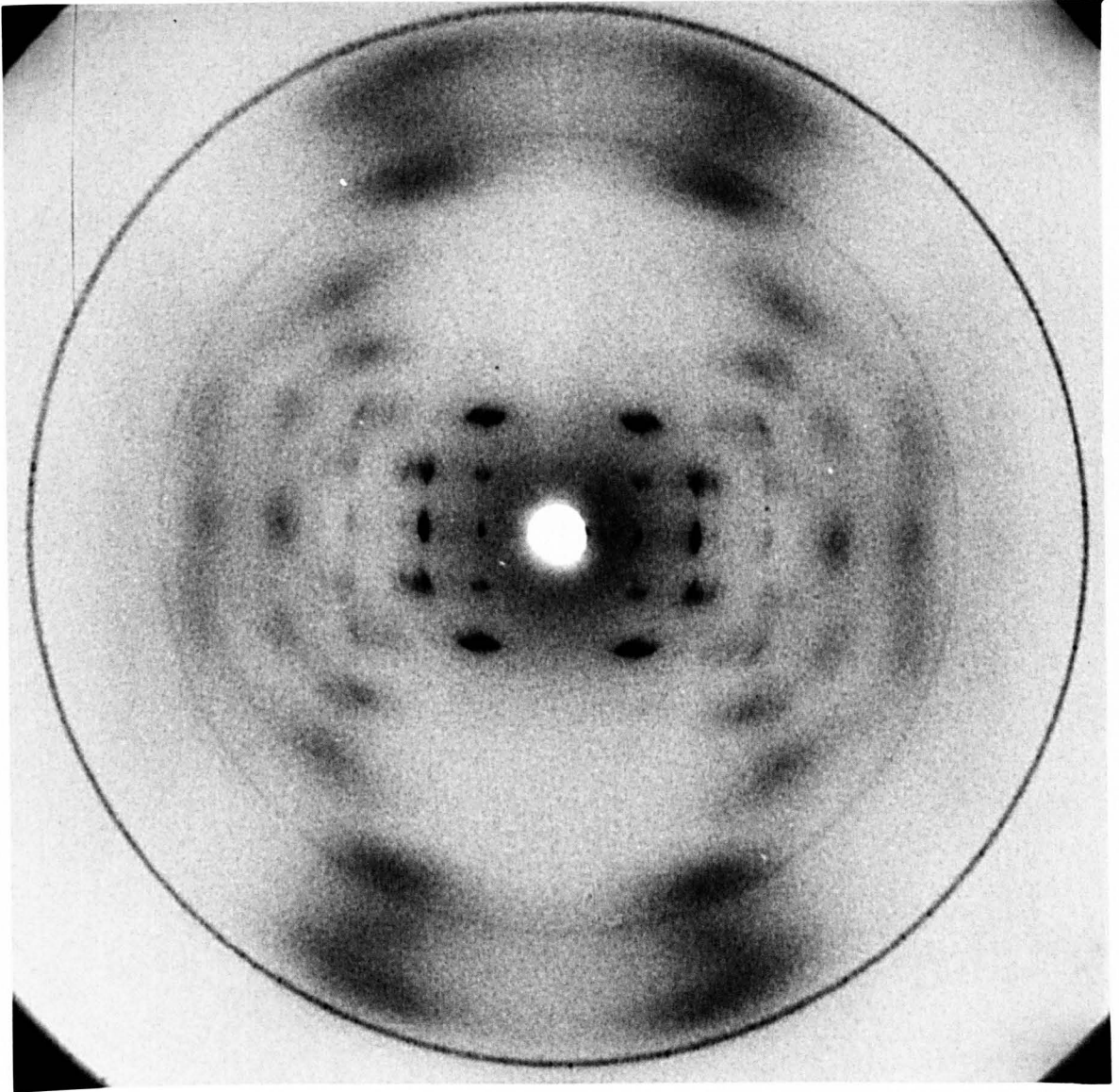


Plate 5.3

Fibre SP 16 at 44% rh. Under these conditions the A lattice is beginning to collapse.

This spacing is just beyond the range of 1.66-1.90nm found for the  $d_{110}$  spacings of the C conformation of Li poly[d(A-C)].poly[d(G-T)] fibres described in chapter 4. It may well indicate the presence of the C conformation in some regions of the fibre.

The fibre was next subjected to a relative humidity of 92% and the completely crystalline A pattern was recovered. At 98% rh a second multi-component diffraction pattern was obtained as shown in Plate 5.4. Again the predominant component contributing to this pattern is that of A. The minor component is most obviously represented by intensity streaks on layer lines one, two and three which are at a smaller reciprocal spacing than the layer lines of the A lattice. There are spots on the first and second of these layer lines at  $\rho = 0.054 \pm 0.006 \text{nm}^{-1}$  and  $\rho = 0.075 \pm 0.004 \text{nm}^{-1}$  respectively. There is an intense meridional reflection at  $0.331 \pm 0.007 \text{nm}^{-1}$  and a weak reflection which is also apparently meridional at  $3.25 \pm 0.13 \text{nm}^{-1}$ . In addition there are two equatorial reflections at  $2.11 \pm 0.06 \text{nm}^{-1}$  and  $2.46 \pm 0.19 \text{nm}^{-1}$ . All of these reflections are extraneous to those associated with the A lattice. The layer line streaks are often seen in conjunction with A DNA diffraction and are usually associated with a semi-crystalline B conformation. In this case the streak layer line spacing indicates a pitch of  $3.25 \pm 0.13 \text{nm}$  which together with the meridional reflection at  $0.331 \pm 0.007 \text{nm}^{-1}$  is in accordance with a ten fold helix. However, the Bragg reflection on the first layer line of the minor component is not normally seen in semi-crystalline B DNA. A diffraction pattern from the fibre which was more completely in the phase represented by the minor component of Plate 5.4 was later obtained. It was shown to represent the modified B conformation,  $\alpha\text{-B}'$ , which was first observed in Na'poly(dA).poly(dT) by Arnott and Selsing, 1974. However, this explanation does not account for the equatorial reflection at  $2.46 \text{nm}^{-1}$  or the meridional intensity on the first layer line streak. The former reflection may be due to a partial semi-crystalline B packing arrangement within the fibre. Thus the diffraction

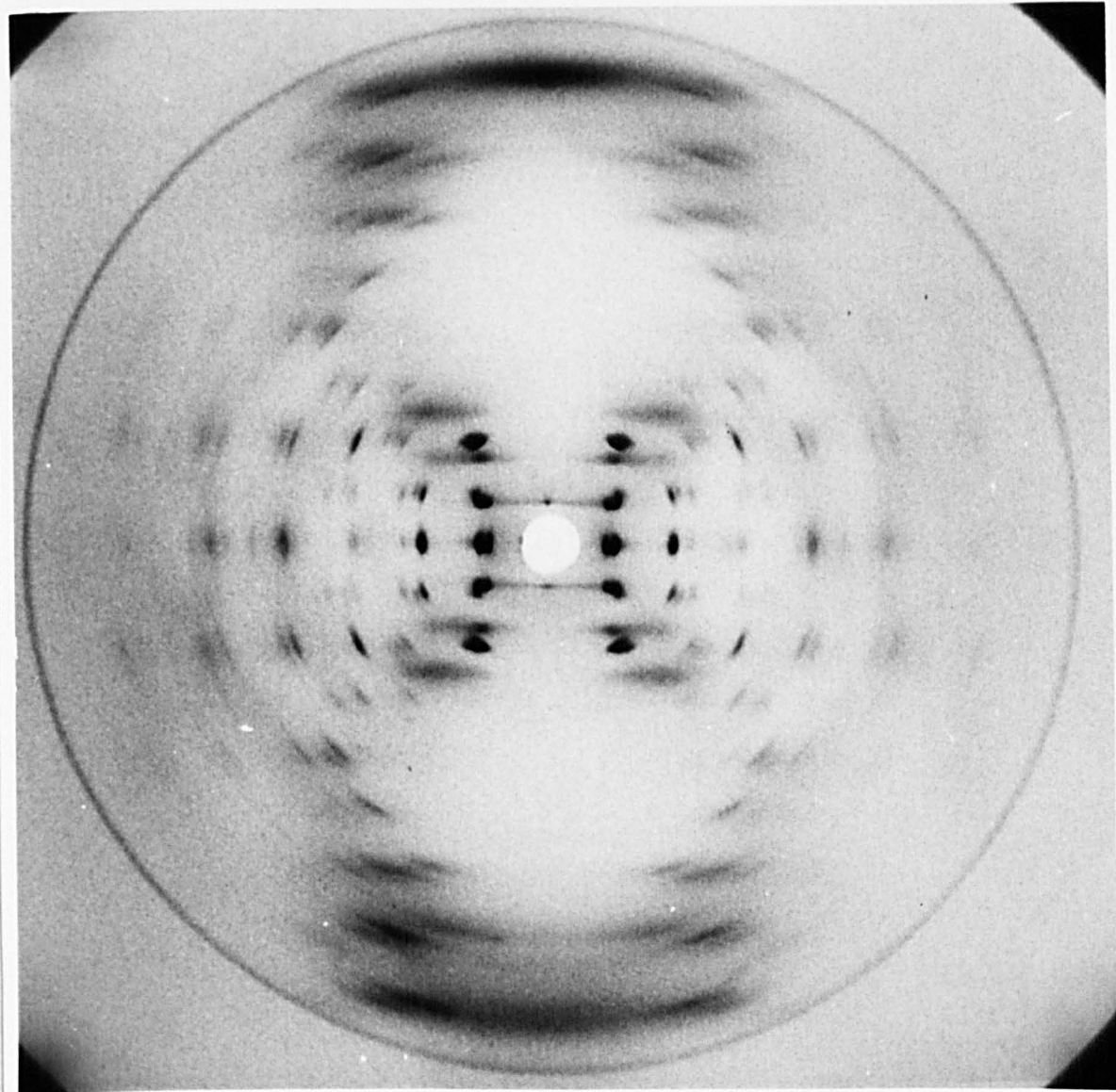


Plate 5.4

Fibre SP 16 at 98% rh. A multicomponent diffraction pattern which is predominantly A. The streaks in the centre of the pattern, the intense meridional reflection at 0.33nm and the first two equatorial reflections are probably representative of the  $\alpha$ -B' and semi-crystalline B conformations.

pattern shown in Plate 5.4 represents a fibre exhibiting at least three different conformations. The meridional reflection at 3.25nm has been observed on several other diffraction patterns from this fibre as shown in Plates 5.5, 5.6, 5.7 and 5.8. It probably arises as a result of  $\text{Na}^+$  associated with the polynucleotide double helix whose z coordinates differ by exactly one pitch length.

In an attempt to induce the fibre to completely adopt the  $\alpha\text{-B}'$  conformation it was sealed in a pinhole camera and humidified at 98% rh for  $\sim 8$  days. The fibre was then transferred to a Franks camera and humidified for a further 10 hours at 98% rh before commencing the exposure. An  $\alpha\text{-B}'$  type pattern was obtained with no A component present, but the overall intensity of the pattern was weak. This procedure was repeated twice more in order to obtain a more clearly defined pattern. The first of these repeats again resulted in a weakly exposed  $\alpha\text{-B}'$  pattern while the next pattern much more closely resembled the semi-crystalline B structure of Na calf thymus DNA as shown in Plate 5.5.

An exposure was then recorded at 95% rh as shown in Plate 5.6. This represents the best  $\alpha\text{-B}'$  pattern of Na poly[d(A-T)].poly[d(A-T)] obtained to date. In order to confirm the assignment of  $\alpha\text{-B}'$  to this pattern x and y coordinates of the diffraction spots from the negative of Plate 5.6 were measured with the aid of a two dimensional travelling microscope.  $\zeta$ ,  $\xi$ ,  $\rho$  and d-spacings were calculated for each reflection using the computer program 'Film'. With this information a xi-zeta plot was constructed and the lattice was shown to index on a hexagonal system. A xi-zeta plot of the first three layer lines of Plate 5.6 is given in Figure 5.1. The  $\rho$ -spacings of the unambiguously identified spots were used in conjunction with their assigned Miller indices to calculate lattice parameters. These were subjected to a cyclic least squares refinement procedure using the computer program 'Hex'. The observed and refined  $\rho$ -spacings together with their assigned Miller indices are given in Table 5.1. The refined lattice



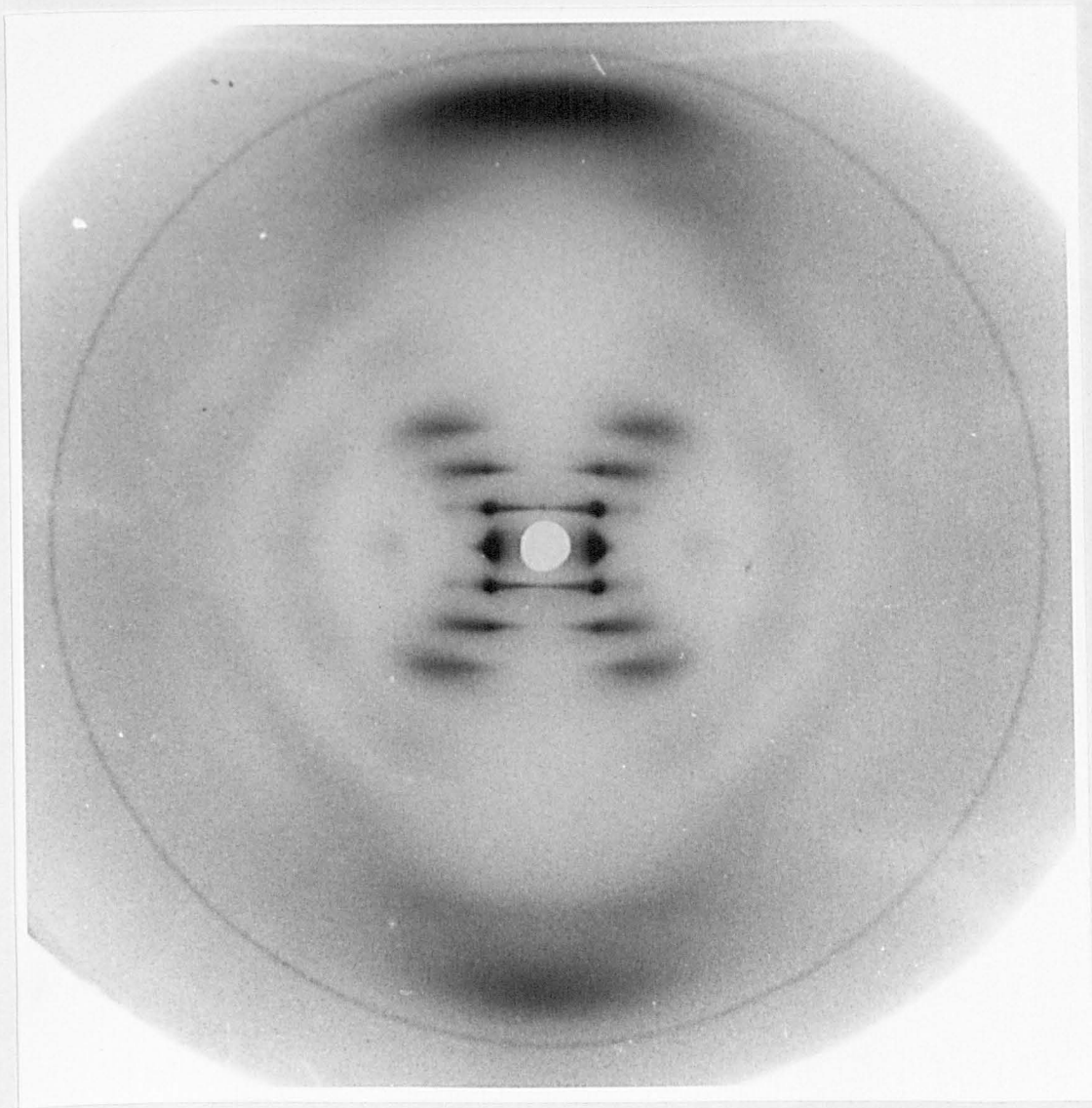


Plate 5.5

Fibre SP 16 at 98% rh. This diffraction pattern is much more similar to that of semi-crystalline B calf thymus DNA than to the  $\alpha$ -B' pattern of Plate 5.6.

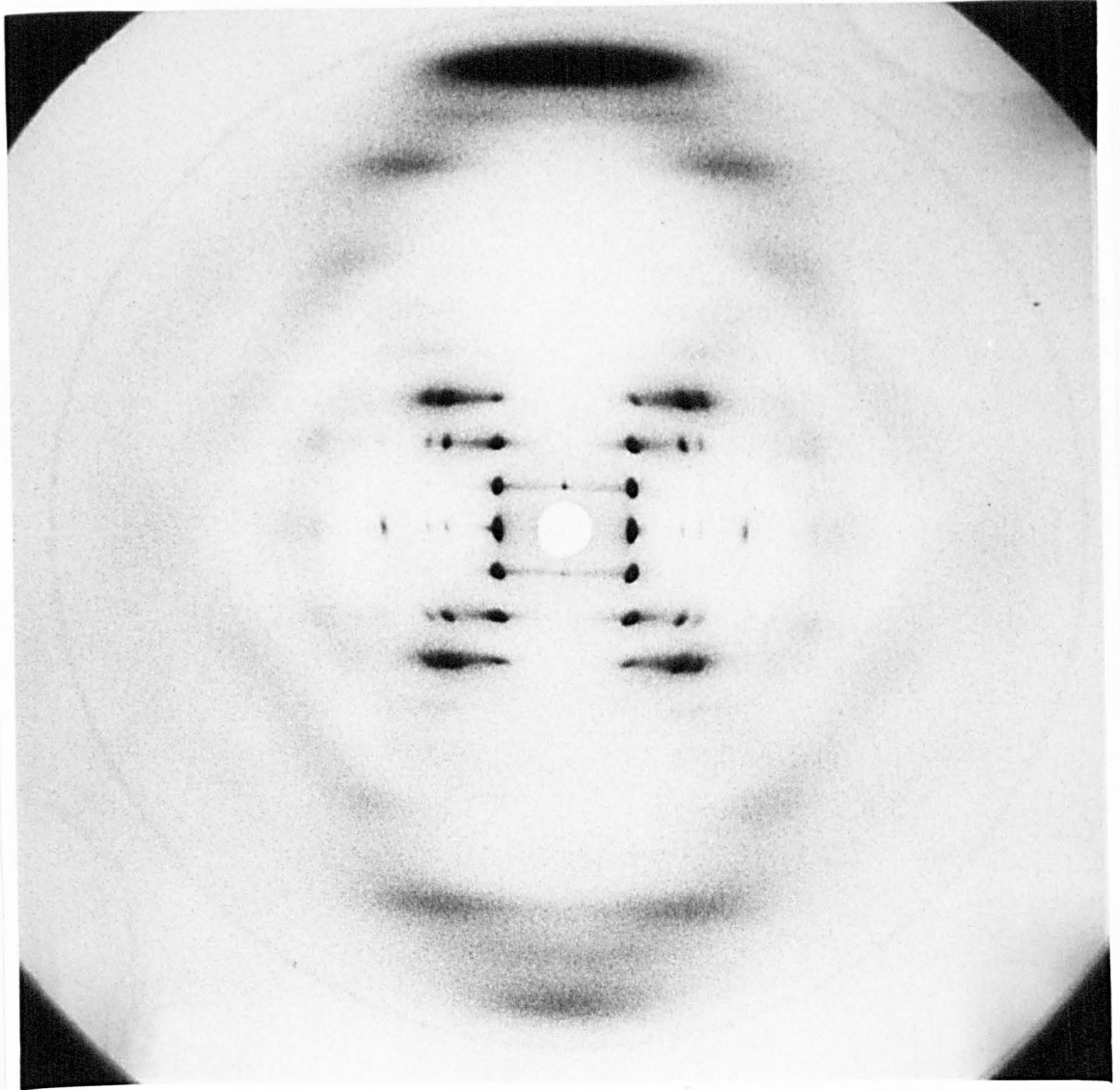


Plate 5.6

Fibre SP 16 at 95% rh. An  $\alpha$ -B' diffraction pattern which closely resembles the  $\alpha$ -B' pattern of Na poly(dA).poly(dT), Arnott and Selsing, 1974.

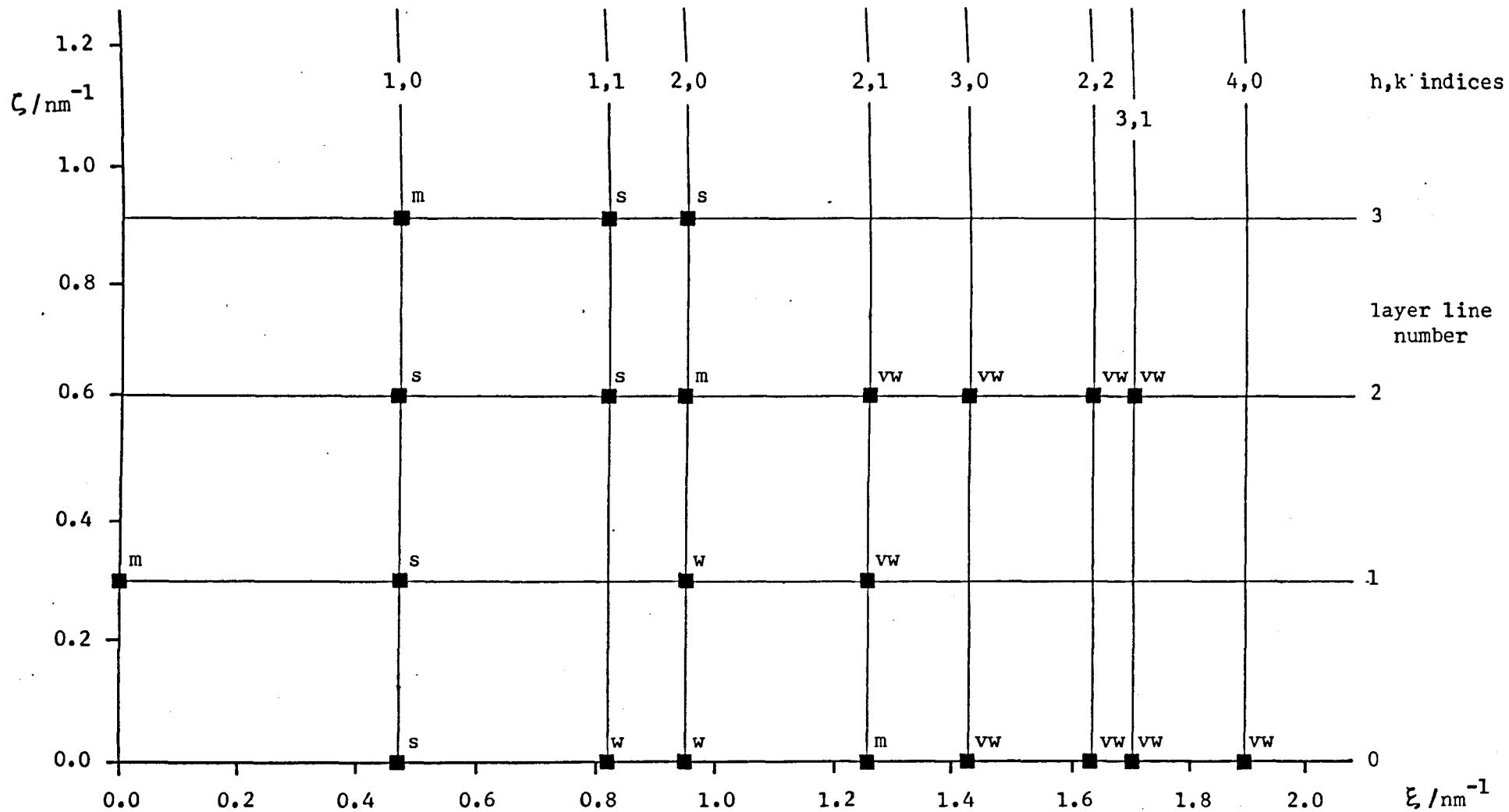


Figure 5.1

A xi-zeta plot of the first three layer lines of the diffraction pattern shown in Plate 5.6. ■ indicates the observation of a Bragg reflection while the letters s, m, w or vw indicate the apparent relative intensity of that reflection. The plot indexed on the basis of a hexagonal lattice with  $a = 2.46\text{nm}$  and  $c = 3.28\text{nm}$ .

Assigned h,k,l Value	$\rho$ Observed /nm <sup>-1</sup>	$\rho$ Calculated /nm <sup>-1</sup>	Apparent Relative Intensity	Intensity of $\alpha$ -B' Conf. Arnott and Selsing, 1974
100	0.470	0.473	s	3.2
110	0.818	0.819	w	1.2
200	0.946	0.945	w	1.3
210	1.252	1.251	m	2.0
300	1.412	1.418	vw	-
220	1.632	1.638	vw	1.3
310	1.711	1.704	vw	2.4
400	1.892	1.891	vw	-
001	0.310	0.305	m	-
101	0.561	0.562	s	3.7
201	0.998	0.993	w	-
211	1.290	1.287	vw	-
102	0.770	0.771	s	2.8
112	1.021	1.021	s	2.0
202	1.125	1.125	m	1.6
212	1.391	1.391	vw	1.8
302	1.546	1.543	vw	1.9
222	1.741	1.747	vw	1.9
312	1.812	1.810	vw	2.7
103	1.027	1.029	m	3.1
113	1.224	1.227	s	5.4
203	1.319	1.315	s	4.9
114	-	-	-	1.5
204	-	-	-	1.9
214	-	-	-	2.4

Table 5.1

The observed and calculated  $\rho$ -spacings together with their assigned Miller indices for the  $\alpha$ -B' pattern of Na poly[d(A-T)].poly[d(A-T)] shown in Plate 5.6. Also given are the corresponding relative intensities of the reflections on a scale s, m, w and vw. These are compared with the observed relative intensities of the  $\alpha$ -B' conformation of Na poly(dA).poly(dT) obtained by densitometry by Arnott and Selsing, 1974. These values have been truncated for convenience.

parameters were  $a = 2.457 \pm 0.009\text{nm}$  and  $c = 3.281 \pm 0.012\text{nm}$ . Measurements of the intense meridional reflection gave an axial rise per residue of  $0.328 \pm 0.004\text{nm}$  thus confirming a ten fold helix. These parameters are in good agreement with the values of  $a = 2.279 \pm 0.006\text{nm}$ ,  $c = 3.287 \pm 0.007\text{nm}$  and an axial rise per residue of  $0.324\text{--}0.329\text{nm}$  given for the  $\alpha\text{-B}'$  conformation of Na poly(dA).poly(dT) by Arnott and Selsing, 1974. Moreover, intensities have been assigned by eye to the reflections observed on the diffraction pattern reproduced in Plate 5.6. These assignments are in qualitative agreement with the densitometry data of Arnott and Selsing, 1974, as shown in Table 5.1. Thus although quantitative intensity measurements have not yet been carried out it seems certain that Plate 5.6 represents an  $\alpha\text{-B}'$  conformation of Na poly[d(A-T)].poly[d(A-T)] which is very similar to that observed by Arnott and Selsing, 1974, for Na poly(dA).poly(dT) and subsequently found for Na poly(dI).poly(dC) and Na poly[d(A-I)].poly[d(C-T)] by Leslie et al., 1980.

On lowering the humidity of the fibre environment to 92% an A/ $\alpha\text{-B}'$  diffraction pattern was once more obtained. However, in this case, the axes of the A and  $\alpha\text{-B}'$  lattices were no longer coincident as in Plate 5.4 but were offset at an angle of  $6 \pm 1^\circ$  as shown in Plate 5.7. This exposure was repeated and the direction of the fibre axis was inscribed on the negative. This result suggested that the lattice axis coincident with the fibre axis was that of the  $\alpha\text{-B}'$  lattice. In this second exposure the angle between the two axes had decreased to  $3.5 \pm 1^\circ$ . It is perhaps significant that in the monoclinic unit cell of A DNA  $\beta = 97^\circ$ , although why this feature should apparently manifest itself in some A/ $\alpha\text{-B}'$  diffraction patterns and not others remains unclear. Mahendrasingam, 1983, recorded two further diffraction patterns from this fibre at 92% rh which were A/ $\alpha\text{-B}'$  mixtures, but no difference was apparent in the axes of the two components in either pattern.

Mahendrasingam, 1983, has investigated the conformations available to

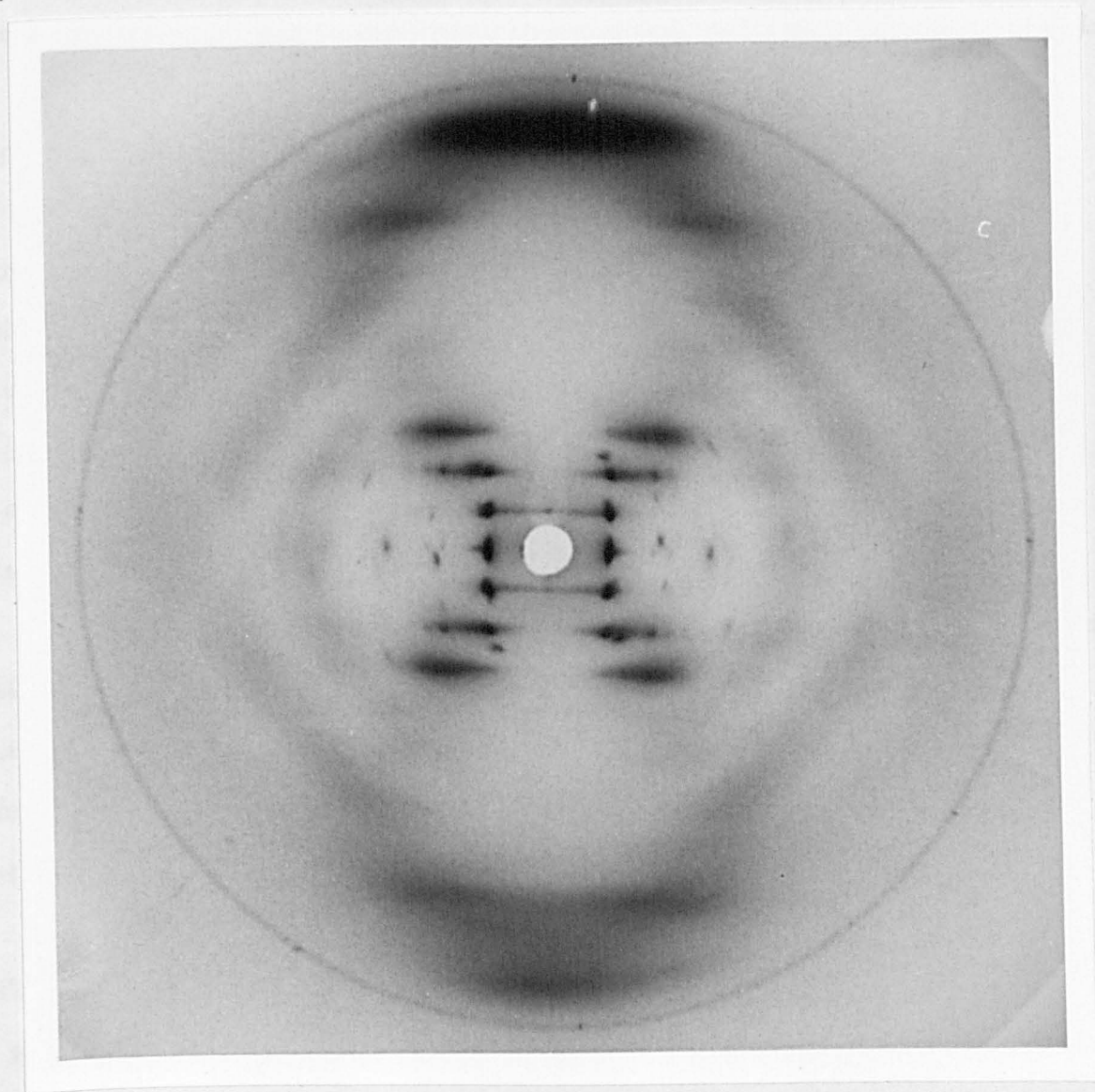


Plate 5.7

Fibre SP 16 at 92% rh. Another A/ $\alpha$ -B' diffraction pattern but in this case the axes of the two lattices are offset by  $6 \pm 1^\circ$ .

Na poly[d(A-T)].poly[d(A-T)] as a function of fibre salt content using the method described in section 5.2. He found that fibres containing  $\text{cCl}^-/\text{PO}_4^-$  ratios  $\geq 1.0$  gave patterns dominated by diffraction from salt crystallites. For fibres containing  $\text{cCl}^-/\text{PO}_4^-$  ratios  $\sim 0.6$  A diffraction patterns were observed at low humidities  $\sim 32-75\%$ , while at higher humidities in the region of  $75-92\%$  diffraction patterns were A/ $\alpha$ -B' or A/B mixtures. Prolonged exposure of these fibres to higher humidities of  $92\%$  or  $95\%$  resulted in a transition to the D conformation as shown in Plate 5.8. At  $98\%$  rh such fibres exhibited the semi-crystalline B conformation. Reduction of the relative humidity below  $98\%$  resulted in a reversion to the D conformation which then persisted even when the relative humidity was as low as  $32\%$ . Other fibres with concentrations of excess salt in this range assumed the D conformation over a period of a few months without being subjected to high humidities.

For fibres containing  $\text{cCl}^-/\text{PO}_4^-$  ratios  $\sim 0.4$  the sequence of transitions was similar to that described above except that at low humidities the patterns were A/C mixtures which changed to A patterns  $\sim 66-75\%$  rh. Transitions from A patterns to A/ $\alpha$ -B' or A/B mixtures also occurred at rather higher relative humidities.

Fibres containing  $\text{cCl}^-/\text{PO}_4^-$  ratios  $< 0.2$  gave C patterns from  $33-75\%$  or  $92\%$  rh as shown in Plate 5.9, above which they changed reversibly into the  $\bar{B}$  form. Neither A nor D conformations were observed for these fibres.

For the A, semi-crystalline B and C diffraction patterns lattice geometries and intensity distributions did not differ significantly from those observed for the natural Na DNA's. Orientation and crystallinity were generally very good although the C patterns were not so well defined as those of Na poly[d(A-C)].poly[d(G-T)], for example Plate 3.7. In the case of the D patterns the crystallinity was significantly better than has previously been reported. In particular the meridional reflection on the eighth layer line could be clearly distinguished from neighbouring reflections while the

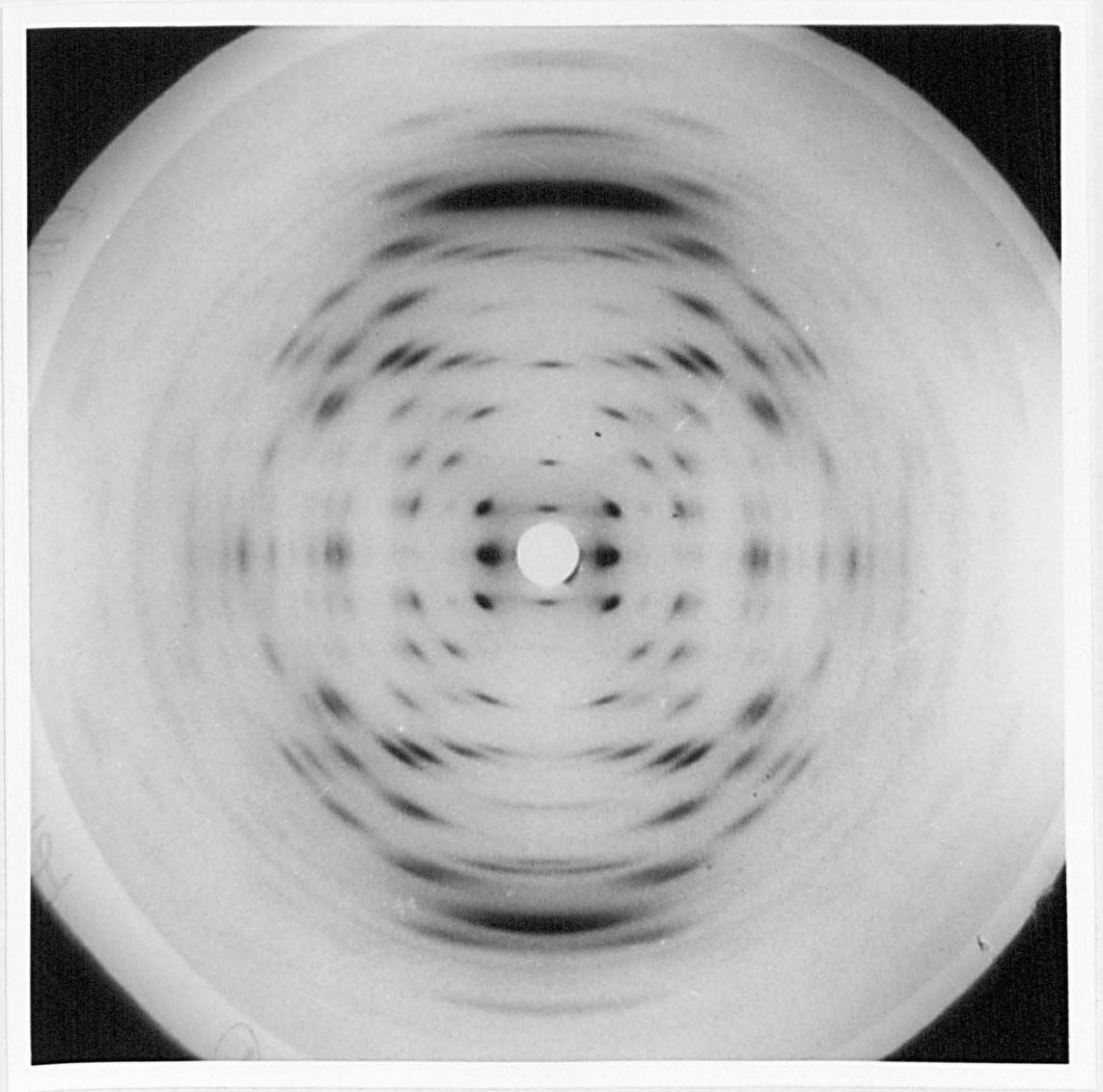


Plate 5.8

A fibre at 95% rh in the D conformation, courtesy of Mahendrasingam, 1983.



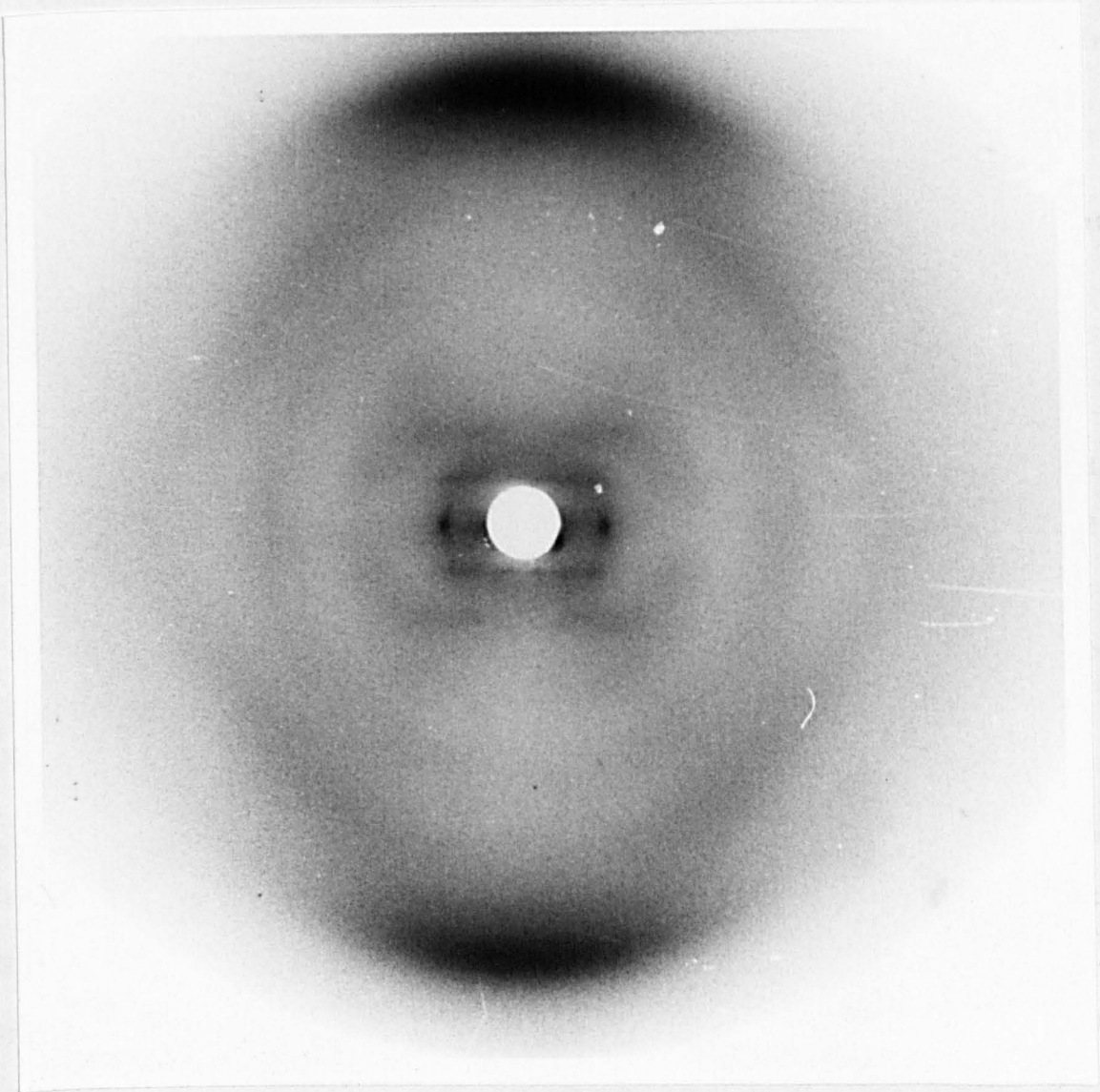


Plate 5.9

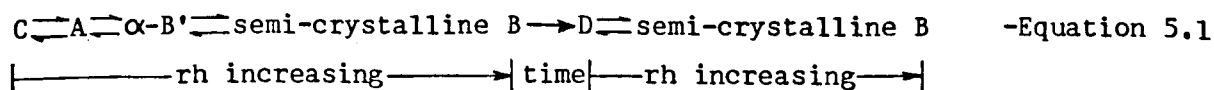
A fibre at 57% rh,  $cCl^-/PO_4^- \sim 0.2$ . This fibre is completely in the C conformation, courtesy of Mahendrasingam, 1983.

crystallinity was so high that sharp reflections were observed at spacings as low as 0.25nm.

#### 5.4 Discussion

X-ray diffraction patterns from the single fibre described in the first part of section 5.3 indicate that the C, A,  $\alpha$ -B' and semi-crystalline B conformations are all available to Na poly[d(A-T)].poly[d(A-T)]. The observation of these conformations is supported by the results of Mahendrasingam, 1983, who has also observed a transition to the D conformation for this polynucleotide. These conformations have all been observed for the sodium cation and this serves to underline the complex diversity of nucleic acid structure when subjected to even very mild environmental changes. Thus Na poly[d(A-T)].poly[d(A-T)] is shown to exhibit the C and  $\alpha$ -B' conformations in addition to those found by Davies and Baldwin, 1963, Arnott et al., 1974, and Leslie et al., 1980.

The fibre in the first section of these results probably has an excess salt content  $> 0.6 \text{ cCl}^-/\text{PO}_4^-$  when compared with Mahendrasingam's results. The diffraction patterns from this fibre together with the results of Mahendrasingam, 1983, have established a specific sequence of conformational transitions in Na poly[d(A-T)].poly[d(A-T)] fibres as a function of relative humidity, excess salt content within the fibre and time. This sequence is shown in Equation 5.1. Which part of this sequence is observed depends on



the excess salt content within a fibre sample. This overall sequence of transitions is able to explain the A  $\rightarrow$  D transitions observed by Davies and Baldwin, 1963, and the D  $\rightarrow$  B transitions of Arnott et al., 1974. However, no evidence has been obtained for the D  $\rightarrow$  A  $\rightarrow$  B transitions as a function of increasing relative humidity reported by Leslie et al., 1980.

For fibres containing  $\text{cCl}^-/\text{PO}_4^- < 0.2$  Mahendrasingam has observed a

departure from this general equation where transitions from the C to the B conformation occur directly. This is a particularly interesting observation and may provide a basis for explaining why fibres of Li DNA or Li polynucleotides do not exhibit the A conformation. Obviously the complete phase diagram of Na poly[d(A-T)].poly[d(A-T)] conformation as a function of  $cCl^-/PO_4^-$  ratio and relative humidity is more complicated than is represented by Equation 5.1. It is hoped that this equation may provide a basis for a more complete explanation of the conformational transitions which occur in this intriguing polynucleotide.

The C conformation has again emerged as a conformation which is available to the sodium salt of a polynucleotide and this further supports the view that the C conformation may be of fundamental biological significance. The C type diffraction patterns are reminiscent of the low pitch B patterns with enhanced intensity on the second layer line as described by Goodwin, 1977, for some natural DNA's of high A,T content. The C conformation may also be representative of the disordered form of DNA described by Pilet and Brahms, 1973.

The irreversible nature of the A/C  $\rightarrow$  A transition at 92% rh for the single fibre of Na poly[d(A-T)].poly[d(A-T)] parallels the A/C  $\rightarrow$  A and C  $\rightarrow$  A transitions found in Na poly[d(A-C)].poly[d(G-T)] fibres described in chapter 3. However, it contrasts with the reversible A/C  $\rightleftharpoons$  A and C  $\rightleftharpoons$  A transitions of native Na DNA and Na poly[d(A-T)].poly[d(A-T)] fibres reported by Mahendrasingam, 1983. The reason for this discrepancy is probably due to the difference in sample preparation. Fibres which exhibited irreversible transitions were all prepared directly from solid polynucleotide. Initially this may have given rise to inhomogeneous distributions of salt within the fibres as discussed in chapter 3.4. Fibres exhibiting reversible transitions were all prepared by the centrifugation technique. Thus in retrospect the observation of the first A/C patterns like that in Plate 5.1 is probably fortuitous. Without such patterns further investigations of fibres with

lower salt content would not have been carried out.

The A conformation of Na poly[d(A-T)].poly[d(A-T)] has been regarded as a metastable state by Arnott et al., 1974. In this work the A conformation of Na poly[d(A-T)].poly[d(A-T)] has been observed over a wide range of conditions for considerable periods of time. This is in agreement with the results of Davies and Baldwin, 1963, and Leslie et al., 1980. Thus the importance of the A conformation of Na poly[d(A-T)].poly[d(A-T)] should not be underestimated. Of specific interest with regard to the A conformation of Na poly[d(A-T)].poly[d(A-T)] is the particularly well resolved diffraction patterns which have been described as representative of a dehydrated A lattice. An example is shown in Plate 5.3. A more complete analysis including intensity measurements of these types of patterns is necessary. Such an analysis may yield information as to whether these patterns represent some intermediate state between that of the A and C conformations. If this is the case it may be possible to obtain some knowledge of the mechanism by which the  $A \rightleftharpoons C$  transition occurs.

This work represents the first reported observation of the  $\alpha$ -B' conformation for Na poly[d(A-T)].poly[d(A-T)]. This observation is important to the question of the effects of sequence specificity on nucleic acid conformation. Leslie et al., 1980, suggested that the observation of the B' conformation for Na poly(dA).poly(dT), which was not apparent for the corresponding alternating co-polymer, was evidence of a base sequence effect. The present results render this suggestion questionable.

The semi-crystalline B conformation of Na poly[d(A-T)].poly[d(A-T)] appears under conditions of highest humidity and excess fibre salt content with which it was possible to discern distinctive diffraction patterns. This is in agreement with the results of Arnott et al., 1974, and Leslie et al., 1980, and is generally the case for the sodium salts of natural DNA's and synthetic polynucleotides.

With regard to the D form of Na poly[d(A-T)].poly[d(A-T)] the results

presented here are in agreement with the work of Davies and Baldwin, 1963, Arnott et al., 1974, and Leslie et al., 1980, in suggesting that this conformation is particularly stable. Once the D form has been assumed in a given fibre it remains over a wide range of relative humidity and the A and C conformations have not been reobtained. The assumption of the D form has been facilitated by raising the relative humidity of the fibre environment to 92% or more when there are moderate amounts of excess salt in the fibre and also by leaving fibres for substantial periods of time (~months) at more moderate humidities.

If the conventional right-handed models for the A conformation, Fuller et al., 1965, and the B conformation, Langridge et al., 1960b, Arnott and Hukins, 1972, 1973, are considered in association with the left-handed model of the D conformation proposed by Mahendrasingam, 1983, then the conformational changes involving the  $A \rightarrow D$  or  $D \rightleftharpoons B$  transitions are extremely complex since they involve a change in the handedness of the helix. A similar transition involving the reversal of the handedness of the helix occurs during the  $B \rightarrow S$  transition, Arnott et al., 1980, Leslie et al., 1980. This latter transition is further complicated by the accompanying change in the orientation of half of the nucleosides which change from the anti to the syn conformation. A series of changes which would account for the transition between a right-handed A or B conformation and a left-handed D conformation has been proposed by Mahendrasingam, 1983. The complexity of these conformational changes may be the reason why Na poly[d(A-T)]. poly[d(A-T)] apparently becomes locked in the D conformation. Such a stable conformation may well be exploited in biological processes which involve alternating A,T sequences in native DNA.

Arnott et al., 1974, have suggested a specific area in which such a stable conformation may be exploited and this is concerned with satellite DNA. In section 5.1 attention was drawn to the close approximation of crab satellite DNA to Na poly[d(A-T)].poly[d(A-T)]. Satellite regions of DNA are

usually clustered near the centromere regions of the chromosome and Hearst et al., 1973, have suggested that these regions may be responsible for the maintenance of the structural integrity of the chromosome. The ability of such regions to maintain a conformation like that of the D conformation which is distinct and not normally available to random sequence DNA could be an important aspect of the role which satellite DNA plays in the function of the genome. The lack of preference of Na poly[d(A-T)].poly[d(A-T)] to persist in the A conformation is in keeping with its importance in a structural rather than a transcriptional role. Although crab satellite DNA is not typical of other satellite DNA's it may be that these DNA's also have unusual molecular geometries and further structural investigations may be important in elucidating their function.

A second area in which the conformational flexibility of Na poly[d(A-T)].poly[d(A-T)] may be biologically exploited involves the enhanced binding of the lac repressor of *E. coli* to Na poly[d(A-T)].poly[d(A-T)]. In order to account for this phenomenon Klug et al., 1979, have proposed an alternating B structure for this polynucleotide. Their model was inspired by the crystal structure of the tetranucleotide [d(A-T)]<sub>2</sub>·[d(A-T)]<sub>2</sub> by Viswamitra et al., 1978. It involves a normal phosphodiester linkage between the adenine and thymine bases, but has an unusual linkage between the thymine and adenine bases specifically in the conformation of the O<sub>3</sub>'-P bond. Klug et al., 1979, quote evidence from the digestion of synthetic poly[d(A-T)].poly[d(A-T)] by pancreatic DNAase I, nmr data from oligonucleotides and fibre x-ray diffraction studies on Li poly[d(A-T)].poly[d(A-T)] by Davies and Baldwin, 1963, to support their contention that the difference in the binding of lac repressor to poly[d(A-T)].poly[d(A-T)] is due to a difference in sugar phosphate backbone conformation rather than due directly to the base sequence. The question arises as to whether the α-B' conformation of Na poly[d(A-T)].poly[d(A-T)] is associated with the alternating B model proposed by Klug et al., 1979. The x-ray diffraction

pattern of the  $\alpha$ -B' conformation reproduced in Plate 5.6 shows enhancement in intensity on the higher ordered, even numbered layer lines as suggested by Klug et al., 1979, for the Li poly[d(A-T)].poly[d(A-T)] B patterns of Davies and Baldwin, 1963, in support of a dinucleotide repeating unit. However, the  $\alpha$ -B' conformation is also observed for the corresponding homopolymer Na poly(dA).poly(dT) by Arnott and Selsing, 1974. In this case there is no reason to assume the existence of an alternating deoxyribose phosphate backbone. Thus there seems little likelihood that the B' conformation is a candidate for the alternating B model of Klug et al., 1979. The semi-crystalline B patterns of Na poly[d(A-T)].poly[d(A-T)] provide a relatively small amount of information and it is not possible to say whether they are representative of an alternating B structure. In order to investigate the alternating B structure further it is necessary to examine diffraction patterns from the lithium salt of poly[d(A-T)].poly[d(A-T)]. In view of the highly resolved patterns which were obtained from Li poly[d(A-C)].poly[d(G-T)] it may well be possible to obtain Li poly[d(A-T)].poly[d(A-T)] patterns which are of superior quality to those of Davies and Baldwin, 1963. More detailed diffraction data may well strengthen the case for an alternating B conformation for poly[d(A-T)].poly[d(A-T)] and provide a basis for a detailed refinement of the structure. Ideally it would be desirable to obtain fully crystalline B diffraction data from the sodium salt of poly[d(A-T)].poly[d(A-T)] as was obtained for Na poly[d(A-C)].poly[d(G-T)] by Leslie et al., 1980.

The effect of base sequence and base composition on nucleic acid secondary structure in terms of x-ray fibre diffraction has centred on the changes in the biologically relevant B conformation as a function of A,T content of the sample, Bram and Tougaard, 1972. During the course of this investigation of Na poly[d(A-T)].poly[d(A-T)] no semi-crystalline B patterns have been observed with intensity distributions markedly different from those of calf thymus DNA reported by Langridge et al., 1960a. Selsing and

Arnott, 1976, Selsing et al., 1976, Goodwin, 1977, and Leslie et al., 1980, have examined semi-crystalline patterns from a wide range of synthetic and natural DNA's of various A,T content and are in agreement with these observations. However, both Goodwin, 1977, and Leslie et al., 1980, have examined oriented but non-crystalline B patterns of synthetic polynucleotides with an enhancement of intensity on the first and third layer lines as described by Bram and Tougard, 1972. Goodwin, 1977, has proposed that such intensity distributions in B patterns may arise due to  $(dA)_n \cdot (dT)_n$  regions adopting a B' conformation like that of poly(dA).poly(dT), Arnott and Selsing, 1974. The superposition of semi-crystalline B and  $\alpha$ -B' diffraction patterns would enhance intensity on the first and third layer lines with respect to that of the second. The observation in the course of this work of the  $\alpha$ -B' conformation for the alternating copolymer Na poly[d(A-T)].poly[d(A-T)] allows Goodwin's suggestion to be extended, encompassing alternating  $[d(A-T)]_n \cdot [d(A-T)]_n$  regions in synthetic polynucleotides and native DNA's. A possible explanation is therefore provided for the observation by Goodwin, 1977, of a Na poly[d(A-T)].poly[d(A-T)] fibre at 98% rh giving a semi-crystalline B diffraction pattern with an intensity distribution similar to those obtained by Bram and Tougard, 1972. If this is the explanation then perhaps the reason why differences in intensity distributions are only observed in oriented but non-crystalline samples is due to the diminishing influence of crystalline forces on nucleic acid conformation. The conformational angles and base stacking in the B' conformation are very similar to those in the B conformation. However, the B' conformation is distinctive enough for its lateral associations (as observed in the  $\alpha$  and  $\beta$  crystalline forms) to be strikingly different from those observed for the B conformation, Arnott and Selsing, 1974. Thus, while it is tempting to agree with Leslie et al., 1980, that the intensity distribution in some semi-crystalline B patterns may arise as a result of differences in packing arrangements, it should be pointed out that the B'



conformation has so far only been observed for Na poly(dA).poly(dT), Arnott and Selsing, 1974, Na poly(dI).poly(dC) and Na poly[d(A-I)].poly[d(C-T)], Leslie et al., 1980, and Na poly[d(A-T)].poly[d(A-T)], this chapter.

Leslie et al., 1980, have pointed out that in some respects I.C base pairs behave like A.T rather than G.C base pairs. Hence the B' conformation has so far only been observed in samples containing A.T or the related I.C base pairs. If this is the case then the observation of the B' conformation is due to a base composition effect. If Goodwin's explanation is correct then it is a base composition effect, albeit indirectly, which is responsible for the differences in the intensity distributions of A,T rich semi-crystalline B DNA diffraction patterns.

The complexity of the above argument illustrates the difficulty of determining the effects of base sequence and base composition on nucleic acid conformation. Leslie et al., 1980, provide a recent review of the conformations so far observed for many of the synthetic polynucleotides. However, the observation of two additional conformations for Na poly[d(A-T)].poly[d(A-T)] during the course of this work suggests that research in this field is not complete even in terms of conformation as a function of relative humidity and excess salt content. In view of the suspected deficiencies in this data the assignment of base sequence and base composition effects remains somewhat speculative. In addition there is evidence that such parameters also influence the ease with which structural transitions occur, Pilet and Brahms, 1972, Brahms et al., 1973. It is difficult to accurately control the amount of excess salt content in fibre samples on which these transitions are critically dependent. Thus at the present time x-ray fibre diffraction provides little information on the ease with which structural transitions occur. Therefore, as well as a more complete investigation on the conformations available to the synthetic polynucleotides there is also a clear need for the accurate determination of the excess salt content of fibre samples together with a knowledge of the distribution of that salt.

These latter two points are further discussed in chapter 6.

## Chapter 6. EXPERIMENTAL TECHNIQUES TO DETERMINE THE AMOUNT OF SALT RETAINED BY NUCLEIC ACIDS

### 6.1 Introduction

It has long been established that the amount of salt present in DNA or polynucleotide fibres plays a major role in determining nucleic acid conformation. The work on polynucleotide conformation reported in chapters 3 - 5 emphasises such an observation. It implies that a knowledge of the total salt content of nucleic acid solutions and samples for x-ray analysis would be an important aid in understanding nucleic acid conformation as a function of environmental conditions. This chapter discusses some of the techniques available to determine the amount of salt retained by nucleic acids. In particular it examines the method of  $\text{Na}^+$  concentration analysis using flame emission spectroscopy (F.E.S.) as described by Blakeley, 1976. Further experiments using a modification of this method are described. Differences in the ability of modified DNA's to retain salt are of great interest since such information may be related to their structural variations. In this respect the analysis of the salt content of  $\phi$ W-14 viral DNA solutions has been re-examined. Finally, preliminary experiments have been performed to measure  $\text{Cl}^-$  concentrations of DNA solutions. Such techniques are potentially extremely sensitive and the implications for x-ray fibre analysis are considered.

### 6.2 The micro-Carius method of chloride analysis

A method for estimating the total salt content of DNA samples by chloride analysis using a micro-Carius method has already been established by Cooper and Hamilton, 1966. In this procedure 3-8mg of sample are placed in a pressure tube together with silver nitrate and halogen free concentrated nitric acid. The pressure tube is then sealed and heated to  $\sim 300^\circ\text{C}$  for 5 hours in an electric furnace. When cool the tube is carefully opened and the quantity of precipitated silver chloride is determined by

gravimetric analysis. Simple calculation then yields the quantity of chloride present in the sample. However, this method uses quantities of material which have not normally been available for polynucleotides, nor is it a particularly convenient method to use.

### 6.3 The quantitative increase of sodium chloride concentration in samples for x-ray analysis

In the work on synthetic polynucleotides in this thesis a method has been developed whereby the salt content of x-ray fibre samples can be quantitatively increased by small increments, chapter 3. In this manner polynucleotide conformation has been examined as a function of the amount of added salt to x-ray samples, but the total salt content of such samples remains unknown.

### 6.4 The determination of $\text{Na}^+/\text{PO}_4^-$ ratios in DNA solutions using F.E.S.

#### a) A re-examination of $\text{Na}^+/\text{PO}_4^-$ ratios determined by Blakeley, 1976.

Blakeley, 1976, has developed a technique to investigate the salt content of DNA solutions using F.E.S. to measure  $\text{Na}^+$  concentrations. The DNA concentrations of the solutions were determined by U.V. spectroscopy and the results were expressed in terms of  $\text{Na}^+/\text{PO}_4^-$  ratios. Blakeley measured  $\text{Na}^+/\text{PO}_4^-$  ratios for commercial DNA solutions and for solutions of commercial DNA's which had been subjected to phenol purification. His results are reproduced in Table 6.1.

Blakeley also examined the  $\text{Na}^+/\text{PO}_4^-$  ratios of DNA gels. In these cases the  $\text{Na}^+/\text{PO}_4^-$  ratios of the solutions of the DNA's to be used in the experiment were first determined. The solutions were then centrifuged, the supernatant poured off and the last traces removed by Pasteur pipette or by washing the gels briefly in 80% ethanol. The gels were redissolved in distilled water and the  $\text{Na}^+$  and  $\text{PO}_4^-$  concentrations were determined by flame emission and U.V. spectroscopy respectively. Blakeley gave the results of four of these runs and the  $\text{Na}^+/\text{PO}_4^-$  ratios of the DNA

DNA Sample	DNA Concentration mM	Na <sup>+</sup> Concentration mM	Na <sup>+</sup> /PO <sub>4</sub> <sup>-</sup>
B.D.H.	6.6	5.0	0.76
Sigma V	5.9	4.5	0.76
Miles VI	2.7	2.75	1.02
Purified Calf Thymus	2.5	1.50	0.60
Purified Calf Thymus	1.6	0.96	0.60
Purified Calf Thymus	1.4	0.91	0.65

Table 6.1 DNA Na<sup>+</sup>/PO<sub>4</sub><sup>-</sup> data from Figure 3.3, Blakeley, 1976.

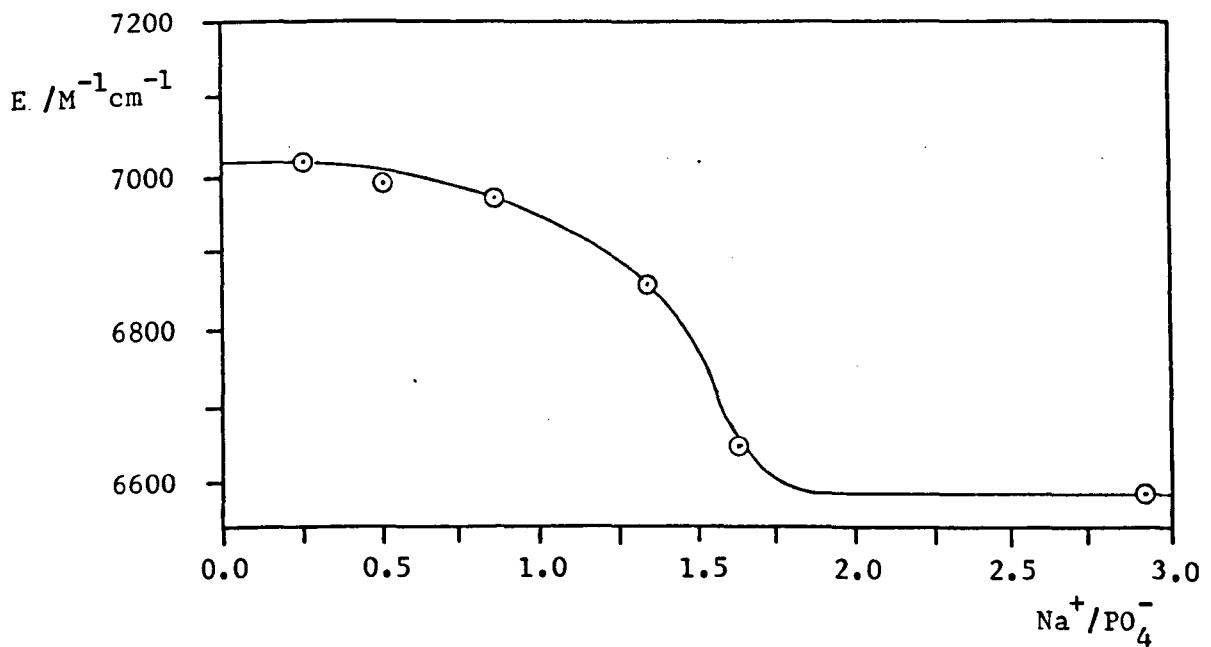


Figure 6.1 The variation of the extinction coefficient  $E_{\lambda 260\text{nm}}$  of DNA with ionic strength. The data is Figure 3.2 of Blakeley, 1976.

gels was seen to increase linearly with the salt concentration of the supernatant.

In Blakeley's results for commercial and purified DNA solutions,  $\text{Na}^+/\text{PO}_4^-$  ratios of less than 1.0 in all but one instance is rather surprising. The DNA solutions used in gel experiments and redissolved gels centrifuged from 0.0 - 0.3M NaCl also gave  $\text{Na}^+/\text{PO}_4^-$  ratios  $< 1.0$ . In order to precipitate DNA from solution the negative charge of the DNA phosphate groups must be neutralized. Since the DNA was precipitated from solutions of relatively high  $\text{Na}^+$  concentration it might be expected that the phosphate groups are neutralized on a 1:1 basis with  $\text{Na}^+$ . Hence taking into account the presence of excess sodium chloride which may be trapped in or complexed with the precipitate, the  $\text{Na}^+/\text{PO}_4^-$  ratio of such DNA should be at least 1.0. DNA precipitates washed in 80% ethanol might be expected to contain less sodium chloride and Blakeley's results (Table 6.1) tend to reflect this concept, but quantitatively it is thought unlikely that  $\text{Na}^+/\text{PO}_4^-$  ratios of DNA's should decrease below 1.0. It is possible that ions other than  $\text{Na}^+$  neutralize the negative phosphate charge of DNA and perhaps at low  $\text{Na}^+$  concentrations this effect is more apparent. Blakeley, 1976, assayed his DNA solutions for the presence of  $\text{Ca}^{2+}$  which is the most likely contaminant of water, but he found  $[\text{Ca}^{2+}] < 10\mu\text{M}$ , which he regarded as negligible. Another alternative is that water in the form of  $\text{H}_3\text{O}^+$  may play a role in charge neutralization, but this is more difficult to demonstrate experimentally.

Blakeley has successfully used his technique to predict the likelihood of an A or B type diffraction pattern from a DNA fibre at a specific relative humidity when formed from a gel centrifuged from a solution of a given salt concentration. His method is very convenient to use and only requires a small quantity of material. The procedure has thus been re-examined in an attempt to establish whether his results are quantitative or whether low  $\text{Na}^+/\text{PO}_4^-$  ratios are due to a systematic error in the

experiments. One factor which may influence these results is that DNA concentrations have apparently been measured from solutions formed by DNA dissolved in distilled water. Under conditions of low salt concentration DNA will denature. Subsequent measurements of  $\text{PO}_4^-$  concentration by U.V. spectroscopy may lead to an over estimation of DNA concentration and hence an under estimation of  $\text{Na}^+/\text{PO}_4^-$  ratios. To compensate for this effect Blakeley, 1976, derived an empirical extinction coefficient for DNA solutions at low salt concentrations. A series of samples of the same DNA concentration but different sodium chloride concentrations were prepared by dialysing 100ml of  $1.2\text{mg ml}^{-1}$  DNA solution in 0.02M NaCl against distilled water at  $4^\circ\text{C}$ . 3ml samples of the Na DNA solution were analysed with respect to time for  $\text{Na}^+$  content and apparent  $\text{PO}_4^-$  content. The dialysate was changed after each sample was taken. The effect of osmosis was shown to be negligible. In this manner a modified extinction coefficient  $E_i$  was derived as shown in Equation 6.1, where  $E_i$  is the extinction coefficient at ionic strength  $i$ , and  $E$  is the extinction coefficient of native DNA at high ionic strength. The variation of  $E_i$  with respect to the  $\text{Na}^+/\text{PO}_4^-$  ratio

$$E_i = \frac{\text{apparent DNA concentration} \times E}{\text{DNA concentration}} \quad \text{- Equation 6.1}$$

in the DNA sample was plotted and is reproduced in Figure 6.1. From this diagram it can be seen that a theoretical DNA solution of  $\text{Na}^+/\text{PO}_4^- = 0.0$  has been assigned an extinction coefficient  $\sim 7000\text{M}^{-1}\text{cm}^{-1}$ . This represents an increase of  $E_{\lambda 260\text{nm}}$  of only 6% compared with the average value of  $E_{\lambda 260\text{nm}} = 6600\text{M}^{-1}\text{cm}^{-1}$  for double stranded DNA. However, melting temperature studies show that the absorbances of Sigma calf thymus DNA solutions increase by an average of 36% upon melting. At room temperature the absorbances of such solutions are still  $\sim 27\%$  higher than those of the original samples, Table 6.2. These results suggest that Blakeley's modified extinction coefficient is not sufficiently large to compensate for the increased

Weight of DNA Sample /ug	Volume of 1mM Potassium Phosphate, 0.1mM EDTA Buffer added /ml	DNA conc. $\times 10^{-5}M$	Melting Temp $^{\circ}C$	% Increase in Absorption at 260nm	
				80 $^{\circ}C$	30 $^{\circ}C$
90	3.00	6.35	51	34.8	28.0
70	2.00	8.67	50	36.7	24.0
205	6.84	7.02	51	36.2	29.8

Table 6.2

Data relating to the thermal analysis of Sigma DNA samples in phosphate EDTA buffer. The absorption of these solutions has increased on average by 27% after melting.

Weight of DNA Sample /ug	Volume of Distilled Water added /ml	DNA conc. $\times 10^{-5}M$	Melting Temp $^{\circ}C$	% Increase in Absorption at 260nm	
				80 $^{\circ}C$	30 $^{\circ}C$
60	2.00	9.50*	-	6.0	0.0
110	3.67	5.42	50	30.7	13.3
200	6.67	9.30*	-	5.7	0.0

Table 6.3

Data relating to the thermal analysis of Sigma DNA samples in distilled water. The change in absorption is much reduced compared with Table 6.2, indicating that the DNA samples are partially or completely denatured.

\* DNA concentrations may be in error by up to 40%.



absorbance of DNA solutions which may have denatured under conditions of low ionic strength. Sigma calf thymus DNA samples dissolved in distilled water at DNA concentrations suitable for U.V. spectroscopic analysis are partially or completely denatured according to melting temperature studies, Table 6.3.

b) A modified F.E.S. routine

Using the experience gained from the experiments of Blakeley, 1976, a modified F.E.S. technique has been devised. Experiments were carried out using Sigma 1 DNA, batch number D1501. A bulk solution of this DNA was prepared by dissolving the DNA in standard 3mM sodium chloride solution at a phosphate concentration of  $\sim 1 \text{mgml}^{-1}$ . The DNA was left for a minimum period of 48 hours at  $4^{\circ}\text{C}$  to dissolve and U.V. spectroscopy was carried out on aliquots of the solution diluted with 3mM sodium chloride to accurately determine the DNA concentration. The use of 3mM sodium chloride solution gives a  $\text{Na}^+/\text{PO}_4^- \sim 1.0$  at DNA concentrations of  $1 \text{mgml}^{-1}$ . This is in addition to salt present in the solid DNA. Although this method reduces the sensitivity of the F.E. spectrometer to detect  $\text{Na}^+$  arising from the DNA, it reduces the risk of denaturing the DNA under normal conditions and allows  $\text{Na}^+$  and  $\text{PO}_4^-$  analysis of samples from the same bulk solution.

$\text{Na}^+$  concentrations were measured on a Unicam SP 1900 F.E. spectrometer. The spectrometer was first zeroed on deionized water used to make up and dilute the bulk DNA solution. Thus, any  $\text{Na}^+$  contamination present in the water will not appear in subsequent  $\text{Na}^+$  concentration measurements. The spectrometer was then calibrated using standard sodium chloride solutions. For each set of samples to be analysed a calibration curve was obtained by plotting sodium chloride concentration against the numerical spectrometer output. DNA samples were prepared by diluting aliquots of the DNA solution with deionized water to give a series of samples of different DNA concentrations. In this manner  $\text{Na}^+/\text{PO}_4^-$  ratio as a function of DNA concentration was investigated. The DNA samples were fed through the

spectrometer and a comparison of the spectrometer output with the appropriate calibration curve gave the total  $\text{Na}^+$  concentration of the samples. For each sample the calculated  $\text{Na}^+$  concentration due to the presence of 3mM standard sodium chloride solution present in the bulk DNA solution was subtracted from the total  $\text{Na}^+$  concentration. The remaining  $\text{Na}^+$  concentration was attributed to the presence of DNA and was expressed in terms of a  $\text{Na}^+/\text{PO}_4^-$  ratio.

After several exploratory experiments the following observations were made:

i) Samples of less than 10ml in volume were found to have a relatively large variation in their  $\text{Na}^+/\text{PO}_4^-$  ratios. This effect seemed to be independent of DNA or  $\text{Na}^+$  concentration.

ii) Samples of  $\text{Na}^+$  concentration  $\geq 5\text{mM}$  tended to give lower  $\text{Na}^+/\text{PO}_4^-$  ratios than expected. This was attributed to the impedance of such salt solutions through the atomizer.

iii) A wider dispersion of  $\text{Na}^+/\text{PO}_4^-$  ratios was obtained from samples made up in  $\sim 10\text{ml}$  glass containers rather than glass test tubes.

In a more critical examination of the effect of the container on  $\text{Na}^+/\text{PO}_4^-$  ratios,  $\text{Na}^+$  concentrations of distilled water in various containers were measured using a flame photometer. The photometer was zeroed on distilled water from a large plastic beaker, calibrated with standard sodium chloride solutions and was sensitive to  $1\mu\text{M}$   $\text{Na}^+$  concentrations. Glass test tubes which had been washed and stored were filled with deionized water and found to contain  $\text{Na}^+$  concentrations of 12-40 $\mu\text{M}$ . After a period of  $\sim 95$  hours the  $\text{Na}^+$  concentration had increased to 20-52 $\mu\text{M}$ . Glass tubes which were thoroughly rinsed with deionized water immediately before use gave  $\text{Na}^+$  concentrations below  $1\mu\text{M}$ . However, after  $\sim 95$  hours the  $\text{Na}^+$  ion concentration had increased up to 12 $\mu\text{M}$ . Pyrex tubes treated in the same manner were found to contain  $\text{Na}^+$  concentrations of  $< 1-6\mu\text{M}$  which increased to 2-10 $\mu\text{M}$  after  $\sim 95$  hours. No  $\text{Na}^+$  could be detected in deionized water

contained in plastic tubes even after prolonged exposure. From these results it seems that ordinary glass tubes may significantly affect the determination of  $\text{Na}^+/\text{PO}_4^-$  ratios at low  $\text{Na}^+$  concentrations. This is a possible explanation of the marked variation of  $\text{Na}^+/\text{PO}_4^-$  ratio in low volume samples and in samples which were made up in vessels which were not so frequently washed. The contribution from individual glass tubes varied considerably. Rinsing the tubes immediately prior to use greatly reduced the possibility of  $\text{Na}^+$  contamination, but the use of wet tubes might give rise to dilution inaccuracies. The increase in  $\text{Na}^+$  concentration of solutions remaining in glass tubes for a significant period of time can be attributed to the leaching of  $\text{Na}^+$  from the silicate. Pyrex tubes give rise to less  $\text{Na}^+$  contamination and no contamination was found to ensue from the use of plastic tubes. In the latter case it is possible that  $\text{Cl}^-$  can be leached from certain plastics and there is the possibility of DNA adsorption to certain plastic surfaces. Hence the use of pyrex glass vessels may represent the best choice of container for  $\text{Na}^+/\text{PO}_4^-$  determination in these types of experiments.

With the above observations in mind two sets of data were obtained giving  $\text{Na}^+/\text{PO}_4^-$  ratios for Sigma 1 DNA, batch No. D1501 and the results are recorded in Table 6.4. In both cases the average  $\text{Na}^+/\text{PO}_4^-$  ratios are significantly greater than 1.0 and there is no obvious change in  $\text{Na}^+/\text{PO}_4^-$  ratios with respect to DNA concentration. Although the variation of  $\text{Na}^+/\text{PO}_4^-$  ratios in the individual sets of results is  $\pm 6\%$  the difference between the two average  $\text{Na}^+/\text{PO}_4^-$  ratios is 18%. This may be due to the use of more anhydrous sodium chloride when making up standard solutions for the second data set. It is tempting to conclude from these results that Sigma 1 calf thymus DNA contains between 1.4 and 1.7  $\text{Na}^+$  per nucleotide.

### c) Conclusions

These results show that F.E.S. is sensitive enough to measure  $\text{Na}^+/\text{PO}_4^-$  values of commercial DNA's dissolved in 3mM NaCl solutions. Under these

Vol. of Bulk DNA soln. /ml	Vol. of Distilled Water added /ml	Calculated DNA conc. /mM	Na <sup>+</sup> conc. y due to 3mM NaCl in Bulk DNA soln. /mM	Total Na <sup>+</sup> conc. x /mM	x-y /mM	Na <sup>+</sup> /PO <sub>4</sub> <sup>-</sup>	Average Na <sup>+</sup> /PO <sub>4</sub> <sup>-</sup>
5.0	5.0	1.61	1.50	4.18	2.68	1.66	1.70 1 <sup>st</sup> run
4.6	5.4	1.48	1.38	3.76	2.38	1.61	
4.2	5.8	1.35	1.26	3.60	2.34	1.73	
3.8	6.2	1.22	1.14	3.18	2.04	1.67	
3.4	6.6	1.09	1.02	2.95	1.93	1.77	
3.0	7.0	0.96	0.90	2.58	1.68	1.75	
2.6	7.4	0.835	0.78	1.88	1.10	1.32	1.39 2 <sup>nd</sup> run
2.2	7.8	0.706	0.66	1.70	1.04	1.47	
1.8	8.2	0.578	0.54	1.37	0.83	1.44	
1.4	8.6	0.449	0.42	1.01	0.59	1.31	
1.0	9.0	0.321	0.30	0.73	0.43	1.34	
1.0	9.0	0.321	0.30	0.74	0.44	1.37	
0.8	9.2	0.257	0.24	0.60	0.36	1.40	

Table 6.4 Data culminating in the determination of Na<sup>+</sup>/PO<sub>4</sub><sup>-</sup> ratios of Sigma 1 calf thymus DNA.

conditions there is little risk of denaturing the DNA and it is no longer necessary to modify the DNA extinction coefficient  $E_{\lambda 260\text{nm}}$  with empirical correction factors.  $\text{Na}^+/\text{PO}_4^-$  ratios of 1.4 - 1.7 were found for Sigma 1 calf thymus DNA using this modified F.E.S. technique. The results do not show that  $\text{Na}^+/\text{PO}_4^-$  ratios obtained by Blakeley, 1976, are incorrect. Further experimentation using this alternative F.E.S. method may yield  $\text{Na}^+/\text{PO}_4^- < 1.0$  for DNA's which, for example have been deproteinated or extensively washed in 80% ethanol to minimize excess salt. These experiments result in a technique which is an attempt to avoid possible errors to which Blakeley's particular method may be prone. They have the potential of yielding  $\text{Na}^+/\text{PO}_4^-$  ratios to within 5%. This gives rise to the possibility of studying  $\text{Na}^+/\text{PO}_4^-$  ratios as a function of nucleic acid conformation, particularly with regard to the many conformations available to the synthetic polynucleotide structures in order to determine the exact environmental conditions under which such structures are favoured.

#### 6.5 A routine for measuring the ability of $\phi$ W-14 DNA to retain $\text{Na}^+$

##### a) Introduction : $\phi$ W-14 DNA, a viral DNA

$\phi$ W-14 is a bacteriophage having as host the bacterium *Pseudomonas acidovorans*, Kropinski and Warren, 1970.  $\phi$ W-14 DNA exhibits unusual physical properties due to the presence of modified thymine bases in which a molecule of putrescine is covalently bound to the methyl group of the thymine, Figure 6.2. Approximately 50% of the thymine bases are modified in this manner, Kropinski, Bose and Warren, 1973. X-ray diffraction patterns of the Na and Li salts of  $\phi$ W-14 DNA indicate that the modified thymine bases do not cause significant changes in the A and B conformations of DNA, Goodwin, 1977, Greenall, 1982. However, a difference in the induction of the  $A \rightleftharpoons B$  transition is observed in fibres of Na  $\phi$ W-14 DNA compared with fibres of Na calf thymus DNA prepared under the same conditions. Generally fibres from calf thymus DNA give B diffraction

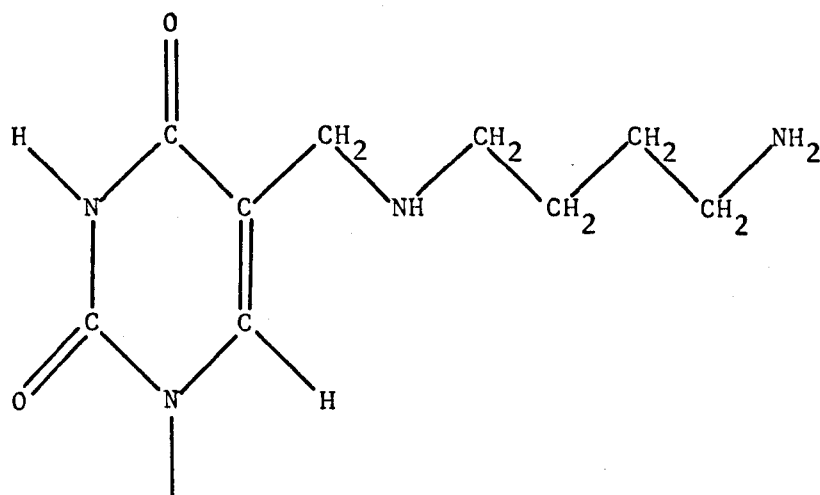


Figure 6.2 The modified thymine base N-thyminylputrescine found in  $\phi$ W-14 DNA.

	Na <sup>+</sup> conc. /mM	DNA conc. after Dialysis /mM	Na <sup>+</sup> /PO <sub>4</sub> <sup>-</sup>	DNA conc. before Dialysis /mM
$\phi$ W-14 DNA	1.49	1.19	1.25	1.14
	1.47	1.21	1.21	1.14
Calf Thymus DNA	1.84	1.06	1.74	1.12
	1.68	1.12	1.50	1.12

Table 6.5 Effective Na<sup>+</sup> and DNA concentrations of  $\phi$ W-14 and calf thymus DNA after dialysis against 1.2mM NaCl solution.

patterns at 92% and higher relative humidities whereas fibres from  $\phi W-14$  DNA regularly give B patterns only at 98% relative humidity and occasionally at 95% relative humidity, Goodwin, 1977.

The fibres used in Goodwin's analysis were prepared from gels centrifuged from DNA solutions containing 2mM Tris.HCl pH 7.6 and 0.01M or 0.02M NaCl. In view of the influence of the ionic strength on the  $A \rightleftharpoons B$  transition, Cooper and Hamilton, 1966, Goodwin pointed out the interest in determining whether the amount of salt present in gels of  $\phi W-14$  DNA was lower than that found in equivalent gels of calf thymus DNA. He suggested that one possible effect of the positive charges of the putrescine group of the  $\phi W-14$  DNA is the neutralizing or partial shielding of some of the DNA phosphate groups resulting in a reduction of the  $Na^+$  concentration in sedimented  $\phi W-14$  DNA gels.

b)  $Na^+/PO_4^-$  ratios of  $\phi W-14$  DNA gels using F.E.S., Goodwin, 1977

In order to investigate the possible reduction of  $Na^+$  concentration in  $\phi W-14$  DNA gels, Goodwin used the F.E.S. technique of Blakeley, 1976, for measuring  $Na^+/PO_4^-$  ratios in DNA gels. In this case Goodwin redissolved  $\phi W-14$  and calf thymus DNA gels in distilled water and allowed them to stand for  $\sim 72$  hours to completely dissolve. The DNA concentrations were measured using U.V. spectroscopy and assuming an extinction coefficient of  $E_{\lambda 260} = 6600M^{-1}cm^{-1}$ . The  $Na^+$  concentration was measured in the same manner as described by Blakeley, 1976. Goodwin gave the  $Na^+/PO_4^-$  ratios for the average of six runs as 0.42 and 0.88 for  $\phi W-14$  DNA and calf thymus DNA respectively when centrifuged from 0.01M NaCl solutions and 0.52 and 1.24 when centrifuged from 0.02M NaCl solutions.

Goodwin concluded that gels prepared from  $\phi W-14$  DNA contain less imbibed salt than equivalent calf thymus DNA gels. He stated that the average difference between  $Na^+/PO_4^-$  ratios in the two DNA's was 0.6 while the putrescine to phosphate ratio is only 0.125. On this basis he suggested that each putrescine molecule would have to neutralize approximately four

phosphate groups in order to account for these differences in  $\text{Na}^+/\text{PO}_4^-$  ratios. An examination of the concentration of other metal ions in the dissolved gels showed that  $\text{Li}^+$ ,  $\text{K}^+$ ,  $\text{Mg}^{2+}$ ,  $\text{Ca}^{2+}$  and  $\text{Cs}^+$  did not significantly contribute to the charge neutralization of the phosphate groups. Goodwin suggested that other charged species may be responsible for the reduction of  $\text{Na}^+$  concentration in  $\phi\text{W-14}$  DNA gels, but this effect is likely to be due, at least in part, to the presence of putrescine groups.

c) An alternative technique for measuring  $\text{Na}^+/\text{PO}_4^-$  ratios of  $\phi\text{W-14}$  DNA

Goodwin's treatment of  $\phi\text{W-14}$  DNA gels is subject to the same comments as recorded for Blakeley's results in section 6.4. In particular the gels were redissolved in distilled water. Hence the salt content of the resultant solutions may be so low as to cause the DNA to denature giving rise to an overestimate in the DNA concentrations. Another experimental difficulty in this procedure is the removal of excess supernatant from the DNA gels without removing part of the gel. Finally  $\phi\text{W-14}$  DNA is very difficult to redissolve once it is precipitated. With these constraints in mind a further experiment has been performed in order to determine whether less  $\text{Na}^+$  are associated with  $\phi\text{W-14}$  DNA compared with calf thymus DNA under conditions where the  $\text{Na}^+/\text{PO}_4^-$  ratio is greater than 1.0.

$\phi\text{W-14}$  DNA was extracted by Professor R.A.J. Warren according to Kropinski and Warren, 1970, and was available in solution in 0.01M Tris.HCl, 0.15M NaCl, 0.01M EDTA, pH 7.4, (TNE). Strips of visking tubing of 1.0cm diameter were boiled for 15 minutes in a conical flask containing 500ml of 0.01M NaCl and a small amount of EDTA. The latter is a divalent chelating agent and strongly interacts with  $\text{Ca}^{2+}$  thus inhibiting the action of DNAase. It also forms complexes with divalent ions generally thus reducing the competition of contaminating ions for the DNA phosphate groups. The tubing was then boiled in deionized water for 30 minutes with two changes and stored in a fresh solution of deionized water until ready for use. One of the dialysis tubes was filled with 15ml of 1.14mM  $\phi\text{W-14}$  DNA in TNE buffer and



a second tube was filled with 15ml of 1.12mM calf thymus DNA in 0.9mM NaCl. The two DNA solutions were dialysed against 5.0dm<sup>3</sup> of 1.2mM NaCl for ~72 hours at 4°C while stirring. The dialysate was changed twice during this time. The tubes were then cut open and their contents transferred to plastic containers. Using these DNA concentrations a dialysate of 1.2mM NaCl might be expected to provide a slight excess of Na<sup>+</sup> per phosphate group.

Standard sodium chloride solutions in the range 0.1 to 1.0mM NaCl were used to calibrate the F.E. spectrometer before Na<sup>+</sup> concentrations of diluted aliquots of the DNA solutions were measured. DNA concentrations were measured before and after dialysis by U.V. spectroscopy. The results were corrected for dilution and are shown in Table 6.5.

The agreement between the two Na<sup>+</sup>/PO<sub>4</sub><sup>-</sup> ratios for calf thymus DNA is rather poor, ~14%. This is surprising since the Na<sup>+</sup>/PO<sub>4</sub><sup>-</sup> ratios for φW-14 DNA differ by less than 4% while measurements on four aliquots of the dialysate give Na<sup>+</sup> concentrations of 1.22 ± 0.02mM or ±2% when taking into account dilution factors. A comparison of the DNA concentrations of the F.E. S. samples with the DNA concentrations of the samples before dialysis shows variations of less than 5%. This suggests that the DNA has not been denatured and osmosis has not significantly affected the results during dialysis. Further it implies that the discrepancy between the calf thymus Na<sup>+</sup>/PO<sub>4</sub><sup>-</sup> ratios is the result of an error incurred when determining the Na<sup>+</sup> concentrations. Ideally a larger number of aliquots should have been examined.

Na<sup>+</sup>/PO<sub>4</sub><sup>-</sup> ratios > 1.0 were obtained for all samples and in this respect the experiment was successful. It is of interest to note that Na<sup>+</sup> concentrations are greater inside the dialysis bags than in the dialysate, despite exhaustive dialysis. This suggests that DNA is able to maintain a relatively high local Na<sup>+</sup> concentration compared with that in the bulk solution.

The Na<sup>+</sup>/PO<sub>4</sub><sup>-</sup> ratios tend to indicate that φW-14 retains less Na<sup>+</sup> than calf thymus DNA when dialysed under the same conditions although these

results are not completely conclusive. This decrease in the  $\text{Na}^+/\text{PO}_4^-$  ratio by  $\sim 0.25$  to  $0.5$  implies that a putrescine group would have to neutralize between two and four phosphate groups of  $\phi\text{W-14}$  DNA to account for the  $\text{Na}^+$  concentration reduction. This is comparable with the neutralization of four phosphate groups obtained by Goodwin, 1977. However, at this time neither these results nor those of Goodwin, 1977, can be regarded in a truly quantitative manner. Nevertheless it is likely that such results indicate that there is some reduction in the ability of  $\phi\text{W-14}$  to retain  $\text{Na}^+$  compared with calf thymus DNA under the same conditions.

Differences in the retention of  $\text{Na}^+$  by  $\phi\text{W-14}$  and calf thymus DNA do not arise from differences in their extinction coefficients. The extinction coefficient  $E_{\lambda 260\text{nm}}$  of  $\phi\text{W-14}$  DNA was determined by Kropinski, Bose and Warren, 1973, by assaying for inorganic phosphate in hydrochloric acid hydrolysates of DNA. They found  $E_{\lambda 260\text{nm}} = 6800\text{M}^{-1}\text{cm}^{-1}$  which is in the range of extinction coefficients of double stranded DNA's, Biswal et al., 1967.  $E_{\lambda 260\text{nm}} = 6800\text{M}^{-1}\text{cm}^{-1}$  represents an increase in the extinction coefficient of  $\phi\text{W-14}$  DNA of 3% compared with  $6600\text{M}^{-1}\text{cm}^{-1}$  used in these results and those of Goodwin, 1977. In view of the relatively large experimental error arising from the determination of  $\text{Na}^+$  concentrations such an error may be regarded as negligible.

#### d) Conclusions

A method has been devised to measure  $\text{Na}^+/\text{PO}_4^-$  ratios for different DNA's under conditions which reflect the ability of a given DNA to retain  $\text{Na}^+$ . Measurements have been carried out under conditions where  $\text{Na}^+/\text{PO}_4^-$  ratios are greater than 1.0 and hence the potential problem of DNA denaturation is greatly reduced.

These results and those of Goodwin, 1977, imply that there is a reduction in the ability of  $\phi\text{W-14}$  DNA to retain  $\text{Na}^+$  compared with calf thymus DNA. Such a reduction may be attributed to the presence of the modified thymine base of  $\phi\text{W-14}$ . It is possible that this modified base is involved

in host controlled modification like glucosylated 5-HmCyt, Revel and Luria, 1970. Alternatively it may facilitate DNA packing in the head of the bacteriophage where neutralization of DNA phosphate groups is important. Developments of this type of experiment should provide quantitative information on the ability of different DNA's to retain cations. Where differences in cation retention are due to the presence of modified bases such information may be important in understanding the function of these modifications.

#### 6.6 The electrode potential method of chloride analysis

A more convenient method of routinely analysing the total chloride ion content of a solution is possible using a chloride meter. This is essentially a device which measures the electrode potential of a cell containing the chloride solution with reference to a standard electrode. An apparatus of this type was constructed to determine the effectiveness of such a device in measuring low concentrations of  $\text{Cl}^-$  in small volumes of DNA solutions.

A silver wire anode was electrolytically plated to give a fine silver chloride coating and a calomel electrode was used as the reference electrode. The plated silver wire was wound around the calomel electrode in a helical fashion to conserve space. Electrical contact between the chloride solution and the calomel electrode was maintained via a salt bridge of 1.0M sodium sulphate solution. The sodium sulphate reservoir was contained in a U-tube, the height of which was found to be critical in maintaining the electrical stability of the apparatus. The electrode potential of the cell was measured using a stabilized millivoltmeter.

Theoretically the electrode potential  $E_m^-$  of an electrode in a solution of its ions of concentration  $[c]$ , is related to the standard electrode potential of hydrogen  $E_m^{\ominus}$  by equation 6.2 where R is the gas constant, F the Faraday constant, T the absolute temperature and z the valency of the ion

concerned. Thus a plot of electrode potential against the log of the ion

$$E_m = E_m^{\ominus} + \frac{RT}{zF} \log_e [c] \quad - \text{Equation 6.2}$$

concentration should be linear. It is not necessary to determine the absolute value of electrode potential since a calibration curve for the apparatus can be obtained by plotting electrode potential as a function of standard chloride ion concentration within the cell. The electrode potential of the cell is then measured for a chloride ion solution of unknown concentration. A comparison of the electrode potential with the calibration curve will give the unknown chloride ion concentration.

The apparatus was first tested using standard sodium chloride solutions and a plot of electrode potential against  $\log_{10} [Cl^-]$  was found linear in the range  $10^{-1} - 10^{-4} M Cl^-$ . In addition there was no significant differences in the electrode potential of 5ml volume samples compared with 50ml volume samples using this equipment. Eventually it was found that the height of the electrode in the solution was unimportant provided that the bottom of the electrode was below the meniscus of the solution. It was thus possible to detect  $10^{-4} M Cl^-$  concentrations in 1ml sample volumes giving a sensitivity of 3.5ppm.  $Cl^-$  concentrations lower than  $10^{-4} M$  could be detected by suitable calibration of the instrument, but the relationship between electrode potential and  $Cl^-$  concentration was no longer linear. Thus the ability of the instrument to detect  $Cl^-$  concentrations differing by the same amount decreased below  $10^{-4} M Cl^-$  concentration. Unfortunately, the apparatus was subject to considerable drift in electrode potential values of the same chloride sample with respect to time. Replating the silver wire electrode had little effect on this drift. Electrode potentials of chloride solutions examined after prolonged contact (up to 7 hours) with plastic containers did not show any obvious trend with respect to time and leaching of  $Cl^-$  from such containers was not thought to be significant. Eventually

the drift in electrode potential was partially attributed to contamination of the sample solution with sulphate ions from the sodium sulphate salt bridge. Optimizing the height of the sodium sulphate reservoir tended to reduce this instability, but it was not entirely removed.

The apparatus was then used to measure  $\text{Cl}^-$  concentrations in DNA solutions. Sigma 1 calf thymus DNA, batch No. D1501 was dissolved in deionized water to give a DNA concentration of 3.61mM. The DNA concentration was calculated assuming 73% of the material was DNA as determined in chapter 3.5. The instrument was calibrated with standard sodium chloride solutions before each run.  $\text{Cl}^-$  concentrations of aliquots of the bulk DNA solution diluted with deionized water were then determined. Table 6.6 presents the results from two successive runs on six DNA samples. The overall  $\text{Cl}^-/\text{PO}_4^-$  ratio for this DNA was found to be  $0.18 \pm 0.014$  or  $\pm 8\%$ . There is no obvious change in these  $\text{Cl}^-/\text{PO}_4^-$  ratios with respect to DNA concentration.

After the second  $\text{Cl}^-$  concentration determination the samples were analysed for  $\text{Na}^+$  concentration. The F.E. spectrometer was calibrated using standard sodium chloride solutions in the range  $10^{-2} - 5 \times 10^{-5} \text{M}$  and a calibration curve of  $\log \text{Na}^+$  concentration against spectrometer output was obtained. Using this curve the  $\text{Na}^+$  concentrations of the samples were subsequently determined. The results are shown in Table 6.7.

The volume of these samples was very low for ideal F.E.S. analysis, but initially  $\text{Na}^+$  and  $\text{Cl}^-$  analysis on the same sample without dilution was deemed desirable. The first  $\text{Na}^+/\text{PO}_4^-$  ratios in Table 6.7 are sequentially increasing. This effect is probably due to  $\text{Na}^+$  concentrations in these samples which are too high, thus impairing the efficiency of the spectrometer atomizer. This causes the  $\text{Na}^+$  concentration to be underestimated, but the effect decreases with decreasing  $\text{Na}^+$  concentration. The last four  $\text{Na}^+/\text{PO}_4^-$  ratios in Table 6.7 are almost constant and are taken to be correct. Using the data from Table 6.6  $(\text{Na}^+ - \text{Cl}^-)/\text{PO}_4^-$  ratios have also been calculated. The last four determinations of the  $(\text{Na}^+ - \text{Cl}^-)/\text{PO}_4^-$  ratio in Table 6.7 are

Vol. DNA from Bulk soln. /ml	Vol. Deionized Water /ml	Calculated DNA conc. /mM	1 <sup>st</sup> Run		2 <sup>nd</sup> Run	
			Cl <sup>-</sup> conc. /mM	Cl <sup>-</sup> /PO <sub>4</sub> <sup>-</sup>	Cl <sup>-</sup> conc. /mM	Cl <sup>-</sup> /PO <sub>4</sub> <sup>-</sup>
1.50	0.00	3.61	0.589	0.163	0.750	0.208
1.25	0.25	3.01	0.490	0.163	0.589	0.196
1.00	0.50	2.41	0.389	0.161	0.452	0.188
0.75	0.75	1.81	0.288	0.159	0.347	0.192
0.50	1.00	1.20	0.214	0.178	0.219	0.183
0.25	1.25	0.60	0.106	0.177	0.119	0.198
Average				0.167		0.194

Table 6.6 Cl<sup>-</sup>/PO<sub>4</sub><sup>-</sup> ratios for Sigma 1 calf thymus DNA.

Vol. DNA from Bulk soln. /ml	Vol. Deionized Water /ml	Calculated DNA conc. /mM	Na <sup>+</sup> conc. /mM	Na <sup>+</sup> /PO <sub>4</sub> <sup>-</sup>	(Na <sup>+</sup> - Cl <sup>-</sup> )/PO <sub>4</sub> <sup>-</sup>
1.50	0.00	3.61	3.55	0.98	0.78
1.50	0.00	3.61	3.63	1.01	0.80
1.25	0.25	3.01	3.47	1.15	0.96
1.00	0.50	2.40	2.95	1.23	1.04
0.75	0.75	1.80	2.29	1.27	1.08
0.50	1.00	1.20	1.51	1.26	1.08
0.25	1.25	0.60	0.74	1.23	1.04

Table 6.7 Chloride and sodium ion analysis of Sigma 1 calf thymus DNA.

1.0 ±8% which is within the limits of experimental error. This implies that in this calf thymus DNA sample there are sufficient  $\text{Na}^+$  in excess of  $\text{Cl}^-$  to exactly neutralize the DNA phosphate groups.

These experimental techniques clearly need further refinement. Nevertheless they show that  $\text{Cl}^-$  concentration can be measured to within one tenth of the phosphate concentration in DNA solutions. The accuracy is sufficient to make the determination of  $\text{Cl}^-/\text{PO}_4^-$  ratios of much interest in the analysis of nucleic acid conformation as a function of ionic strength in samples for x-ray analysis. Furthermore, using this technique in conjunction with  $\text{Na}^+$  analysis it is possible to determine the relative concentration of  $\text{Na}^+$  interacting with the DNA as opposed to their presence as the result of sodium chloride in the DNA sample. It would be of interest to carry out a similar experiment using  $\phi\text{W-14}$  DNA to examine the effect of modified thymine bases to retain  $\text{Cl}^-$  as well as  $\text{Na}^+$ . It may be that not only is the retention of  $\text{Na}^+$  reduced by the positively charged N-thyminyl-putrescine, as indicated in section 6.5, but also that the local  $\text{Cl}^-$  concentration around this DNA is increased. The relevance of such an analysis has already been discussed in the previous section.

### 6.7 Chloride analysis by amperometric titration

A number of commercial instruments are available which measure  $\text{Cl}^-$  concentration by the electrode potential method. Such devices may be expected to have improved electrical stability compared with the apparatus described above. They should also provide  $\text{Cl}^-$  concentrations of greater accuracy but cannot readily measure  $[\text{Cl}^-]$  below  $10^{-4}\text{M}$ . A more accurate method of measuring low  $\text{Cl}^-$  concentration is by an amperometric titration. The most sensitive instrument of this type is the Buchler direct reading chloridometer. In this device current is passed through the sample via two silver generating electrodes. Silver ions are released from the anode and combine with chloride ions in the sample to produce silver chloride which is



insoluble. When all the chloride is precipitated the increasing concentration of free silver ions causes an increase in current which activates a relay and stops a timed readout. The rate of generation of silver ions is constant and therefore the quantity of chloride ion precipitated is proportional to the time elapsed. The apparatus can detect 0.01mEq/l of chloride ions in 0.01ml of sample to an accuracy of 0.5% ie 0.035ug in 0.01ml.

This method is superior to the electrode potential method since the chloridometer output is completely linear with respect to  $\text{Cl}^-$  concentration. In the electrode potential method the measured electrode potential is only linear with  $\text{Cl}^-$  concentration at  $[\text{Cl}^-] > 10^{-4}\text{M}$ .

This chloridometer not only offers accurate and fast  $\text{Cl}^-$  analysis of DNA solutions, but it is sensitive enough to measure  $\text{Cl}^-$  concentrations of solutions of individual fibre x-ray samples. A typical fibre sample of 200ug DNA might be expected to contain  $\sim 3.2\text{ug}$  of  $\text{Cl}^-$ . If the fibre was dissolved in 0.5ml of distilled water, the  $\text{Cl}^-$  concentration of the sample would be twice that at which the Buchler chloridometer is accurate to 0.5%. Such a  $\text{Cl}^-$  assay would use very little sample and the remaining solution could be further diluted for  $\text{Na}^+$  analysis using F.E.S. DNA concentrations of such samples could be estimated by U.V. spectroscopy of other fibres dissolved in saline solutions to prevent DNA denaturation.

This process is obviously a destructive technique and it is necessary to ensure that all x-ray data is collected before  $\text{Cl}^-$  analysis is possible. Nevertheless, such procedures offer the possibility of routine analysis of x-ray fibre samples rather than the analysis of bulk solutions from which such samples are prepared. In view of the varied x-ray diffraction results from fibres made from apparently the same bulk solution and exposed to supposedly similar environmental conditions, this type of microanalysis may prove of value in determining quantitatively the effects of ionic strength on DNA conformation.

## 6.8 Conclusions

A number of experimental techniques relating to the determination of the amount of salt retained by nucleic acids have been discussed.  $\text{Na}^+/\text{PO}_4^-$  ratios of 1.4 - 1.7 have been obtained for Sigma 1 calf thymus DNA using a modified F.E.S. technique to measure  $\text{Na}^+$  concentrations of DNA solutions. Further experimentation is necessary to ascertain whether  $\text{Na}^+/\text{PO}_4^-$  ratios less than 1.0 can be attributed to DNA which has been precipitated from solutions of relatively high salt concentration. A technique has been devised to measure  $\text{Na}^+/\text{PO}_4^-$  ratios of different DNA's under conditions which reflect the ability of a given DNA to retain  $\text{Na}^+$ . Results suggest that  $\phi\text{W-14}$  DNA retains less  $\text{Na}^+$  than calf thymus DNA under similar conditions. Further experimentation is necessary in order to quantify these results. This information may be important in understanding the function of modified DNA's such as  $\phi\text{W-14}$ . An instrument has been constructed to measure  $\text{Cl}^-$  concentrations in DNA solutions using an electrode potential method. Using this instrument  $\text{Cl}^-/\text{PO}_4^-$  ratios of 0.18 have been obtained for Sigma 1 calf thymus DNA. Attributing  $\text{Cl}^-$  concentration to the presence of sodium chloride there was still sufficient  $\text{Na}^+$  present to completely neutralize the DNA phosphate groups. A particularly sensitive method of  $\text{Cl}^-$  analysis by amperometric titration has been discussed. This is relevant to the determination of  $\text{Cl}^-$  concentrations in x-ray fibre samples. The development of these techniques should result in the quantitative determination of  $\text{Na}^+$  and  $\text{Cl}^-$  concentrations present in the x-ray fibre samples. In view of the relevance of ionic strength on nucleic acid conformation the determination of such parameters may be important in understanding why a specific nucleic acid conformation is favoured under certain environmental conditions. F.E.S., electropotential and amperometric titration methods can easily be adapted to measure cation and anion concentrations other than those of  $\text{Na}^+$  and  $\text{Cl}^-$ .

Even with such quantitative micro-analytical techniques available the problem of determining the amount of salt directly associated with DNA is

not completely solved. This is apparent from an examination of x-ray diffraction patterns such as that of Plate 3.7. Here the diffraction ring at 0.282nm is evidence of crystalline sodium chloride within the fibre sample. Thus the distribution of  $\text{Na}^+$  and  $\text{Cl}^-$  in the fibres may be non-homogeneous, at least under conditions of moderate/high salt concentrations and low relative humidity. Transmission electron microscopy, (T.E.M.), has been briefly examined in order to determine the size and distribution of these salt micro-crystals in these DNA fibres. However, there are many problems in the preparation of DNA samples for T.E.M. and this technique has so far proved unsuccessful. An alternative method for estimating the amount of crystalline salt present in fibres is the comparison of the intensity of the salt diffraction ring with the intensity of a reflection from a substance in the fibre of known concentration. Such procedures remain to be investigated.

Chapter 7. AN EXAMINATION OF THE FORMATION OF SMALL MOLECULE CRYSTALLITES  
IN DNA FIBRES

7.1 Introduction

Numerous small molecules possessing planar aromatic groups have been shown to interact with nucleic acids and many of these molecules are of medicinal interest. This subject has been extensively reviewed by Goldberg and Friedman, 1971, and Gale et al., 1981. One type of interaction between these small molecules and DNA is that of intercalation. This interaction involves the insertion of a planar drug chromophore in between two adjacent base pairs of DNA and may give rise to stable drug/DNA complexes with consequential disruptions in DNA replication and transcription processes. An intercalation model was first proposed by Lerman, 1961, in order to explain the x-ray diffraction patterns obtained from proflavine/DNA complexes. The proposal was subsequently supported by a number of physico-chemical experiments by Luzzati et al., 1961, Lerman, 1963, and Lerman, 1964a,b. A more detailed analysis of x-ray diffraction patterns in conjunction with optical transformations and spectrophotometric measurements from proflavine/DNA and acridine orange/DNA complexes was carried out by Neville and Davies, 1966. Their results were shown to be in qualitative agreement with the intercalation model of Lerman, 1961. X-ray fibre diffraction results in conjunction with molecular model building techniques have shown that a number of other small molecule/DNA complexes are consistent with an intercalation model. For example, Fuller and Waring, 1964, Pigram et al., 1972, Bond et al., 1975, and Porumb, 1976, have produced intercalation models for ethidium bromide, daunomycin, PtTS and adriamycin respectively. Diffraction patterns from fibres of drug/DNA complexes are much less well resolved than the relatively well ordered fibres of DNA alone. Thus the structural information provided by x-ray fibre diffraction of drug/DNA complexes is rather limited. In particular, little information is available

with regard to the changes which intercalation must impose on the DNA sugar-phosphate backbone. Linked atom least squares molecular model building has been used to calculate plausible models for proflavine intercalation into both the A form (Alden and Arnott, 1977) and the B form of DNA (Alden and Arnott, 1975). However, the analysis of drug/DNA complexes has not yet provided data at atomic resolution. To some extent such information has been obtained from single crystal x-ray analyses of drug/dinucleotide complexes. However, the direct relevance of such structures to nucleic acid complexes is unclear at present, Neidle, 1982. The ability to synthesize and crystallise longer oligonucleotide sequences which has proved so successful in providing data of the Z and B conformations (Wang et al., 1979, and Wing et al., 1980) may well have an important role to play in elucidating the structure of drug/DNA complexes. Equally, synthetic polynucleotides, which are now more readily available in larger quantities, may be used to provide more detailed information with regard to the interaction of drugs with nucleic acids. A more exact knowledge of the structure and mechanism by which different drug molecules interact with nucleic acids is a desirable prerequisite in the search and design of chemotherapeutic drugs which are more specific in their mode of interaction and give rise to less harmful side effects. Equally important is the realization as to which of the millions of small molecule compounds now being synthesised are likely to be harmful to man and his environment and to the extent of this toxicity for a given molecular species.

During fibre x-ray diffraction investigations of small molecule/DNA complexes crystallization of the small molecules within DNA fibres has occasionally been observed. This observation is interesting for a number of reasons. Firstly, diffraction from the crystallites has been well resolved in some drug/DNA systems. A knowledge of the structure of the small molecules within the crystallites may provide useful information with respect to the DNA structure or that of the drug/DNA complex. Secondly, a

knowledge of the conditions under which these crystallites are formed may well lend some insight into the mechanism of the small molecule/DNA interaction. A third point of interest is concerned with the use of small molecules in drug treatment regimes. Although molecules of this type have been used as anticarcinogens those which have so far been effective are extremely cytotoxic. Such drugs have been administered either orally or intravenously and a problem arises in conveying the selected drug to the infected area without destroying normal, healthy tissue. As an alternative means of administration, drug crystals could be implanted in a tumour site and thus provide a slow, continuous dose of antibiotic to an infected area. This is in preference to the massive indiscriminant dose incurred during oral or intravenous administration.

The initial objective of this work was to determine the conditions for observing the crystallization of a particular small molecule, that of steffimycin B, in DNA fibres. Steffimycin B provides well resolved diffraction patterns of a crystalline small molecule within DNA fibres. Steffimycin B has not proved to be an effective antibacterial agent although it is highly inhibitory against gram positive bacteria in vitro and has shown potential antitumour activity in an in vitro screen, Brodasky and Reusser, 1974, Reusser, 1975. However steffimycin B is structurally related to the far more potent daunomycin and adriamycin anthracycline antibiotics. The most well resolved diffraction patterns of crystalline steffimycin B/DNA fibres were obtained by Blakeley, 1976, and these patterns have been examined in detail. A series of five acridine derivatives have been briefly examined with respect to their ability to crystallize in DNA fibres. The structural features of compounds which have shown evidence of crystallization in drug/DNA fibres have been discussed.

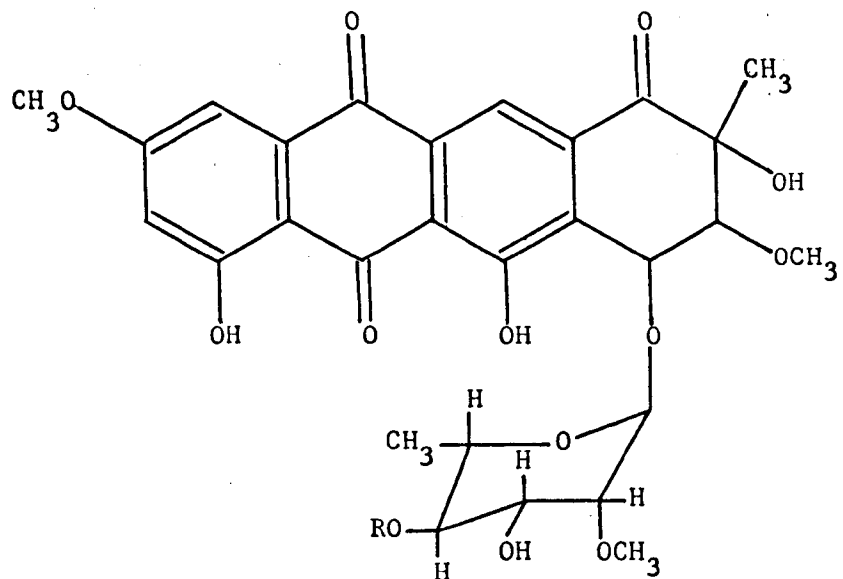
## 7.2 Previous observations of the crystallization of small molecules in DNA fibres

### a) The steffimycins

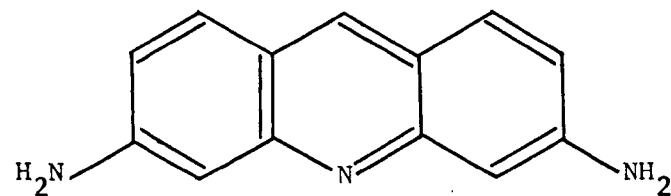
Some of the most well resolved diffraction patterns of the crystallization of small molecules in DNA fibres have been obtained from steffimycin B/DNA samples. Steffimycin was isolated from *Streptomyces steffisburgensis* by Bergy and Reusser, 1967, and Steffimycin B was isolated from *Streptomyces elgreteus* by Brodasky and Reusser, 1974. Both crystalline compounds are orange-yellow in colour. In acidic aqueous solutions these antibiotics exhibit a bright yellow colour, which turns purple upon addition of strong base. These compounds have been shown to inhibit various biological activities including DNA-directed RNA synthesis. This effect has been attributed to the binding of these antibiotics to adenine or thymine or both of these bases of the DNA template, Reusser, 1967, 1975. However, these antibiotics have been curiously ineffective in vivo. Brodasky and Reusser, 1974, showed that steffimycin B differed from steffimycin as a result of the substitution of an oxymethyl group for an hydroxyl group on the sugar ring. A more detailed structural analysis of the steffimycins has been carried out by Kelly et al., 1977, on the basis of spectral analyses and chemical degradation studies. Their proposal for the steffimycin structures is depicted in Figure 7.1a.

Blakeley, 1976, has examined the effects of the steffimycin antibiotics on DNA using U.V. and visible spectroscopy, x-ray fibre diffraction and model building techniques. He proposed that both these antibiotics interact with DNA by intercalation and that at P/D ratios  $< 18.2$  external binding of the steffimycins to DNA also occurs. From a consideration of the interaction of the steffimycins with Na poly[d(A-T)].poly[d(A-T)], Blakeley concluded that both these antibiotics have a preference for A-T binding sites.

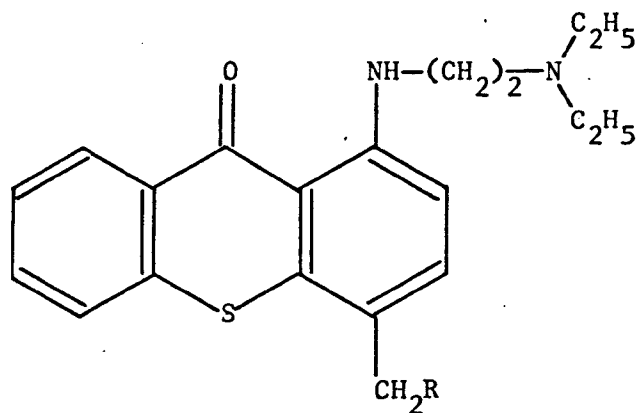
Dall'Acqua et al., 1979, have also examined the interaction of the



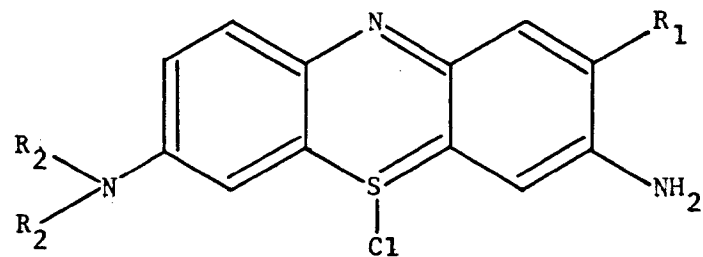
a) Steffimycin, R = H ; Steffimycin B, R = CH<sub>3</sub>



b) Proflavine



c) Miracil D, R = H ; Hycanthone R = OH



d) Toluidine Blue, R<sub>1</sub> = CH<sub>3</sub> R<sub>2</sub> = CH<sub>2</sub> ; Thionine, R<sub>1</sub> = R<sub>2</sub> = H

Figure 7.1 Graphic formulae of small molecules associated with crystallization in DNA fibres.



steffimycin antibiotics with DNA's of various base compositions and with synthetic polynucleotides. On the basis of spectrophotometric and fluorimetric data, thermal transition studies and gel filtration analysis they concluded that the steffimycins formed stable complexes with DNA. Flow dichroism measurements were interpreted as direct evidence that the interaction of the steffimycins with DNA was by intercalation. Association constants and the frequency of the binding sites were obtained from the spectrophotometric and fluorimetric data according to the method of McGhee and von Hippel, 1974. These results suggested that an alternating A-T sequence in DNA represents the preferential receptor site for the steffimycins which is in agreement with Blakeley, 1976. The association constant of steffimycin B was found to be slightly higher than for steffimycin but both were an order of magnitude below that obtained for adriamycin/DNA complexes under similar conditions. The authors suggest that the reduced binding affinity of the steffimycins may partially explain the lack of in vivo activity of the steffimycins.

The crystallization of steffimycin B within DNA fibres was discovered by Blakeley, 1976. Blakeley had prepared steffimycin/DNA and steffimycin B/DNA fibres from gels centrifuged from solutions in a similar manner to that described in chapter 2.4. Prior to centrifugation the solutions contained 0.33 or 0.66mM deproteinized calf thymus DNA, 10.5mM NaCl and sufficient steffimycin B to give P/D ratios in the range of 4-60. Steffimycin B preparations contained ~26% v/v methanol in order to ensure the solubility of this antibiotic which is only sparingly soluble in aqueous solution.

X-ray diffraction patterns of these fibres were usually reminiscent of B DNA patterns with increased values of pitch and decreased intermolecular spacings according to the quantity of antibiotic present and consistent with present concepts of drug binding by intercalation. However, fibres of P/D ratio  $< 12$  often exhibited 0.7nm meridional reflections superimposed on non-modified B DNA diffraction patterns. The observation of such meridional

reflections tended to occur more frequently in patterns from steffimycin B/DNA fibres than from steffimycin/DNA fibres. In the former case Blakeley obtained several patterns with a large number of crystalline drug reflections superimposed on an intensity distribution associated with that of B DNA similar to that shown in Plate 7.1.

Blakeley recorded the positions of 34 crystalline drug reflections and showed that these reflections indexed on a hexagonal lattice with  $a = 2.993 \pm 0.002\text{nm}$  and  $c = 0.770 \pm 0.001\text{nm}$ . Blakeley pointed out that the  $a$  lattice parameter of B DNA was 1.5 times that of steffimycin B and it may be possible to superimpose the nucleic acid lattice over the drug lattice. However, Blakeley found it difficult to arrange steffimycin B and DNA molecules in the same unit cell without appreciable steric hindrances and concluded that the steffimycin B molecules crystallize in sites between the DNA microcrystals.

Blakeley has suggested that under conditions of low relative humidity hydrophobic drug molecules leave intercalation sites giving rise to a 0.68nm or 0.70nm meridional reflection and that in some cases these drug molecules rearrange to form crystallites with a  $c$  dimension of 0.77nm. Blakeley has reported an increased tendency for steffimycin B molecules to leave DNA intercalation sites under hydrophobic conditions compared with steffimycin molecules. He suggested that this occurs as a result of the formation of only one hydrogen bond in the steffimycin B/DNA complex compared with two hydrogen bonds in the steffimycin/DNA complex. This conclusion was based on model building studies and may be in contrast to the work of Dall'Acqua et al., 1979, who obtained slightly higher association constants for steffimycin B than steffimycin DNA receptor sites. However, it should be remembered that while Blakeley's studies were carried out on fibres, those of Dall'Acqua et al. were performed in solution.

b) Proflavine

Proflavine (3,6-diaminoacridine), Figure 7.1b, is a member of the

Plates 7.1 - 7.8 : X-ray diffraction patterns from steffimycin B/DNA and acridine derivative/DNA fibres

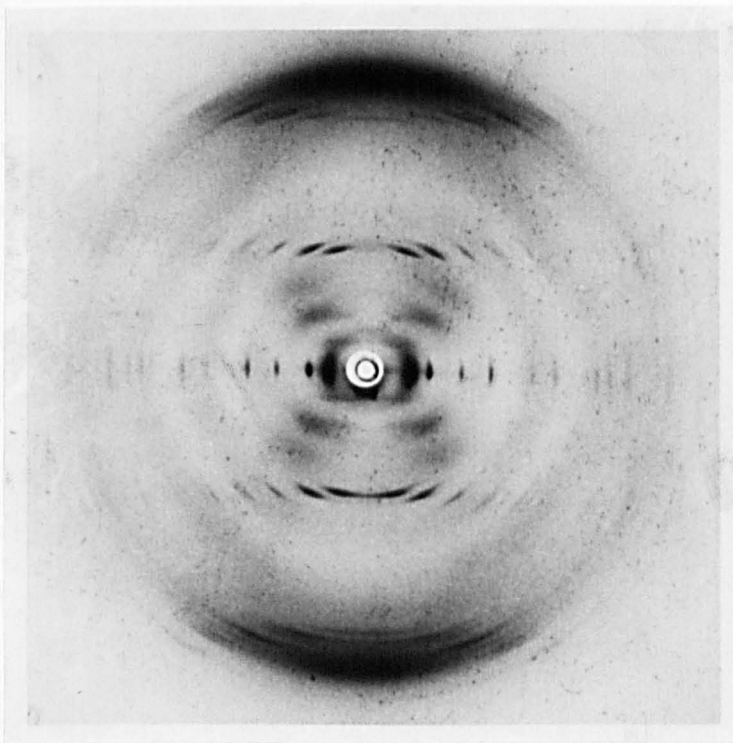


Plate 7.1

Crystalline steffimycin B/DNA fibre,  $P/D = 12.2$ ,  $rh = 92\%$ , courtesy of Blakeley, 1976.

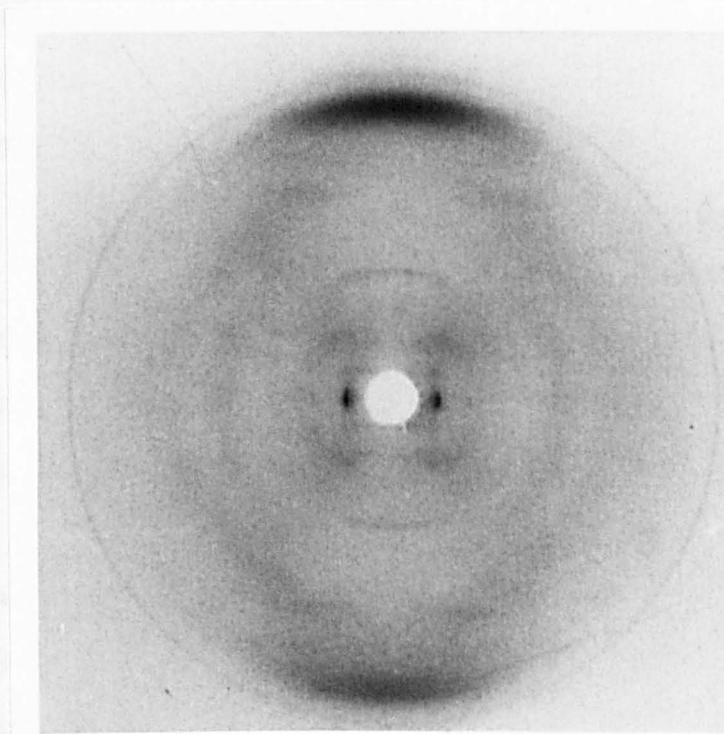


Plate 7.2

Steffimycin B/DNA fibre,  $P/D \sim 6.0$ ,  $rh = 44\%$ , from gel 1 showing a semi-crystalline B diffraction pattern with an additional meridional reflection at  $0.72\text{nm}$  attributed to the presence of steffimycin B.

acridines which have long been used as antibacterial and antimalarial agents. Their biological activity is associated with the inhibition of RNA and DNA synthesis, Albert, 1973, Acheson, 1973, and believed to be as a result of intercalation, for example, Lerman, 1961, Neidle et al., 1977. The acridines are widely used as histological stains for nucleic acid-containing structures in cells while some acridines including proflavine are powerful mutagens, Brenner et al., 1961.

In examining x-ray diffraction patterns of proflavine/DNA fibres at  $P/D = 5.9$  and 100% rh, Neville and Davies, 1966, observed disordered B type diffraction patterns with meridional reflections  $\sim 0.68\text{nm}$ . These reflections were superimposed on diffuse scattering, were of weak intensity and not reproducibly observed. No explanation was given as to their origin.

c) Miracil D

Miracil D, Figure 7.1c, is clinically useful as an antischistosome drug that has also shown anticancer activity in a number of test systems, Hirschberg, 1975. It is also known to inhibit RNA synthesis by blocking the action of DNA dependent RNA polymerase, Hirschberg et al., 1968, Weinstein and Hirschberg, 1971. Crystalline miracil D/DNA diffraction patterns have been obtained by Davies, 1973, which are of similar quality to the crystalline steffimycin B/DNA patterns of Blakeley, 1976. Model building studies showed that the intercalation of miracil D from the direction of the small groove of DNA was stereochemically feasible. However, the intensity distribution from crystalline miracil D/DNA diffraction patterns was very similar to that observed on patterns from thin needle shaped crystals of miracil D. In addition, no evidence of intercalation was apparent from diffraction patterns of miracil D/DNA fibres which did not exhibit crystalline miracil D reflections. Davies thus concluded that miracil D binds weakly to DNA along the outside of the sugar phosphate chain and crystallizes out separately from the DNA molecules under specific fibre conditions. The binding of miracil D to DNA was shown to be critically

dependent on the ionic strength. Davies has suggested that the presence of a sulphur atom in the ring system of miracil D may reduce its binding affinity for DNA either as a result of charge effects or due to puckering of the ring system about the sulphur atom.

In contrast to the proposed non-intercalation of miracil D nmr evidence supports an intercalative mode of miracil D binding to poly(rA). poly(rU), Heller et al., 1974. In addition Hycanthon, Figure 7.1c, which is a derivative of miracil D, affects circular DNA in a manner consistent with that of other simple intercalating drugs, Waring, 1970. However, differences in the interpretation of the binding mode of this drug to DNA may have resulted from examination of drug/DNA interactions in solution as opposed to the solid state. Neidle, 1976, has determined the crystal structure of miracil D and shown that the ring system of the molecule is planar  $\pm 0.005\text{nm}$ . The hydrogen atom of the  $N_1$  nitrogen atom is in a favourable position to form an intramolecular hydrogen bond with the carbonyl oxygen atom. Alkyl substitution abolishes this hydrogen bond forcing a rotation of the  $N_1$  substituent out of the plane of the chromophore giving a substantial increase in the effective van der Waals thickness of the thioxanthone ring. This is consistent with the inhibition of biological activity and the decrease in the strength of miracil D binding to DNA upon alkyl substitution. During intercalation the side chain of miracil D may well be stabilized by electrostatic interaction between terminal nitrogen and phosphate oxygens on the nucleic acid back bone, Weinstein and Hirschberg, 1971. This suggestion is supported by model building studies, Neidle, 1976.

#### d) Toluidine blue

Toluidine blue, Figure 7.1d, is a phenothiazine derivative which has medicinal uses as a heparin inhibitor and as an antihaemorrhagic and antimenorrhagic agent.

X-ray diffraction patterns of toluidine blue/DNA fibres showing crystalline drug reflections were again obtained by Davies, 1973, and were

similar to those of crystalline miracil D/DNA patterns. Davies has suggested that this compound is unable to intercalate with DNA since in addition to the sulphur atom in the ring system, intercalation is further inhibited by the presence of bulky methyl substituents. Thionine, Figure 7.1d, which does not have these methyl substituents gave typical intercalation type diffraction patterns and no evidence of crystallization in the DNA fibres was observed.

### 7.3 Materials and methods

In an attempt to reproduce the crystalline steffimycin B/DNA diffraction patterns of Blakeley, 1976, fibres were prepared from gels centrifuged from solutions as described in chapter 2.4. The contents of the solutions prior to centrifugation are shown in Table 7.1. The solution from which gel 3 was centrifuged gave a similar pH to that of solution 2 despite the absence of Tris.HCl pH 7.4. Solutions from which gels 4 and 5 were centrifuged were prepared in the absence of Tris.HCl pH 7.4 and although their pH was not measured it was probably  $\sim 7.1$  in both cases. Similarly, the pH of the solution from which gel 6 was centrifuged was likely to be close to that of solution 2  $\sim 7.3-7.4$ .

The P/D ratios of the gels were determined by absorption spectroscopy. U.V. absorption of solutions containing DNA but no drug showed that only 5% of the DNA remained in the supernatant after centrifugation. This quantity of DNA was considered to have a negligible effect on the visible absorption spectra of drug solutions. Thus for the purpose of analysis the supernatants of drug/DNA solutions were deemed to contain only non-bound drug. The DNA phosphate concentration of a gel was calculated assuming 95% of the DNA in the solution prior to centrifugation was obtained in the sedimented gel. The drug concentration of the gel was calculated from the difference between the drug concentration in the solution prior to centrifugation and the concentration of the drug in the supernatant after centrifugation. One or more fibres were selected from each gel and diffraction patterns were

Gel No.	DNA conc./mM	NaCl conc./mM	Tris.HCl/mM	pH	Steffimycin B conc./mM	Methanol conc./%	P/D
1	0.30	10.0	10.0	8.5	49	15.5	~6.0
2	0.33	10.0	10.0	7.3	73	26.8	6.6
3	0.31	10.0	-	7.1	68	25.0	8.6
4	0.33	10.0	-	-	44	23.6	10.9
5	0.22	10.0	-	-	37	20.0	8.4
6	0.19	32.0	32.0	-	32	39.5	8.4

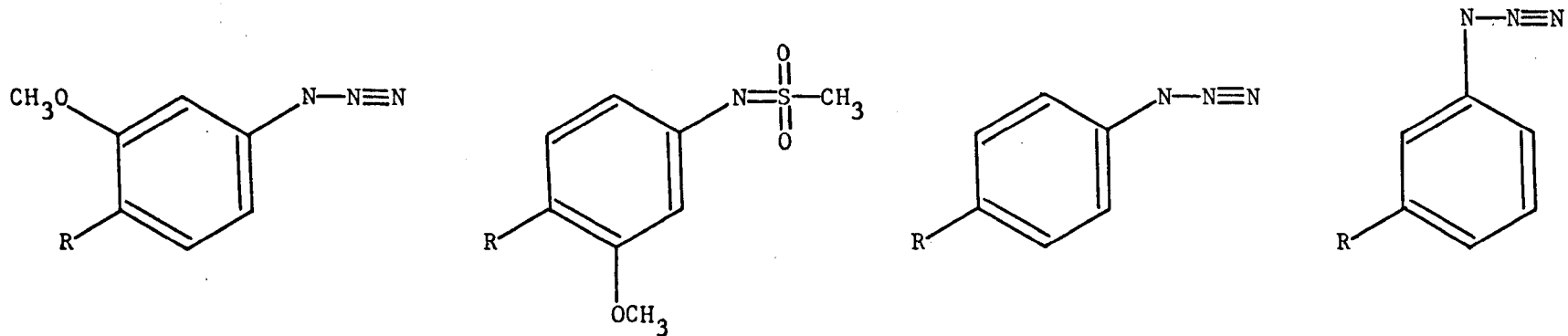
Table 7.1 Contents of steffimycin B/DNA solutions prior to centrifugation.

recorded at various humidities using pinhole and toroidal optics.

In addition to the properties of the acridines already discussed these compounds are important as potential antitumour agents. This is especially true of members of the acridinyl methane sulphonanilide (AMSA) series which are active against a number of experimental tumours in animals as well as in man, Cain and Atwell, 1974, Cain et al., 1974. Mr. C. Wong of the Department of Pharmacy, University of Aston, Birmingham has synthesised four derivatives of the m-AMSA compound in order to further investigate the enhanced biological activity of these acridines, Wong, 1979. The graphic formula of these acridine derivatives are given in Figure 7.2. The x-ray diffraction patterns of fibres of these compounds complexed with DNA has been examined.

These compounds were kept frozen until ready for use since some of them decompose rapidly on exposure to light. Stock solutions of the acridine derivatives were prepared by dissolving 10.0mg of each compound in 5.0ml of dimethyl sulphoxide, DMSO. DMSO is a powerful organic solvent and its use was necessary since the derivatives are only sparingly soluble in aqueous solution. Fibres were prepared from each of the acridine derivatives complexed with DNA from gels centrifuged from solution as described in chapter 2.4. Prior to centrifugation the concentrations of the solutions were 0.38mM deproteinized calf thymus DNA, 10mM NaCl, 1.0mM Tris.HCl pH 7.4, 62.5µM drug giving a P/D = 6.0 and ~1% v/v DMSO. A DNA control gel was also prepared from a solution of the same concentration of DNA, NaCl and Tris. HCl pH 7.4 but contained no acridine derivative or DMSO. Owing to the lack of information regarding the extinction coefficients of these acridine derivatives no attempt was made to calculate a more accurate P/D ratio for the sedimented gels as previously described for steffimycin B/DNA gels. One or more fibres were selected from each gel and diffraction patterns were usually recorded at 75%, 92%, 98%, 92%, 75% and 57% rh using pinhole or toroidal optics.



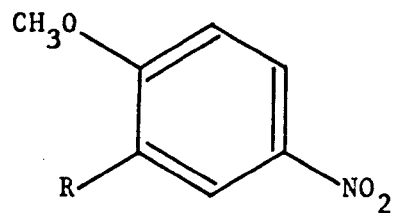


9-(2-Methoxy-4-azidoanilino)~  
acridine hydrochloride

9-[4-(9-acridinylamino)~  
methanesulphon-m-anisidide hydro~  
chloride [m-AMSA]

9-(4-Azidoanilino)~  
acridine hydrochloride

9-(3-Azidoanilino)~  
acridine hydrochloride



9-(2-Methoxy-5-nitroanilino)~  
acridine hydrochloride

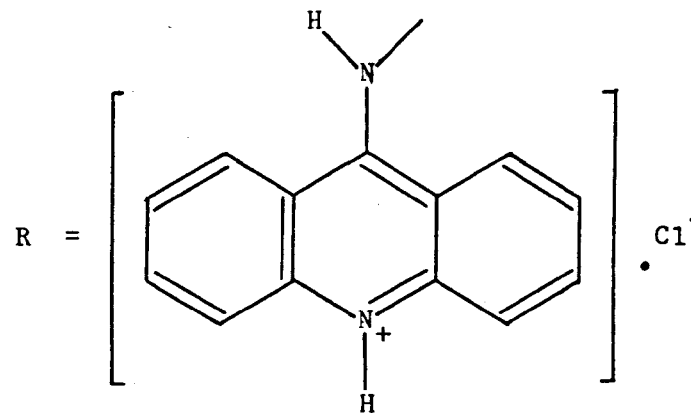


**Figure 7.2** Graphic formulae of the acridine derivatives synthesized by Wong, 1979.

#### 7.4 Results

a) X-ray diffraction patterns of steffimycin B/DNA fibres produced from gels 1 to 6.

Fibres from gel 1 generally gave A diffraction patterns at 75% rh and semi-crystalline B patterns at 98% rh. Superimposed on the B patterns was a reflection  $\sim 0.72\text{nm}$  as shown in Plate 7.2. On reducing the relative humidity, the B conformation remained stable in one fibre but changed to the A conformation at 75% rh in the other fibres. In all cases the meridional reflection at  $0.72\text{nm}$  remained.

Fibres from gel 2 gave B or A/B diffraction patterns at 66% and 92% rh and showed some evidence of crystalline steffimycin B reflections although the degree of crystallinity was very poor compared with Blakeley's patterns.

Fibres from gel 3 gave B diffraction patterns in the humidity range of 0-92% and one of the fibres exhibited crystalline steffimycin B reflections similar to those observed from fibres of gel 2.

Fibres from gels 4 and 5 all gave B diffraction patterns in the relative humidity range of 44-98% and no patterns were obtained exhibiting crystalline drug reflections. An example of the type of diffraction pattern obtained from these fibres is shown in Plate 7.3.

Fibres from gel 6 all gave B type diffraction patterns at 92% and 98% rh with no evidence of crystalline steffimycin B reflections. The gel was inadvertently allowed to dry out and was then redissolved in glass distilled water. On producing a new fibre from this gel crystalline steffimycin B reflections were obtained similar to those observed in patterns from fibres of gels 2 and 3. An example of this type of diffraction pattern is shown in Plate 7.4. A variation in the relative humidity of the fibre environment produced no apparent changes in the crystalline reflections.

As gels 2, 3, 4 and 6 dried out thin needle shaped crystals of steffimycin B were visible to the naked eye.

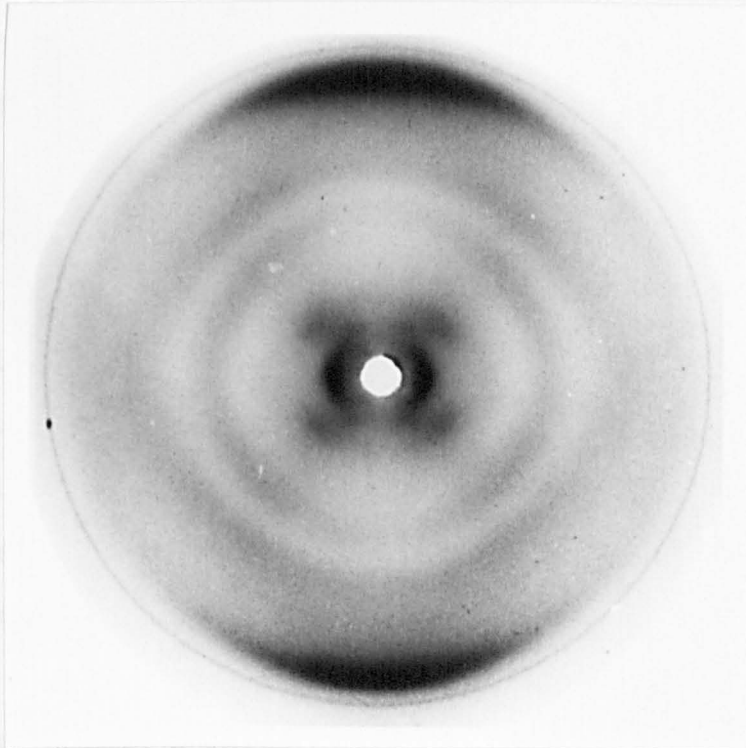


Plate 7.3

Steffimycin B/DNA fibre,  $P/D = 8.4$ ,  $rh = 92\%$ , from gel 5 showing the type of B diffraction pattern obtained in the absence of crystalline steffimycin B.

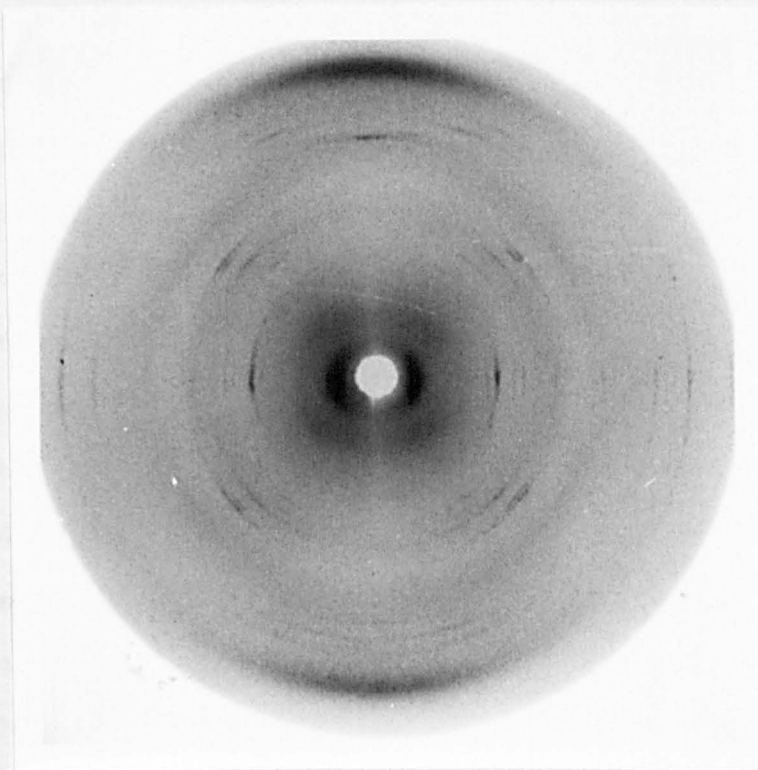


Plate 7.4

Steffimycin B/DNA fibre,  $P/D = 8.4$ ,  $rh = 98\%$ , from gel 6 showing some evidence of crystalline steffimycin B diffraction superimposed on that of B DNA diffraction.

b) Analysis of the best crystalline steffimycin B/DNA diffraction pattern

Of the diffraction patterns so far recorded at the University of Keele, the steffimycin B/DNA patterns obtained by Blakeley, 1976, are the best examples of a small molecule crystallizing in a DNA fibre. Attempts to reproduce these patterns with a similar degree of crystallinity have not been successful. In order to see whether any further information could be obtained from Blakeley's patterns one of them was reexamined.  $x$  and  $y$  coordinates of the crystalline steffimycin B reflections were measured using the Pye microscope.  $\zeta$ ,  $\xi$ ,  $\rho$  and  $d$ -spacings were calculated using the computer program 'Film' and a  $\xi$ - $\zeta$  plot was constructed as shown in Figure 7.3. The patterns indexed on a hexagonal lattice as described by Blakeley, 1976.  $\rho$ -spacing of unambiguously identified reflections were used in conjunction with their assigned Miller indices to calculate lattice parameters which were subjected to a cyclic least squares refinement using the computer program 'Hex'. Blakeley's x-ray negative was then reproduced onto a 15" x 12" photographic plate. An accurately ruled 0.5mm grid on a glass plate was also reproduced onto a 15" x 12" plate which was carefully measured. Distortions due to misalignment of the enlarging equipment and non-linear shrinkage of the emulsion were shown to be negligible. The refined lattice parameters from the computer program 'Hex' were used to calculate the radii for all possible reflections of the steffimycin B lattice out to 15.0cm using the computer program 'Find E'. A specimen to film distance was used in this program which took account of the enlargement factor involved in the production of the photographic plate. The radii of the steffimycin B reflections on the photographic plate of Blakeley's pattern were determined using a beam compass and steel rule. Particular attention was given to the regions of the plate where a reflection was predicted by the 'Find E' program, but where no reflection had previously been observed using the Pye microscope. The updated set of  $\rho$ -spacings so obtained was again used in the computer program 'Hex' to give final lattice parameters

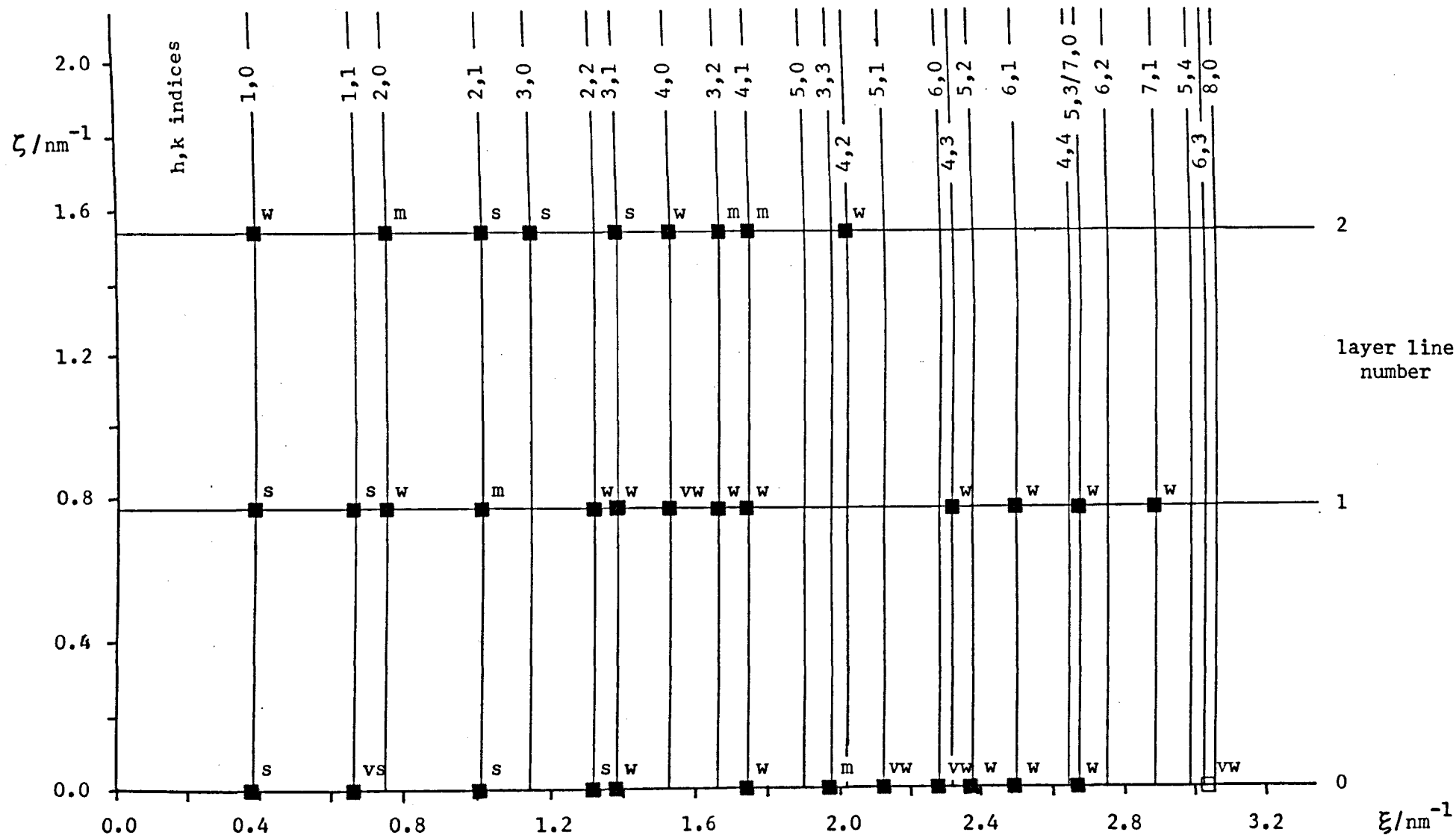


Figure 7.3

A xi-zeta plot of the diffraction pattern shown in Plate 7.1. ■, □ indicates the observation of a Bragg reflection while shading indicates the use of the  $\rho$ -spacing of that reflection in the lattice refinement program. The letters vs, s, m, w and vw refer to the apparent relative intensities of the reflections. The plot corresponds to a hexagonal lattice with  $a = 3.024\text{nm}$  and  $c = 0.7712\text{nm}$ .

of  $a = 3.024 \pm 0.003\text{nm}$  and  $c = 0.7712 \pm 0.0007\text{nm}$ . The observed and calculated  $\rho$ -spacings together with their assigned Miller indices are recorded in Table 7.2. There is little difference in the spacings of the reflections recorded by Blakeley, 1976, compared with those in Table 7.2 and the final lattice parameters determined from the two data sets are not significantly different.

In an attempt to examine further the structure of steffimycin B radial traces of the reflections on Blakeley's negative were recorded using the microdensitometer. However, several problems were encountered. Blakeley's patterns had been recorded on Kodirex film and the background intensity is very high. Therefore the error in determining the intensities of the reflections is large and may be as much as 50%. In addition, although the diffraction pattern was recorded on two x-ray films placed one behind the other several of the reflections gave intensities well in excess of 1.0 O.D. In this region of optical density the blackening of the film is no longer proportional to the intensity of the incident radiation. In order to obtain a more accurate and complete set of intensity measurements it is necessary to record the diffraction patterns on several x-ray films to get a large range of intensity measurements. It is also important to use an x-ray film which is not highly susceptible to extraneous radiation. In this respect although Ilford Industrial G is no longer marketed the Swedish film Cea seems to be superior to the current Kodak alternative, Kodak No Screen film. In view of the large variation in the size of the reflections which increase rapidly with diffraction angle it is necessary to determine intensity measurements from both radial and tangential traces, Marvin et al., 1961. Alternatively the intensity data from the diffraction patterns could be digitalized using an Optronics rotating drum densitometer. The SERC unit at Daresbury provide a service to this end. A number of corrections should be applied to the intensity measurements of these types of diffraction patterns and these have been concisely reviewed and updated by Fraser et al.,

Assigned h,k,l Value	$\rho$ Observed /nm <sup>-1</sup>	$\rho$ Calculated /nm <sup>-1</sup>	Apparent Relative Intensity
1 0 0	0.380	0.382	s
1 1 0	0.660	0.661	vs
2 1 0	1.011	1.010	s
2 2 0	1.321	1.323	s
3 1 0	1.379	1.377	w
4 1 0	1.749	1.750	w
3 3 0	1.980	1.984	m
5 1 0	2.126	2.126	vw
6 0 0	2.295	2.291	vw
5 2 0	2.388	2.384	w
6 1 0	2.508	2.504	w
5 3 0/7 0 0	2.676	2.673	w
6 3 0 or 8 0 0	3.035	-	vw
1 0 1	1.351	1.352	s
1 1 1	1.456	1.456	s
2 0 1	1.507	1.505	w
2 1 1	1.634	1.644	m
2 2 1	1.852	1.852	w
3 1 1	1.893	1.891	w
4 0 1	2.001	2.004	vw
3 2 1	2.112	2.110	w
4 1 1	2.180	2.178	w
4 3 1	2.657	2.660	w
6 1 1	2.816	2.820	w
5 3 1/7 0 1	2.961	2.971	w
7 1 1	3.163	3.161	w
1 0 2	2.628	2.621	w
2 0 2	2.697	2.704	m
2 1 2	2.782	2.783	s
3 0 2	2.838	2.835	s
3 1 2	2.936	2.936	s
4 0 2	3.015	3.010	w
3 2 2	3.083	3.082	m
4 1 2	3.128	3.129	m
4 2 2	3.286	3.288	w

Table 7.2

Observed and calculated  $\rho$ -spacings together with their assigned Miller indices for the steffimycin B/DNA pattern shown in Plate 7.1. The corresponding relative intensities are also shown.

1976.

In an effort to obtain a more complete set of intensity measurements Blakeley's fibres were re-x-rayed but they were found to be extremely brittle and better diffraction patterns were not forthcoming. Attempts to produce better diffraction patterns from new steffimycin B/DNA fibres met with little success as described in section 7.4a.

Using the refined lattice parameters of crystalline steffimycin B obtained from the computer program 'Hex' the volume of the steffimycin B unit cell was found to be  $6.12\text{nm}^3$ . Assuming that the density of steffimycin B is similar to that of the related anthracycline daunomycin monohydrochloride, Neidle and Taylor, 1977, then the number of molecules per unit cell is given in Equation 7.1.

$$\begin{aligned}
 N &= \frac{\rho \times \text{Vol. unit cell} \times L}{\text{M.Wt.}} && \text{- Equation 7.1} \\
 &= \frac{1.36\text{gcm}^{-3} \times 6.12 \times 10^{-21}\text{cm}^3 \times 6.023 \times 10^{23}}{588\text{g}} \\
 &= 8.65
 \end{aligned}$$

where N is the number of molecules in the unit cell

$\rho$  is the assumed density of steffimycin B

Vol. unit cell is the volume of the steffimycin B unit cell

M.Wt. is the molecular weight of steffimycin B

L is Avogadro's number

The fraction of solvent in the unit cell of steffimycin B in a hydrated fibre is probably greater than that found in the crystal of daunomycin monohydrochloride. Thus it is likely that the value of density used in Equation 7.1 has been overestimated leading to an overestimation in N. Since the unit cell of steffimycin B is hexagonal the most likely value for N is 6.

The steffimycin B molecule is asymmetric and thus of the hexagonal space groups those containing mirror, glide or inversion elements cannot



describe the steffimycin B unit cell. The remaining hexagonal space groups are given in Table 7.3 together with the number of asymmetric units per unit cell and the number of asymmetric units in the c direction of the unit cell for each space group. The unit cell of steffimycin B has a c dimension of only 0.77nm and the thickness of the steffimycin B chromophore is 0.34nm. Thus it is unlikely that the number of steffimycin B molecules in the c direction of the unit cell is more than two. It is also unlikely that this number is less two owing to the tendency for the non-polar chromophores of these types of molecules to stack in aqueous environments. From Table 7.3 it can be seen that only the P3, P312, P321 and P6<sub>3</sub> space groups fill the criteria of 6 molecules per unit cell and two asymmetric units in the c direction of the unit cell. Mr. F. Bingham has attempted to arrange CPK models of steffimycin B according to the symmetries imposed by the most likely space groups. The easiest packing arrangements were obtained using P312 or P321 space group symmetry and Plate 7.5 shows steffimycin B CPK models arranged in a unit cell with the latter symmetry. The only systematic absences which may occur as a result of the general conditions of symmetry associated with the P3, P312, P321 and P6<sub>3</sub> space groups are that  $l = 2n$  for the 00l reflections of the P6<sub>3</sub> space group. On this basis it was not possible to distinguish which of the space groups best described the steffimycin B lattice.

c) X-ray diffraction patterns of acridine derivative/DNA fibres

All the diffraction patterns obtained from the acridine derivative/DNA fibres gave disordered or semi-crystalline B type diffraction patterns. A typical example of this type of pattern is provided by a fibre of the 4-azide derivative/DNA complex at 75% rh as shown in Plate 7.6. The diffraction patterns were not sufficiently well resolved to make accurate measurements of pitch and intermolecular spacing values and no evidence was obtained as to whether the compounds interact with DNA by intercalation. Fibres from m-AMSA and 5-nitro derivative/DNA complexes gave disordered or semi-

Space Group	No. of Asymmetric Units per Unit Cell	No. of Asymmetric Units in the $a$ Direction	Comments
P3	3	1	Possible if there is an asymmetric unit of 2 molecules.
P3 <sub>1</sub>	3	3	
P3 <sub>2</sub>	3	3	
R3	3	3	
P312	6	2	Possible
P321	6	2	Possible
P3 <sub>1</sub> 12	6	6	
P3 <sub>1</sub> 21	6	6	
P3 <sub>2</sub> 12	6	6	
P3 <sub>2</sub> 21	6	6	
R32	6	6	
P6	6	1	2 molecules per asymmetric unit leads to 12 molecules per unit cell.
P6 <sub>1</sub>	6	6	
P6 <sub>5</sub>	6	6	
P6 <sub>2</sub>	6	3	
P6 <sub>4</sub>	6	3	
P6 <sub>3</sub>	6	2	Possible
P622	12	2	
P6 <sub>1</sub> 22	12	12	
P6 <sub>5</sub> 22	12	12	
P6 <sub>2</sub> 22	12	6	
P6 <sub>4</sub> 22	12	6	
P6 <sub>3</sub> 22	12	4	

Table 7.3

The set of hexagonal space groups excluding those containing mirror and inversion elements, with information relating to their suitability in describing the steffimycin B lattice.

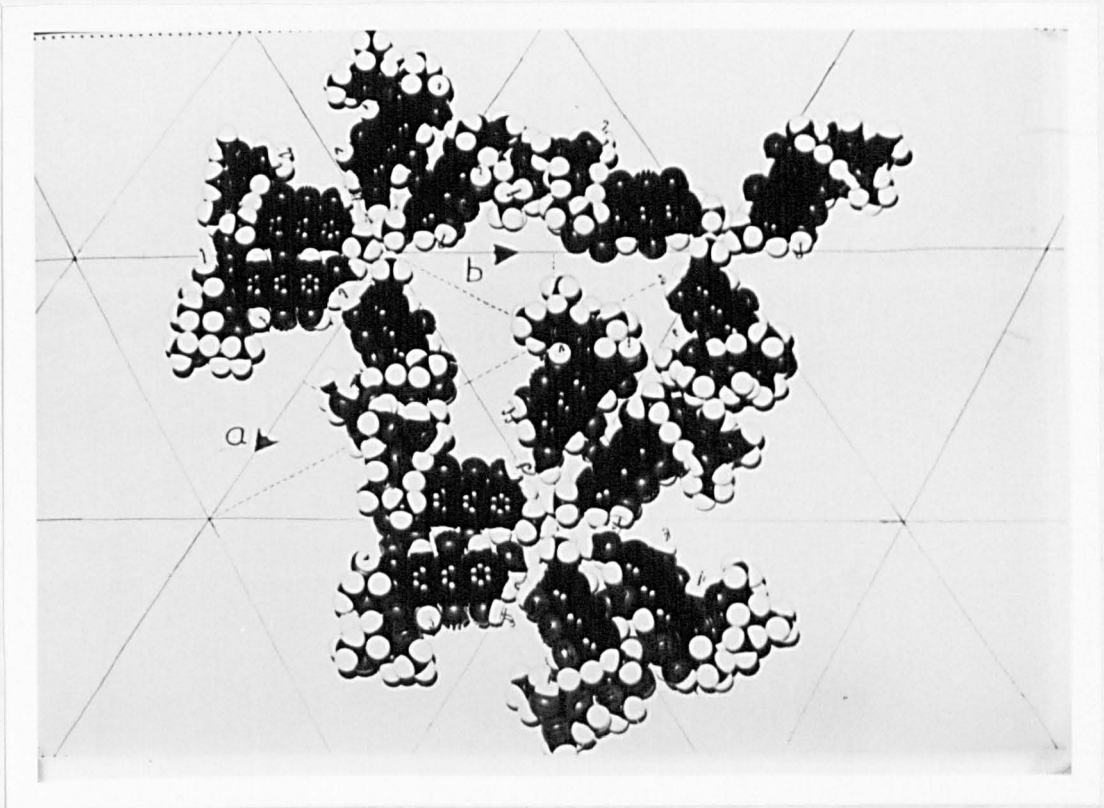


Plate 7.5

The arrangement of steffimycin B CPK molecules in a hexagonal unit cell using P321 symmetry. For the sake of clarity not all the steffimycin B molecules are shown. Courtesy of Bingham, 1977.

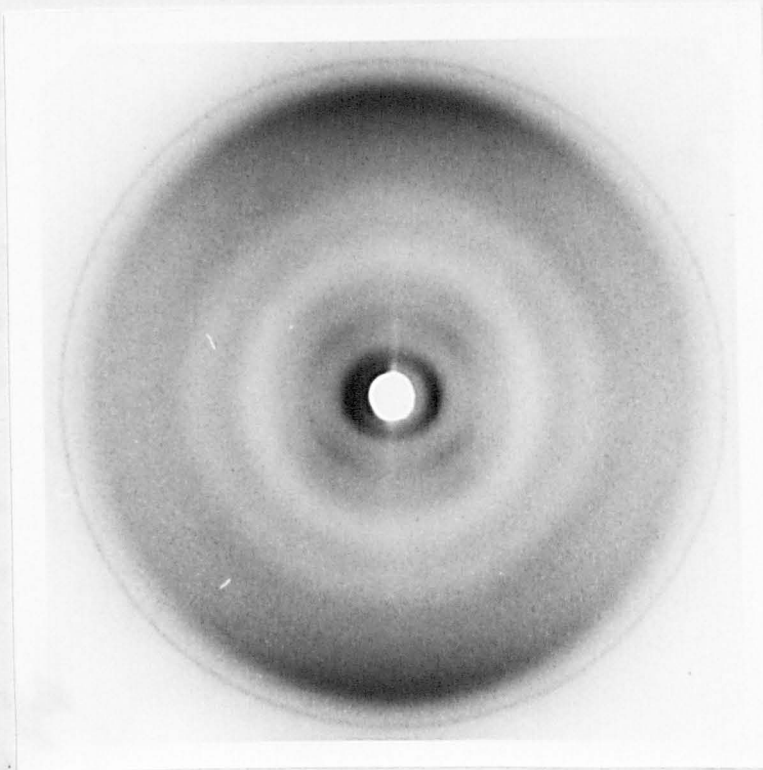


Plate 7.6

4-azide acridine derivative/DNA fibre, P/D  $\sim 6.0$ , rh = 75%, showing a disordered B type diffraction pattern.

crystalline B patterns on which were superimposed crystalline acridine derivative reflections as shown in Plates 7.7 and 7.8 respectively. In these patterns the acridine derivative reflections appear particularly extended and often circular indicating little orientation of the molecules within the DNA fibres. Owing to the lack of well resolved x-ray data no attempt has been made to compare this data with that obtained for steffimycin B, by Blakeley, 1976.

Changing the relative humidity of the fibre environment had little apparent effect on the appearance of either the disordered semi-crystalline B patterns or the reflections associated with the crystalline acridine derivatives.

Evidence of some interaction between the acridine derivatives and DNA was apparent from the diffraction patterns from the DNA control gel. These fibres gave A/B diffraction patterns at 75% rh, A/B or B patterns at 92% rh and B patterns at 98% rh. The absence of A diffraction patterns for the acridine derivative/DNA fibres at low humidity suggest that these derivatives stabilize DNA in the B conformation. The nature of this interaction is not clear at present.

### 7.5 Discussion

In attempting to determine the conditions for the crystallization of steffimycin B in DNA fibres well resolved x-ray diffraction patterns were not obtained. The inferences given below are based on patterns from poorly crystalline steffimycin B/DNA fibres and are somewhat tentative.

Generally steffimycin B/DNA fibres exhibited the B conformation throughout the range of humidities investigated. The observation of fibres from gel 1 in the A conformation at low relative humidity suggest that at the higher pH of 8.5 steffimycin B/DNA complexes are less stable. It is interesting that fibres of this gel only exhibited the meridional reflection  $\sim 0.72\text{nm}$  on assumption of the B conformation at

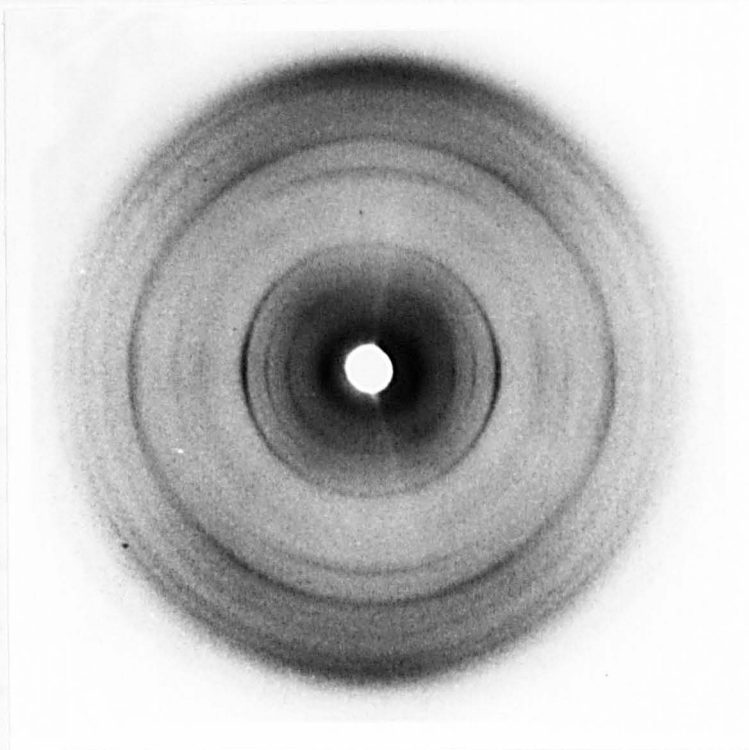


Plate 7.7

m-AMSA/DNA fibre, P/D  $\sim 6.0$ , rh = 75%, showing crystalline acridine derivative reflections superimposed on a disordered B type diffraction pattern.

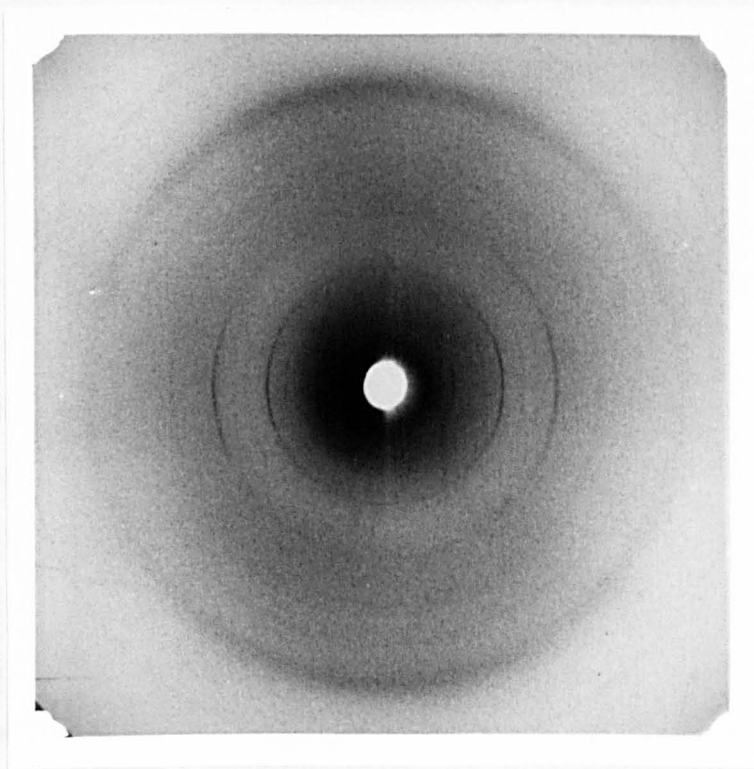


Plate 7.8

5-nitro acridine derivative/DNA fibre, P/D  $\sim 6.0$ , rh = 92%, showing crystalline acridine derivative reflections superimposed on a disordered B type diffraction pattern.

high humidity, while this reflection remained when the relative humidity of the fibre environment was lowered despite a change in DNA conformation to that of A in some fibres. The 0.72nm reflection is similar to the 0.68nm reflection observed on x-ray diffraction patterns from proflavine/DNA fibres, Neville and Davies, 1966. The 0.72nm reflection may arise as the result of the stacking of steffimycin B molecules to form dimers. However, whether this occurs as a result of high humidity or is initiated by a change in DNA conformation remains unclear. Once formed the structure giving rise to the meridional reflection seems unaffected by changes in relative humidity or DNA conformation.

Variation of P/D ratio in the range 6.6-10.9 produced no obvious trend in the appearance of crystalline steffimycin B reflections on steffimycin B/DNA diffraction patterns. A comparison of diffraction patterns from fibres of gels 2 and 3 showed no evidence of any effects on steffimycin B crystallization due to the presence of 10mM Tris.HCl pH 7.4 in the steffimycin B/DNA solutions prior to centrifugation.

The appearance of crystalline steffimycin B reflections in patterns from fibres of gel 6 may have occurred as the result of the increase of sodium chloride concentration in the solution from which the gel was centrifuged. This probably causes a decrease in steffimycin/DNA interaction due to increased competition from  $\text{Na}^+$  and  $\text{Cl}^-$ . However, the concentrations of Tris.HCl and methanol were also increased in this solution prior to centrifugation and it has not been shown whether these factors have contributed to the crystallization of steffimycin B.

Crystalline and non-crystalline steffimycin B/DNA diffraction patterns have been obtained from fibres prepared from the same gel and it seems likely that fibre preparation plays an important role in the crystallization of steffimycin B in DNA fibres. The conditions pertaining at the time of fibre preparation which may be important for the production of crystalline steffimycin B/DNA fibres include temperature and relative humidity at which

the fibre is formed and the extent to which the gel has dried out. In these experiments none of these effects could be associated with the production of even poorly crystalline steffimycin B/DNA fibres. The appearance of steffimycin B crystals in gels 2, 3, 4 and 6 as they dried out may be relevant to the lack of success in obtaining crystalline steffimycin B/DNA fibres. Blakeley, 1976, did not observe steffimycin B crystals in his gels or the fibres produced from them. This suggests that in Blakeley's gels the rate of nucleation has proceeded at a faster rate than crystal growth while the converse is true for the experiments described above. The conditions responsible for such effects have not been established.

The analysis of Blakeley's diffraction pattern of crystalline steffimycin B/DNA gives some indication of the space groups which may describe crystalline steffimycin B in DNA fibres. However, the space group has not been unambiguously identified and it is unlikely that further information can be obtained from these patterns for reasons already discussed. Well defined x-ray diffraction patterns of crystalline steffimycin B/DNA fibres from which complete sets of intensity data can be obtained are necessary in order to proceed with this structure problem. It is of particular interest as to whether steffimycin B crystallization is influenced by the presence of DNA since this may provide information with regard to the steffimycin B/DNA structure prior to crystallization and as to how this structure was formed. It is also important to determine the crystal structure and the conditions of its formation from the point of view of chemotherapeutic exploitation.

The x-ray diffraction patterns of the acridine derivative/DNA fibres demonstrated the crystallization of the m-AMSA and 5-nitro compounds in DNA fibres. However, whether these compounds gave rise to crystalline reflections in DNA fibres as a result of their structural differences or differences in their physico-chemical properties, compared with the remaining three acridine derivatives examined has not been established. The appearance of crystalline reflections in these samples may have occurred

due to differences in sample preparation which were not apparent at that time.

In examining the structure and properties of the compounds which are known to exhibit crystalline reflections in DNA fibres poor solubility in aqueous solvents seemed to be a common feature. Crystalline drug/DNA complexes were prepared from steffimycin B dissolved in methanol and acridine derivatives dissolved in DMSO, the solvents being necessary in order to obtain P/D ratios  $\sim 6.0$ . The situation is complicated by the potential role of the solvents in drug crystallization.

Proflavine/DNA fibres indicative of intercalation were only obtained at relative humidities of 100%+ in which the fibres had first been exposed to a fine mist of water, Neville and Davies, 1966. Diffraction patterns of fibres under these conditions exhibited meridional reflections at 0.68nm and this again seemed to emphasize the association of the lack of solubility of the drug in aqueous solution with the appearance of crystalline drug reflections on drug/DNA diffraction patterns. However, miracil D and toluidine blue which are adequately soluble in water give well resolved crystalline small molecule/DNA diffraction patterns. The possibility that miracil D crystallizes in DNA fibres owing to its inability to intercalate in DNA, as suggested by Davies, 1973, is not in agreement with the work of Heller et al., 1974, and Waring, 1970. The proposed non-planar ring system of miracil D as a feature preventing intercalation also contrasts with the results of Neidle, 1976. However, drug/DNA interactions in the fibre and solution states may not be identical.

Pigram, 1968, Pigram et al., 1972, and Porumb, 1976, have examined daunomycin and adriamycin/DNA fibres using x-ray diffraction techniques but have not obtained any evidence of crystallization of these antibiotics in DNA fibres. Daunomycin and adriamycin each have an amino substituent on their sugar residues which is able to form an additional hydrogen bond with the oxygen phosphate atoms of the DNA backbone, increasing the stability of



the antibiotic/DNA complex. Evidence of this increased stability is provided by measurements of the binding affinities for DNA of these compounds, Dall'Acqua et al., 1979. These antibiotic/DNA complexes have so far remained stable during changes in the environmental conditions of the fibres. In the case of the steffimycins, which exhibit a lower binding affinity for DNA, then it is probable that fibre conditions give rise to free energies of drug/drug interactions which are greater in magnitude than those of drug/DNA interactions thus resulting in dimer or crystal formation.

The results of Dall'Acqua et al., 1979, suggest that factors other than binding affinity for DNA affect the ability of a drug to crystallize in DNA fibres. Dall'Acqua et al. report a slightly higher binding affinity of steffimycin B for DNA receptor sites compared with steffimycin although the latter compound which was more extensively studied by Blakeley, 1976, failed to give well resolved crystalline drug/DNA diffraction patterns. However, again there is the danger of applying the results of solution experiments to the fibre state.

Blakeley, 1976, has suggested that DNA affects the crystal structure of steffimycin B and that it is the orientation of the chromophore in contact with the DNA which seeds crystal formation. Blakeley has concluded that the formation of crystalline steffimycin B regions in the presence of oriented DNA is a stable arrangement and is initiated by hydrophobic conditions.

In the course of this work little evidence was obtained to support or contradict Blakeley's proposed mechanism for the crystallization of steffimycin B in DNA fibres. No changes were apparent in the diffraction patterns of partially crystalline steffimycin B/DNA and acridine derivative/DNA fibres as a result of changes in the relative humidity of the fibre environment. However, initially steffimycin B/DNA fibres prepared from gel 1 only gave diffraction patterns exhibiting meridional reflections at 0.72nm under hydrophilic conditions. A similar result was obtained for

proflavine/DNA fibres, Neville and Davies, 1966. It is possible that diffraction patterns exhibiting these reflections represent a drug structure which is not an intermediate stage in the complete crystallization of the drug compounds.

It seems likely that a drug with low solubility in aqueous solution and a relatively low binding affinity for DNA are possible indicators that it will crystallize in DNA fibres. However, the conditions of gel and fibre preparation exert a strong influence on the ability of small molecules to crystallize in DNA fibres.

Once the conditions for the crystallization of a specific small molecule in DNA fibres have been established it would be of interest to examine the crystallization phenomenon in Na poly[d(A-T)].poly[d(A-T)] fibres. The steffimycins have been shown to exhibit strong A,T specificity, Blakeley, 1976, and Dall'Acqua et al., 1979. Thus both intercalation and crystallization of these antibiotics in Na poly[d(A-T)].poly[d(A-T)] fibres may result in very regular structures giving well resolved x-ray diffraction patterns from which a greater degree of information may be obtained than has so far been possible using native random sequence DNA. It would also be of interest to determine whether any of the conformations known to be available to Na poly[d(A-T)].poly[d(A-T)], other than the B form, can occur in the presence of crystalline drug reflections. The absence of the A conformation in crystalline steffimycin B/DNA fibres provides some evidence for the interaction of steffimycin B with DNA. However, whether this is due to residual steffimycin B intercalating with DNA or whether it arises from crystalline steffimycin B/DNA interaction is not known. It may well be possible to exploit the homogeneous sequence of synthetic polynucleotides to provide further information on the crystallization of small molecules in nucleic acid fibres.

Chapter 8. AN X-RAY INVESTIGATION INTO THE COMPLEX FORMED BETWEEN BOVINE  
SERUM ALBUMIN AND MONTMORILLONITE

8.1 Introduction

A large variety of substances have been shown to participate in interlamellar adsorption when complexed with the clay mineral, montmorillonite. Mooney et al., 1952, Norrish, 1954, Fink, 1977, and Cebula et al., 1979, have investigated montmorillonite swelling in the presence of water and inorganic cations. Hendricks, 1941, and Greene-Kelly, 1955, have examined montmorillonite complexed with many different organic cations while Greenland, 1956, has analysed montmorillonite swelling as a result of sugar adsorption. An extensive review of the montmorillonite minerals and their interactions is given by MacEwan, 1961. Methods for analysing the x-ray data of these systems have been devised by Norrish, 1954, Height et al., 1960, 1962, and MacEwan, 1956.

The interaction of proteins with montmorillonite has received relatively little attention. However, Ensminger and Gieseck, 1940, have examined the interaction of albumin with montmorillonite and observed that the  $d_{001}$  spacings of the complexes increased from 2.4nm to 4.8nm as the protein/clay ratio was increased from 0.5 to 4.0. They obtained similar results for gelatin/montmorillonite complexes. Ensminger and Gieseck, 1941, showed that other protein/montmorillonite complexes had enhanced d-spacings and reduced base-exchange capacities compared with uncomplexed montmorillonite which was consistent with protein adsorption in the interlamellar regions of montmorillonite. Talibudeen, 1955, has also found that a number of other protein/montmorillonite complexes gave large  $d_{001}$  spacings corresponding to interlamellar protein adsorption.

The early work of Ensminger and Gieseck, 1940, 1941, was carried out in order to determine interactions between organic matter and the clay fraction of the soil. This area of research is relevant to the question

of soil fertility. The adsorption by clays of a great variety of smaller molecules and ions is of importance to the oil and mining industries where the production of slurries of optimum constitution for transportation is of vital commercial interest.

The experiments in this work were carried out to confirm the adsorption of albumin in the interlamellar regions of montmorillonite as reported in the earlier literature and to obtain some information with regard to the orientation of the complexed albumin. These experiments also provide an opportunity to optimise sample preparation. This work provides a basis for a much wider range of experiments.

Lyklema and Norde, 1973, using adsorption techniques showed that human serum albumin is adsorbed onto the surface of polystyrene latex (PSL) beads. Diffraction methods give a more direct means of determining the structure of such complexes. The comparison of montmorillonite and PSL substrates with the same adsorbate would be of great interest. In addition the interaction of different proteins with the same substrate may give useful information with regard to the different types of protein interaction on the same substrate. A more complete understanding of how these substrates behave under various environmental conditions may also yield a method for obtaining structural information of proteins.

Protein/montmorillonite complexes bear a useful resemblance to protein/membrane systems. A specific example is in the interaction of protein with arterial walls. Similarly, protein/PSL particles are reminiscent of spherical virus particles. The results gained from these types of partially synthetic systems may provide information with regard to the more complex native systems.

The advantages of using neutron diffraction methods to investigate montmorillonite/water systems have been discussed by Cebula et al., 1979. The main advantage of such techniques with regard to protein/montmorillonite or protein/PSL systems is that suitable variation of the hydrogen to

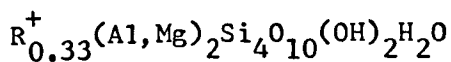
deuterium ratio in the solvent allows the substrate or protein to be contrast matched out of the system. This allows the individual contributions from the solvent and protein to interlamellar swelling to be determined.

It is envisaged that these albumin/montmorillonite experiments will form a basis for a wider range of experiments involving protein/montmorillonite and protein/PSL complexes using both x-ray and neutron diffraction techniques.

## 8.2 Materials and methods

### a) Montmorillonite

The name montmorillonite is currently used in three senses which must be clearly distinguished. In its most general sense montmorillonite is used to identify a group of hydrated silicates of different chemical composition giving essentially similar x-ray diffraction patterns. More specifically the name refers to a sub group of the hydrated silicates which contain mainly silica and alumina with usually a little magnesia and some replacement of alumina by ferric oxides. In particular montmorillonite is applied to a mineral of this sub group having the formula shown in Equation 8.1.



- Equation 8.1

Where R includes  $K^{+}$ ,  $Mg^{2+}$ ,  $Ca^{2+}$  and others.

It is in this latter sense that the name montmorillonite is used in this work. As a result of the amorphous nature of montmorillonite it has not been possible to deduce its precise structure from the available x-ray data. However, it is generally believed that the silicate sheet structure of montmorillonite closely resembles that of pyrophyllite and talc, although the silicate tetrahedra are thought to be irregularly superimposed while  $Al^{3+}$  is replaced by  $Mg^{2+}$  in octahedral sites. The

resultant charge on the silicate sheets is balanced by interlamellar cations. A schematic diagram of the supposed structure is shown in Figure 8.1.

b) Bovine serum albumin (BSA)

Bovine serum albumin is a plasma protein which serves in the regulation of pH and osmotic pressure and in the transportation of metal ions, fatty acids, steroids, hormones and amino acids. It consists of a single polypeptide chain of 590 amino acids and has a molecular weight of 69,000. BSA is thought to be approximately ellipsoidal in shape, but the estimated axial lengths of the molecule have varied according to the experimental method of investigation. Riddiford and Jennings, 1966, have reported values of 11.6nm and 2.7nm for the major and minor axes of the ellipsoid using low angle x-ray diffraction while Squire et al., 1968, have given values of 14.0nm and 4.0nm based on measurements of sedimentation coefficients and diffusion constants. Low, 1952, has described the shape of BSA in terms of a modified right prism of dimensions 14.8nm, 2.2nm and 4.5nm, again using low angle x-ray diffraction. The differences in these values may result from the inclusion or exclusion of the volume of the water of hydration in the volume occupied by the dehydrated protein.

c) Sample preparation

Sodium montmorillonite was prepared from Wyoming bentonite according to the procedure used by Callaghan and Ottewill, 1974. The sodium counter ion was then removed by dialysis and an alkaline water suspension of the clay was thoroughly mixed with an alkaline water suspension of BSA at definitive ratios. Under these conditions a homogeneous mixture was easily obtained since the two substances are negatively charged. The pH of the resultant suspension was lowered by the addition of dilute acetic acid to a value of 3.5. This is below the isoelectric point of the BSA and thus leaves the protein with a net positive charge. Flocculation of the protein with the negatively charged mineral then takes place during continued mixing over a period of some 50 hours. From this stage the flocculate can

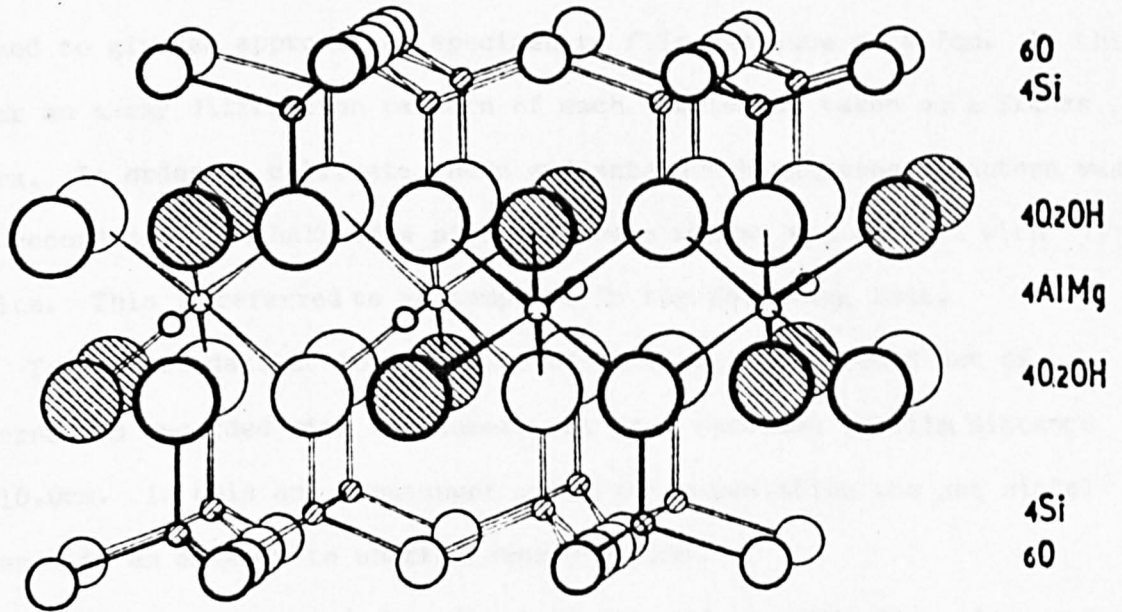
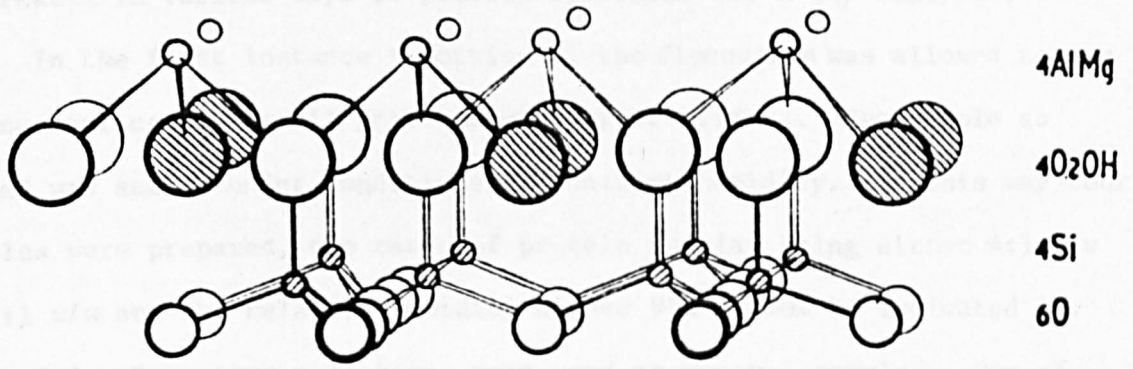


Figure 8.1 The structure of montmorillonite, reproduced from MacEwan, 1961.

be treated in various ways to provide specimens for x-ray analysis.

In the first instance a portion of the flocculate was allowed to dry on one surface of a small pill box with mylar windows. The sample so formed was sealed under conditions of constant humidity. In this way four samples were prepared, the ratio of protein to clay being either 4:1 w/w or 1:1 w/w and the relative humidity either 90% or 30% as indicated in Table 8.1. Two other pill boxes were used as control samples. One of these contained montmorillonite alone and the other was used empty.

Both surfaces of a pill box were cleaned with a small amount of ethanol on a tissue before irradiating. The cell was then attached to a normal Searle camera specimen holder with the aid of plasticine and aligned to give an approximate specimen to film distance of 4.7cm. In this manner an x-ray diffraction pattern of each sample was taken on a Franks camera. In order to calibrate these and subsequent patterns a pattern was also recorded of one half of a pill box whose window was covered with calcite. This is referred to as sample G in the following text.

To collect data at lower angles of diffraction a second set of patterns was recorded with the camera set at a specimen to film distance of  $\sim 10.0$ cm. In this and subsequent cases the x-radiation was not nickel filtered in an attempt to shorten exposure time.

Sample C was removed from its pill box and attached to a glass rod with the aid of bostic. This allowed the effects of radiation scattered from the mylar windows to be examined and also permitted the relative humidity of the sample environment to be varied in a similar manner to that described for DNA fibres in chapter 2.6. Diffraction patterns of samples D and F were also recorded for comparison purposes. In this and the following experiments the Franks camera was realigned to give a specimen to film distance  $\sim 7.6$ cm in an effort to optimize resolution with exposure time.

Finally a second set of samples was prepared by making slide smears



Sample Identification	BSA/Montmorillonite w/w	Relative Humidity %
A	4:1	90
B	4:1	30
C	1:1	90
D	1:1	30
E	All montmorillonite	90
F	Blank cell	Ambient humidity

Table 8.1 Preparation details of samples A - F

of the montmorillonite or montmorillonite complex suspensions on glass microscope slides and allowing them to dry to thin films  $\sim 30\mu$  thick. A small flake was then cut from each film, mounted in a 2mm diameter quartz capillary tube and sealed with wax under specific environmental conditions.

This technique was adopted in an attempt to improve orientation of these samples compared with the previous specimens. Moreover, such samples could be aligned with the x-ray beam parallel to the plane of the lamella in order to increase the intensity of the 001 reflections. Such samples, like their counterparts in the pill boxes, have the advantage that they can be allowed to equilibrate with a specific environment for much longer periods than is practically possible if enclosed simply by the x-ray camera.

In addition to montmorillonite and BSA/montmorillonite samples, samples of montmorillonite complexed with other substances have also been examined to determine whether these results are in agreement with those reported in the existing literature. The detailed preparation of these samples is shown in Table 8.2.

The capillary tubes are very fragile and in order to facilitate mounting in the x-ray camera, the thicker end of each tube was glued into the cleft of an L-shaped block of balsa wood. A further block was glued to the other side of the tube as shown in Figure 8.2. This complete jig could then be attached to the specimen holder of a Searle camera with the aid of double sided tape.

An x-ray pattern of each sample was obtained with the lamellar perpendicular to the axis of the x-ray beam and several patterns were recorded with the lamellar parallel to the beam axis.

The positions of the reflections on all the x-ray patterns obtained were measured either with a travelling microscope or more often with a compass and steel rule. This latter method was employed since it was found easier to determine boundaries of faint and weakly contrasting adjacent bands by observing the patterns at oblique angles, often in

Sample Number	Method of Preparation	Environment
1	Na montmorillonite.	90% rh
2	Na montmorillonite dialysed against H <sub>2</sub> O and dried.	90% rh
3	Na montmorillonite.	Immersed in glycerol
4	Na montmorillonite.	Immersed in 95% pyrimidine
5	Na montmorillonite dissolved in 0.5M NaCl soln., dialysed against this soln. and dried.	Immersed in 0.5M NaCl soln.
6	Albumin/H <sub>2</sub> O dialysed Na montmorillonite mixed in an alkaline medium at a ratio of 1:1 w/w then slowly acidified and dried.	90% rh
7	As per 6	Immersed in acetic acid soln. pH 5
8	Albumin/H <sub>2</sub> O dialysed Na montmorillonite mixed at a ratio of 1:1 w/w and dried.	90% rh
9	As per 8	Immersed in acetic acid soln. pH 5
10	Albumin/H <sub>2</sub> O dialysed Na montmorillonite mixed at a ratio of 2:1 w/w and dried	90% rh

Table 8.2 Preparation details of samples 1 - 10

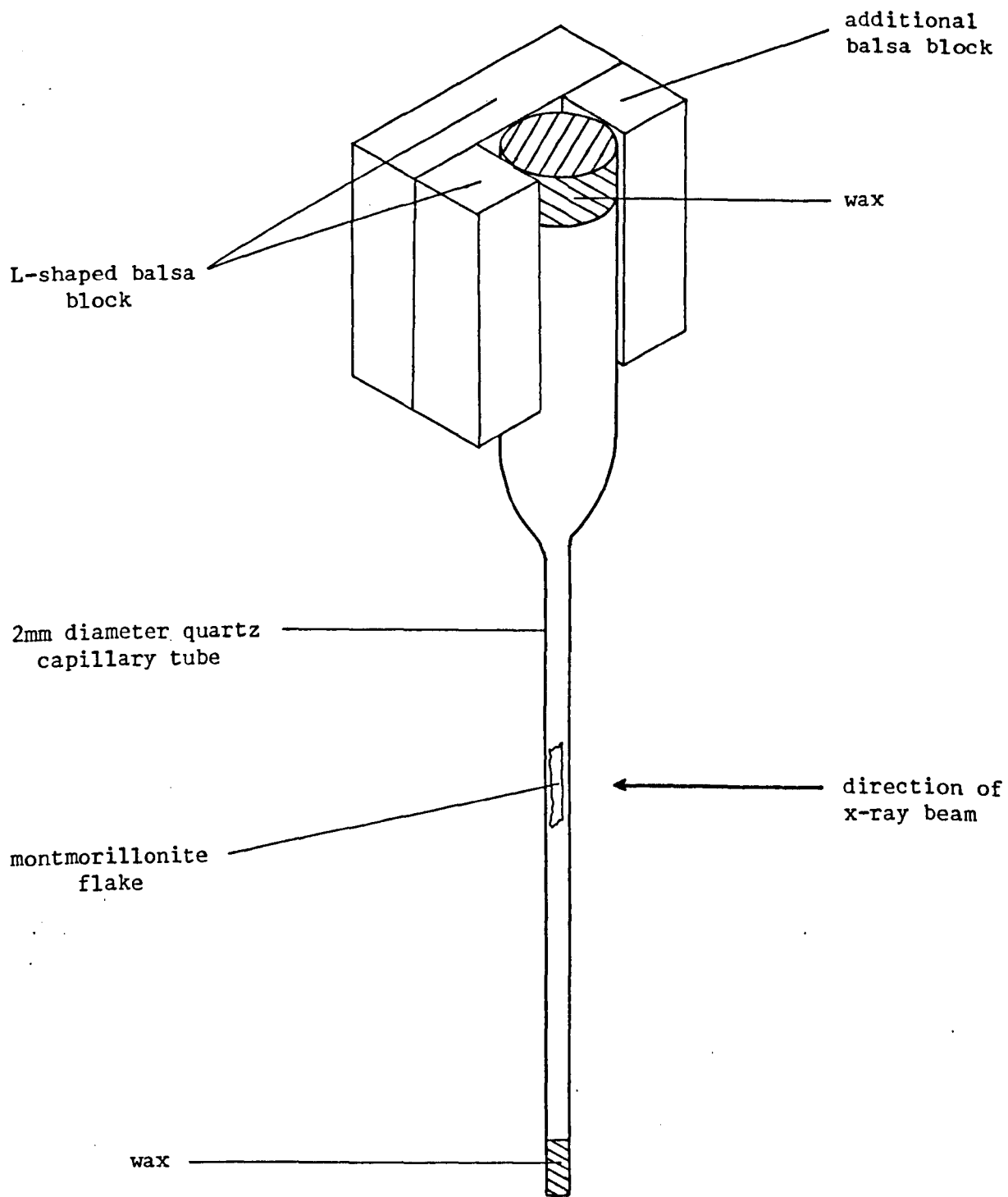


**Figure 8.2** A diagram of the balsa-wood jig used for mounting capillary tubes onto the Searle camera holder.

conjunction with a bright light source of variable intensity. A low power microscope stage proved ideal for this latter purpose. The reduction in light intensity in measuring the positions of reflections on these patterns using either the travelling microscope or the Stoe film measuring device could not be tolerated. The accuracy with which the positions of these reflections could be determined was  $\pm 0.2\text{mm}$ . The error in calculating the corresponding d-spacings in nm depends on the specimen to film distance employed. Table 8.3 shows the equivalent errors in d-spacing as a function of specimen to film distance for some relevant reflections. In cases where the reflections were particularly diffuse the error maybe somewhat larger than is shown in this table.

### 8.3 Results

In the following text diffraction patterns are referred to according to the letter or number of the sample from which a given pattern was obtained.

#### a) X-ray diffraction patterns of samples A - G recorded at a specimen to film distance, $D \sim 4.7\text{cm}$

A d-spacing of  $0.3035\text{nm}$  was assigned to the most intense calcite reflection of pattern G and a value of  $0.5403 \pm 0.004\text{nm}$  was obtained for the d-spacing of the principal mylar reflection. This value was used to calibrate patterns A - F and the results are shown in Table 8.4. Diffraction patterns of samples A - G were recorded using two negative films in each case. The d-spacings in Table 8.4 usually represent the average d-spacings obtained from measurements of the top and bottom films. The number 1 in brackets implies that the corresponding d-spacing was only observed on one of the two negatives. A range in the value of d-spacings is given in cases where the difference in d-spacings on the two negatives are thought to be too great to average.

Mylar reflections on patterns A - E and pattern G were identified by

d-spacing/nm	Error in d-spacing at Specimen to Film Distance D/nm		
	D = 4.7cm	D = 7.6cm	D = 10.0cm
0.336	0.002	0.002	0.001
0.447	0.005	0.003	0.002
1.00	0.027	0.017	0.013
1.50	0.060	0.038	0.029
2.00	0.112	0.067	0.052
2.30	0.142	0.090	0.068
3.00	0.254	0.154	0.117
3.30	0.303	0.192	0.141
4.00	0.454	0.280	0.208
5.00	0.757	0.446	0.325
6.00	1.04	0.517	0.469
8.00	1.89	1.22	0.839

Table 8.3 The error in d-spacings of some relevant reflections at various specimen to film distances assuming an error in determining the corresponding radius of a specific reflection of 0.2mm.

Sample	$C_1$	$C_2$	$C_3$	$C_4$	$I_0$	$I_3$	$I_4$	$I_5$	$I_6$	Exposure Time in Hours
A		0.334	0.425	0.446	1.01	1.70(1)	2.50(1)	3.51	5.6(1)	21.4
B		0.337	0.428	0.452	0.99			3.84	5.7-6.9	8.6
C		0.336	0.428	0.454	1.03		2.32(1)	2.96	4.8(1)	32.3
D		0.336	0.430	0.454	1.00			3.22	4.8-5.6	Unknown
E	0.332	0.337	0.430	0.449		x = 1.45 - 1.65 y = 1.90 - 2.46				22.5
F								[3.3-4.2]	5.3-6.2	20.6

Table 8.4 d-spacings /nm of reflections observed on patterns of samples A - F at a specimen to film distance of  $\approx 4.7$ cm. See text for details.

comparison with pattern F of the empty mylar cell. Generally mylar reflections appeared as a series of broad bands of four fold rotational symmetry as shown in Plate 8.1. Mylar diffraction was observed at d-spacings of 0.275, 0.314, 0.335, 0.359, 0.501 and 0.540nm and these reflections are referred to by the letters  $M_1 - M_6$  respectively. For ease of documentation these reflections are not recorded in the following tables.

Diffraction from montmorillonite intra-sheet structure on patterns A - D was identified by comparison with pattern E which is reproduced in Plate 8.2. These montmorillonite reflections usually appeared as discrete rings although the intensity profile of the rings was sharper on the high angle side of a given reflection. The d-spacings of these reflections are denoted by  $C_1 - C_4$  in Table 8.4.

In addition to mylar and montmorillonite intra-sheet reflections, patterns A - D exhibited diffuse intensity extending from 0.86 - 1.20nm. The average value of this extent has been recorded in column  $I_0$  of Table 8.4. The centres of patterns A - D showed adjacent broad bands whose intensities increased towards the centres of the patterns in a stepwise fashion. These features are illustrated in Plate 8.3. The d-spacings obtained from measurements of the maximum diameters of these bands are denoted by  $I_3 - I_6$  in Table 8.4. The central strong intensity region of pattern E was elliptical in shape and the entries  $I_x$  and  $I_y$  in Table 8.4 refer to the extent of diffuse intensity along the major and minor axes of the ellipse respectively. The square bracketed d-spacing of sample F in Table 8.4 refers to diffuse intensity, surrounding an intense central region. The diameter of the backstop in this camera arrangement corresponded to a d-spacing  $\sim 9.0$ nm.

b) X-ray diffraction patterns from samples A - F recorded at  $D \sim 10.0$ cm

A second set of diffraction patterns of samples A - F was recorded at an increased specimen to film distance in order to improve the resolution of the reflections in the central regions of these patterns.



Plates 8.1 - 8.7 : X-ray diffraction patterns relating to BSA/  
montmorillonite samples

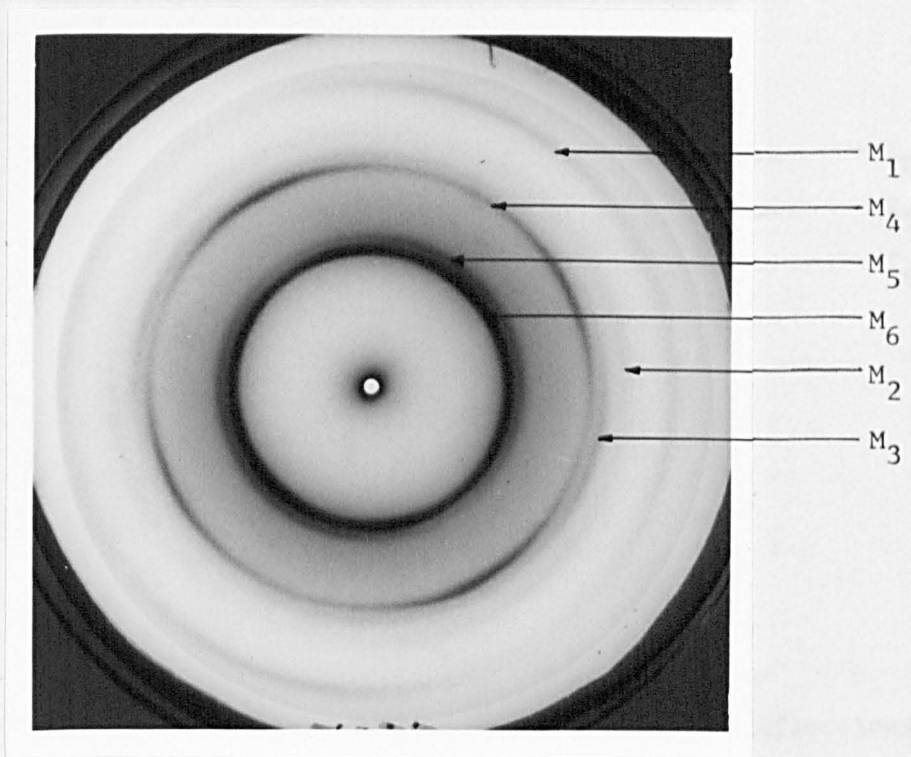


Plate 8.1

Pattern F at D  $\sim$ 3.5cm showing mylar reflections. The symbols on these and subsequent patterns are described in the text.

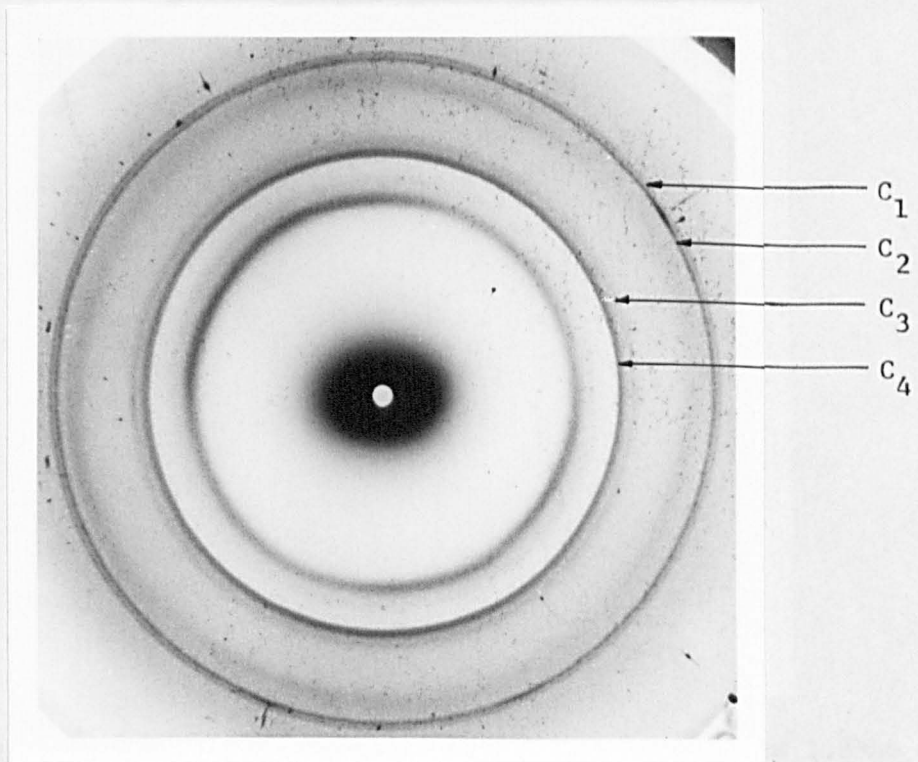
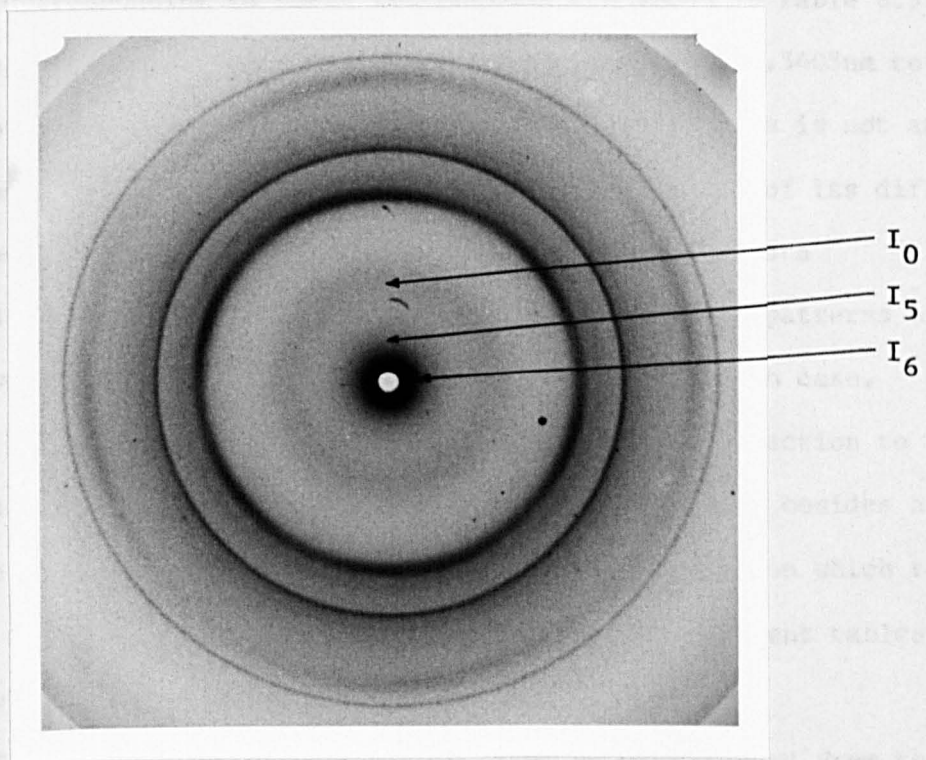


Plate 8.2

Pattern E at D  $\sim$ 4.7cm showing mylar and montmorillonite reflections.



**Plate 8.3**

Pattern B at  $D \sim 4.7\text{cm}$  showing mylar and BSA/montmorillonite reflections.

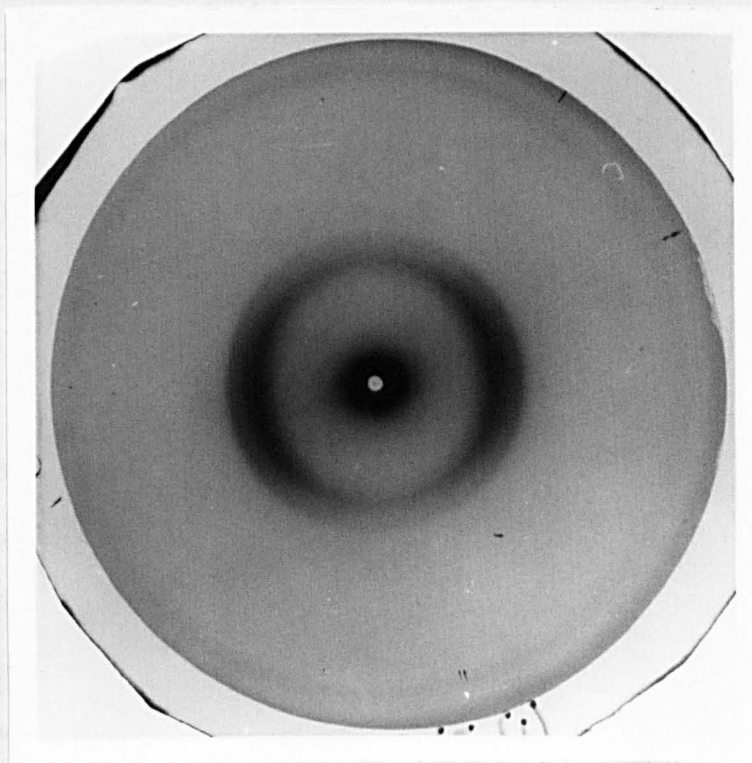


**Plate 8.4**

Pattern E at  $D \sim 10.0\text{cm}$ . The intersheet spacings at  $1.12\text{nm}$  and  $1.38\text{nm}$  are clearly resolved compared with Plate 8.2.

The d-spacings corresponding to these reflections are shown in Table 8.5. The spacings were again calculated on the basis of assigning 0.5403nm to the d-spacing of the principal mylar reflection. Although this is not an ideal reflection with which to calibrate the patterns because of its diffuse nature, the specimen to film distance was such as to exclude data collection at d-spacings of less than 0.5nm. The diffraction patterns of these samples were recorded on up to six negative films in each case. This allowed a greater variation of intensity for a given reflection to be recorded than when using two films. The number in brackets besides a specific d-spacing in Table 8.5 indicates the number of films on which that reflection was measured. The symbols used in this and subsequent tables are as described for Table 8.4 except where stated.

Pattern F exhibited an intense central band which extended from the observable limit  $\sim 20.0$ nm out to 6.0nm. The extent of this region decreased with decreasing intensity as indicated in Table 8.5. To check that this band was not due to camera misalignment a 200 $\mu$ m diameter DNA fibre was exposed for a similar period of time using the same camera arrangement. Only diffuse scatter was present in the central region of the pattern. This suggested that the mylar windows of the sample containers limited the potential resolution of the system.

In pattern E the elliptical region of the pattern of this sample recorded at  $D \sim 4.7$ cm was resolved into an arced reflection at 1.38nm and a second almost circular reflection at 1.12nm as shown in Plate 8.4. An elliptical central region was still apparent corresponding to d-spacings of  $I_{2x}$ ,  $I_{2y}$  and this was surrounded by a more diffuse region,  $I_{1x}$ ,  $I_{1y}$ , as recorded in Table 8.5.

In patterns A - D the broad reflection centred  $\sim 1.0$ nm was still apparent, but it was too faint to measure accurately and it has not been recorded in Table 8.5. Patterns A - D showed no evidence of the arced montmorillonite reflections of pattern E. The central regions of patterns

Sample	$I_0$	$I_1$	$I_3$	$I_4$	$I_5$	$I_6$	$I_7$	$I_8$	Exposure Time in Hours
A				2.21(1)	3.46(3)		5.9-7.6(5)		38.5
B				2.36(2)	3.34(4)		5.2-7.7(6)		36.0
C					3.23(2)		5.5(2)	9.3-10.6(6)	34.3
D			1.78(1)		2.66(5)		5.0(6)	7.7-8.5(5)	75.2
E	1.12(3)	1.38(4)				$x_1 = 4.4-8.0(3)$ $x_2 = 6.1-10.2(4)$ $y_1 = 5.3-9.9(3)$ $y_2 = 6.8-14.6(5)$			32.2
F							6.1-8.8(5)		31.1

Table 8.5 d-spacings /nm of reflections observed on patterns of samples A-F at a specimen to film distance  $\sim 10.0$ cm.

A - D still appeared as broad bands which merged into neighbouring more intense bands closer to the centres of the patterns, as shown in Plate 8.5. Measurements were again taken to the outermost edge of a given band providing a minimum d-spacing for that reflection. Only in cases where the correct exposure was taken did a band appear ring like and then its intensity was usually very weak and difficult to measure. The d-spacings obtained for these bands were very similar to those of the patterns recorded at 4.7cm specimen to film distance. However patterns C and D clearly showed reflections  $\sim 5.5\text{nm}$  and  $\sim 5.0\text{nm}$  respectively, which did not appear in patterns of those samples recorded at the smaller specimen to film distance.

c) X-ray diffraction patterns from samples C, D and F recorded at D  $\sim 7.6\text{cm}$

A specimen to film distance of 7.6cm was chosen in order to optimise resolution with exposure time. It also enabled montmorillonite reflections at 0.447nm to be recorded. The diameter of the backstop in this camera arrangement corresponded to a d-spacing of 14.0nm. Patterns were obtained of sample C which had been removed from its pill box and subjected to a camera environment of 92%, 44% and 33% rh. In each case the sample was allowed to equilibrate overnight at the appropriate humidity before commencing exposure. For comparison purposes patterns were also recorded of samples D and F using the same camera arrangement. The patterns were calibrated by assigning a value of 0.447nm to the d-spacing of the  $C_4$  montmorillonite reflection as described in section 8.4 a). The d-spacings of the reflections observed on these patterns are shown in Table 8.6. The central reflections on some of these patterns did not always merge into adjacent reflections as seen in Plate 8.6. Where this is the case an average d-spacing has been calculated for that reflection rather than a minimum d-spacing. This is denoted by an asterisk in Table 8.6. If other negatives in the same film pack of the diffraction pattern did not show such a well resolved reflection then the range of minimum d-spacings for

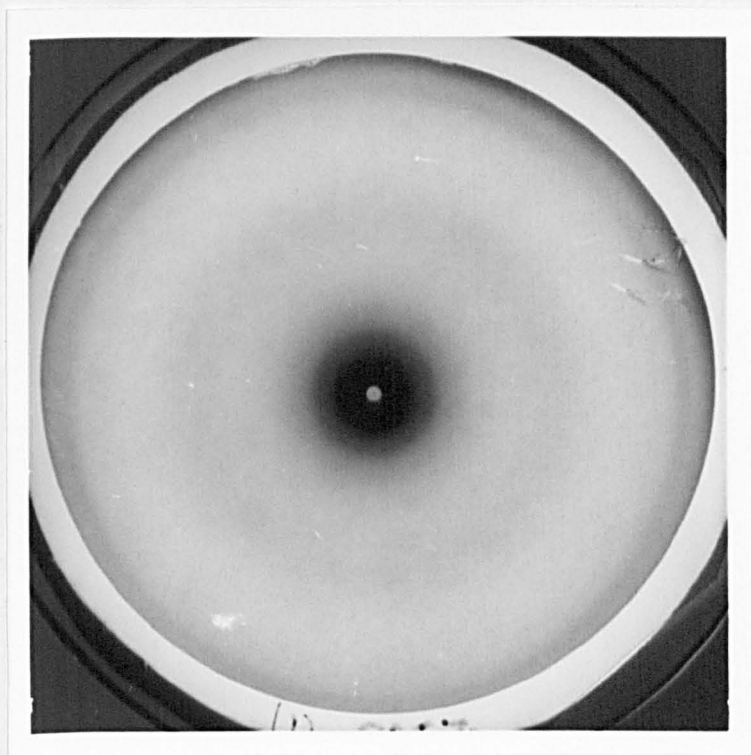


Plate 8.5

Pattern D at  $D \sim 10.0\text{cm}$  showing the BSA/montmorillonite diffraction at high  $d$ -spacing.

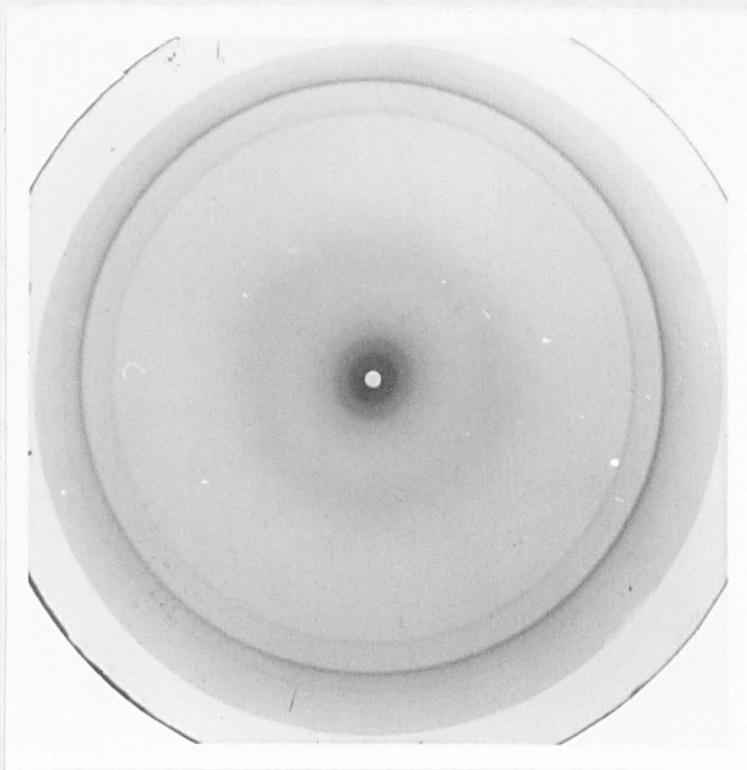


Plate 8.6

Pattern C at  $D \sim 7.6\text{cm}$  and  $rh = 92\%$ . The central reflections are better resolved in this pattern, particularly the  $I_5$  reflection at  $3.3\text{nm}$ .

Sample	Rh%	C <sub>3</sub>	C <sub>5</sub>	C <sub>6</sub>	I <sub>0</sub>	I <sub>2</sub>	I <sub>3</sub>	I <sub>5</sub>	I <sub>7</sub>	I <sub>8</sub>	Exposure Time in Hours
C	92	0.422(3)	0.468(3)	0.494(4)	1.03(2)	1.63(1)	2.13(3)	3.54*(3) 2.9-3.1(4)	7.16*(1) 4.9-6.0(4)		29.7
C	44	0.423(3)	0.468(1)	0.494(4)	1.01(2)	1.51(1)	1.95(2)	3.30*(4) 2.6-2.9(5)	6.75*(2) 4.6-5.7(4)		26.3
C	33	0.423(3)	0.464(1)	0.495(4)	1.04(2)		1.94(2)	3.29*(3) 2.7-3.3(5)	6.24*(2) 4.9-5.7(4)		25.7
D		0.424(2)		0.495(4)	1.02(1)		1.89(1)	3.07*(1) 2.8-3.2(4)	4.9-5.7(4)	8.0-9.8(3)	19.6
F								3.5-4.0(3)	4.6-7.9(5)		35.6

Table 8.6 d-spacings /nm of reflections observed on patterns of samples C, D and F at a specimen to film distance ~7.6cm.

that reflection is also given. In these cases measurements of the negative which received the least amount of diffracted radiation tended to give a larger d-spacing. This feature is also apparent from the data in Tables 8.4, 8.5 and 8.7. It arises because minimum d-spacings have been determined for the central reflections, but less intense bands appear less broad and measurements of the minimum d-spacings thus give rise to larger values, although the average d-spacing remains constant. The most accurate measurements of the central reflections are thus obtained when the reflections appear as discrete rings rather than adjacent bands. For this reason the data in Table 8.6 is probably the most accurate, despite the reduction in specimen to film distance compared with the data in Table 8.5.

One feature apparent from the absence of mylar diffraction was the appearance of two other montmorillonite reflections  $C_5$  and  $C_6$  at 0.467nm and 0.494nm.

The  $I_3$ ,  $I_5$  and  $I_7$  reflections for sample C tended to decrease slightly with decreasing relative humidity, but no dramatic changes were apparent. Height et al., 1962, have suggested that a considerable time ~6 weeks is necessary to obtain equilibrium conditions for these types of samples. The data in Table 8.6 is compatible with this suggestion.

In general the  $I_0 - I_8$  reflections of the patterns referred to in Table 8.6 are similar to those obtained previously and an interpretation of these results is given in section 8.4 a).

d) X-ray diffraction patterns of samples 1 - 10 recorded at  $D \sim 7.0\text{cm}$

The diffraction patterns of these samples were again calibrated by assigning a value of 0.447nm to the  $C_4$  montmorillonite reflection. The d-spacings of the reflections observed in these patterns are shown in Table 8.7.

The diffraction pattern from sample 3 gave considerable diffuse scattering which was attributed to the glycerol in which the montmorillonite flake was immersed. To decrease this scattering the remaining samples of



Sample	$C_6$	$I_0$	$I_1$	$I_2$	$I_3$	$I_4$	$I_5$	$I_6$	$I_7$	$I_8$	Exposure Time in Hours
1	0.494(3)			1.55(3)	1.71(1)			4.9(1)	6.4-9.6(3)		24.0
1//	0.495(2)		1.26(2)	1.52(2)					6.7-8.6(3)		21.8
2	0.493(2)		1.29(2)		1.69(2)					7.5-8.2(2)	unknown
3					1.75(3)						36.4
4	0.494(4)		1.18(3)			2.36*(4)	2.60(3)			7.5(2)	42.6
5	0.494(2)			1.55(3)							47.3
6	0.494(3)	1.02(4)		1.55(2)		2.38(4)		3.9-5.6(3)		7.7-7.9(4)	32.5
6//	0.493(2)	1.03(3)	1.21(2)	1.44(3)	2.14(3)	2.42(2)		4.1(2)	5.5(1)		73.5
7	0.493(3)	1.02(1)	1.36(1)		1.77(3)		2.53(4)		4.6-7.1(3)		40.0
8	0.494(3)	1.05(4)		1.42(3)	1.71(4)		2.68(3)				22.6
9	0.495(2)	0.93(1)		1.52(1)	1.95(2)	2.50(1)	2.89(2)		5.8(2)	7.6-8.6(2)	40.6
10		1.01(1)		1.57(1)			3.29*(2)		6.3*(1) 5.0-9.3(4)		unknown

Table 8.7 d-spacings /nm of the reflections observed on patterns of samples 1-10 recorded at a specimen to film distance  $\sim 7.6$ cm.

this type were shaken vigorously just before x-raying to remove the bulk of the solution from a region of the montmorillonite flakes. The exposed portions of the flakes were aligned in the x-ray beam and overall scattering was reduced while the fibres remained sealed in an environment containing their bathing solutions.

The symbol // in Table 8.7 indicates that that sample was aligned with the large face of the montmorillonite flake parallel rather than perpendicular to the axis of the x-ray beam. The type of BSA/montmorillonite diffraction pattern obtained when sample 6 was aligned in this manner is shown in Plate 8.7. Although there is some evidence of orientation the central diffraction maxima did not exhibit a greater degree of resolution. For samples aligned in this manner the  $I_0 - I_8$  reflections in Table 8.7 are representative of the minimum d-spacing and the radii of reflections perpendicular to the long axis of the intensity distributions were not measured. The remaining notation in Table 8.7 is as described previously.

#### 8.4 Discussion

##### a) Interpretation of the diffraction from samples A - G

An examination of the data in Tables 8.4 - 8.6 suggests little variation in the diffraction patterns of samples A - D as a function of protein/clay ratio and relative humidity at which the samples were sealed. The intensity of the central reflections appear to increase rapidly with increasing d-spacing. Whether such a reflection was observed on a given negative seemed more dependent on exposure time than any differences in sample preparation. Too weak an exposure rendered a specific reflection invisible, while too strong an exposure caused it to be obscured by the adjacent strong intensity reflection at the higher d-spacing.

There were no significant differences in the montmorillonite intra-sheet spacings of the samples of the protein/clay complexes compared with those of the sample of clay alone. Thus there is no evidence of any

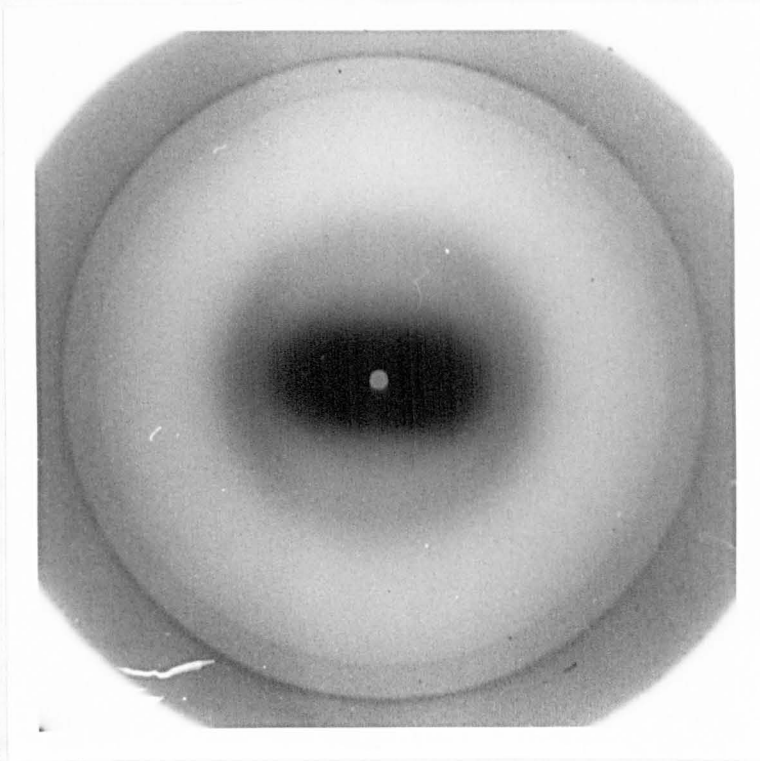


Plate 8.7

Pattern 6// at  $D \sim 7.0\text{cm}$ . The central reflections show some evidence of orientation but there is little apparent increase in resolution.

changes within the silicate sheets themselves as a result of the formation of the protein/clay complexes. Once this had been established it was possible to use the C4 montmorillonite reflection for a more accurate calibration of the patterns.

Correlating the data in Tables 8.4 - 8.6 gives clay intra-sheet d-spacings at 1.38(vs), 1.12(vs), 0.495(w), 0.467(vw), 0.451(s), 0.426(m), 0.336(s) and 0.332(w)nm, where vs, s, m, w and vw refer to the relative intensities of the reflections as assessed by eye. One of the montmorillonite structures listed in ASTM tables has d-spacings of 1.36, 0.447, 0.334, 0.323 etc. ... nm which corresponds reasonably well with the strong intensity reflections observed for the clay samples at 1.38, 0.451 and 0.336nm. The remainder of these d-spacings do not correspond with those of any of the other montmorillonite structures given in the ASTM tables and probably arise as a result of the presence of impurities in the clay samples.

The reflections at 1.38 and 1.12nm in sample E are due to interlamellar distances. These reflections are no longer apparent in samples of the protein/clay complexes which instead show a broad reflection centred at  $\sim 1.0$ nm and extending from 0.85 - 1.25nm. Norrish, 1954, has shown that water molecules are adsorbed between the silicate sheets of montmorillonite in monolayers and that structures of up to four interlamellar water layers are possible. He gives interlamellar spacings of 0.95, 1.24, 1.54 and 1.90nm for Na montmorillonite during water uptake. Upon further hydration of Na montmorillonite samples the water layers dissociate completely and the interlamellar spacings increase linearly with water content. Thus the data in columns  $I_0 - I_3$  of Tables 8.4 - 8.6 are indicative of water layers between the montmorillonite platelets. The difference in intensity distribution in this region of samples A - D compared with sample E suggests that the presence of the protein is causing a disruption in the water structure. In some samples more than one reflection is observed in this range and this may be due to

a mixed layer silicate structure arising from impurities within the montmorillonite samples or due to an inhomogeneous distribution of water content.

Generally samples A - D gave reflections corresponding to d-spacings of 2.3 and 3.2nm while reflections at 5.5 and 5.0nm were apparent from patterns C and D at the highest specimen to film distance used. In considering the reflection at 2.3nm Norrish, 1954, has reported that H montmorillonite in the presence of acidic solutions undergoes an ageing process. Over a period of 24 hours H montmorillonite releases  $Al^{3+}$  ions from the silicate structure into the interlamellar region giving rise to a d-spacing of 2.2nm. Height et al., 1962, have observed a similar phenomenon for dilute H bentonite suspensions which age over a period of approximately four months. The conversion of the H clay to an Al clay may be responsible for the reflection at 2.2nm since the BSA/montmorillonite samples were prepared under acid conditions.

The reflection at 3.3nm is attributed to the presence of albumin within the interlamellar regions of the montmorillonite. Taking into account the dimensions of the silicate sheets hydrated with a single layer of water molecules, a 3.3nm interlamellar spacing corresponds to a protein diameter  $\sim 2.3$ nm. This is within the range reported in section 8.2 b). A value of 3.3nm was observed for the  $d_{001}$  spacings of albumin/Na montmorillonite complexes of ratio 1:1 w/w by Ensminger and Gieseck, 1940. Talibudeen has also reported  $d_{001}$  spacings  $\sim 3.0$ nm for haemoglobin/montmorillonite complexes.

Samples C and D exhibit reflections  $\sim 5.5$ nm which may result from the presence of two layers of protein molecules within some interlamellar regions. If this is the case then clearly the protein molecules pack with their major axes parallel rather than perpendicular to the silicate sheets.

b) Interpretation of the diffraction patterns of samples 1 - 10

The d-spacings in columns  $I_0 - I_3$  in Table 8.7 are indicative of water layers between silicate sheets. A d-spacing of  $\sim 1.0\text{nm}$  for the BSA/montmorillonite samples compared with higher d-spacings in this region for the non-protein containing samples suggests that the presence of the BSA is again causing a disruption in the water structure. As was the case for samples A - E there is evidence of an inhomogeneous distribution of water within the samples.

Sample 1 of the Na montmorillonite at 90% rh gave a very similar diffraction pattern to that of sample 2 of H montmorillonite and in particular neither of these samples gave diffracted intensity in the region of  $2.0\text{nm} - 4.0\text{nm}$ . The reduction in the d-spacings of the  $I_0 - I_4$  reflections of the Na montmorillonite sample lying parallel rather than perpendicular to the axis of the x-ray beam maybe due to evaporation when the tube was accidentally broken before being resealed.

Samples 3,4 and 5 were examined to determine whether the non-protein/montmorillonite complex samples used in this work gave similar results to those previously reported in the literature. For sample 3 the reflection at  $1.75\text{nm}$  is in good agreement with the  $d_{001}$  spacings of  $1.77\text{nm}$  for glycerol/Na montmorillonite complexes reported by MacEwan, 1956. Greenland, 1956, gave a  $d_{001}$  spacing of  $1.81\text{nm}$  for this complex and interpreted this value in terms of two layers of glycerol molecules in each interlamellar region.

Other information which may have been present on the diffraction pattern of this sample was obscured by diffuse intensity attributed to the glycerol. Pattern 4 gave a strong reflection at  $2.36\text{nm}$  which is in good agreement with the  $d_{001}$  spacing of  $2.33\text{nm}$  for montmorillonite flakes saturated with pyrimidine as reported by Green-Kelly, 1955. The reflection at  $2.6\text{nm}$  may arise as the result of the inclusion of a layer of water molecules between some interlamellar regions. The cause of the reflection at  $7.5\text{nm}$  for this sample is not known. Norrish, 1954, showed that

montmorillonite flakes gave  $d_{001}$  spacings  $\sim 1.6\text{nm}$  in the presence of 4 - 1.8M NaCl solution and  $d_{001}$  spacings of 1.90nm in the presence of 1.8M - 0.3M NaCl solution. In more dilute solutions the  $d_{001}$  spacings increased linearly from 4.0nm with respect to  $[\text{NaCl}]^{-\frac{1}{2}}$ . The diffraction pattern of sample 5 giving a  $d_{001}$  spacing of 1.55nm is not inconsistent with these results and the lower than expected  $d_{001}$  spacing may again arise as the result of evaporation when the capillary tube was accidentally broken.

Samples 6 and 7 which were prepared by acidification and samples 7 and 9 which were immersed in an acetic acid solution all exhibited  $d$ -spacings in the range 2.4 - 2.5nm. These reflections may be due to the ageing of H montmorillonite as described in section 8.4 a). Samples 8 and 10 which were not treated with acid only gave one reflection in the 2.0 - 4.0nm range. Samples 7 - 10 indicated diffracted intensity in the region of 2.9nm which is similar to the 3.3nm reflections observed in samples A - D and is believed to arise as a direct result of albumin adsorption within the montmorillonite interlamellar spacings. Again these BSA/montmorillonite samples gave diffracted intensity at higher spacings indicating the possibility that more than one protein layer was adsorbed in some interlamellar regions. Sample 10 at a BSA/montmorillonite ratio of 2:1 w/w gave particularly distinctive reflections at 3.3nm and 6.3nm.

Aligning the specimens parallel rather than perpendicular to the axis of the x-ray beam demonstrated that some degree of orientation was present in the samples. However, such orientation was not sufficient to improve the resolution of the reflections and patterns were not generally recorded in this manner.

There seemed little advantage in slowly acidifying the BSA/montmorillonite samples during preparation, or immersing them in acetic acid solution and there remains the possibility that these processes promote ageing of the H-montmorillonite.

c) Future experiments

The diffraction patterns from these samples are not well resolved and an improvement in molecular orientation is desirable. During sample preparation dialysing Na montmorillonite against water not only removes the interlamellar cations but it also leaves the edges of broken clay platelets with a net positive charge. These edges may act as alternative binding sites for the BSA molecules, or cause disorientation of the platelets as a result of edge/face binding. Neutralization of this positive charge by the addition of sodium chloride may prevent protein binding at these sites and reduce edge/face binding, giving rise to a more ordered structure, Fink, 1977. However, care in utilizing this procedure is necessary since weak sodium chloride solutions can give rise to large increases in interlamellar spacings.

The poor resolution of the diffraction patterns may be due to the presence of mixed layer structures. If this is the case a more extensive method of sample purification may help to improve resolution.

There is some evidence to suggest that the distribution of water and protein molecules within the samples are not homogeneous. Hence an improvement in resolution may also be obtained by allowing longer periods of time for the samples to attain equilibrium.

More information from the diffraction patterns may be forthcoming if they are subjected to a more detailed analysis such as that described by MacEwan, 1956. However, it is unlikely that profitable results can be obtained from such analysis in view of the poor diffraction data available at the present time.

Despite extensive room for improvement the results indicate that diffraction is present which is associated with the uptake of BSA in the interlamellar regions of the montmorillonite. There is also some evidence that the BSA is aligned with its major axis parallel to the montmorillonite sheets. Thus the use of neutron diffraction techniques to further examine



BSA/montmorillonite complexes seems justifiable. Neutron diffraction is essential since it enables phase contrasting techniques to distinguish between the individual contributions of the water and BSA molecules to the interlamellar expansion of the montmorillonite.

Chapter 9. CONCLUSIONS

A method of fibre preparation has been developed which takes into account the small quantity of synthetic polynucleotide material available and allows the salt content of individual fibres to be quantitatively increased by small increments. In this manner synthetic polynucleotide conformations in fibre samples have been examined as a function of added salt per phosphate.

This work has shown that the A, B and C conformations found for naturally occurring DNA's are all available to the sodium salt of poly[d(A-C)].poly[d(G-T)]. The C conformation is stabilized in fibres by conditions of low relative humidity and the sequence of conformational changes with increasing relative humidity is C → A → B. This is in contrast to the A → C → B sequence suggested by Leslie et al., 1980. A comparison of these results with those subsequently obtained for naturally occurring Na DNA's and the synthetic polynucleotide Na poly[d(A-T)].poly[d(A-T)] suggests that the C conformation of Na poly[d(A-C)].poly[d(G-T)] is stabilized in fibres of low salt content. Such a comparison also implies that the same sequence of transitions is observed on increasing the sodium chloride content of these fibres as on increasing the relative humidity.

This work has thus established that the C conformation of poly[d(A-C)].poly[d(G-T)] can be reproducibly obtained in fibres where sodium is the associated cation. Since poly[d(A-C)].poly[d(G-T)] contains all of the four nucleotides commonly found in native DNA's it might be expected that the occurrence of the C conformation in these fibres is not an effect of base composition. This has been confirmed by a parallel study of the C conformation on a wide variety of naturally occurring Na DNA's, Mahendrasingam, 1983, Rhodes et al., 1982. The routine observation of the C conformation in DNA's and polynucleotides when the associated cation is sodium suggests that this conformation may be of greater biological

significance than has so far been assumed.

Semi-crystalline C and B diffraction patterns have been obtained from Li poly[d(A-C)].poly[d(G-T)] fibres under similar conditions to those observed for naturally occurring Li DNA's, Marvin et al., 1961, Zimmerman and Pfeiffer, 1980. Analysis of the most well resolved diffraction patterns have shown that the C form of Li poly[d(A-C)].poly[d(G-T)] crystallizes in a hexagonal lattice with  $a = 3.48 \pm 0.02\text{nm}$  and  $c = 5.84 \pm 0.03\text{nm}$ . Some of the diffraction patterns showed intensity streaks on low, odd numbered layer lines implying a random translation of the molecules in the unit cell by  $\pm 1/2 z$ . In such cases a slightly smaller lattice was indicated with  $a = 3.216 \pm 0.004\text{nm}$  and  $c = 5.807 \pm 0.007\text{nm}$ . The a parameters tended to increase with increasing relative humidity although there was little variation in pitch under these conditions and the molecular packing appeared to remain hexagonal.

The C conformation in Li poly[d(A-C)].poly[d(G-T)] fibres has been observed over an extensive range of environmental conditions including those in which orthorhombic crystalline B patterns would be expected in fibres of naturally occurring Li DNA's. This suggests that the C conformation of Li poly[d(A-C)].poly[d(G-T)] is more stable than its random sequence counterpart. The observation of only hexagonal C patterns in Li poly[d(A-C)].poly[d(G-T)] fibres as opposed to both hexagonal and orthorhombic C patterns in fibres of naturally occurring Li DNA's implies that molecular packing may be an important contribution to this stability. Such a stability may be due to the alternating dinucleotide sequence of Li poly[d(A-C)].poly[d(G-T)] which appears to manifest itself in the  $9_2$  helical symmetry of this C conformation.

The C diffraction patterns obtained from Li poly[d(A-C)].poly[d(G-T)] fibres observed here are the most crystalline and well resolved C patterns which have yet been reported. A more complete analysis of these patterns

is currently being undertaken (Rhodes et al., to be submitted) and should provide a more accurate model of the C conformation than is available at the present time. A greater understanding of this conformation is important in view of its potential biological significance.

In conjunction with the results of Mahendrasingam, 1983, this work has shown that the A, B,  $\alpha$ -B', C and D conformations are all available to the sodium salt of poly[d(A-T)].poly[d(A-T)]. A sequence of transitions between these conformations has been proposed in Equation 5.1.

The A conformation of Na poly[d(A-T)].poly[d(A-T)] has previously been regarded as a metastable state by Arnott et al., 1974. In contrast this work has shown that the A conformation of Na poly[d(A-T)].poly[d(A-T)] has been observed over a wide range of conditions for considerable periods of time.

The observation of the  $\alpha$ -B' conformation for Na poly[d(A-T)].poly[d(A-T)] implies that this conformation is not a sequence dependant of Na poly(dA).poly(dT) as suggested by Leslie et al., 1980. It is possible to explain the modified intensity distributions of semi-crystalline B diffraction patterns from DNA fibres of high A,T content (Bram and Tougard, 1972) in terms of mixtures of semi-crystalline B and  $\alpha$ -B' patterns.

Again the C conformation has been reproducibly observed for a polynucleotide structure under conditions where the associated cation is sodium. This supports the contention of Mahendrasingam, 1983, and Rhodes et al., 1982, that the C conformation may be more biologically significant than has previously been supposed.

Once the D conformation of Na poly[d(A-T)].poly[d(A-T)] had been assumed in a given fibre it remained stable over a wide range of relative humidity and transitions to the A and C conformations were no longer possible. The stability of the D conformation may occur as a result of a transition from a right handed A or B helix to a left handed D helix, Mahendrasingam,

1983. Such a stable conformation may be exploited biologically in maintaining the structural integrity of the chromosome, Arnott et al., 1974.

A transition from the C directly to the semi-crystalline B conformation in Na poly[d(A-T)].poly[d(A-T)] fibres of low salt content has been observed by Mahendrasingam, 1983. This departure from the transitional sequence given in Equation 5.1 is interesting in that it parallels the transition observed in fibres of Li DNA and Li polynucleotides. It may provide a basis for explaining why the A conformation has never been observed in these fibres when the associated cation is lithium.

A knowledge of the detailed conformation of Na poly[d(A-T)].poly[d(A-T)] is important in explaining the enhanced binding affinity of this synthetic polynucleotide for the lac repressor of E.coli and whether this is due to the assumption of an alternating B conformation as proposed by Klug et al., 1979.

At the present time there are difficulties in establishing base sequence or base composition effects on nucleic acid conformation on the basis of the observation of a specific conformation for a particular synthetic polynucleotide. This is demonstrated by the observation of two Na poly[d(A-T)].poly[d(A-T)] conformations which have not been previously reported. Thus there is a need for more extensive research into the conformations available to synthetic polynucleotides.

This work has emphasised the importance of salt on nucleic acid conformation and underlined the need for accurately determining the salt content in x-ray fibre diffraction samples of polynucleotides. As a basis for determining the total salt content in such fibres a number of techniques have been investigated.

$\text{Na}^+/\text{PO}_4^-$  ratios of DNA in sodium chloride solutions have been measured by F.E.S. and U.V. absorption spectroscopy using a modification of the technique described by Blakeley, 1976. Excluding  $\text{Na}^+$  due to its presence

in standard sodium chloride solution,  $\text{Na}^+/\text{PO}_4^-$  ratios  $\sim 1.4-1.7$  were obtained from Sigma 1 calf thymus DNA. This method seeks to avoid denaturation of the DNA which may have resulted in Blakeley obtaining  $\text{Na}^+/\text{PO}_4^-$  ratios  $< 1.0$  for some DNA's dissolved in distilled water.

A routine has been developed to measure the ability of different DNA's to retain  $\text{Na}^+$  under dialysis conditions. Measurements were carried out under conditions of  $\text{Na}^+/\text{PO}_4^-$  ratios  $> 1.0$  to reduce the risk of DNA denaturation. In comparing calf thymus and  $\phi\text{W-14}$  DNA there is evidence to suggest that the latter DNA retains less  $\text{Na}^+$ ; a fact which may be attributed to the partial shielding or neutralization of the DNA phosphate groups by the putrescine residues. This may explain the apparent stability of the A conformation of this viral DNA in x-ray fibre samples compared with calf thymus DNA under similar conditions. The results obtained are not yet quantitative and further improvements are needed to achieve this end. Such data is important in relating the structural modifications of these DNA's to their chemical and biological functions.

An electrode potential method for measuring the concentration of  $\text{Cl}^-$  in small volumes of DNA solutions has been successfully demonstrated. Sigma 1 calf thymus DNA was shown to contain  $\text{Cl}^-/\text{PO}_4^-$  ratios  $\sim 0.18$  and subsequent  $\text{Na}^+$  analysis suggested that this  $\text{Cl}^-$  concentration could all be accounted for by the presence of excess sodium chloride in the DNA.

Amperometric titration methods offer the possibility of measuring  $\text{Cl}^-$  concentrations in solutions of individual fibre samples. Thus the salt content of fibres could be routinely analysed, rather than determining the properties of the bulk solutions from which these samples are made. Such an analysis still does not allow the salt directly associated with the DNA to be determined in every case since the salt may partially crystallize within fibre samples. Nevertheless a more quantitative analysis of the total salt content in individual fibre samples may lead to a better understanding of the effects of salt on nucleic acid conformation. It will

also allow more reproducible sample preparation and a more direct comparison of the results obtained by workers in different laboratories using different preparative techniques.

The conditions for the crystallization of steffimycin B in DNA fibres have been examined. However, diffraction patterns indicated only partial crystallization of this molecule and lacked the resolution of earlier patterns obtained by Blakeley, 1976. From these results it appeared that steffimycin B crystallization in DNA fibres was not significantly affected by variations in phosphate/drug ratios in the fibres, relative humidity of the fibre environment or by the presence of 10mM Tris.HCl pH 7.4 in the solutions from which the gels were centrifuged. There is some indication that higher salt concentrations  $\sim 32\text{mM}$  NaCl in the solutions prior to centrifugation may promote crystallization. However, it is likely that fibre preparation and the environmental conditions pertaining at that time play an important role in the crystallization process.

The analysis of Blakeley's diffraction pattern has confirmed that steffimycin B crystallizes in a hexagonal lattice with  $a = 3.024 \pm 0.003\text{nm}$  and  $c = 0.7712 \pm 0.0007\text{nm}$ . A comparison of the unit cell dimensions with those of a molecule of steffimycin B has indicated possible space groups which may describe the steffimycin B lattice. A particular space group has not been unambiguously identified and further well defined crystalline steffimycin B/DNA diffraction patterns are needed to continue the analysis of this problem.

m-AMSA and a 5-nitro acridine derivative have been shown to exhibit partially crystalline drug/DNA diffraction patterns. Three azido acridine derivatives examined under the same conditions showed no crystalline drug diffraction patterns. It is not known whether this result is due to the structural differences between these compounds or due to unintentional differences during sample preparation.

A comparison has been made between these results and fibre x-ray diffraction studies of other crystalline and non-crystalline drug/DNA studies. This suggests that a drug which has low solubility in aqueous solution and a relatively low binding affinity for DNA are possible indicators that it will crystallize in DNA fibres.

The crystallization process of small molecules in DNA fibres is important with regard to the information on DNA structure which an understanding on this process may provide and the mechanism by which these types of molecules interact with DNA. It may also be possible to exploit this crystallization process in drug treatment regimes. Further information on this crystallization process may be provided from an analysis of small molecule interactions with synthetic polynucleotides.

In investigating the complex formed between BSA and montmorillonite, x-ray diffraction results consistently indicate the presence of a repeating structure  $\sim 3.3\text{nm}$ . This was attributed to albumin within the interlamellar regions of the montmorillonite and corresponded to a protein diameter  $\sim 2.3\text{nm}$ . This value is in keeping with estimates of BSA dimensions, Low, 1952, and with earlier protein/montmorillonite adsorption experiments carried out by Ensminger and Gieseck, 1940, and Talibudeen, 1955. Reflections  $\sim 5.5\text{nm}$  from some samples may occur due to the presence of two layers of protein molecules within some interlamellar regions which suggests that the BSA molecules pack with their major axes parallel to the silicate sheets. Protein adsorption appears to disrupt the arrangement of the lamellar and/or the structured water molecules on the lamellar surfaces. This is apparent from the broad reflection at  $1.0\text{nm}$  on BSA/montmorillonite diffraction patterns which was not visible on patterns of the montmorillonite alone. Non-protein samples complexed with the montmorillonite used in this work generally gave rise to interlamellar d-spacings consistent with those previously reported in the literature. Little improvement in the resolution



of diffraction patterns was apparent as a result of the various methods of sample preparation. Nevertheless the results obtained provide a basis for subsequent neutron diffraction experiments to clearly establish the individual contributions of water and BSA to the interlamellar expansion of montmorillonite. It is hoped that an understanding of the surface interactions in this partially synthetic complex will be useful in analysing surface interactions which occur in more intricate biological systems.

Appendix A. THE USE OF A JIG TO FACILITATE THE ALIGNMENT OF FRANKS  
OPTICS ON A SEARLE CAMERA

Franks optics mounted in Searle x-ray diffraction cameras were used to obtain many of the x-ray photographs for this work. These cameras were operated in conjunction with a GEC-Elliott GX6 rotating anode x-ray generator in which the cathode was mounted in the horizontal position. With these constraints in mind a jig was developed to facilitate the determination of the film plane of the cameras which varies according to the maximum chosen specimen to film distance.

To achieve optimum resolution and exposure time it is necessary to have the smallest total x-ray path length which is compatible with the required specimen to film distance. Thus it is necessary to vary the focal conditions of the camera according to the information required from the sample under investigation. The jig has been designed as an aid to obtaining the optimum focal conditions of the camera. A schematic diagram of the device is shown in Figure A.1 while Plate A.1 shows the device in use on a Franks camera.

The jig consists of a milled central brass block that is in three parts. A 'v' section has been milled from the inside surfaces of these parts so that when screwed together they house the arms of the jig. The latter are made of silver steel, are 0.3cm square in cross section and support brass rider blocks. The riders are made in a similar fashion to the central block, two running on the front arm of the jig and one on the rear arm. The lower arm of each rider is extended into a brass boss through which a hole is drilled to contain a silver steel pointer of appropriate height. The pointer is held in position by means of a screw and can be varied in  $\sim 1$ cm in height. A screw at the end of each arm of the jig prevents the riders from being accidentally disengaged from the jig.

A lug protrudes from the central block and is milled to the same

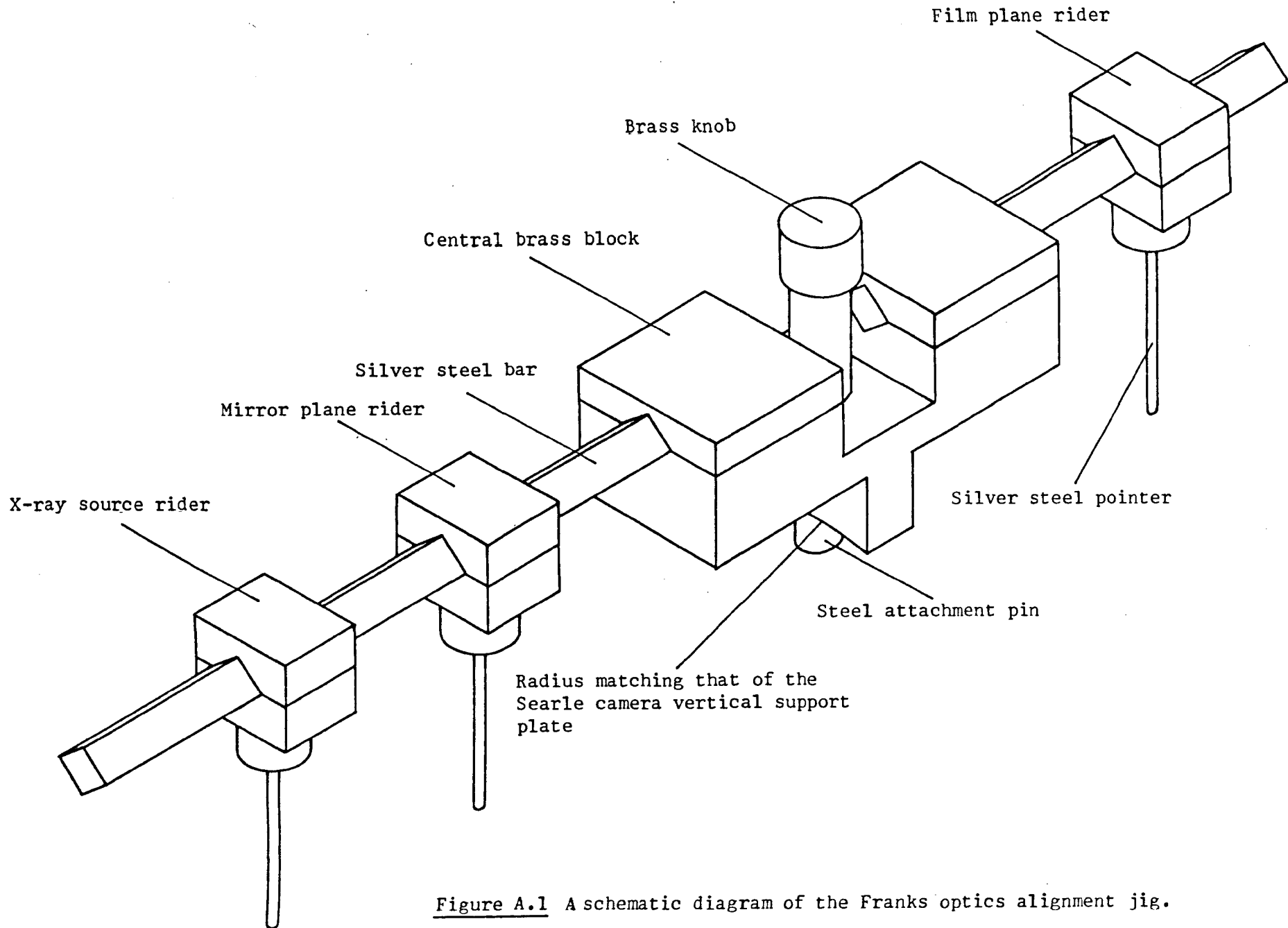


Figure A.1 A schematic diagram of the Franks optics alignment jig.

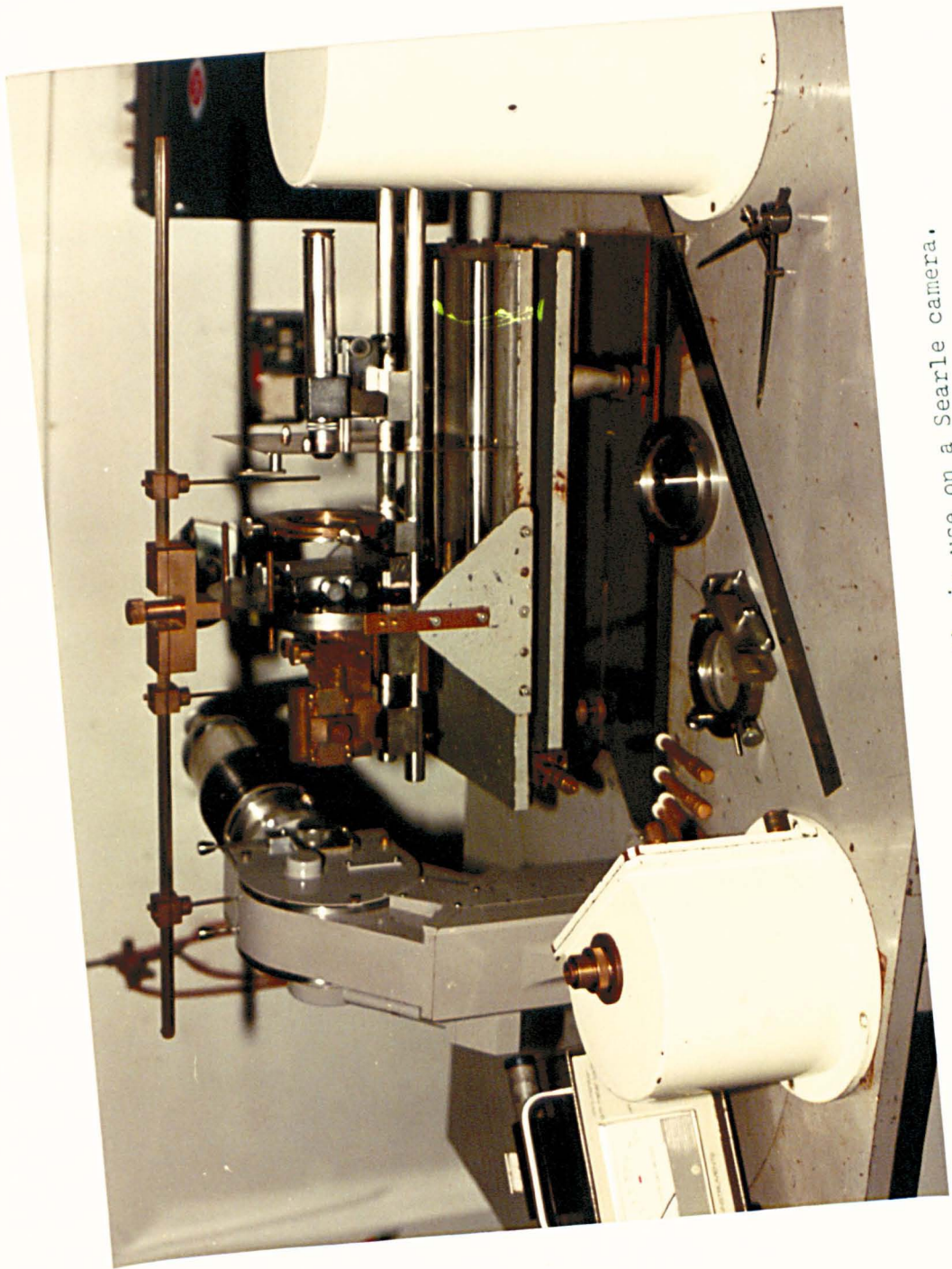


Plate A.1 The Franks optics alignment jig in use on a Searle camera.

thickness and radius as the vertical support plate of the camera stand. A steel pin with one end tapped  $3/5''$  at 26 tpi is inserted through a hole in the lug and central block. A cut out in this block allows a knurled brass knob to be attached to the pin from the top of the block. The knob is held in position by means of a grub screw and the dimensions of the knob are such as to prevent it slipping through the hole in the central block. Thus with the jig in position above the camera stand, rotating the knob will screw the steel pin into the hole in the vertical support plate created by the removal of the gas inlet tube.

The arms of the jig and the pointers are made of silver steel which is readily available in accurately ground quantities. The central block and riders are made of brass which is easy to machine and does not rust. All screws used in the jig are 4 BA allen cap screws. A steel pin lends strength to the attachment device.

To set up the Franks camera the base plate is bolted to the work surface of the generator at the correct angle and the camera stand is aligned in the conventional manner. The mirror mounts are placed on the optical bench in the desired positions and the lower part of the front vacuum chamber cover is attached to the vertical support plate. Lead shielding is used to enclose the gap between the front vacuum chamber cover and the first mirror assembly, but at this stage the shielding around the mirror assemblies is not positioned. The chosen nose piece is attached to the front vacuum chamber cover and the camera assembly is slowly advanced along the base plate towards the anode housing of the generator until the nose piece engages with the x-ray window. The jig is gently screwed into position on the vertical support plate, but before tightening, a small block is placed against the vertical support plate and the protruding lug of the central jig so as to position the jig perpendicular to the support plate.

A line is drawn on the anode housing, midway between the shutters

and at right angles to the anode axis. Rider 1 is moved along the front arm of the jig and its pointer is adjusted in height in order to lie on the line. The pointer thus represents the position of the x-ray source. Rider 2 is similarly adjusted so that its pointer coincides with the mid point of the two mirror assemblies. The distance between these pointers is determined and rider 3 is manipulated so that the distance between its pointer and that of rider 2 is the same as that between the pointers of riders 1 and 2. The distances between the pointers are most conveniently rendered equal with the aid of a beam compass.

The microscope assembly is placed on the optical bench and focused on the fluorescent screen. The screen is removed from the field of view and the assembly is moved along the bench until the pointer of rider 3 appears in focus. It may be necessary to adjust the height of the pointer during this process. A piece of masking tape is then attached to the top half of one of the rods of the optical bench immediately behind the rear of the base block of the microscope assembly. The jig can now be removed from the camera and replaced by the gas inlet tube. After placing lead shielding around the mirror assemblies the alignment of the camera is carried out in the conventional manner.

Provided that the camera stand is not moved it is only necessary to place the microscope assembly on the optical bench and carefully move it to bring the rear end of the assembly block up against the masking tape in order to determine the film plane. The accuracy of this arrangement is probably  $\sim 1\text{mm}$  but its main advantage is the ease with which it can be carried out. This is a great asset when the maximum specimen to film distance is often changed, or when the camera on the water bridge side of the generator has to be periodically realigned after generator maintenance procedures.

By attaching a second rider to the rear arm of the jig and adjusting the height of the pointers, the jig could easily be adapted for use in the

alignment of apertures and stops on the 'v' block of the Searle camera when using toroidal optics.

Appendix B. A BRACKET TO CONSTRUCT CPK MODELS IN THE B CONFORMATION OF DNA

Molecular models allow visualization of the three dimensional structure of molecules enabling the space relationships between atoms of molecules to be examined. This is of great importance to research and teaching in the biophysical and biochemical sciences where biological structure and function at the molecular level so often depend on molecular conformation.

CPK models, Koltun, 1965, are lightweight precision space filling models which are particularly useful for constructing macromolecules of biological interest. Photographs of CPK models corroborating experimental molecular structure are found throughout the scientific literature. In keeping with the design concepts of the CPK models a bracket has been developed which facilitates the assembly of up to two turns of DNA helix in the B conformation. The design of the bracket was based on an earlier version by Pigram, 1968, but provides a greater degree of support for the final model while use of a thinner central supporting rod allows a greater degree of accuracy to be maintained.

The atomic coordinates of B DNA given by Arnott and Hukins, 1972, were used to calculate the average distance between  $N_1$  purine and  $N_3$  pyrimidine atoms in A.T and G.C base pairs. Using this distance the bracket was designed as an integral part of a base pair occupying the positions normally taken by the  $N_1$  purine and the associated hydrogen CPK atoms. The dimensions of the bracket were determined by the covalent and van der Waals radii specifications of the CPK atoms and allowances were made for distances resulting from the use of the interatomic connector links. A plan orthographic projection of the bracket is given in Figure B.1 while Plate B.1 shows the brackets incorporated in two base pairs of DNA.

A standard CPK connector link screwed into a recess in the base of the bracket was used to connect the bracket to the CPK  $N_3$  atom of the



$a = 0.0625''$  diameter hole tapped for a brass screw  
 $b = 0.125''$  diameter hole tapped for a grub screw  
 $c = e = 0.05''$   
 $d = 0.0625''$  radius hole drilled at an angle of  $6^\circ$  to the plane of projection

All dimensions are in inches  
 Scale 4 : 1  
 The bracket is milled from a 1.0'' thick aluminium block

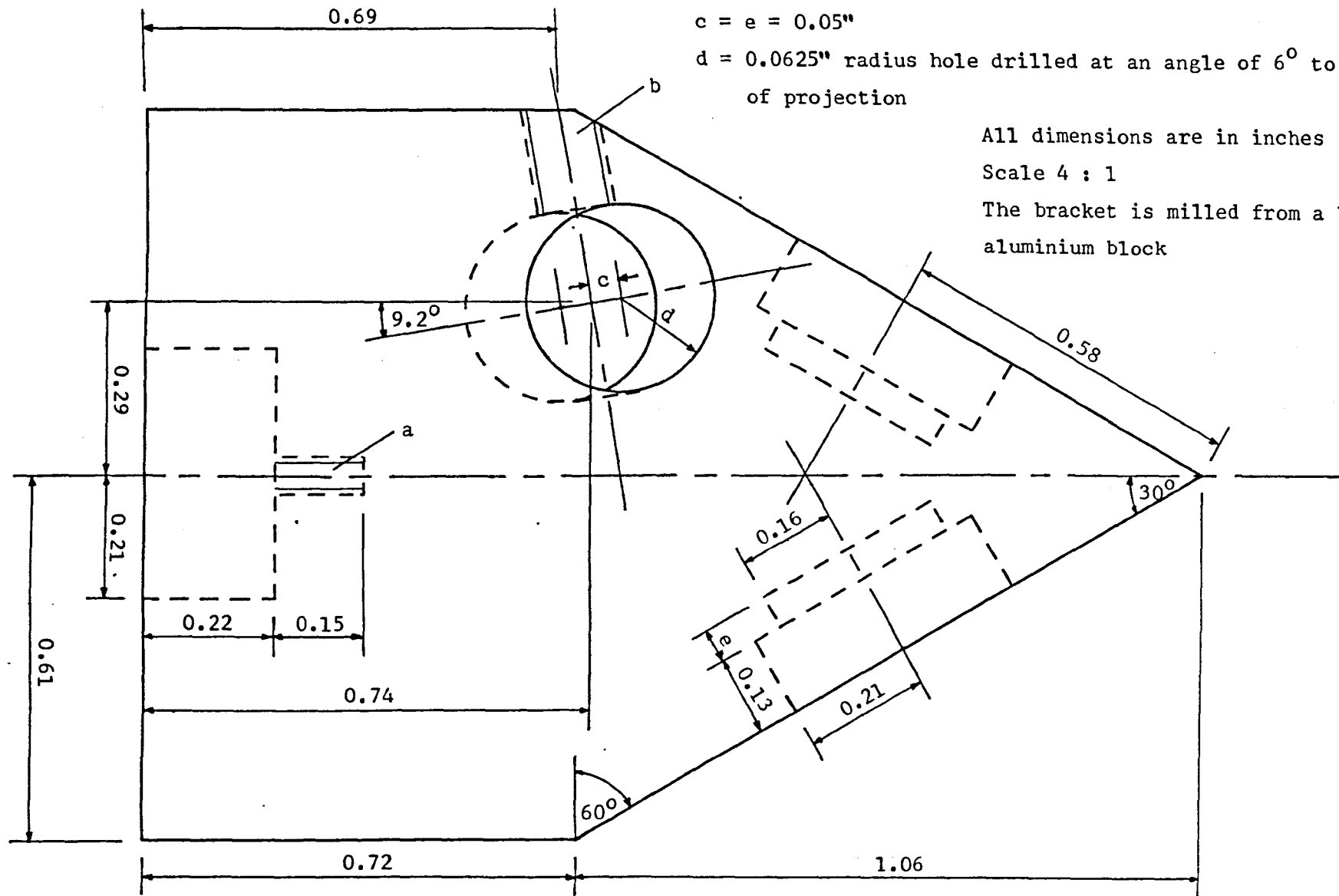


Figure B.1 A projection of the support bracket used to construct CPK models of DNA in the B conformation.

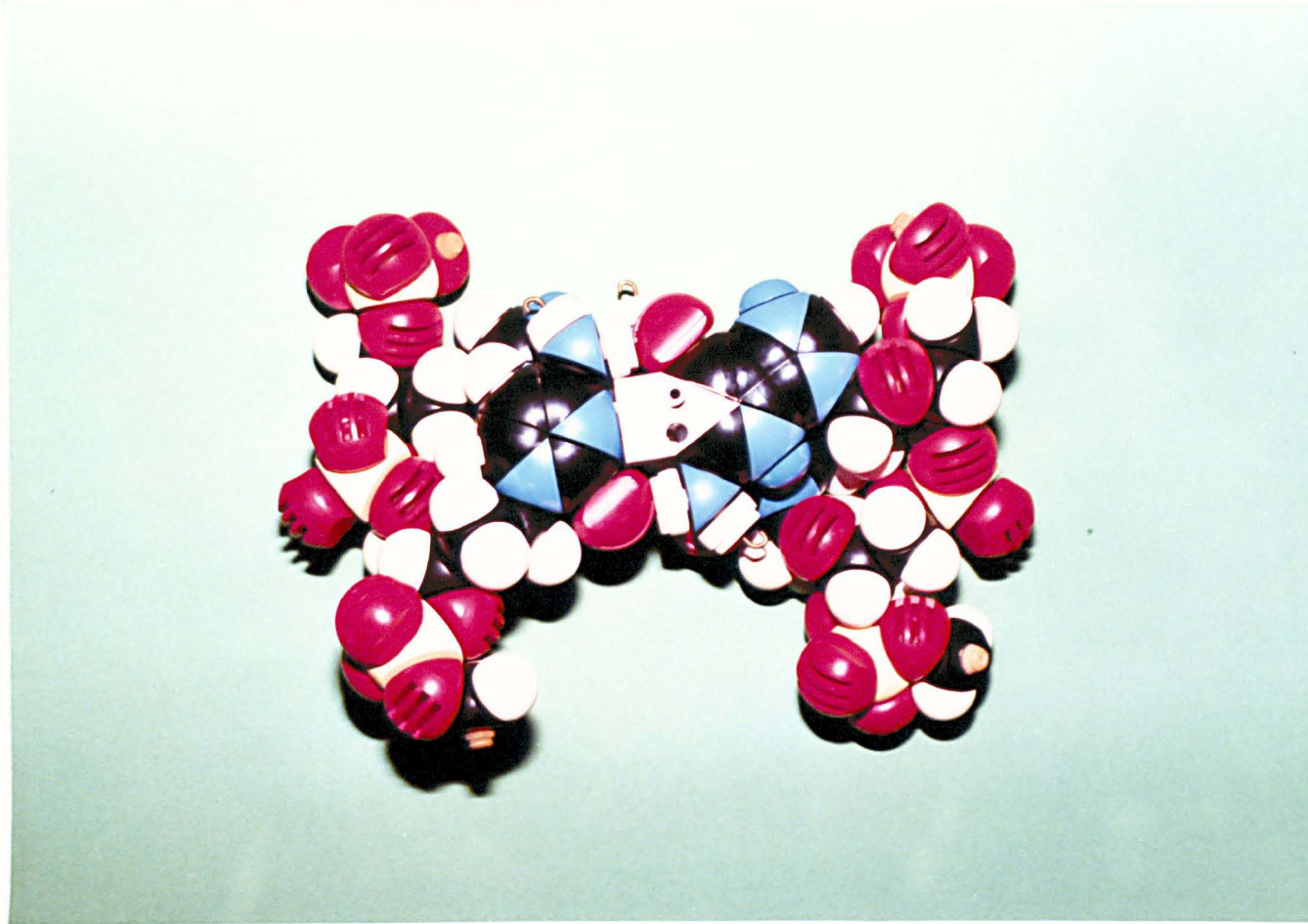


Plate B.1 The incorporation of the support brackets into two base pairs of CPK DNA viewed from the direction of the helix axis.

pyrimidine residue. Standard length CPK gluing connectors were cemented into the recesses in the head of the bracket using araldite. A CPK carbon aromatic 6 atom was araldited to each of these connectors and then the remainder of the base pair was constructed in the normal manner.

A hole in the bracket at an angle of  $84^\circ$  to the plane of the base pair allowed the bracket to be mounted onto a central steel support rod of  $5/16$ " diameter. The angled hole in the bracket provided a base pair tilt of  $6^\circ$  to the helix axis. No attempt was made to incorporate into the bracket design the  $2.1^\circ$  base pair twist of the Arnott and Hukins B DNA model which has a less pronounced effect on the DNA structure. If desired, this effect could be embodied into the bracket by drilling the hole for the central support rod to take account of this effect and by refacing the sides and base of the bracket and repositioning the holes for the connector links.

An attachment screw in the bracket located into a dimple in the central support rod attaching the bracket and base pair to the rod in the correct orientation. The dimples on the rod were machined such that they lie on a right-handed helix with an angle of  $36^\circ$  rotation per residue and a translation equivalent to 0.338nm. The position of the attachment screw in the bracket was coincident with the dyad axis of the base pair so that inversion of the bracket allowed either purine or pyrimidine residues to be located in either strand of the resultant DNA model.

The bracket was constructed from aluminium which is light, cheap and easy to machine. However, care had to be taken in tapping the hole for the attachment screw since it was easy to significantly deviate from the direction of the drill hole giving rise to large variations in the angle of rotation per residue. This problem was overcome by tapping the hole with the tap mounted in the chuck of a vertical drill and the bracket held in the appropriate position in a vice.

A central supporting rod of steel was chosen in order that the

diameter of the rod could be small enough to be sufficiently contained by the brackets when the axis of the rod was coincident with the DNA helix axis, yet strong enough to bear the weight of two turns of CPK DNA helix. The central support rod was mounted in a heavy metal base plate to lend stability to the model. The base plate was contained in a veneered wooden box for cosmetic purposes. Additional support for the model was provided by a second rod of larger diameter attached to the base plate and connected to the top of the central support rod by a horizontal arm. This was particularly useful when moving the model to prevent undue flexing of the central support rod. It could easily be removed for greater accessibility to the DNA model during model building studies.

In constructing a DNA model it was found easier to first assemble the base pairs around the brackets and then attach these to the central support rod in the desired orientations. Furanose rings were then attached to each base pair and the residues were finally linked by the phosphate groups. Plate B.2 shows a completed 1.5 turn CPK B DNA model incorporating these brackets.

In addition to the standard CPK B DNA models a 2.0 turn intercalation CPK B DNA model was also constructed using these brackets. This model was again based on an earlier design by Pigram, 1968. In this model the central supporting rod was cut into two parts mid-way between the location of the tenth and eleventh base pairs. Correct alignment of the two halves of the model was maintained by a steel pin which located in holes in the halves of the central support rod. Additional support was again provided by a non-centred support rod of larger diameter attached to the top of the central support rod by a horizontal support arm. In this model the support arm could be tracked vertically in a key-way in the larger rod and held in any desired position by the clamping pin. Thus the top half of the DNA model could be separated from the lower half to expose an intercalation gap in the DNA helix. If desired, two intercalation gaps could be created in the

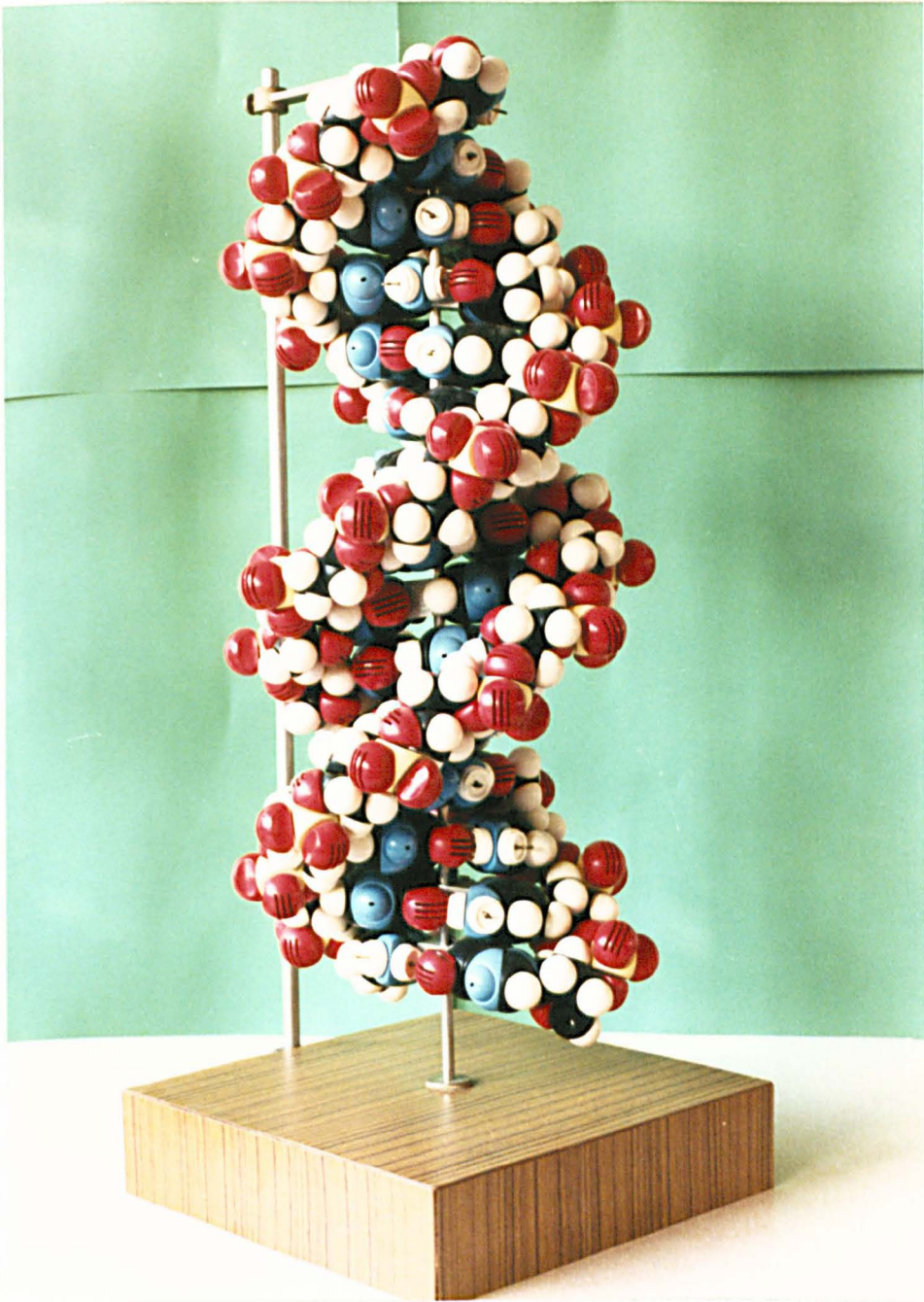


Plate B.2

A 1.5 turn CPK DNA model in the B conformation constructed using the support brackets.

model, separated by 1, 2 or 3 nucleotide pairs, by suitable insertion of a segment of central support rod containing the appropriate number of residues. This model allowed trial drug/DNA intercalation arrangements to be constructed. Once a promising arrangement was discovered further model building could be carried out using computer techniques. However, CPK model building was particularly useful in carrying out preliminary studies where non-feasible models could be quickly eliminated.

Brackets of similar design to that discussed could be used to construct DNA models in the related C or D conformations. Alternatively, individually designed brackets may be used in a DNA model to construct the side by side structure proposed by Rodley et al., 1976, or the B conformation of the CGCGAATTCGCG structure of Wing et al., 1980, which details the conformations of the individual base pairs in the dodecamer sequence.

It should not be envisaged that the B DNA model represents a definitive rigid conformation of DNA. In solution DNA structure is undergoing continual conformational change and thus the B conformation probably represents an averaged structure. Even in the fibre state Zimmerman and Pfeiffer, 1980, have suggested that continual smooth conformational transitions may occur between B and C conformations and this is supported by the results in chapter 4. In this respect the very rigidity of the B DNA model constructed using these brackets prevents manipulation of the model into conformations even closely resembling that of the B conformation. The intercalation model is an exception which applies to a specific case. What this bracket design does provide is a unit which is compatible with the design concepts of the CPK model and which allows a DNA model to be readily assembled in a specific conformation without the need to measure values of rotation per residue, rise per residue, helix displacement and base pair tilt. It gives the model sufficient rigidity such that subsequent examinations of the model do not displace the conformational characteristics. The model readily enables the essential features of the three dimensional structure of DNA in the B

conformation to be visualized. It also provides an adequate basis for preliminary drug/DNA model building analysis.

References

- Acheson, R.M. (Ed.) (1973) *Acridines* (2<sup>nd</sup> ed.) Wiley, London.
- Albert, A. (1973) *Selective Toxicity* (5<sup>th</sup> ed.) Chapman and Hall, London.
- Alden, C.J. and Arnott, S. (1975) *Nucl. Acids Res.*, 2, 1701.
- Alden, C.J. and Arnott, S. (1977) *Nucl. Acids Res.*, 4, 3855.
- Arnott, S. (1982) in *Topics in Nucleic Acid Structure* vol. 1 (Ed. S. Neidle) Macmillan Publishers Ltd., p 65.
- Arnott, S. and Hukins, D.W.L. (1972) *Biochem. Biophys. Res. Commun.*, 47, 1504.
- Arnott, S. and Hukins, D.W.L. (1973) *J. Mol. Biol.*, 81, 93.
- Arnott, S. and Selsing, E. (1974) *J. Mol. Biol.*, 88, 509.
- Arnott, S. and Selsing, E. (1975) *J. Mol. Biol.*, 98, 265.
- Arnott, S. and Wonacott, A.J. (1966) *Polymer*, 7, 157.
- Arnott, S., Hutchinson, F., Spencer, M., Wilkins, M.H.F., Fuller, W. and Langridge, R. (1966) *Nature*, 211, 227.
- Arnott, S., Wilkins, M.H.F., Fuller, W. and Langridge, R. (1967) *J. Mol. Biol.*, 27, 535.
- Arnott, S., Fuller, W., Hodgson, A.R. and Prutton, I. (1968) *Nature*, 220, 561.
- Arnott, S., Dover, S.D. and Wonacott, A.J. (1969) *Acta Crystallogr.*, B25, 2192.
- Arnott, S., Hukins, D.W.L., Dover, S.D. Fuller, W. and Hodgson, A.R. (1973) *J. Mol. Biol.*, 81, 107.
- Arnott, S., Chandrasekaran, R., Hukins, D.W.L., Smith, P.J.C. and Watts, L. (1974) *J. Mol. Biol.*, 88, 523.
- Arnott, S., Chandrasekaran, R., Birdsall, D.L., Leslie, A.G.W. and Ratliff, R.L. (1980) *Nature*, 283, 743.
- Bergy, M.E. and Reusser, F. (1967) *Experientia*, 23, 254.
- Berman, H.M. (1982) in *Topics in Nucleic Acid Structure* vol. 1 (Ed. S. Neidle) Macmillan Publishers Ltd., p 1.
- Bingham, F. (1977) B.Sc. Project, Dept. of Physics, University of Keele.
- Biswal, N., Kleinschmidt, A.K., Spatz, H.C. and Trautner, T.A. (1967) *Mol. Gen. Genet.*, 100, 39.
- Blakeley, P.J. (1976) Ph.D. Thesis, Dept. of Physics, University of Keele.
- Bond, P.J., Langridge, R., Jennette, K.W. and Lippard, S.J. (1975) *Proc. Natl. Acad. Sci. U.S.A.*, 72, 4825.
- Bram, S. (1971) *Nature New Biol.*, 232, 174.



- Bram, S. (1973) Proc. Natl. Acad. Sci. U.S.A., 70, 2167.
- Bram, S. and Baudy, P. (1974) Nature, 250, 414.
- Bram, S. and Tougard, P. (1972) Nature New Biol., 239, 128.
- Brahms, G.J., Pilet, J., Lan, T.-T.P. and Hill, L.R. (1973) Proc. Natl. Acad. Sci. U.S.A., 70, 3352.
- Brenner, S., Barnett, L., Crick, F.H.C. and Orgel, A. (1961) J. Mol. Biol., 3, 121.
- Brodasky, T.F. and Reusser, F. (1974) J. Antibiot., 27, 809.
- Cain, B.F. and Atwell, G.J. (1974) Europ. J. Cancer, 10, 539.
- Cain, B.F., Seelye, R.N. and Atwell, G.J. (1974) J. Med. Chem., 17, 922.
- Callaghan, I.C. and Ottewill, R.H. (1974) Farad. Disc. Chem. Soc., 57, 110.
- Cebula, D.J., Thomas, R.K., Middleton, S., Ottewill, R.H. and White, J.W. (1979) Clay Clay M., 27, 39.
- Conner, B.N., Takano, T., Tanaka, S., Itakura, K. and Dickerson, R.E. (1982) Nature, 295, 294.
- Cooper, P.J. and Hamilton, L.D. (1966) J. Mol. Biol., 16, 562.
- Crawford, J.L., Kolpak, F.J., Wang, A.H.-J., Quigley, G.J., van Broom, J.H., van der Marel, G. and Rich, A. (1980) Proc. Natl. Acad. Sci. U.S.A., 77, 4016.
- Crick, F.H.C. and Watson, J.D. (1954) Proc. R. Soc., A223, 80.
- Dall'Acqua, F., Vedaldi, D. and Gennaro, A. (1979) Chem-Biol. Interactions, 25, 59.
- Davies, D.R. (1960) Nature, 186, 1030.
- Davies, D.R. and Baldwin, R.L. (1963) J. Mol. Biol., 6, 251.
- Davies, M.E. (1973) unpublished.
- Dickerson, R.E. and Drew, H.R. (1981) J. Mol. Biol., 149, 761.
- Drew, H.R. and Dickerson, R.E. (1981a) J. Mol. Biol., 151, 535.
- Drew, H.R. and Dickerson, R.E. (1981b) J. Mol. Biol., 152, 723.
- Drew, H.R., Dickerson, R.E. and Itakura, K. (1978) J. Mol. Biol., 125, 535.
- Drew, H.R., Takano, T., Tanaka, S., Itakura, K. and Dickerson, R.E. (1980) Nature, 286, 567.
- Drew, H.R., Wing, R.M., Takano, T., Broka, C., Tanaka, S., Itakura, K. and Dickerson, R.E. (1981) Proc. Natl. Acad. Sci. U.S.A., 78, 2179.
- Ensminger, L.E. and Giesecking, J.E. (1940) Soil Sci., 48, 467.
- Ensminger, L.E. and Giesecking, J.E. (1941) Soil Sci., 51, 125.

- Erfurth, S.C., Bond, P.J. and Peticolas, W.L. (1975) *Biopolymers*, 14, 1245.
- Fink, D.H. (1977) *Clay Clay M.*, 25, 196.
- Fraser, R.D.B., Macrae, T.P., Miller, A. and Rowlands, R.J. (1976) *J. Apply. Cryst.*, 9, 4.
- Fuller, W. (1961) Ph.D. Thesis, Dept. of Biophysics, King's College, University of London.
- Fuller, W. and Waring, M.J. (1964) *Ber. Bunsenges. Physik. Chem.*, 68, 805.
- Fuller, W., Wilkins, M.H.F., Wilson, H.R. and Hamilton, L.D. (1965) *J. Mol. Biol.*, 12, 60.
- Fuller, W., Hutchingson, F., Spencer, M. and Wilkins, M.H.F. (1967) *J. Mol. Biol.*, 27, 507.
- Gale, E.F., Cundliffe, E., Renyolds, P.E., Richmond, M.H. and Waring, M.J. (1981) *The Molecular Basis of Antibiotic Action* (2<sup>nd</sup> ed.) John Wiley and Sons, London.
- Goldberg, I.H. and Friedman, P.A. (1971) *Ann. Rev. Biochem.*, 40, 775.
- Goodwin, D.C. (1977) Ph.D. Thesis, Dept. of Physics, University of Keele.
- Greenall, R.J. (1982) Ph.D. Thesis, Dept. of Physics, University of Keele.
- Greenall, R.J., Pigram, W.J. and Fuller, W. (1979) *Nature*, 282, 880.
- Greene-Kelly, R. (1955) *Trans. Farad. Soc.*, 51, 412.
- Greenland, D.J. (1956) *J. Soil Sci.*, 7, 319.
- Gupta, G., Bansal, M. and Sasisekharan, V. (1980) *Int. J. Biol. Macromol.*, 2, 368.
- Hearst, J.E., Botchan, M., Kram, R. and Beals, E. (1973) *Biochim. Biophys. Acta*, 294, 173.
- Height, R., Jr., Higdon, W.T. and Schmidt, P.W. (1960) *J. Chem. Phys.*, 33, 1656.
- Height, R., Jr., Higdon, W.T., Darley, H.C.H. and Schmidt, P.W. (1962) *J. Chem. Phys.*, 37, 502.
- Heller, M.J., Tu, A.T. and Maciel, G.E. (1974) *Biochemistry*, 13, 1623.
- Hendricks, S.B. (1941) *J. Phys. Chem.*, 45, 65.
- Hirschberg, E. (1975) in *Antibiotics III Mechanism of Action of Antimicrobial and Antitumour Agents* (Eds. J.W. Corcoran and F.E. Hahn) Springer-Verlag, Heidelberg, p 274.
- Hirschberg, E., Weinstein, I.B., Gersten, N., Marnier, E., Finkelstein, T. and Carchman, R. (1968) *Cancer Res.*, 28, 601.
- Kelly, R.C., Schletter, I., Koert, J.M., MacKellar, F.A. and Wiley, P.F. (1977) *J. Org. Chem.*, 42, 3591.

- Klug, A., Jack, A., Viswamitra, M.A., Kennard, O., Shakked, Z. and Steitz, T.A. (1979) *J. Mol. Biol.*, 131, 669.
- Koltun, W.L. (1965) *Biopolymers*, 3, 665.
- Kropinski, A.M.B. and Warren, R.A.J. (1970) *J. Gen. Virol.*, 6, 85.
- Kropinski, A.M.B., Bose, R.J. and Warren, R.A.J. (1973) *Biochemistry*, 12, 151.
- Langridge, R. (1969) *J. Cell. Physiol.*, 74, sup. 1, 1.
- Langridge, R., Wilson, H.R., Hooper, C.W., Wilkins, M.H.F. and Hamilton, L.D. (1960a) *J. Mol. Biol.*, 2, 19.
- Langridge, R., Marvin, D.A., Seeds, W.E., Wilson, H.R., Hooper, C.W., Wilkins, M.H.F. and Hamilton, L.D. (1960b) *J. Mol. Biol.*, 2, 38.
- Lerman, L.S. (1961) *J. Mol. Biol.*, 3, 18.
- Lerman, L.S. (1963) *Proc. Natl. Acad. Sci. U.S.A.*, 49, 94.
- Lerman, L.S. (1964a) *J. Cell. Comp. Physiol.*, 64, sup. 1, 1.
- Lerman, L.S. (1964b) *J. Mol. Biol.*, 10, 367.
- Leslie, A.G.W., Arnott, S., Chandrasekaran, R. and Ratliff, R.L. (1980) *J. Mol. Biol.*, 143, 49.
- Low, B.W. (1952) *J. Amer. Chem. Soc.*, 74, 4830.
- Luzzati, V., Masson, F. and Lerman, L.S. (1961) *J. Mol. Biol.*, 3, 634.
- Lyklema, J. and Norde, W. (1973) *Croat. Chem.*, 45, 67.
- MacEwan, D.M.C. (1956) *Kolloid-Z.*, 149, 96.
- MacEwan, D.M.C. (1961) in *X-ray Identification and Crystal Structure of Clay Minerals* (Ed. G. Brown) Mineralogical Society, London, p 143.
- Mahendrasingam, A. (1983) Ph.D. Thesis, Dept. of Physics, University of Keele.
- Marvin, D.A., Spencer, M., Wilkins, M.H.F. and Hamilton, L.D. (1961) *J. Mol. Biol.*, 3, 547.
- McGhee, J.D. and von Hippel, P.H. (1974) *J. Mol. Biol.*, 86, 469.
- Milman, G., Langridge, R. and Chamberlin, M.J. (1967) *Proc. Natl. Acad. Sci. U.S.A.*, 57, 1804.
- Mitsui, Y., Langridge, R., Shortle, B.E., Cantor, C.R., Grant, R.C., Kodama, M. and Wells, R.D. (1970) *Nature*, 228, 1166.
- Mokul'skaya, T.D., Smetanina, E.P., Myshko, G.E. and Mokul'skii, M.A. (1975) *Mol. Biol.*, 9, 446.
- Mokul'skii, M.A., Kapitonova, K.A. and Mokul'skaya, T.D. (1972) *Mol. Biol.*, 6, 716.
- Mooney, R.W., Keenan, A.G. and Wood, L.A. (1952) *J. Amer. Chem. Soc.*, 74, 1367.

- Neidle, S. (1976) *Biochim. Biophys. Acta*, 454, 207.
- Neidle, S. (1982) in *Topics in Nucleic Acid Structure* vol. 1 (Ed. S. Neidle) Macmillan Publishers Ltd., p 177.
- Neidle, S. and Taylor, G. (1977) *Biochim. Biophys. Acta*, 479, 450.
- Neidle, S., Achari, A., Taylor, G.L., Berman, H.M., Carrel, H.L., Glusker, J.P. and Stallings, W.C. (1977) *Nature*, 269, 304.
- Neville, D.M., Jr. and Davies, D.R. (1966) *J. Mol. Biol.*, 17, 57.
- Norrish, K. (1954) *Farad. Disc. Chem. Soc.*, 18, 120.
- O'Brien, F.E.M. (1948) *J. Sci. Instr.*, 25, 73.
- O'Brien, E.J. and MacEwan, A.W. (1970) *J. Mol. Biol.*, 48, 243.
- Peacocke, A.R. and Walker, I.O. (1962) *J. Mol. Biol.*, 5, 550.
- Pigram, W.J. (1968) Ph.D. Thesis, Dept. of Biophysics, King's College, University of London.
- Pigram, W.J., Fuller, W. and Hamilton, L.D. (1972) *Nature New Biol.*, 235, 17.
- Pilet, J. and Brahm, G.J. (1973) *Biopolymers*, 12, 387.
- Porumb, H. (1976) Ph.D. Thesis, Dept. of Physics, University of Keele.
- Reusser, F. (1967) *J. Bacteriol.*, 93, 65.
- Reusser, F. (1975) *Biochim. Biophys. Acta*, 383, 266.
- Revel, H.R. and Luria, S.E. (1970) *Ann. Rev. Genet.*, 4, 177.
- Rhodes, N.J., Mahendrasingam, A., Pigram, W.J., Fuller, W., Brahm, G.J., Vergne, J. and Warren, R.A.J. (1982) *Nature*, 296, 267.
- Riddiford, C.L. and Jennings, B.R. (1966) *Biochim. Biophys. Acta*, 126, 171.
- Riggs, A.D., Lin, S.-Y. and Wells, R.D. (1972) *Proc. Natl. Acad. Sci. U.S.A.*, 69, 761.
- Rodley, G.A., Scobie, R.S., Bates, R.H.T. and Lewitt, R.M. (1976) *Proc. Natl. Acad. Sci. U.S.A.*, 73, 2959.
- Rusconi, A. (1966) *Biochim. Biophys. Acta*, 123, 627.
- Seeman, N.C., Rosenberg, J.M., Suddath, F.L., Kim, J.J.P. and Rich, A. (1976) *J. Mol. Biol.*, 104, 109.
- Selsing, E. and Arnott, S. (1976) *Nucl. Acids Res.*, 3, 2443.
- Selsing, E., Leslie, A.G.W., Arnott, S., Gall, J.G., Skinner, D.M., Southern, E.M., Spencer, J.H. and Harbers, K. (1976) *Nucl. Acids Res.*, 3, 2451.
- Shakked, Z., Rabinovich, D., Cruse, W.B.T., Egert, E., Kennard, O., Sala, G., Salisbury, S.A. and Viswamitra, M.A. (1981) *Proc. R. Soc.*, B213, 479.

- Squire, P.G., Moser, P. and O'Konski, C.T. (1968) *Biochemistry*, 7, 4261.
- Sueoka, N. and Cheng, T.-Y. (1962a) *J. Mol. Biol.*, 4, 161.
- Sueoka, N. and Cheng, T.-Y. (1962b) *Proc. Natl. Acad. Sci. U.S.A.*, 48, 1851.
- Sundaralingam, M. (1969) *Biopolymers*, 7, 821.
- Sundaralingam, M. and Jensen, L.H. (1965) *J. Mol. Biol.*, 13, 930.
- Talibudeen, O. (1955) *Trans. Farad. Soc.*, 51, 582.
- Viswamitra, M.A., Kennard, O., Jones, P.G., Sheldrick, G.M., Salisbury, S.A., Falvello, L. and Shakked, Z. (1978) *Nature*, 273, 687.
- Wang, A.H.-J., Quigley, G.J., Kolpak, F.J., Crawford, J.L., van Boom, J.H., van der Marel, G. and Rich, A. (1979) *Nature*, 282, 680.
- Wang, A.H.-J., Quigley, G.J., Kolpak, F.J., van der Marel, G., van Boom, J.H. and Rich, A. (1981) *Science*, 211, 171.
- Wang, A.H.-J., Fujii, S., van Boom, J.H. and Rich, A. (1982a) *Proc. Natl. Acad. Sci. U.S.A.*, 79, 3968.
- Wang, A.H.-J., Fujii, S., van Boom, J.H., van der Marel, G.A., van Boeckel, S.A.A. and Rich, A. (1982b) *Nature*, 299, 601.
- Waring, M.J. (1970) *J. Mol. Biol.*, 54, 247.
- Watson, J.D. and Crick, F.H.C. (1953a) *Nature*, 171, 737.
- Watson, J.D. and Crick, F.H.C. (1953b) *Nature*, 171, 964.
- Weinstein, I.B. and Hirschberg, E. (1971) *Progr. Mol. Subcell. Biol.*, 2, 232.
- Wing, R.M., Drew, H.R., Takano, T., Broka, C., Tanaka, S., Itakura, K. and Dickerson, R.E. (1980) *Nature*, 287, 755.
- Wong, C. (1979) Ph.D. Thesis, Dept. of Pharmacy, University of Aston, Birmingham.
- Zimmerman, S.B. and Pfeiffer, B.H. (1979) *Proc. Natl. Acad. Sci. U.S.A.*, 76, 2703.
- Zimmerman, S.B. and Pfeiffer, B.H. (1980) *J. Mol. Biol.*, 142, 315.
- Zimmerman, S.B. and Pfeiffer, B.H. (1981) *Proc. Natl. Acad. Sci. U.S.A.*, 78, 78.